Altered NMDA and GABA-A Receptor Subunit Expression in the Hypothalamic Paraventricular Nucleus of Hypertensive and Pregnant Rats

CORK, SIMON,CHRISTOPHER

Altered NMDA and $GABA_A$ Receptor Subunit Expression in the Hypothalamic Paraventricular Nucleus of Hypertensive and Pregnant Rats

Simon Christopher Cork

B.Sc. (Hons) (Dunelm)

A thesis submitted to the University of Durham in accordance with the requirements for the degree of Doctor of Philosophy

School of Biological and Biomedical Sciences

University of Durham

2013

Supervisor: Dr Susan Pyner

“No one, unless he is grossly ignorant of what science has done for mankind, can entertain any doubt of the incalculable benefits which will hereafter be derived from physiology”

Charles Darwin, 1809 - 1882

Abstract

Hypertension and pregnancy are both accompanied by increases in sympathetic nerve activity. This has been attributed in part, to changes in the neurochemistry of the hypothalamic paraventricular nucleus (PVN).

In hypertension, physiological studies have revealed that decreases in GABAergic inhibition and increases in glutamatergic excitation within the PVN contribute to this sympathoexcitation. In late-term pregnancy however, the sympathoexcitation appears to be mediated by decreases in GABAergic inhibition, with no glutamatergic contribution.

This study aimed to examine the molecular characteristics of the $GABA_A$ and NMDA receptor to ascertain whether changes in their subunit expression in the PVN could contribute to the sympathoexcitation observed in these physiological states. Whole PVN micropunches subjected to quantitative immunoblotting were combined with semi-quantitative analysis of immunohistochemistry to ascertain which subunits were altered, and whether the alteration was confined to specific parvocellular subnuclei of the PVN.

The results of this study show that both hypertension and pregnancy are accompanied by significant decreases in both the α1 and α5 subunit of the $GABA_A$ receptor in the PVN. Furthermore, hypertension is also accompanied by a significant increase in the expression of the GluN2A subunit of the NMDA receptor, which was associated with increases in the number of GluN2A-immunoreactive neurones in specific parvocellular subnuclei of the PVN. Conversely, pregnancy was associated with a significant increase in GluN2B subunit expression which was not associated with changes in cell immunoreactivity in any parvocellular subnuclei.

The results from this study suggest that decreases in α1 and α5 subunits of the $GABA_A$ receptor may be important in mediating the sympathoexcitation observed in both of these physiological states, with the greater level of sympathoexcitation observed in hypertension possibly attributed to increases in GluN2A-mediated NMDA receptor expression.

Table of Contents

List of Illustrations

Chapter 1 - Introduction:

Chapter 2 - Methods:

Chapter 3 - Physiological Parameters of Animals Used:

Chapter 4 - CTB Labelling of Spinally Projecting Neurones:

Chapter 5 - Localisation of NMDA Receptor Subunits in the PVN:

Chapter 6 - Localisation of $GABA_A$ Receptors in the PVN:

Chapter 7 - Co-localisation of GABAA and NMDA Receptors with Presympathetic Spinally Projecting PVN Neurones:

Chapter 8 - Discussion:

List of Abbreviations

2,3-dioxo-6-nitro-1,2,3,4-tetrahydrobenzo[f]quinoxaline-7-sulfonamide disodium	NBQX
2a-amino-3-hydroxy-5-methyl-4-isoxazolepropionic acid	AMPA
3'3-diaminobenzidine	DAB
3rd Ventricle	3V
3α-hydroxy-5α-pregnan-20-one	3α-OH-DHP Allopregnanolone
4,5,6,7-tetrahydroisoxazolo-[5,4-c]pyridine-3-ol	THIP
5β-pregnan-3α-ol-20-one	Pregnanolone
5β-pregnane-3,20-dione	Pregnanedione
6-cyano-7-nitroquinoxaline-2,3-dione	CNQX
Adrenal Medulla	AM
Ammonium Persulphate	APS
Angiotensin II	AngII
Angiotensin Type 1 Receptor	AT1
Anterior Parvocellular Subnucleus	PaAP
Arterial Blood Pressure	ABP
Bovine Serum Albumin	BSA
Casein kinase 2	CK2
Caudal Ventrolateral Medulla	CVLM
Central Nervous System	CNS

Cholera Toxin Subunit B	CTB
Cornu Ammonis	CA
Corticotrophin Releasing Hormone	CRH
Dahl Salt-Resistant Rat	DSR
Dahl Salt-Sensitive Rat	DSS
Distilled water	dH_2O
Dithiothreitol	DTT
DL-2-amino-5-phosphonovaleric acid	AP-5
Dorsal Cap	PaDC
Ethylenediaminetetraacetic acid	EDTA
Ethyleneglycoltetraacetic acid	EGTA
Excitatory Post-Synaptic Current	EPSC
Fluorogold	FG
Gamma aminobutyric acid	GABA
Glutamate Vesicular Transporter	VGLUT
Glutamic Acid Decarboxylase	GAD
Granule cells of the dentate gyrus	DGGC
Green Fluorescent Protein	GFP
Heart Failure	HF
Heart Rate	HR
Herpes Simplex Virus	HSV
High Frequency	HiF
Horseradish Peroxidase	HRP
Immunoreactive	IR

Inhibitory Post-Synaptic Potential	IPSC
Intermediolateral Cell Column	IML
Intracerebroventricular	i.c.v.
Intravenous	i.v.
K^+-Cl^- cotransporter-2	KCC2
Kynurenic Acid	Kyn
Lateral Parvocellular Subunit	PaLP
Liberate Antibody Binding Solution	L.A.B.
Low Frequency	LF
Lumbar Sympathetic Nerve Activity	LSNA
Mean Arterial Blood Pressure	MAP
Medial Parvocellular Subnucleus	PaMP
Messenger RNA	mRNA
Muscle Sympathetic Nerve Activity	MSNA
N (G)-nitro-L- arginine methyl ester	L-NAME
Na^+-K^+-$2Cl^-$ cotransporter-1	NKCC1
Nitric Oxide	NO
N-methyl-D-aspartate	NMDA
Nucleus Tractus Solitarius	NTS
Paraformaldehyde	PFA
Paraventricular Nucleus	PVN
Phosphate Buffer	PB
Poly-acrylamide gel electrophoresis	PAGE
Posterior Parvocellular Subnucleus	PaPO

Renal Sympathetic Nerve Activity	RSNA
Ribonucleic Acid	RNA
Rostral Ventrolateral Medulla	RVLM
Single Unit MSNA	sMSNA
SKF 105111- 17β-17-[bis (1methylethyl) amino-carbonyl] androstane-3,5-diene-3-carboxylic acid	SKF
Sodium dodecyl sulphate	SDS
Sodium Nitroprusside	SNP
Spontaneous IPSC	sIPSC
Spontaneously Hypertensive Rat	SHR
Sprague Dawley Rat	SD
Supraoptic Nucleus	SON
Sympathetic Nerve Activity	SNA
Sympathetic Preganglionic neurones	SPN
Tetrahydrodeoxycorticosterone	THDOC
Tetramethylethylenediamine	TEMED
Transmembrane	TM
Tris-buffered saline	TBS
Ventral Parvocellular Subnucleus	PaVP
Wild Type	WT
Wistar-Kyoto Rat	WKY

Declaration

The research contained in this thesis was carried out by the author between 2008 and 2012 while a postgraduate student at the School of Biological & Biomedical Sciences, University of Durham. No part of the material presented has previously been submitted for a degree in this or any other university.

The injections of cholera toxin-B and Fluorogold presented in chapters 4 and 7 respectively were carried out by either the author, Ms Valerie Affleck or Dr Susan Pyner.

Acknowledgements

This work would not have been possible without the help of many people. First and foremost, I am eternally indebted to Dr Susan Pyner for her unfaltering support and guidance over the course of this project. I am thankful to be able to call her my supervisor and friend.

A great deal of thanks also goes to Dr Paul Chazot for his support throughout this project, as well as his expertise on $GABA_A$ and NMDA receptors, and the use of many of the antibodies used in this thesis. I also wish to thank Prof. John Coote for his general guidance, wisdom, enthusiasm and inspiration.

Special thanks go to Claire Robinson and Heather Crawford (LSSU), Helen Grindley and Christine Richardson (Imaging Suite) and Valerie Affleck for technical support.

I am lucky to have met many friends over the course of my research at Durham, these include, but are not limited to Drs Gavin Richardson, Andrew Lemin, Piers Hemsley, Kamila Wojciechowicz, Mwape Katabe and Rushdie Abuhamdah; all of whom have provided both practical and social support over the years.

Finally I wish to thank my partner Natalie and my parents for their constant and unwavering support throughout my life. They are the reason I have been able to achieve this thesis.

Chapter 1. Introduction

Maintenance of cardiovascular homeostasis is a complex neural reflex, required to preserve adequate blood flow to organs. This regulation involves the integration of signals from peripheral baroreceptors and results in reflex adjustment of the sympathetic nervous system (Heesch, 1999). Cardiovascular diseases such as heart failure and hypertension are multifactoral in nature; but a common characteristic is increased sympathetic nerve activity to areas of the cardiovascular system, the origins of which are within the brain (Grassi *et al.*, 2009). This increased sympathetic outflow is also a characteristic feature of pregnancy (Greenwood *et al*, 2001; Jarvis *et al*, 2012). A key site for this aberrant control of sympathetic outflow is the hypothalamic paraventricular nucleus (PVN; Guyenet, 2006)

This thesis aims to bring together the current literature regarding the role of the PVN and its contribution to normal cardiovascular homeostasis, as well as its role in cardiovascular disease.

I. Anatomy of the PVN

The architecture and anatomy of the PVN have been described extensively in various animals including the rat (Swanson & Sawchenko, 1983; Simmons & Swanson, 2008), mouse (Kadar *et al.*, 2010), rabbit (Schimchowitsch *et al.*, 1989), cat (Caverson *et al*, 1984), sheep (Papadopoulos *et al*, 1990) platypus (Ashwell *et al.*, 2006) and human (Koutcherov *et al.*, 2000). It is now well accepted that in the rat the PVN consists of five anatomically distinct parvocellular subnuclei and two magnocellular subnuclei (Swanson &

Sawchenko, 1983). The exact anatomical boundaries of these subnuclei have changed depending on the method of detection (e.g. characterisation of efferent projections, neurochemical immunoreactivity), however the nomenclature ascribed to these five parvocellular subnuclei has remained largely unchanged. The five parvocellular subnuclei of the rat PVN are termed the anterior parvocellular (PaAP), medial parvocellular (PaMP), dorsal cap (PaDC), ventral parvocellular (PaVP) and posterior parvocellular (PaPO – alternatively referred to as the lateral parvocellular (PaLP); Figure 1**;** Swanson *et al.*, 1980; Swanson & Sawchenko, 1983; Paxinos & Watson, 1998).

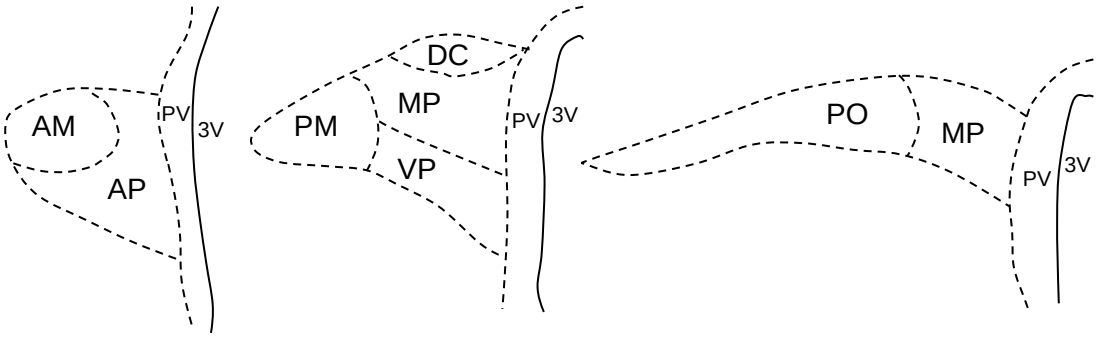

Figure 1 Schematic representation of the rat PVN showing the anatomically distinct subnuclei. Abbreviations: AM = anterior magnocellular, AP = anterior parvocellular, PV = periventricular area, DC = dorsal cap, MP = medial parvocellular, VP = ventral parvocellular, PM = posterior magnocellular, PO = posterior parvocellular, 3V = 3rd ventricle. Adapted from Swanson *et al*, 1980.

The PVN has long been known to send descending projections from its magnocellular neurosecretory regions to the neurohypophysis (Sherlock *et al.*, 1975). In addition to this, the PVN is known to send efferent projections to the median eminence, locus coeruleus, parabrachial nuclei and dorsal vagal complex from its parvocellular regions (Swanson, 1977).

Importantly, in the rat the PVN is also known to send descending projections to other central nuclei involved in autonomic regulation of the cardiovascular system (Ranson *et al,* 1998; Pyner & Coote, 2000). A significant descending projection to the intermediolateral cell column of the spinal cord (IML) originates from all parvocellular subnuclei of the PVN, with the majority arising from the mid- to caudal levels of the PVN that includes the medial, posterior, ventral and dorsal cap regions (Swanson *et al.*, 1980; Oldfield *et al.*, 2001). This descending projection also closely apposes sympathetic preganglionic neurones (SPN) which target both the stellate ganglion (which sends sympathetic postganglionic neurones to the heart; Xie *et al*, 2011) and the adrenal medulla (which secretes adrenaline in response to sympathetic activation; Ranson *et al.*, 1998; Motawei *et al.*, 1999). Immunohistochemical and electrophysiological studies in rats have identified that these descending projections utilise either oxytocin or vasopressin as their predominant neurotransmitter (Cechetto & Saper, 1988; Yang *et al.*, 2009).

Of the cardiovascular command centres, the rostral ventrolateral medulla (RVLM) is the most important site in setting vascular tone, and therefore an important site in determining blood pressure (Guyenet, 2006; Kumagai *et al.*, 2012). The PVN is known to send a dense efferent projection to the RVLM, which closely targets spinally projecting neurones emanating from this nucleus (Pyner & Coote, 1999; Hardy, 2001). Furthermore, the PVN has also been shown to send a branching connection, which targets neurones in both the IML and the RVLM (Shafton *et al.*, 1998; Pyner & Coote, 2000). The distribution of these PVN-RVLM projecting neurones is similar to that observed for PVN-IML descending projections, with PVN-RVLM neurones being present in all

parvocellular subnuclei (Pyner & Coote, 2000), with a more dense distribution in the caudal PVN (Figure 2; Pyner & Coote, 2000; Oldfield *et al.*, 2001).

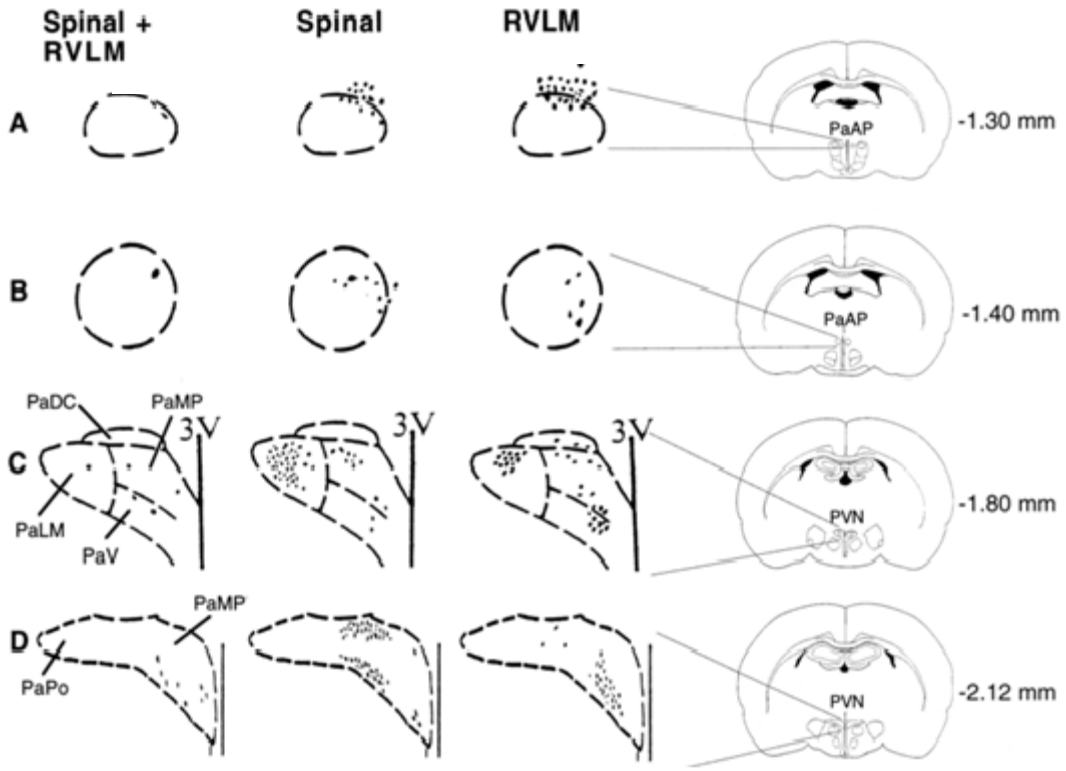

Figure 2 Schematic representation of the location of neurones projecting to the IML and RVLM, IML alone or RVLM alone throughout the rostrocaudal extent of the PVN. Neurones projecting to both the IML and RVLM were mainly confined to the mid-caudal levels (C-D). 3V = 3rd ventricle, Subnuclei abbreviations are as in Figure 1. PaLM = Lateral Magnocellular. Coordinates refer to Bregma level (Pyner & Coote, 2000)

II. Peripheral Monitoring of Arterial Blood Pressure

Central control of cardiovascular homeostasis begins with a constant monitoring of the peripheral environment, achieved through the activation or inhibition of baroreceptors. Baroreceptors are specialised nerve endings that respond to stretch (Kougias *et al.*, 2010). Those which are concerned with blood pressure regulation are located in the carotid sinus and the aortic arch (Kougias *et al.*, 2010). Their role is to create a negative feedback loop, through which mean arterial blood pressure (MAP) is tightly regulated around a "set point". These cardiovascular baroreceptors are activated by a rise in arterial blood pressure, or fall silent if blood pressure falls. This information is transmitted via cranial nerves IX (glossopharyngeal) and X (vagus) to the nucleus tractus solitarii (NTS); located within the medulla (Andresen & Kunze, 1994; Kougias *et al.*, 2010; Kumagai *et al.*, 2012). Baroreceptors are key components which help to maintain mean arterial blood pressure by monitoring of peripheral blood pressure that results in reflex changes in sympathetic activity to specific organs, chiefly the heart and kidneys (Guyenet, 2006).

The most common method of assessing baroreflex function is to construct baroreflex curves, marrying alterations in blood pressure with reflex alterations in either heart rate or sympathetic nerve activity (Figure 3).

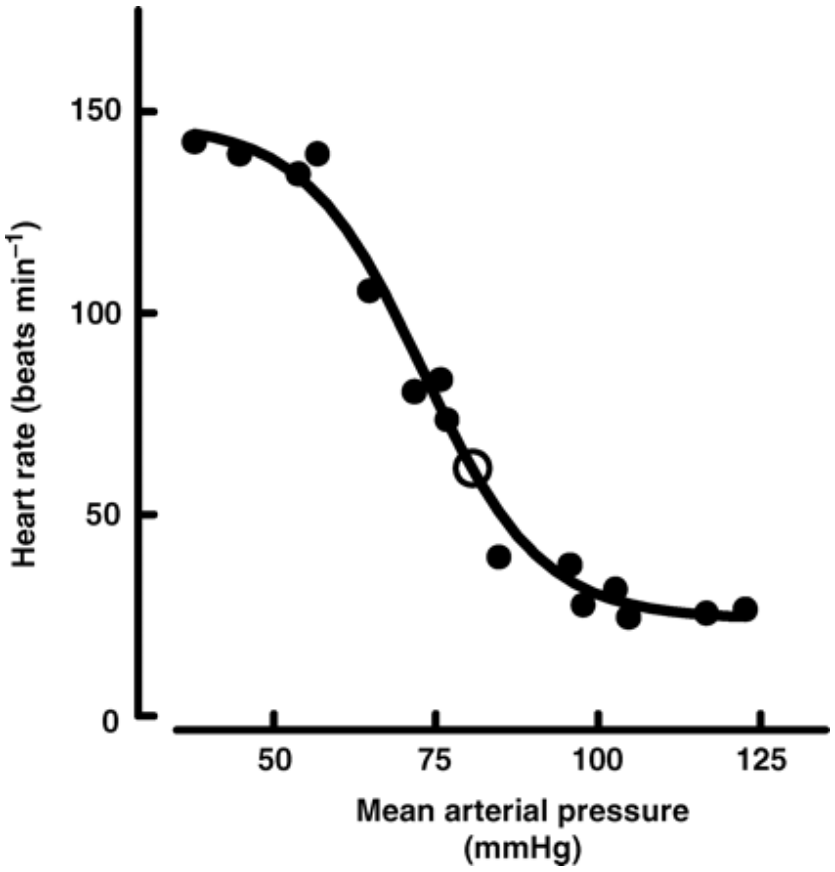

Figure 3 Typical heart rate baroreflex curve from un-anaesthetised female sheep. Decreases in blood pressure; evoked by i.v. infusion of nitroprusside elicit a reflex tachycardia, whereas increases in blood pressure; evoked by i.v. infusion of phenylephrine, elicit reflex bradycardia. Open circle represents the "set point" of blood pressure (Thomas & Woods, 2004)

Increases in blood pressure, experimentally elicited by intravenous (i.v.) infusion of the potent vasoconstrictor phenylephrine in rats (Crandall & Heesch, 1990; Page *et al.*, 2011), cats (Schmidt & DiMicco, 1984), sheep (Thomas & Woods, 2004) and rabbits (Quesnell & Brooks, 1997), results in a reflex bradycardia and a renal sympathoinhibition. Conversely, decreases in blood pressure; elicited by i.v. infusion of nitroprusside, results in a reflex tachycardia and renal sympathoexcitation (Quesnell & Brooks, 1997; Page *et al.*, 2011). The result of which is restoration of blood pressure towards the central "set point".

These baroreceptor inputs enter the brain via the NTS (Andresen & Kunze, 1994; Kougias *et al.*, 2010). The NTS is a key site for integration of visceral inputs and receives information from gustatory, gastrointestinal and respiratory, as well as cardiovascular afferents (Andresen & Kunze, 1994). Microinjection of glutamate into the NTS of awake rats produces dose-dependent pressor and bradycardic responses. Furthermore, the reflex bradycardia induced by i.v. phenylephrine was blocked by prior application of the *N*-methyl-D-aspartate (NMDA) receptor antagonist kynurenic acid, suggesting that the NTS is a vital nucleus in mediating the baroreflex, and that glutamatergic inputs play a major role in mediating this mechanism (Colombari *et al.*, 1994).

Neuroanatomical tracing studies in rats have demonstrated that cardiovascular areas of the NTS have reciprocal connections with the PVN (Kannan *et al.*, 1984; Bailey *et al.*, 2006; Affleck *et al.*, 2012). Furthermore, PVN-RVLM and PVN-spinal cord projecting neurones have been shown to be barosensitive. *In vivo* measurements of the electrical activity of PVN-RVLM and PVN-IML projecting neurones showed that acute increases in blood pressure reduces their firing activity, whereas acute decreases in blood pressure increases their firing activity (Lovick & Coote, 1988a; Chen & Toney, 2010). Recent evidence has shown that NTS-PVN projecting neurones make close apposition to both γ-aminobutyric acid (GABA)-ergic and nitrergic interneurones surrounding the PVN (Figure 4**;** Affleck *et al.*, 2012). It is therefore possible to speculate that baroreceptor activation leads to activation of NTS-PVN projecting neurones which may in turn activate inhibitory networks within the PVN.

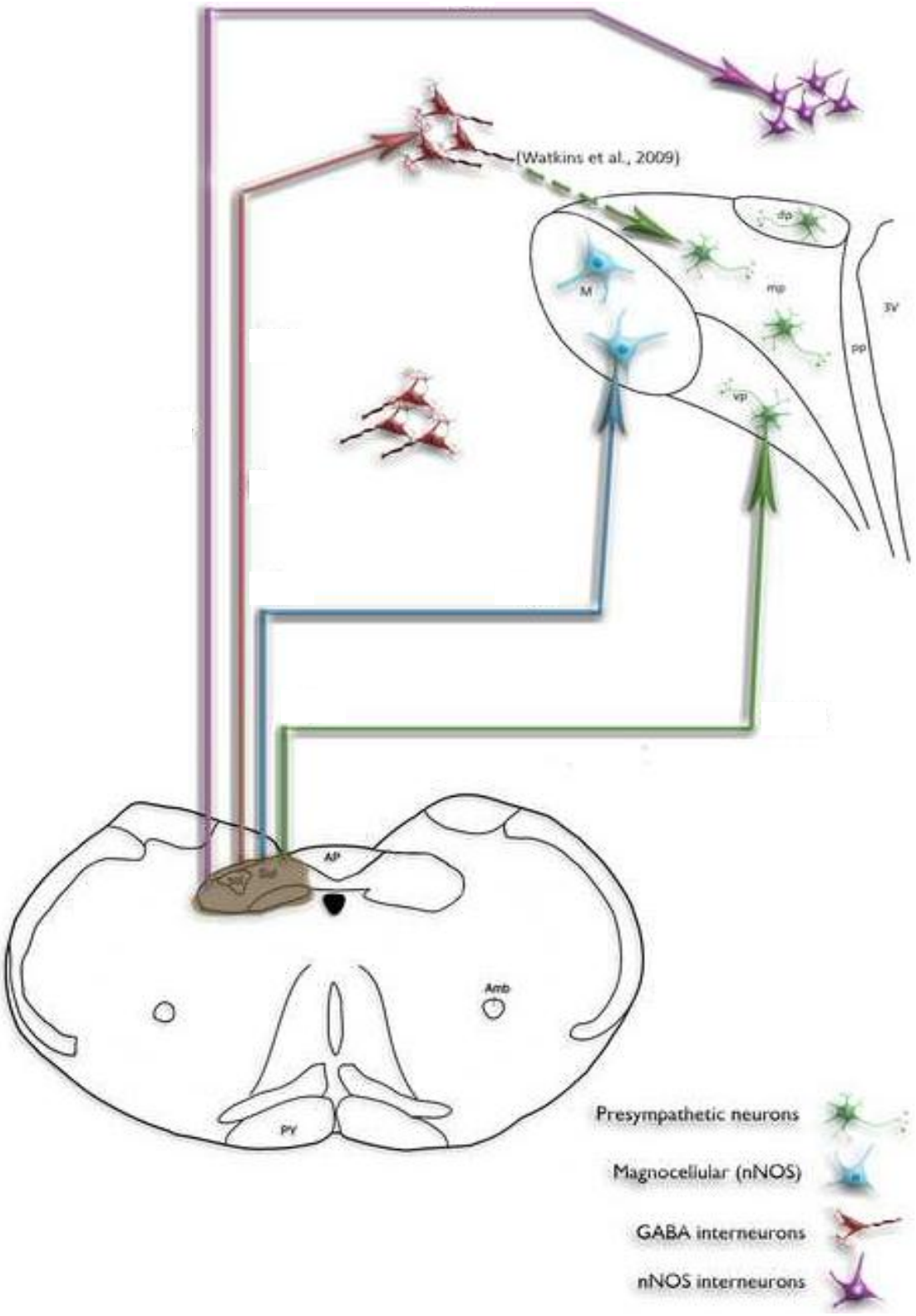

Figure 4 Schematic representation of ascending projections from the NTS to the PVN. Projections directly target spinally projecting presympathetic neurones as well as GABAergic interneurones located around the dorsal and lateral boundaries of the PVN and both intra- and extra-PVN nitrergic neurones (Affleck *et al.*, 2012).

III. Role of the PVN in Cardiovascular Homeostasis

As previously described, the PVN sends a dense descending projection from parvocellular subnuclei to the IML region of the spinal cord (Hosoya, 1980; Swanson *et al.*, 1980; Ranson *et al.*, 1998; Motawei *et al.*, 1999; Pyner & Coote, 2000). In a series of experiments examining the electrophysiological properties of PVN-IML projecting neurones in rats, it was observed that 97% of neurones in this population are quiescent under basal conditions (Lovick & Coote, 1988a). Application of glutamate directly onto these neurones only increased the firing activity of 41% of neurones, however following unilateral vagotomy; which prevents the integration of afferent baroreceptor activity, firing activity was increased to 69%, suggesting that at least a proportion of these neurones are under tonic baroreceptor-mediated inhibition (Lovick & Coote, 1988a). Furthermore, the firing rate of neurones, which did respond to glutamate application was significantly attenuated following either a hypertensive or hypervolaemic challenge, or augmented following a hypotensive challenge (Lovick & Coote, 1988b, a). The hypervolaemic challenge used in this study did not significantly alter blood pressure, suggesting that these neurones are capable of responding to fluctuations in blood volume independent of blood pressure changes. This was further evidenced in a series of experiments in which a non-hypotensive haemorrhage in rats (withdrawal of 2ml blood) resulted in a significant increase in expression of c-fos, a marker of neuronal activation, in 12% of PVN-IML projecting neurones, suggesting that these neurones are directly activated following hypovolaemic challenges (Badoer *et al.*, 1993).

In rats, hypervolaemic challenges are known to result in an inhibition of renal vascular resistance (Lovick *et al.*, 1993) and renal sympathetic nerve activity (Haselton *et al.*, 1994), mediated through activation of atrial volume receptors (Karim *et al.*, 1972). Studies have shown that the PVN is the critical central site in mediating this response. Volume loading in rats resulted in a significant increase in the number of c-fos positive neurones in the PVN (Pyner *et al.*, 2002). Furthermore, the renal vasodilatory response to an increase in blood volume equivalent to 1% of total body weight was abolished following specific lesioning of parvocellular neurones of the PVN in the rat (Lovick *et al.*, 1993). To specifically identify whether atrial volume receptors were involved in initiating this response, inflation of a balloon at the junction of the superior vena cava and right atria in the rat resulted in a significant increase in c-fos positive neurones, predominantly located in the medial to posterior regions of the PVN (Pyner *et al.*, 2002).

Taken together, these results suggest a significant role for the PVN in mediating the renal response to hypervolaemia. However, although both spinally projecting and RVLM-projecting PVN neurones are barosensitive (Lovick & Coote, 1988a; Chen & Toney, 2010), the role of the PVN as an integral component in the setting of basal vascular tone appears to be minimal.

The main evidence for this observation comes from studies in which PVN input to sympathetic vasomotor nerves has been removed in rats, either by complete transection of the brain caudal to the hypothalamus (Yamori & Okamoto, 1969), electrolytic lesion (Herzig *et al.*, 1991) or radiofrequency ablation of the PVN (Ernsberger *et al.*, 1985). In all the studies, removal of the PVN failed to significantly alter blood pressure, suggesting the influence of the

PVN on blood pressure is minimal. However, this does not conclusively prove that the PVN plays a minor role in controlling blood pressure under normal circumstances, since ablation of the RVLM; the major brain site for vasomotor control, also fails to significantly alter blood pressure (Cochrane & Nathan, 1989, 1993). This suggests that other brain areas may be able to compensate for the loss of these brain regions.

IV. Neurochemistry of the PVN

Modulation of sympathetic outflow from the PVN involves the complex interaction between inhibitory and excitatory neurotransmitters. In the rat PVN, over 30 neuroactive substances have been identified, including serotonin, dopamine, angiotensin, oestrogen, glucagon-like peptide 1, vasopressin, oxytocin and neuropeptide Y (Pyner, 2009). Although detailed studies' examining the distribution of these neuroactive substances is limited, it is clear from those that have been studied that their expression throughout the PVN is differential. For example, angiotensin type 1a (AT_{1A}) receptors are distributed predominately in the medial and dorsal cap regions (Lenkei *et al.*, 1995) whereas oestrogen receptors (ER-β) were localised to the ventral and posterior parvocellular subnuclei (Bingham *et al.*, 2006). Given that different subnuclei of the PVN have different efferent projections (Swanson *et al.*, 1980; Oldfield *et al.*, 2001), these distinct patterns of distribution mean that neuroactive substances can modulate the activity of specific populations of neurones in the PVN, thus producing distinct physiological responses.

Some of these neuroactive substances appear to be more important than others in regulating the sympathetic outflow from the PVN in the rat. Descending projections from the PVN to the spinal cord are known to be predominantly oxytocinergic or vasopressinergic (Sofroniew, 1980; Yang *et al.*, 2009). Within the PVN, γ-aminobutyric acid (GABA) is the most common inhibitory neurotransmitter (Decavel & Van den Pol, 1990), with glutamate being a predominant excitatory neurotransmitter (Li *et al.*, 2006; Busnardo *et al.*, 2009).

Importantly, modulation of these two neurotransmitter systems also occurs within the PVN. Nitric oxide (NO), acting as a diffuse gaseous molecule (Stern, 2004), has been shown to stimulate the release of GABA in the PVN *in vivo* (Horn *et al.*, 1994). Microinjection of the NO donor sodium nitroprusside (SNP) or the nitric oxide synthase inhibitor L-NAME produced a significant decrease and increase in renal sympathetic nerve activity (RSNA) respectively (Zhang & Patel, 1998; Yang & Coote, 2003). Furthermore, *in vivo* studies in rats have shown that NO in the PVN is released following *N*-methyl-D-aspartate (NMDA) receptor activation, acting in a negative feedback manner to reduce NMDA receptor activation (Li *et al.*, 2001).

The remainder of this chapter will focus on the role of GABA and glutamate in the PVN and its role in modulating the sympathetic outflow in normal cardiovascular homeostasis, as well as their contribution to the exacerbated sympathetic outflow observed in hypertension and late-term pregnancy.

V. GABA and $GABA_A$ Receptors

Synthesised from the enzymatic decarboxylation of glutamate by glutamic acid decarboxylase (GAD; Petroff, 2002), GABA is the most abundant inhibitory neurotransmitter in the hypothalamus and the central nervous system (CNS), composing around 50% of all cortical and hypothalamic synapses (Decavel & Van den Pol, 1990; Macdonald & Olsen, 1994).

GABA is released from presynaptic terminals of GAD-positive neurones at high concentrations (0.3 – 1.0mM. Mody & Pearce, 2004). Once released, the half-life of GABA within the synapse is <1ms (Mody & Pearce, 2004). Recycling of GABA predominantly takes place by GABA transporters (GAT), of which four have so far been identified (Schousboe *et al.*, 2004). GABA transporters are expressed by astrocytes, and upon uptake GABA is shunted to the Krebs cycle, whereupon it is metabolised into glutamine, which is then taken up by GABAergic neurones (Brambilla *et al.*, 2003).

Once GABA has diffused across the synapse it acts at postsynaptic $GABA_A$, $GABA_B$ or $GABA_C$ receptors. Of these, the $GABA_A$ receptor is the most abundantly expressed (Chebib & Johnston, 1999).

The $GABA_B$ receptor is a G-protein coupled receptor (GPCR) which acts at both pre- and postsynaptic sites (Bettler & Tiao, 2006). $GABA_B$ receptors assemble as heteromers composed of the $GABA_{B1}$ and $GABA_{B2}$ subunits, with molecular diversity arising from the existence of $GABA_{B1a}$ and $GABA_{B1b}$ subunits (Bettler & Tiao, 2006).

Conversely, the $GABA_C$ receptor, like the $GABA_A$ receptor detailed below, is an ionotropic chloride channel (Enz & Cutting, 1998). It is distinct from the $GABA_A$

receptor in that it is insensitive to $GABA_A$ receptor modulators such as benzodiazepines and barbiturates, is composed uniquely of ρ subunits, and is expressed exclusively in the retina (Enz & Cutting, 1998).

The $GABA_A$ receptor is a member of a superfamily of Cys-loop transmitter-gated ion channels, which includes the nicotinic acetylcholine receptor and the $5HT_3$ receptor (Macdonald & Olsen, 1994; Johnston, 1996; Chebib & Johnston, 1999; Arancibia-Carcamo & Kittler, 2009). As well as GABA, $GABA_A$ receptors contain binding sites for many allosteric modulators, including ethanol, barbiturates and anaesthetics (Macdonald & Olsen, 1994). Upon activation, the $GABA_A$ receptor opens a chloride channel, leading to rapid hyperpolarisation of the membrane and thereby preventing action potential generation (Arancibia-Carcamo & Kittler, 2009).

Like all members of the Cys-loop gated ion channels, the $GABA_A$ receptor is composed of five subunits, acquired from a genetic repertoire of 19 so far discovered (α1-6, β1-3, γ1-3, δ, ε, π, θ and ρ1-3; Mehta & Ticku, 1999; Sieghart *et al.*, 1999). Each subunit consists of a large extracellular N-terminus domain and four transmembrane loops (TM1-4) with a large intracellular domain between TM3 and TM4 (Figure 5). It is widely believed that the TM2 domains, of each subunit join in such a way as to form the inner lining of the pore, whereas the function of the TM1, TM3 and TM4 domains is to interface with lipids. The intracellular loop between TM3 and TM4 provides the main site for protein-protein interactions as well as acting as the main site for protein modification through phosphorylation, palmitoylation or ubiquitination (Chebib & Johnston, 1999; Sieghart *et al.*, 1999; Arancibia-Carcamo & Kittler, 2009; Zheleznova *et al.*, 2009).

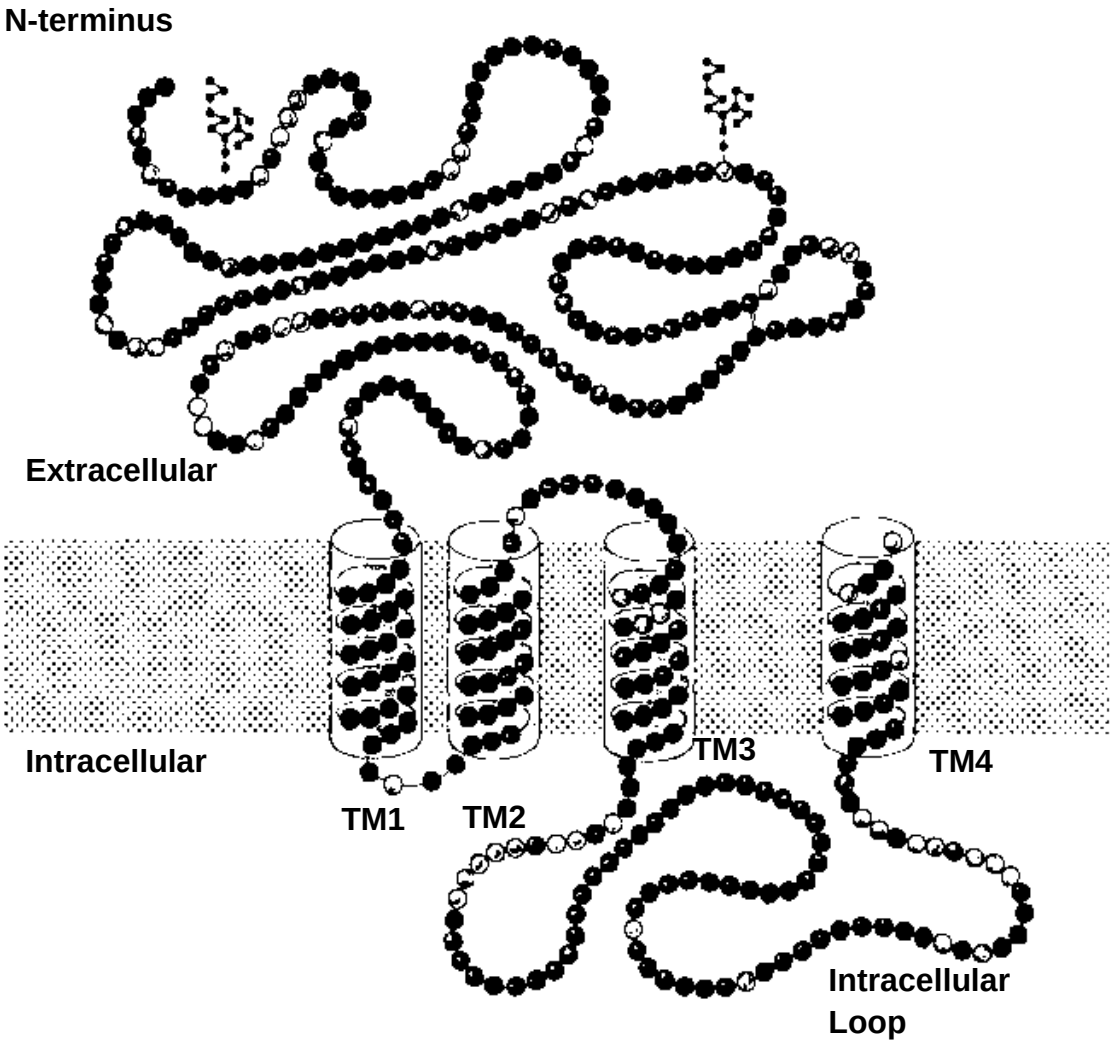

Figure 5 Schematic representation of a $GABA_A$ receptor subunit, showing the large extracellular N-terminus, four transmembrane domains and large intracellular loop between TM3 and TM4. Abbreviations – TM = Transmembrane (Macdonald & Olsen, 1994)

Although there are theoretically thousands of receptor subunit combinations, expression studies have shown that α, β and γ subunits have to combine to produce $GABA_A$ receptors which pharmacologically resemble native receptors. In addition, the δ, ε and π subunits appear to be able to replace the γ subunit, producing receptors with distinct physiological and kinetic properties (Sieghart *et al.*, 1999). The preferred combination of subunits within native $GABA_A$ receptors is two α, two β and one γ subunit (Mehta & Ticku, 1999).

Individual $GABA_A$ receptor subunits have distinct anatomical distributions throughout the brain (Pirker *et al.*, 2000). Furthermore, both individual subunits and receptor subunit conformations confer distinct physiological and pharmacological properties, as well as determining the subcellular localisation of $GABA_A$ receptors (Macdonald & Twyman, 1991; Sun *et al.*, 2004).

Activation of $GABA_A$ receptors requires the binding of two GABA molecules to the receptor, and binding of GABA is slow relative to its diffusion and clearance rates (Farrant & Nusser, 2005). Because of this, not all synaptic $GABA_A$ receptors are opened in response to a single action potential. This allows for a greater depth of modulation at inhibitory post-synaptic sites, with the strength of transmission being determined by the number of post-synaptic receptors and quantity of GABA released from fusing vesicles.

Synaptically-mediated inhibition, characterised by fast decay properties of the GABA current, is known as “phasic inhibition”. This typically requires the release of high levels of GABA, in the region of 3-5mM and is degraded within 500μs (Farrant & Nusser, 2005; Cherubini, 2012). In physiological terms for the PVN, phasic inhibition is most likely to occur following physiological stimuli, such as that from baroreceptors signalling an increase in blood pressure. Such input is likely to activate NTS-PVN projecting neurones which have been shown to closely appose GABAergic interneurones in the PVN (Watkins *et al.*, 2009; Affleck *et al.*, 2012), leading to a release of presynaptic GABA.

As well as phasic inhibition, a significant proportion of neuronal inhibition arises from extrasynaptic $GABA_A$ receptors located outside of the synaptic cleft, mediating so called “tonic inhibition”. In mouse hippocampal neurones studied

in vitro, tonic inhibition has been found to be responsible for generating 75% of the total inhibitory charge (Mody & Pearce, 2004; Glykys *et al.*, 2008). Effectively, the role of tonic inhibition is to lower the size and duration of the excitatory post-synaptic current (EPSC), such that the probability of an action potential is reduced (Farrant & Nusser, 2005). $GABA_A$ receptors mediating tonic inhibition are typically able to respond to much lower concentrations of GABA than their synaptic counterparts. The concentration of GABA outside of the synaptic cleft is estimated to be within the tens of nanomolar, and is determined by the activity of GABAergic synapses, as well as the activity of sodium and chloride transporters (Farrant & Nusser, 2005).

Both phasic and tonic inhibition are mediated by receptors with physiologically and pharmacologically distinct properties. Receptors mediating tonic inhibition are primarily composed of α5 or δ subunits that preferentially target the receptor to the extrasynaptic membrane. Conversely, receptors located within the synapse and thus mediating phasic inhibition are primarily composed of the γ2 subunit typically in combination with the α1 and β2 subunits (Benke *et al.*, 1991; Farrant & Nusser, 2005; Glykys *et al.*, 2008). However, electron microscopic analysis of the subcellular location of $GABA_A$ receptors is yet to find subunits that are exclusively located in either position (Farrant & Nusser, 2005).

Indeed, $GABA_A$ receptors containing the α5 subunit have been identified within the synapse (Serwanski *et al.*, 2006). To this effect however, *in vitro* electrophysiological studies in the hippocampus of mice genetically bred without the α5 subunit of the $GABA_A$ receptor (gabra5$^{-/-}$ mice) showed no reduction in

the response to phasic release of GABA (Glykys & Mody, 2006). This suggests that although the α5 subunit may be present in synapses, it may be present in the synapse in conjunction with other subunits that confer physiologically distinct properties or that they are located in quiescent or silent synapses.

Studies investigating the role of the α5 subunit in mediating tonic inhibition have found that application of the α5-specific inverse agonist L-655,708 onto hippocampal slices significantly increases the spontaneous activity of neurones within the CA3 region (Figure 6**.;** Glykys *et al.*, 2008). Furthermore, α5 knock-out mice have significantly higher levels of basal neuronal activity with no alteration in phasic inhibition (Glykys & Mody, 2006).

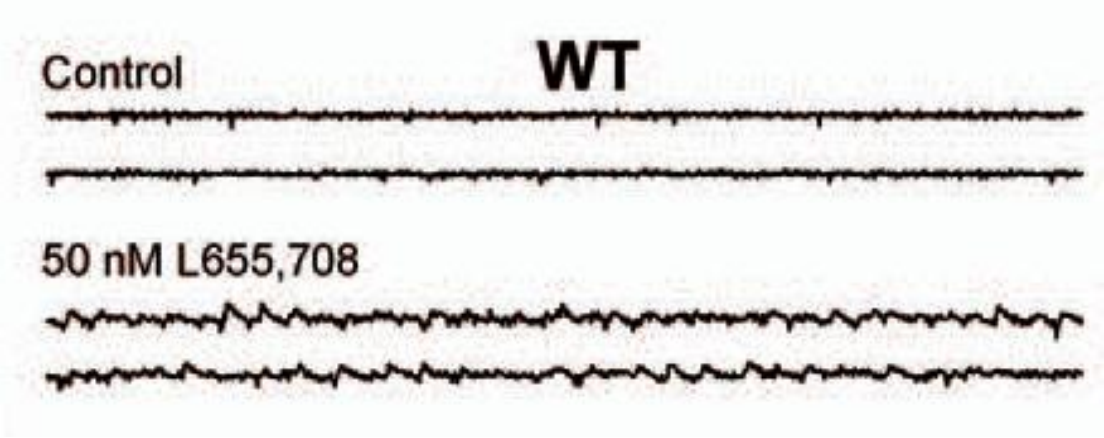

Figure 6 Neurones in the CA3 region of hippocampal slices in wild type (WT) mice show little spontaneous activity *in vitro*. Application of the α5-specific inverse agonist L655,708 significantly increases spontaneous gamma wave formation (Glykys *et al.*, 2008).

Within the hypothalamus, *in vitro* electrophysiological studies in rats have found that in the supraoptic nucleus (SON), the α5 subunit contributes to tonic inhibition to a much greater extent that the δ subunit (Jo *et al.*, 2011).

Furthermore, the α5 subunit has a 400 times greater level of expression than the δ subunit (Figure 7; Jo *et al.*, 2011). Although the SON and PVN are two anatomically distinct nuclei, their similar neurochemistry and cellular makeup (Swanson & Sawchenko, 1983) suggest that the control of tonic inhibition could be controlled in a similar manner.

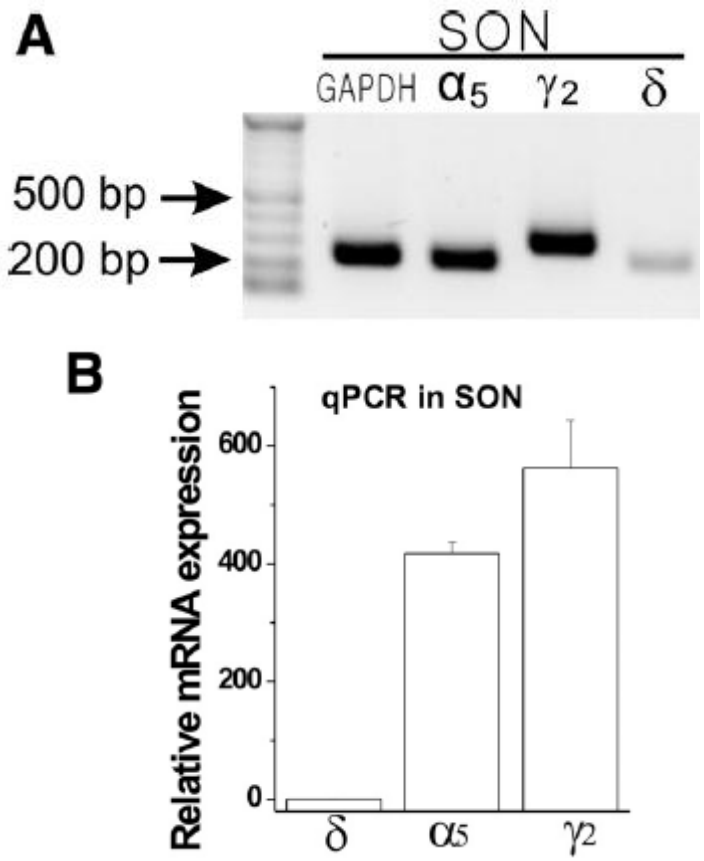

Figure 7 RT-PCR analysis of α5, γ2 and δ subunit mRNA expression in the SON of SD rats. Minimal expression of the δ subunit was observed (A). Expression of α5 mRNA was 400% higher than δ subunit (B; Jo *et al.*, 2011)

Within the PVN, 9 of the 19 $GABA_A$ receptor subunits have been identified using immunohistochemical staining (α1, α2, α5, β1, β2, β3, γ2, γ3 and δ; Pirker *et al.*, 2000). The contribution each of these subunits makes in mediating GABAergic inhibition within the PVN has yet to be elucidated.

Regardless of this, the studies detailed below provide compelling evidence that GABAergic inhibition is important for the PVN to control cardiovascular homeostasis, as well as contributing to the increased neuronal excitability observed in both hypertension and pregnancy.

VI. Role of GABA in the PVN for the Normal Control of Cardiovascular Homeostasis

GABA is the most abundant inhibitory neurotransmitter in the CNS (Chebib & Johnston, 1999; Pirker *et al.*, 2000) and acts as the primary inhibitory neurotransmitter in the hypothalamus, making up over half of all synaptic inputs in this area (Decavel & Van den Pol, 1990).

Anatomically, neurones which are immunoreactive (IR) for GABA, revealed by immunofluorescent staining of GABA or the GABA synthesising enzyme, GAD67 (Monnerie & Le Roux, 2007), are found to surround the dorsal and ventral boundaries of the rat PVN as well as surrounding the lateral boundaries of the dorsal cap (Watkins *et al.*, 2009). Transynaptic tracing of descending PVN projections to the adrenal medulla (AM), using Herpes-Simplex virus conjugated to green fluorescent protein (HSV-GFP) revealed that GABA-IR neurones make direct synaptic contact with PVN-IML-AM neurones, suggesting these neurones are under direct GABAergic inhibitory control (Watkins *et al.*, 2009). In addition, the relatively sparse number of HSV-GFP that co-localised with GABA, in comparison to the large number of GABA-IR neurones that were shown to surround the PVN, suggest that other descending PVN projections, such as those to the RVLM or NTS, as well as interneurones, may be under either direct or indirect GABAergic inhibition. To this effect, there is evidence of GABAergic inhibition of glutamatergic interneurones within the PVN (Li *et al.*, 2006). Furthermore, it was revealed through immunofluorescent identification of PVN-IML projecting neurones that this population does not co-localise with GABA, suggesting that these neurones are unable to influence their own activity in an autocrine manner (Watkins *et al.*, 2009).

It has long been known that manipulation of GABAergic inputs within the PVN produces profound effects on the cardiovascular system, influencing sympathetic outflow, arterial blood pressure (ABP) and heart rate (HR), amongst others (Akine *et al.*, 2003; Li *et al.*, 2006; Li & Pan, 2007b). Numerous studies utilising *in vivo* preparations have identified that inhibition of autonomic outflow from the PVN is governed by both $GABA_A$ and $GABA_B$ receptors (Li & Pan, 2007b).

Bilateral microinjections of the $GABA_A$ receptor agonist muscimol into the PVN significantly reduced ABP, HR and RSNA in male Wistar Kyoto (WKY) rats (Figure 8 A; Allen, 2002; Akine *et al.*, 2003). Conversely, disinhibition of the PVN by bilateral microinjection of the $GABA_A$ receptor antagonists bicuculline or gabazine resulted in a significant increase in ABP, HR, plasma adrenaline and noradrenaline as well as lumbar sympathetic nerve activity (LSNA) in Sprague-Dawley (SD) and WKY rats (Figure 8 B; Martin *et al.*, 1991; Li & Pan, 2007b, a)

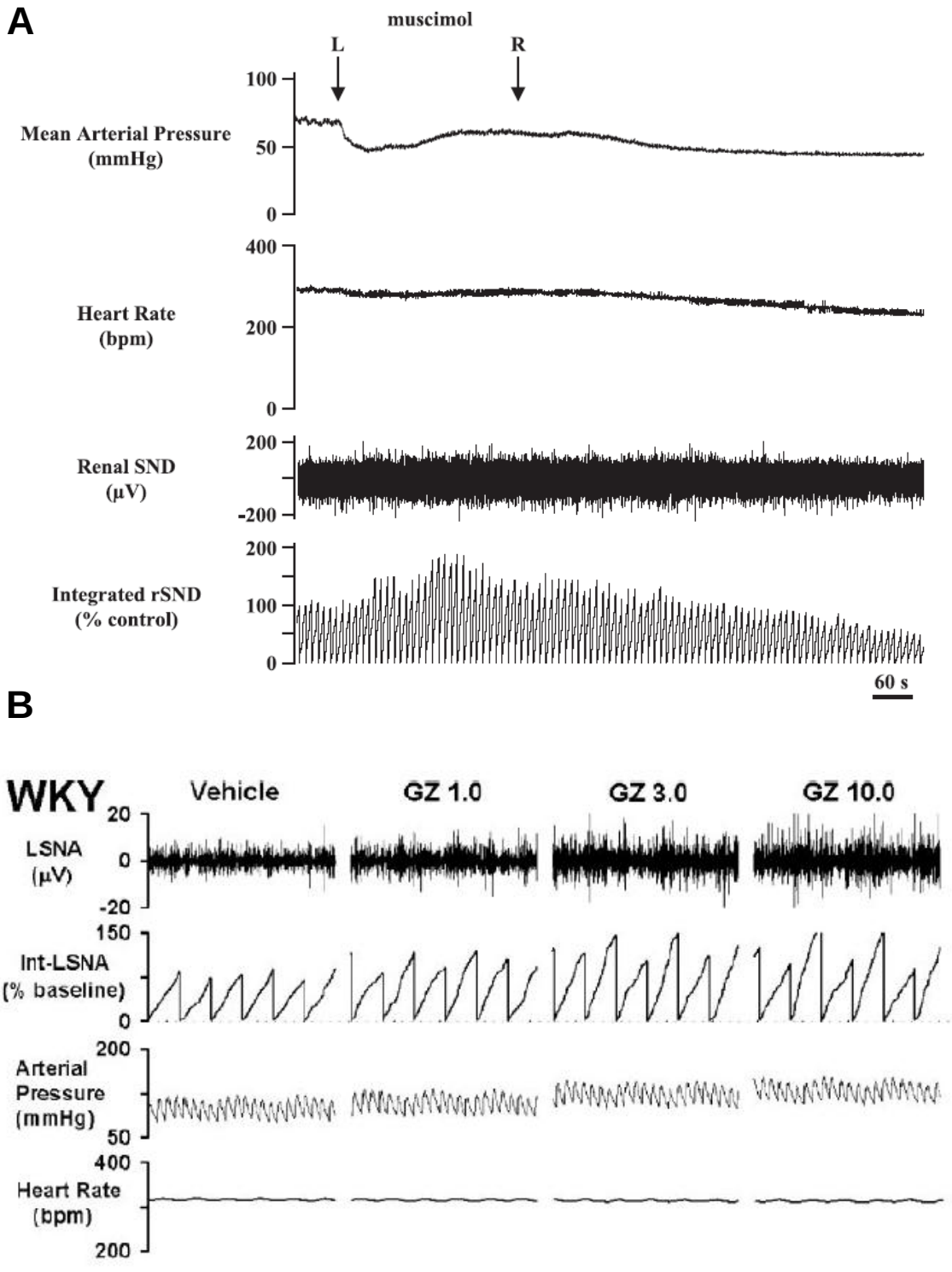

Figure 8 A – Raw trace examples showing decreases in ABP, HR and RSNA following bilateral microinjection of 1nmol muscimol into the PVN L & R refer to the time of each unilateral injection. (Akine et al, 2003). B – Raw trace examples showing increases in LSNA, ABP and HR following bilateral microinjections of increasing concentrations of the $GABA_A$ receptor antagonist gabazine into the PVN compared with vehicle control. GZ = gabazine concentration (nmol/50nl). (Li & Pan, 2007a)

Coupled with this finding is the observation that unilateral bicuculline microinjection into the PVN of virgin female rats increases baroreflex gain and shifts the baroreflex curve upwards and to the right, such that alterations in blood pressure are met with higher levels of LSNA and HR (Figure 9; Page *et al.*, 2011).

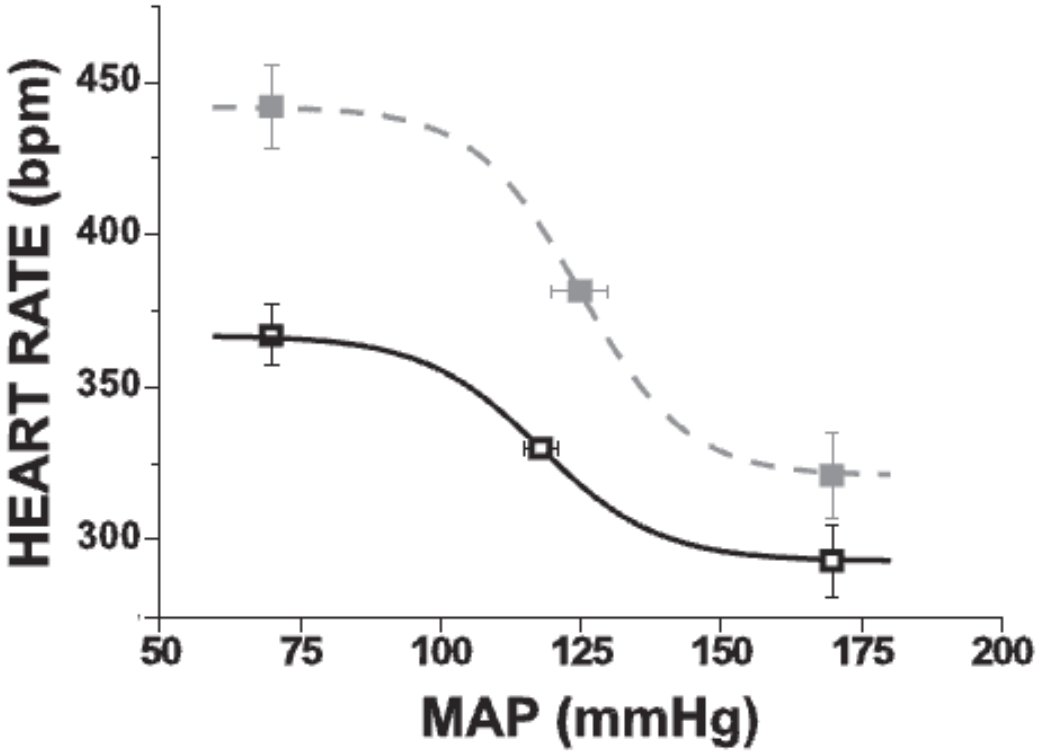

Figure 9 Baroreflex curve from virgin female rats. Dashed line shows baroreflex response following unilateral bicuculline microinjection into the PVN compared to control (solid line). Bicuculline microinjection increased baroreflex gain and shifted the curve upwards and to the right (Page *et al.*, 2011)

Using *in vitro* rat hypothalamic slice preparations, in which PVN-RVLM projecting neurons had been retrogradely labelled with rhodamine-labelled microspheres; application of bicuculline significantly increased the number of glutamate-mediated EPSCs (Li *et al.*, 2006). In a separate set of experiments in which the same population of PVN-RVLM neurones had been labelled, the

benzodiazepine diazepam was also shown to significantly increase the decay time and amplitude of evoked inhibitory post-synaptic currents (IPSCs) and inhibited the spontaneous activity of PVN neurones shown to be responsive to bicuculline (Zahner *et al.*, 2007).

Furthermore, *in vivo* application of baclofen, an agonist of the $GABA_B$ receptor, in the PVN resulted in a significant reduction in LSNA, ABP and HR in WKY and SD rats, however only at high doses (4.5nmol). Bilateral microinjection of the $GABA_B$ antagonist CGP52432 produced no significant effects on LSNA, ABP or HR at doses up to 3.0nmol in both WKY and SD rats (Li & Pan, 2007b). In an *in vitro* hypothalamic slice preparation, application of baclofen significantly inhibited the spontaneous firing potential of PVN-spinally projecting neurones and decreased their membrane potential (-59.6 ± 1.5 to -64.3 ± 2.5mV. $P<0.05$; Li *et al.*, 2008b).

These studies suggest that inhibition of sympathetic outflow from the PVN is mediated predominantly through the $GABA_A$ receptor, and that the $GABA_B$ receptor has a minimal inhibitory role under normal physiological conditions. In addition, efferent outputs from the PVN are also under tonic inhibitory control mediated through both $GABA_A$ and $GABA_B$ receptors.

Studies have been undertaken examining the method through which disinhibition of the GABAergic system within the PVN results in a sympathoexcitatory response. Chen *et al* (2003) observed that, in agreement with previous experiments such as those mentioned above, unilateral microinjection of the $GABA_A$ receptor antagonist bicuculline into the PVN of anaesthetised male SD rats, produced dose-dependent increases in ABP, HR

and sympathetic nerve activity. However, prior injection with either the non-selective excitatory amino acid antagonist kynurenic acid (Kyn), the NMDA receptor antagonist DL-2-amino-5-phosphonovaleric acid (AP-5) or the non-NMDA receptor antagonist 2,3-dioxo-6-nitro-1,2,3,4-tetrahydrobenzo[f]quinoxaline-7-sulfonamide disodium (NBQX), significantly attenuated the sympathoexcitatory, pressor and tachycardic effects of bicuculline injection into the PVN (Figure 10).

Li *et al* (2006) confirmed this by showing that prior injection of AP-5 significantly attenuated the effects of ipsilateral bicuculline injection, in a dose-dependent manner. Furthermore, this study showed that bicuculline injections into the PVN increased the release of glutamate.

These two studies show that the sympathoexcitatory, pressor and tachycardic responses to disinhibition of the PVN through $GABA_A$ receptor antagonism require activation of excitatory amino acid receptors, and that both NMDA and non-NMDA receptors are required for this effect.

These studies also noted that microinjection of either AP-5 (Chen *et al.*, 2003; Li *et al.*, 2006), Kyn or NBQX (Chen *et al.*, 2003) alone did not alter baseline parameters. Taken together, these results suggest that under normal physiological conditions, GABAergic inhibition dominates the neurochemical milieu of the PVN, maintaining control of sympathetic outflow and therefore control of cardiovascular homeostasis.

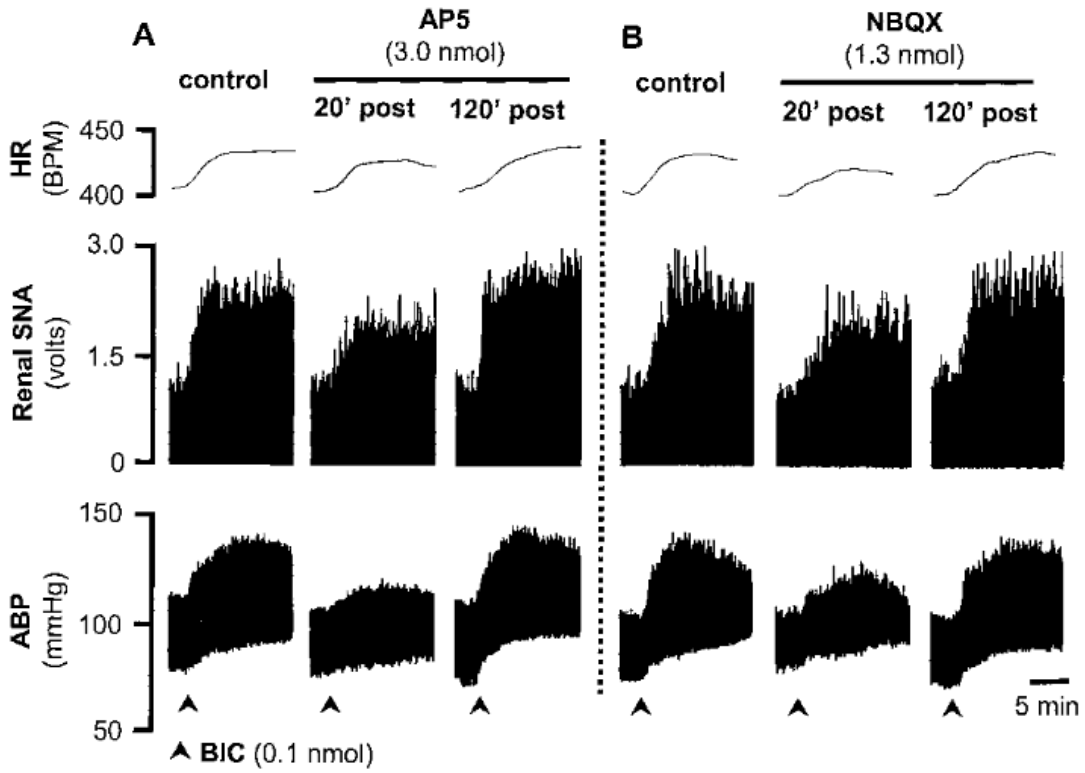

Figure 10 Increases in renal sympathetic nerve activity, blood pressure and HR following application of the $GABA_A$ receptor antagonist bicuculline (arrow heads) are significantly blunted following pre-treatment with either the NMDA receptor antagonist AP-5 (A) or the non-NMDA receptor antagonist NBQX (B; Chen *et al.*, 2003)

Studies have examined the mechanism by which GABA, acting via the $GABA_A$ receptor mediates inhibitory actions within the PVN (Park *et al.*, 2007). Two distinct functional classes of $GABA_A$ receptors exist within the CNS; those which mediate phasic transmission, and those which respond to low-levels of GABA and mediate tonic inhibition.

In slice preparations of retrograde labelled PVN-RVLM projecting neurones from rats, application of 4,5,6,7-tetrahydroisothiazolo-[5,4-c]pyridine-3-ol (THIP), a $GABA_A$ receptor agonist which preferentially activates extrasynaptic $GABA_A$ receptors significantly increased the holding potential of these neurones above

that of spontaneously evoked inhibitory postsynaptic currents (sIPSCs; Park *et al*, 2007). Application of $GABA_A$ receptor antagonists such as bicuculline and pictrotoxin abolished any sIPSC (Park *et al.*, 2007). The authors of this study conclude that PVN-RVLM projecting neurones respond to both phasic and tonic GABAergic inhibition and that tonic inhibition is dependent on synaptic spillover of GABA (Park *et al.*, 2007).

Through these studies, GABAergic inhibition has been shown to play an important role in modulating sympathetic outflow from the PVN, as well as contributing to the maintenance of cardiovascular homeostasis. Under normal physiological conditions, this inhibition seems to be mediated primarily through the fast ionotropic $GABA_A$ receptors, and although activation of $GABA_B$ receptors has been shown to influence sympathetic outflow from the PVN (Li *et al.*, 2008b) they are unlikely to play a major role in contributing to the overall inhibitory milieu of this nucleus. Furthermore, GABAergic inhibition of PVN autonomic neurones has been shown to be dependent on both phasic (synaptic) and tonic (extrasynaptic) receptors (Park *et al.*, 2007).

VII. Glutamate Neurotransmission and Receptors

N-methyl-d-aspartate (NMDA) receptors are glutamate-gated ionotropic channels with a high permeability to calcium (Paoletti & Neyton, 2007). At resting membrane potential, the NMDA receptor pore contains a magnesium block, the removal of which is voltage dependent (Carvalho *et al.*, 2000). NMDA receptors therefore require prior depolarisation to activate. This is achieved through activation of neighbouring α-amino-3-hydro-5-methyl-4-isoxazole propionate (AMPA) receptors, which depolarise the membrane sufficiently to remove the magnesium block and thus allow for activation of NMDA receptors (Carvalho *et al.*, 2000).

N-methyl-d-aspartate (NMDA) receptors are one of three major ionotropic glutamate receptors found in the mammalian CNS (Dingledine *et al.*, 1999). NMDA receptors are heterotetrameric receptors, composed from a repertoire of three subtypes (GluN1, GluN2A-D, GluN3A-B), with alternative splicing of the GluN1 gene rendering eight splice variants termed GluN1-1a/b to GluN1-4a/b (Stephenson, 2001; Paoletti & Neyton, 2007). In native mammalian NMDA receptors, the GluN1 subunit is regarded as being an obligatory subunit, forming the binding site for the co-agonist glycine. These typically co-assemble with the glutamate-binding GluN2 subunits to form fully functioning receptors (Kohr, 2006). Most native NMDA receptors are composed of two GluN1 subunits with two of the same subtype of GluN2 subunits (i.e. GluN1/GluN2A), however there is evidence that more than one type of GluN2 subunit can coassemble in the same receptor (i.e. GluN1/2A/2B), producing unique biophysical properties (Chazot *et al.*, 1994).

All of the NMDA receptor subunits share common structural membrane topology. GluN1 and GluN2 subunits share around 20% amino acid sequence homology, whereas GluN2A and GluN2B subunits share around 70% subunit homology (Stephenson, 2001). Each subunit has a common membrane structure, comprising a large extracellular N-terminus, three transmembrane segments and a cytoplasmic C-terminus (Figure 11).

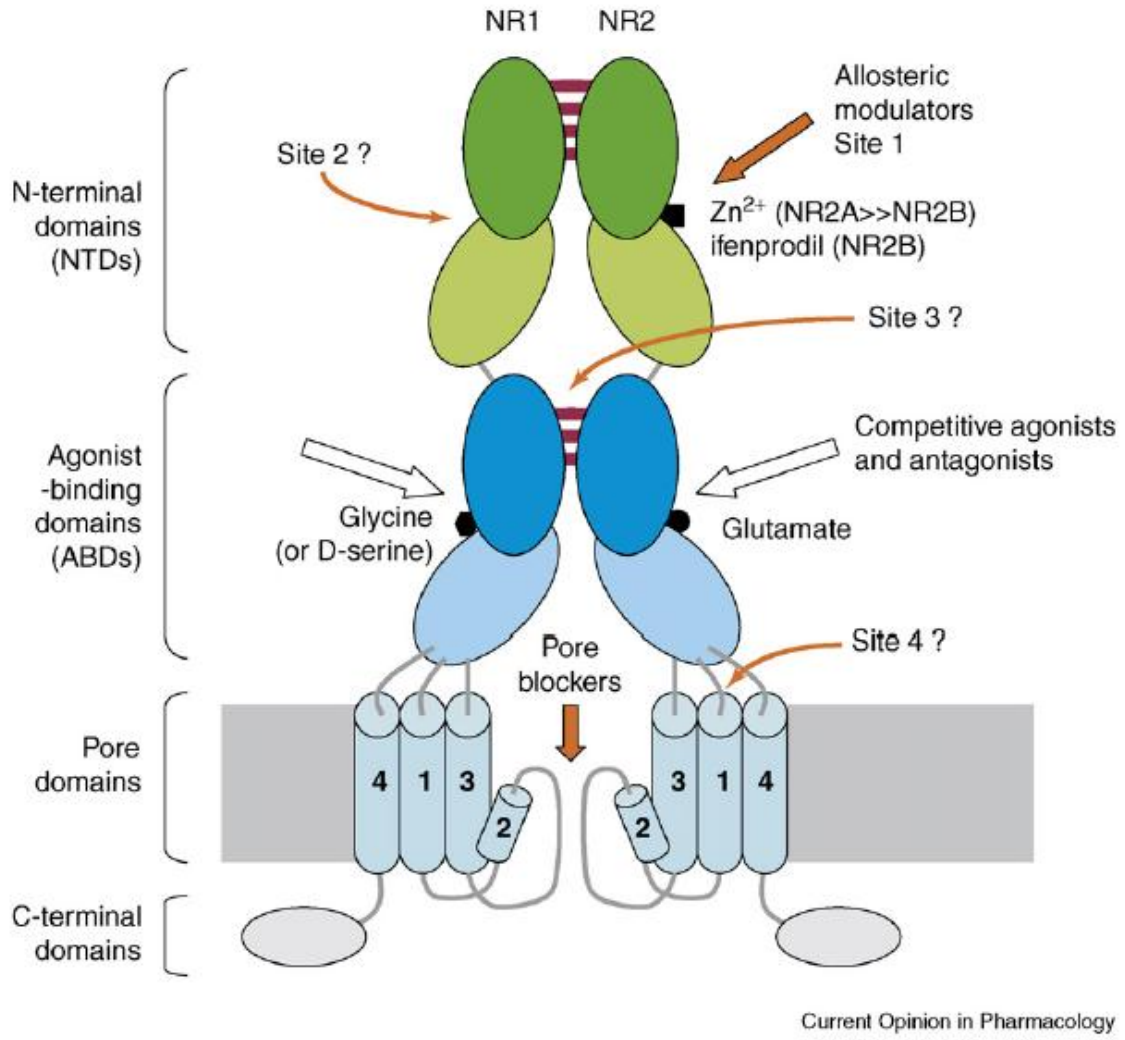

Figure 11 Schematic representation of a NMDA receptor showing potential sites for ligand binding. GluN1 subunits are required for binding of the co-agonist glycine, whereas GluN2 subunits bind glutamate (Paoletti & Neyton, 2007).

Of the four GluN2A subunits, the GluN2A and GluN2B subunits are the most ubiquitously expressed throughout the CNS. During early development GluN2B-containing receptors predominate, switching to GluN2A-containing receptors around birth (Monyer *et al.*, 1994). Both of these subunits confer distinct physiological properties on the NMDA receptor. For example, GluN2A receptors display greater currents and faster decay properties than GluN2B containing receptors (Figure 12).

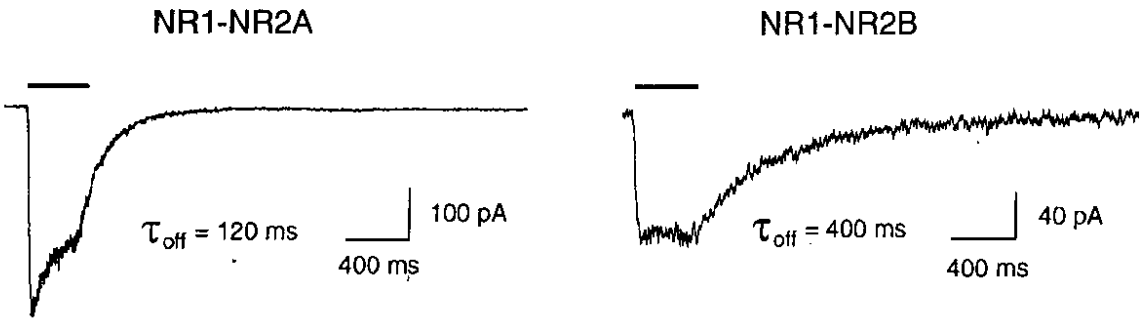

Figure 12 Decay kinetics of GluN2A and GluN2B containing NMDA receptors in transfected HEK cells subjected to 300ms of 100μM glutamate (Monyer *et al.*, 1994).

The density of NMDA receptors at the synapse is differentially regulated for the GluN2A and GluN2B subunits. GluN2B subunit incorporation into the synapse is constitutive and its mobility into the synapse increases when the synapse is quiescent (Gambrill *et al.*, 2011). Conversely, GluN2A incorporation into the synapse requires binding of glutamate to NMDA receptors. Therefore, GluN2A synaptic incorporation increases in response to increased synaptic activity (Barria & Malinow, 2002; Storey *et al.*, 2011). Given the developmental

profile of high GluN2B vs. low GluN2A expression in early embryos (Monyer *et al.*, 1994), the prevailing theory is that the activity-independent GluN2B-containing receptors first accumulate at synapses. Once the synapse becomes active, these GluN2B subunits are internalised and replaced with GluN2A subunits in an activity-dependent fashion (Barria & Malinow, 2002).

VIII. Role of Glutamate in the PVN in Normal Cardiovascular Homeostasis

Given the widespread distribution of ionotropic glutamate receptors within the PVN (Herman *et al.*, 2000), it is unsurprising the glutamate application exerts a potent effect on neuronal excitability and sympathetic outflow emanating from this nucleus (Yang *et al.*, 2001; Li *et al.*, 2006; Li *et al.*, 2008a).

Electron microscopy has shown that glutamatergic inputs synapse onto parvocellular neurones within the PVN (van den Pol, 1991). Further immunohistochemical studies have demonstrated that synaptic boutons immunopositive for the glutamate vesicular transporter VGLUT2 make close apposition to corticotrophin releasing hormone (CRH) positive neurones within the medial parvocellular subnuclei (Ziegler *et al.*, 2005).

The PVN receives a dense glutamatergic input from many hypothalamic and extrahypothalamic nuclei. Brain regions which send an efferent glutamatergic projection to the PVN were retrogradely labelled with [^{3}H]D-aspartate (D-aspartate is an analogue of L-glutamate and is selectively taken up by high affinity transporters located on the presynaptic endings of glutamatergic neurones (Csaki *et al.*, 2000)). Many of the regions labelled with [^{3}H]D-aspartate were within the hypothalamus and included the arcuate nucleus, lateral hypothalamic area and dorsomedial nucleus. Extrahypothalamic innervation originated from areas including the amygdala and bed nucleus of the stria terminalis (Csaki *et al.*, 2000). No brainstem areas were labelled with [^{3}H]D-aspartate, however recent evidence has shown that ascending projections from the NTS that innervate GABAergic neurones within the PVN express small

amounts of VGLUT2, suggesting that glutamate may be a neurotransmitter involved in this pathway (Affleck *et al.*, 2012).

Studies have shown that microinjection of NMDA into the PVN of normotensive rats dose dependently increases heart rate, blood pressure and RSNA, an effect which is blocked by prior application of the NMDA receptor antagonist AP-5 (Li *et al.*, 2006). Interestingly however, application of AP-5 alone does not produce any significant effect on HR, ABP or RSNA (Li *et al.*, 2006). Furthermore, and as previously described (section 1.VI), bicuculline induced sympathoexcitation is attenuated following NMDA receptor blockade (Chen *et al.*, 2003). Collectively, these results suggest that glutamate, acting through NMDA receptors, does not contribute to the tonic regulation of sympathetic outflow in the PVN of normotensive animals. Moreover, glutamatergic inputs appear to be under a dominant tonic inhibition from GABAergic terminals.

The studies outlined so far detail the role of the PVN in the normal control of cardiovascular homeostasis and how the modulation of GABAergic and glutamatergic inputs results in a carefully orchestrated level of sympathetic outflow. However evidence is accumulating which implicates the PVN as a major candidate in contributing to the sympathoexcitation observed in cardiovascular disease states; such as hypertension and heart failure, as well as in pregnancy. The remainder of this chapter will examine the literature relating to this and how alterations in GABAergic and glutamatergic neurotransmission in the PVN have been shown to significantly contribute to this sympathoexcitation.

IX. Hypertension

The increased risk of developing cardiovascular and renal disease in patients with hypertension was first reported in the early 20th century (Janeway, 1913). Recently "The Global Burden of Disease Study 2010" was published in The Lancet at the end of 2012. In this study, hypertension was ranked as a major risk factor for serious cardiovascular and circulatory diseases (Lim *et al*, 2012). It is estimated that hypertension alone resulted in between 8.5 – 10 million deaths globally in 2010 alone (Lim *et al*, 2012). Hypertension is defined as two readings of diastolic blood pressure ≥90mmHg, combined with 2 readings of systolic blood pressure ≥140mmHg (Carretero & Oparil, 2000).

Essential hypertension accounts for around 95% of all hypertensive cases, and is defined as hypertension in the absence of any secondary cause (i.e. renal disease, aldosteronism; Carretero & Oparil, 2000). It is now well established that essential hypertension has a strong neurogenic component, particularly a significant up regulation of sympathetic nerve activity (Grassi *et al.*, 2009), however the mechanism behind this sympathoexcitation remains poorly understood. Furthermore, given that two-thirds of patients who take anti-hypertensive medication fail to meet adequate blood pressure levels (Chobanian *et al.*, 2003; Kougias *et al.*, 2010); it is clear that much more work is required to fully understand the mechanisms underlying hypertension in order to design better therapeutics.

Both animal models of hypertension and studies in humans have shed considerable light on the mechanism by which neurochemical changes in specific brain nuclei contribute to the pathogenesis of hypertension.

X. Altered Cardiovascular Control in Extra-Hypothalamic Sites

Studies in hypertensive humans and rats have identified that baroreflex control of heart rate and SNA is attenuated (Judy & Farrell, 1979; Grassi *et al.*, 1998). In humans and various animal models of hypertension, the baroreflex curve is consistently shifted to the right (Figure 13; Head, 1995; Grassi *et al.*, 1998).

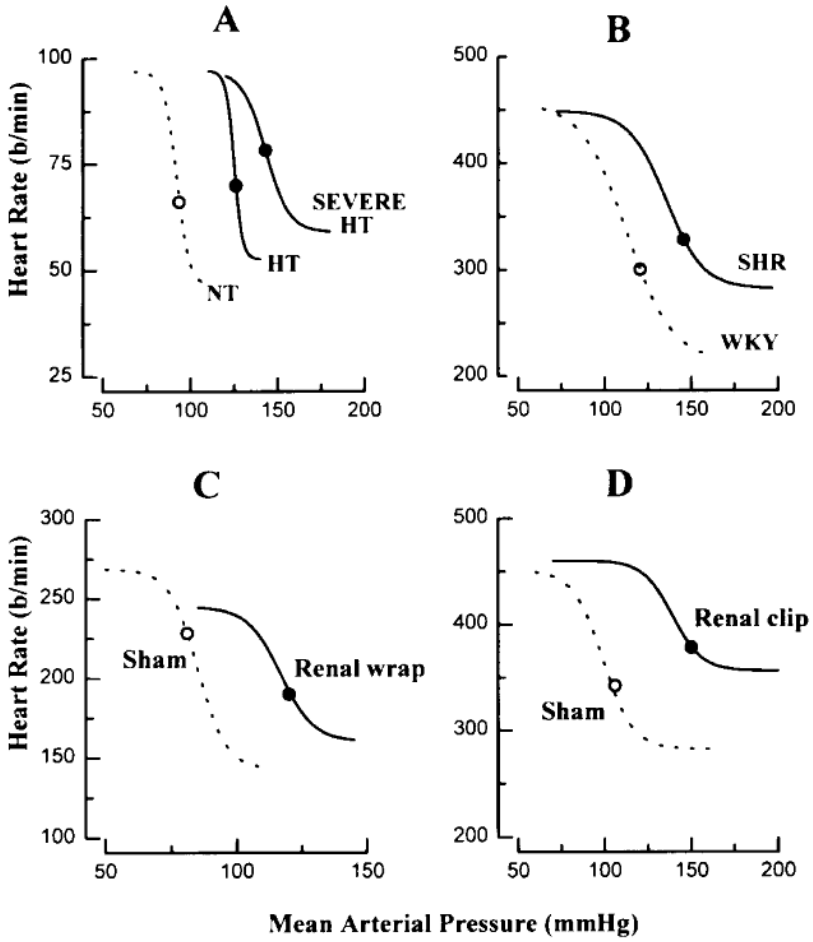

Figure 13 Altered baroreflex control of heart rate in various models of hypertension (B-D), including humans (A) (Head, 1995).

The cause of this reduced baroreflex gain and resetting is unclear, however the reduced gain is most likely the result of both vascular stiffening and cardiac hypertrophy, resulting in a reduced distension of the baroreceptors during hypertensive challenges (de Andrade *et al.*, 2008; Kougias *et al.*, 2010). Under normal physiological conditions, alterations in ABP result in increased activity of

a number of brain sites in the rabbit, including the NTS, RVLM and PVN (Li & Dampney, 1994). Decreased baroreceptor input to the NTS in response to high blood pressure in hypertensive animals is likely to therefore result in decreased drive to other autonomic centres in the brain. The caudal ventrolateral medulla (CVLM) is one such site known to receive excitatory input from the NTS (Sved *et al.*, 2000). The CVLM projects dense inhibitory processes to the RVLM, thereby reducing vasomotor tone in response to baroreceptor activation (Cravo & Morrison, 1993).

Therefore, reduced baroreceptor input resulting from reduced distension of peripheral baroreceptors is likely to result in a reduced NTS-CVLM excitatory input and a subsequent disinhibition of the RVLM. *In vivo* studies in the spontaneously hypertensive rat (SHR) and the Goldblatt model of hypertension show that a major source of these excitatory inputs in the RVLM are glutamatergic (Bergamaschi *et al.*, 1995; Ito *et al.*, 2000), however the origins of these glutamatergic inputs to the PVN remains to be fully determined.

One known area of excitatory glutamatergic input into the RVLM is the PVN (Stocker *et al.*, 2006). Significant advancement has been made over the past few decades into the role of the PVN in hypertension and the mechanisms by which it can sustain the sympathoexcitatory environment observed.

XI. Evidence for the Involvement of the PVN in Hypertension

The hypothalamus has long been believed to contribute to the aetiology of essential hypertension. Early studies showed that transection of the brain caudal to the hypothalamus resulted in a significantly greater decrease in blood pressure in the SHR compared with normotensive WKY controls (-34 ± 11mmHg vs. -18 ± 5 mmHg respectively; Yamori & Okamoto, 1969). Furthermore, neurones within the posterior hypothalamic area had higher levels of spontaneous neuronal firing rates in the adult SHR compared with normotensive WKY controls (3.66 ± 0.55 Hz vs. 2.11 ± 0.29 Hz respectively, Shonis & Waldrop, 1993).

These studies provided convincing evidence that the hypothalamus is involved in the pathogenesis of essential hypertension in the adult rat. Furthermore a study by Eilam et al (1991), showed that transplantation of hypothalamic tissue from embryonic SHR into adult normotensive WKY rats resulted in a 31% increase in blood pressure and an 80% increase in heart weight over a period of 6 weeks. Taken together, these results suggest that hypothalamic control of blood pressure contributes significantly to increased vasomotor tone in hypertension, and that this may be genetically predetermined in the SHR.

A study by Ernsberger *et al* (1985) began to provide evidence that the PVN is the main hypothalamic site responsible for the generation of increased sympathetic activity in hypertension. Radiofrequency lesions of the PVN prevented the rise in blood pressure in the Dahl salt-sensitive (DSS) rat fed a high salt diet. This rise in blood pressure was not observed in Dahl salt-resistant rats, or in DSS rats with lesions placed outside the PVN. A similar study employing electrolytic lesions of the PVN in SHR, also found that ablation

of the PVN significantly reduced blood pressure in adult SHR with established hypertension, but also reduced blood pressure in young, pre-hypertensive SHR compared with sham-operated age matched controls (Ciriello *et al.*, 1984). These studies add weight to the argument that the PVN does not contribute significantly to the control of blood pressure in the normotensive animal; however increased neuronal activity within the hypothalamus, specifically the PVN dramatically increases blood pressure in the hypertensive state.

XII. Role of GABA in the Aetiology of Sympathoexcitation

Activation of the PVN, either by blockade of inhibitory GABAergic networks or by activation of excitatory receptors, has been consistently shown to increase MAP in rats and rabbits by increasing sympathetic outflow (Martin *et al.*, 1991; Deering & Coote, 2000; Allen, 2002; Chen *et al.*, 2003). Given the role of the PVN in regulating sympathetic outflow (Kannan *et al.*, 1989; Kenney *et al.*, 2003) and the characteristic sympathoexcitation in hypertension in both humans and animals (Greenwood *et al.*, 1999; Grassi *et al.*, 2009), studies have long focused on the role of the PVN in the development of hypertension.

It is known that blockade of the GABAergic system in the PVN of normotensive rats produces similar effects to those observed in hypertension (i.e. sympathoexcitation, increased ABP; Martin *et al.*, 1991) and that GABA plays a dominant role in the PVN under normal physiological conditions (Decavel & Van den Pol, 1990). It is therefore perhaps unsurprising that much work has been undertaken to examine the role of GABA in the PVN in the aetiology of sympathoexcitation in hypertension.

Early studies examining the role of the hypothalamus in hypertension identified that the posterior hypothalamus (which encompasses the PVN), showed higher levels of spontaneous neuronal activity in the SHR than in age-matched WKY controls (Shonis & Waldrop, 1993). Since excitatory networks are heavily inhibited in the PVN of normotensive rats (Li *et al.*, 2006), the increase in neuronal excitability in the hypothalamus of hypertensive rats must in part be due to a removal of the inhibitory inputs that are normally present. Indeed to this effect, autoradiographic studies of $GABA_A$ receptor binding sites in the PVN of pre- and established hypertensive SHR (4 weeks and 12 weeks

respectively), showed significantly lower binding of [^{35}S]*t*-butylbicycleophosphorothionate ([^{35}S]TBPS; a $GABA_A$ receptor ligand) to the $GABA_A$ receptor at both ages compared with age-matched WKY controls (Kunkler & Hwang, 1995). In lieu of this, these results would suggest that the ability for GABA to elicit its inhibitory effects within the PVN is blunted, even prior to the onset of hypertension.

However, the physiological effect of GABA activation within the PVN of hypertensive rats has produced conflicting results.

In one series of experiments, bilateral microinjection of the $GABA_A$ receptor agonist muscimol into the PVN of anaesthetised SHR produced a more profound decrease in ABP, HR and LSNA than age matched WKY controls (Allen, 2002; Akine *et al.*, 2003). However, in a second set of experiments, bilateral microinjection of muscimol into the PVN of SHR produced an attenuated decrease in ABP, HR and LSNA at similar concentrations to those used in the previous experiment (Li & Pan, 2007b). Furthermore, the sympathoexcitatory, pressor and tachycardic response to disinhibition of the PVN with bicuculline has been shown to be both attenuated (Li & Pan, 2007b) and augmented (Ito *et al.*, 2002) in SHR compared with WKY controls.

In vitro analysis of $GABA_A$ receptor activity revealed that bicuculline application on PVN-RVLM projecting neurones significantly increased the firing rate of all labelled, spontaneously active neurones in young (6 weeks) and adult (13 weeks) WKY and SD rats. Furthermore, bicuculline application also induced spontaneous firing in a subset of quiescent neurones in WKY and SD rats. However in the SHR, bicuculline application increased the firing rate of only 48.9% of labelled neurones, failed to exert an effect on 21.3% of labelled

neurones, and surprisingly decreased the firing rate of 29.8% of labelled neurones. In addition, bicuculline application failed to evoke spontaneous firing in all but 1 of 12 silent neurones tested (Li & Pan, 2006). This latter, *in vitro* result reinforces the evidence towards a reduced GABAergic influence in the PVN of rats with established hypertension.

Changes in GABAergic inhibition have also been identified in different models of hypertension. In the chronic renal-wrap model of hypertension; in which a ligature in the form of a figure-8 loop is tied around a kidney, followed by removal of the contralateral kidney, bilateral microinjection of bicuculline into the PVN of conscious rats produced an increase in arterial blood pressure that was 31% greater than sham operated rats (Haywood *et al.*, 2001). Furthermore, $GABA_A$ binding sites, measured by autoradiographic labelling with [^{3}H] Flunitrazepam, and mRNA expression of the $GABA_A$ α1 subunit within the PVN were not different between hypertensive and normotensive sham operated rats (Haywood *et al.*, 2001).

However, in acute models of renal-wrap induced hypertension, the sympathoexcitatory effects of bilateral microinjection of bicuculline into conscious rats was attenuated compared with sham operated controls (Martin & Haywood, 1998).

Analysis of GABA synthesis potential; as identified by immunofluorescent-identification of the GABA-synthesising enzyme glutamic-acid decarboxylase (GAD67) expression, in the PVN of renovascular hypertensive rats; in which hypertension is achieved following unilateral occlusion of the renal artery,

showed that GAD67 expression was increased in the medial and caudal aspects of the PVN (Biancardi *et al.*, 2010).

The discrepancies observed in these series of experiments are not fully understood. It is possible that different genetic lineages of strains, injection techniques, injection sites and anaesthesia could contribute to these differences. Moreover, it is possible that these differential changes in GABAergic activity within the PVN are age and disease progression-dependent. In the experiments in which GABAergic inhibition appeared blunted, the animals were either younger (12-13 weeks) in the case of the SHR, or hypertension was in the progressive, rather than established phase (4 days post-surgical renal-wrap). This is compared with the experiments showing augmented GABAergic inhibition within the PVN, in which the animals were older (14 weeks SHR) or chronic renal-wrap had produced established hypertension (≥3 week's post-surgery). Indeed in the renovascular model of hypertension; which showed an increase in GAD67 expression in specific PVN subnuclei, this does not conclusively relate to an increase in GABAergic tone. Analysis of GABA function or post-synaptic GABA receptor densities; which are significant limiting factors in the function of GABA, were not measured in this study, nor were levels of GAD65 expression, and have not been previously measured in this model.

It is therefore possible to speculate that GABAergic tone is altered in early hypertension and is increased as the disease progresses. Given that blood pressure was significantly higher in the younger compared with older SHR (142.3 ± 10.3 mmHg vs. 119 ± 7 mmHg respectively; Allen, 2002; Li & Pan,

2007b), this is a plausible hypothesis. Compensatory increases in presynaptic GABA release and/or postsynaptic $GABA_A$ receptor density could account for these differences. However the effects of using differently sourced strains of SHR and control rats as a possible cause of this discrepancy, as well as the different sites of ABP measurement (carotid vs. femoral), can also not be ruled out.

Indeed recent evidence in a rat model of heart failure points towards differential control of sympathoexcitation in early and late phases. The sympathoexcitation observed in the early stages of heart failure was not dependent upon nitrergic inputs but was mediated by angiotensin II, whereas this was NO dependent in later stages (Pyner *et al,* 2009; Barrett *et al*, 2012). Although this study was not directly related to GABAergic control in hypertension, it provides evidence that the chronic sympathoexcitation characteristic of cardiovascular disease has the potential to be differentially regulated over time.

Very recent evidence has been published shedding some light onto one mechanism by which GABAergic inhibition within the PVN is reduced in hypertension. $GABA_A$ receptor activity is dependent upon intracellular chloride concentrations ($[Cl^-]_i$), the balance of which is maintained through cation-chloride co-transporters. The Na^+-K^+-$2Cl^-$ cotransporter-1 (NKCC1) regulates chloride influx across the membrane, whereas the K^+-Cl^- cotransporter-2 (KCC2) channel regulates chloride efflux (Payne *et al.*, 2003). *In vitro* analysis of the $GABA_A$ receptor activity of spinally projecting PVN neurones showed a significant reduction in activity in the SHR compared with normotensive controls, as well as a significant increase in basal firing rate. However, following 2-4 hour incubation with bumetanide, a specific blocker of NKCC1

channels, $GABA_A$ receptor function was restored and basal firing rate was significantly reduced. Furthermore, expression of the glycosylated isoform of NKCC1 was significantly increased in the SHR compared with WKY rats. Incubating brain slices from SHR with a blocker of N-glycosylation also normalised GABA activity. *In vivo* analysis of the contribution of NKCC1 in the aetiology of hypertension showed that intracerebroventricular infusion of bumetanide in SHR significantly decreased LSNA, ABP and HR as well as significantly increasing the response to muscimol (Ye *et al.*, 2012a). Taken together, these results suggest a significant role for the activity of NKCC1, particularly the glycosylated isoform, in mediating the decreased GABAergic activity within the PVN of hypertensive rats, most likely through disrupting transmembrane chloride homeostasis.

Furthermore, evidence from animals subjected to chronic, unpredictable stress were found to show significant reductions in mRNA levels for extrasynaptic $GABA_A$ receptor subunit (α5 and δ), but not synaptic $GABA_A$ receptor subunits (α1, α3 and γ2) in parvocellular neurones of the PVN Verkuyl *et al.*, 2004)). Although blood pressure levels were not measured in this study, levels of corticosterone, which is known to increase blood pressure (Goodwin & Geller, 2012), were significantly enhanced in the stressed group compared with unstressed controls. It is therefore possible that, rather than a global downregulation of all $GABA_A$ receptors in the PVN, hypertension and pregnancy could be associated with downregulation of specific $GABA_A$ receptor subunits.

As described earlier, the sympathoinhibitory, depressor and bradycardic effects of $GABA_B$ receptor activation within the PVN only manifest at high (4.5nmol) concentrations in normotensive rats (Li & Pan, 2007b). In an *in vitro*

preparation, baclofen application to PVN-spinally projecting neurones produces modest, but significant reductions in spontaneous firing potential (Li *et al.*, 2008b). However, the effects of bilateral microinjection of baclofen into the PVN of SHR were augmented compared with WKY controls. Furthermore, application of baclofen to PVN-spinally projecting, pre-labelled neurones produced a more significant decrease in firing activity compared with WKY controls (Figure 14; Li & Pan, 2007b; Li *et al.*, 2008b)

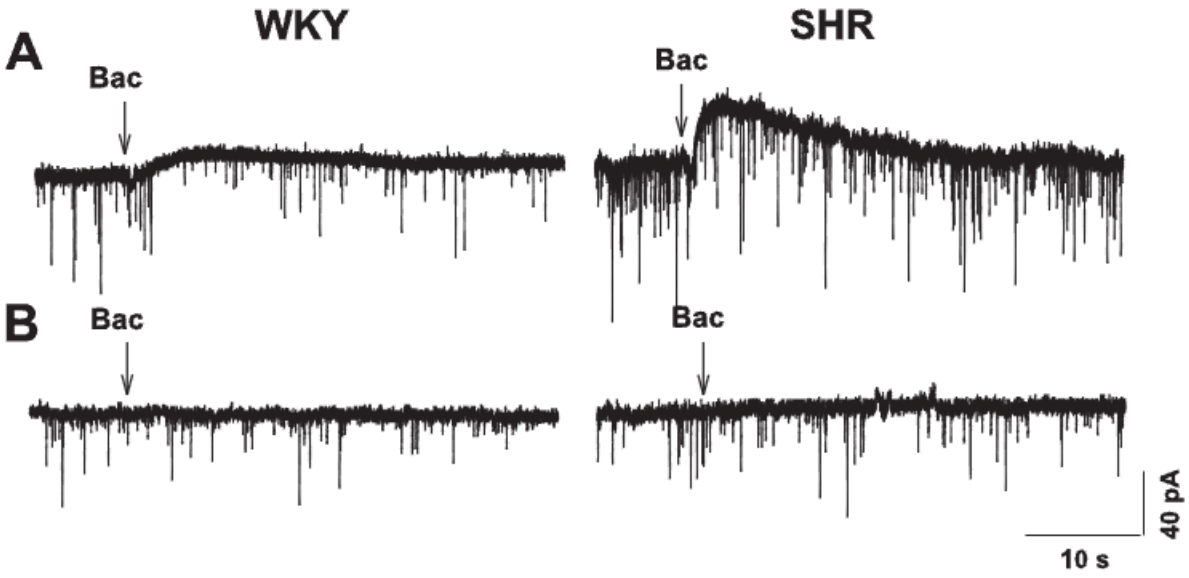

Figure 14 Effect of baclofen on firing rate of PVN-spinally projecting neurones. A: Application of 100μM baclofen evoked an outward current in 54% of recorded neurones in WKY rats and 85% in SHR. The evoked current was significantly greater in the SHR compared with age-matched WKY controls. B: This response was blocked by prior administration of the GPCR blocker GDPβS in both WKY and SHR (Li *et al*, 2008).

In a hypothalamic brain slice preparation, bath application of the $GABA_B$ receptor antagonist CGP-55845 produced no significant changes in the firing activity of PVN-RVLM projecting neurones in 6- or 13- week old WKY, 6 – or 13-week old SD or 6-week old SHR at either low (1μM) or high (5μM) concentrations. Conversely, application of 1μM CGP-55845 to hypothalamic

brain slices from 13-week old SHR produced significant increases in the on-going firing activity of 75% of PVN-RVLM neurones measured. Application of CGP-55845 also induced spontaneous firing in 75% of silent PVN-RVLM neurones measured in the 13-wk old SHR (Li & Pan, 2006).

The results of these studies clearly show that $GABA_B$ receptors play little role in mediating tonic inhibition of PVN-RVLM neurones in normotensive rats. However, the effects of $GABA_B$ receptor activation or inhibition in the PVN of 13-week old SHR are significantly increased.

The reason for the increased $GABA_B$ receptor-mediated inhibition in the PVN of the SHR is not fully understood. Since a decrease in the activity of $GABA_A$ receptors in the PVN was noted in these studies (Li & Pan, 2006, 2007b; Li *et al.*, 2008b), it is possible that increased $GABA_B$ receptor activity is compensatory.

The $GABA_B$ receptor exists as both a pre- and postsynaptic receptor (Li & Pan, 2010). As a presynaptic receptor, $GABA_B$ receptors inhibit neurotransmitter release and have been shown to inhibit the release of glutamate and GABA in the basolateral amygdala (Yamada *et al.*, 1999). It is therefore possible that activation of $GABA_B$ receptors in the PVN could act to inhibit presynaptic GABA release, and that an increase in $GABA_B$ activity in the SHR could act to inhibit GABA release to a greater effect than in normotensive controls, thereby contributing to the reduced $GABA_A$-receptor mediated inhibition. To this effect, reduced concentrations of endogenous GABA have been reported in the hypothalamus of 10 week and 17 week old SHR (Hambley *et al.*, 1984).

The work described above encompasses the range of studies that have been undertaken examining the role of GABA in the PVN of hypertensive rats. Concluding a specific role for GABA in the PVN in the aetiology of hypertension remains difficult and it is therefore clear that more work needs to be undertaken to fully elucidate the changes that occur in the inhibitory environment.

One way of examining the potential contribution that PVN-GABA plays in the development of hypertension is to examine its role in heart failure (HF). Heart failure shares with hypertension a characteristic sympathoexcitation in both animals (Zhang *et al.*, 2002) and humans (Charkoudian & Rabbitts, 2009; Floras, 2009). In addition, not only has PVN activity been shown to be significantly increased in HF, as shown by Fos expression; a marker of neuronal activity (Vahid-Ansari & Leenen, 1998), but the firing rate of PVN-RVLM projecting neurones has also been shown to be significantly increased in HF (Han *et al.*, 2010), as is also observed in hypertension (Li & Pan, 2006).

Experiments examining the physiological effect of GABA activation and blockade, similar to those mentioned above in the hypertensive rat have been undertaken in rats with HF. The sympathoexcitatory effects following unilateral microinjection of bicuculline into the PVN of rats that had undergone left coronary artery ligation, resulting in a characteristic heart failure profile (hypertrophic heart, infarct, sympathoexcitation and increased left ventricular end diastolic pressure), were found to be significantly blunted compared with sham operated rats (Zhang *et al.*, 2002; Wang *et al.*, 2009). Furthermore, the sympathoinhibitory, depressor and bradycardic effect of muscimol injection into the PVN were also significantly blunted in HF rats (Zhang *et al.*, 2002; Wang *et*

al., 2009). Moreover, mRNA expression of the α1 subunit of the $GABA_A$ receptor is significantly reduced in the PVN of rats with HF compared with sham operated rats (Wang *et al.*, 2009). This conclusion of a reduced GABAergic inhibition in the PVN of HF rats is in agreement with *in vitro* work examining the firing properties of PVN-RVLM projecting neurones in HF rats. The spontaneous activity of PVN-RVLM projecting neurones was significantly greater in HF rats compared with sham operated rats (Han *et al.*, 2010). Furthermore there were also significantly fewer spontaneous inhibitory post-synaptic currents (sIPSCs) in these neurones, which were a result of reduced pre-synaptic GABA release (Han *et al.*, 2010). Bicuculline-evoked increases in the firing rate of PVN-RVLM projecting neurones were also decreased in HF, where bicuculline failed to evoke a response in any of the labelled neurones tested, compared to 80% in sham operated controls (Han *et al.*, 2010). These results were distinct from PVN-IML projecting neurones, which displayed a normal firing pattern and sIPSC rate (Han *et al.*, 2010).

In addition; and in contrast to that which is observed in hypertension, the activity of $GABA_B$ receptors is also blunted in the PVN of rats with HF, since application of the $GABA_B$ receptor agonist baclofen produces blunted decreases in RSNA, HR and ABP (Wang *et al.*, 2009).

These results provide interesting insight into the role of PVN-GABA in the aetiology of sympathoexcitation in rats with chronic heart failure. Given that both hypertension and HF display significant increases in sympathetic activity

emanating, at least in part, from the PVN, HF provides an interesting model for the potential mechanisms that are taking place in hypertension.

However caution does need to be observed when extrapolating data observed in HF to that in hypertension. Although both conditions do elicit sympathoexcitation and increased PVN activity, some differences in this activity do exist. For example, in rats with HF, there is an increase in activity of PVN-RVLM projecting neurones only (Han *et al.*, 2010), whereas in hypertensive rats, the firing rate of PVN-RVLM and PVN-IML projecting neurones is increased (Li & Pan, 2006; Li *et al.*, 2008b). Moreover, rats with HF show no significant change in blood pressure compared with sham controls (Zhang *et al.*, 2002), which could indicate towards a differential control of sympathetic outflows in these two conditions.

Regardless of the effects of GABA in the PVN of HF rats, the current understanding of the role of PVN-GABA in hypertension remains poorly understood. The results obtained from studies in HF can and should be used as a framework to examine potentially similar changes in hypertension.

XIII. Role of Glutamate in the Aetiology of Sympathoexcitation

It is known that under normal physiological circumstances, GABAergic inhibition plays a dominant role in regulating sympathetic outflow in the rat PVN. To this effect, application of the NMDA receptor antagonist AP-5 into the PVN produces no effect on blood pressure (Chen *et al.*, 2003). However, although the role of GABA in the PVN of hypertensive rats is contested, results largely suggest that GABAergic inhibition is blunted. Given that the PVN is known to widely express both NMDA and non-NMDA receptors (Herman *et al.*, 2000), it is possible that this would lead to disinhibition and the ability for glutamatergic excitation to predominate.

As previously described, microinjection of AP-5 into the PVN of normotensive rats produces no significant change in blood pressure, heart rate or both RSNA and LSNA (Chen *et al.*, 2003; Li & Pan, 2007a). This is most likely due to the high level of GABAergic inhibition observed in the PVN. However, bilateral microinjection of AP-5 into the PVN of 13 week old SHR produced a significant reduction in ABP, HR and LSNA (27.6 ± 2.8 mmHg, 14.8 ± 5.6 bpm, 24.1 ± 8% respectively compared with age matched WKY; Li & Pan, 2007a). In addition, bilateral application of the selective non-NMDA receptor antagonist 6-cyano-7-nitroquinoxaline-2,3-dione (CNQX) into the PVN produced no significant effects in the normotensive rat, however produced significant reductions in ABP, HR and LSNA in the SHR (20.6 ± 2.5 mmHg, 16.5 ± 8.2bpm, 23.6 ± 1.9% respectively; Li & Pan, 2006). These observations suggest that the sympathoexcitation emanating from the PVN in hypertensive rats is due, at least in part to activation of both NMDA and non-NMDA receptors. Furthermore,

given that the reductions in these parameters to both NMDA and non-NMDA receptor blockade are similar in magnitude, it is possible to suggest that both of these receptor subtypes contribute equally. This is further evidenced by the bilateral application of Kyn into the PVN. Microinjection of Kyn into the PVN of normotensive WKY rats produced no significant cardiovascular effect, whereas when applied to the PVN of the SHR ABP, HR and LSNA were reduced by 40.9 ± 3.9mmHg, 30.1 ± 3.6bpm and 32.3 ± 1.8% respectively (Li & Pan, 2006).

The role of glutamate in contributing to the increased activity of the PVN in other models of hypertension has also been investigated. The Dahl Salt Sensitive (DSS) rat is a genetic model of salt sensitive-hypertension. The degree of hypertension that this rat model exerts is dependent on dietary salt intake, with even normal salt intake producing mild hypertension (Pinto *et al.*, 1998). This differs from the SHR, which produces hypertension regardless of salt intake. The Dahl Salt Resistant (DSR) rat is produced by substituting chromosome 13 for that of the salt resistant Brown Norway rat (Gabor & Leenen, 2012). Dahl Salt Sensitive rats fed a normal salt diet (0.1% NaCl) had a resting ABP of 109 ± 3mmHg compared with 106 ± 4mmHg for the DSR rat fed on the same diet. When fed high salt diets (8% NaCl), DSS rats recorded a ABP of 153 ± 8mmHg compared with 112 ± 3mmHg in the DSR rats (Gabor & Leenen, 2012). Bilateral infusion of Kyn into the PVN of DSS rats fed normal salt diets produced no alteration in ABP or HR. However, when infused into the PVN of DSS fed high salt diets, Kyn produced significant decreases in both ABP and HR (Gabor & Leenen, 2012). Given that these results mirror those observed in the SHR, it would appear that glutamatergic inputs are an important component of multiple models of hypertension.

These results can be replicated in a hypothalamic *in vitro* preparation. Application of AP-5, CNQX or Kyn failed to elicit any effect on the firing rate or membrane potential of PVN-IML projecting neurones in WKY rats. Conversely, AP-5, CNQX and Kyn all elicited a significant decrease in the firing rate of PVN-IML projecting neurones in 11-13 week old SHR (Li *et al.*, 2008a). Puff application of NMDA onto these neurones also elicited significantly greater inward currents in SHR compared to WKY, whereas inward currents elicited by puff application of AMPA were similar in SHR and WKY (Li *et al.*, 2008a). These results not only show that the increased response to both NMDA and non-NMDA stimulation *in vivo* is, at least in part due to stimulation of presympathetic neurones targeting the spinal cord, but also the activity of post-synaptic NMDA receptors is somehow increased on these neurones, whereas the activity of AMPA receptors remains the same.

What remains unclear from the studies discussed previously is whether the increased influence of the glutamatergic network in the PVN of hypertensive rats is due to an increase in the activity of postsynaptic glutamate receptors, a withdrawal of the inhibition, which normally prevents activation of these receptors, or a combination of the two.

To evidence this latter part, microinjection of either the $GABA_A$ receptor antagonist gabazine or bicuculline into the PVN produces a significant increase in ABP, HR and SNA in both normotensive and SHR (Chen *et al.*, 2003; Li & Pan, 2007a). However, the cardiovascular and sympathoexcitatory effects of $GABA_A$ receptor antagonism were blocked by prior antagonism of glutamatergic receptors with Kyn (Chen *et al.*, 2003; Li & Pan, 2007a). These results suggest that withdrawal of GABAergic inhibition results in the activation of glutamatergic

inputs within the PVN. Given that evidence suggests GABAergic inputs are reduced in the PVN of hypertensive rats (Li & Pan, 2007b), it is possible to suggest that this withdrawal would result in the activation of glutamate receptors.

Furthermore, recent evidence also suggests that the expression of postsynaptic NMDA receptors is up-regulated in the PVN of hypertensive rats. Analysis of whole PVN protein and mRNA expression of the GluN2A and GluN2B subunits of the NMDA receptor show an increase in expression in the SHR compared with age-matched WKY controls (Ye *et al.*, 2012b). In addition, casein kinase 2 (CK2) phosphorylation of GluN2B subunits, phosphorylation of which results in internalisation of the GluN2B subunit and a selective enhancement of synaptic GluN2A subunits (Sanz-Clemente *et al.*, 2010), was increased in the PVN of SHRs compared with WKY controls (Ye *et al.*, 2012b).

The evidence therefore appears to suggest that the increased influence of glutamatergic inputs in the PVN of hypertensive rats results from both reduced GABAergic inhibition of glutamatergic networks, as well as an increase in the expression of postsynaptic NMDA receptors.

As with PVN-GABA, much work has been undertaken examining the role of glutamate in the sympathoexcitatory actions of heart failure.

Experiments have shown that microinjection of NMDA into the PVN of rats with HF show an augmented pressor and sympathoexcitatory response than sham operated controls (Li *et al.*, 2003). Conversely, blockade of NMDA receptors with AP-5 produced significant decreases in ABP and RSNA in HF, but not in sham operated controls (Li *et al.*, 2003). Furthermore, expression of the GluN1

subunit of the NMDA receptor was also increased in the PVN of HF rats (Li *et al.*, 2003). This data points toward a heightened activity of NMDA receptor activity within the PVN of rats with HF, and generally correlates with the data observed from hypertensive animals and discussed previously. In addition, it has been shown that chronic blockade of AT1 receptors within the PVN of rats with HF reverses the augmented response to NMDA microinjection and normalises the GluN1 expression (Kleiber *et al.*, 2010).

The influence of glutamate in the PVN on the sympathoexcitation and cardiovascular characteristics observed in hypertension has been extensively studied, and the results appear to be more conclusive than those observed for GABA, which shows considerable variability in its physiological response in hypertension. Furthermore, studies examining the role of glutamatergic hyperactivity in the PVN of HF animals show striking similarities in the augmented responses observed between the two physiological states. Taken together, these results suggest a significant role for glutamate in maintaining the sympathoexcitation observed in these two cardiovascular disease states.

XIV. Pregnancy and Neurosteroidal Modulation of $GABA_A$ Receptors

Pregnancy is associated with an increase in blood volume (40% increase on pre-pregnancy levels), cardiac output (30-35% increase on pre-pregnancy levels) and sympathetic nerve activity in both animals and humans (Longo, 1983; Heesch & Rogers, 1995; Greenwood *et al.*, 2001; Jarvis *et al.*, 2012). Coupled with these changes are increases in both plasma and brain concentrations of certain hormones, including oestrogen, progesterone and chorionic somatomammotropin (Figure 15; Longo, 1983; Concas *et al.*, 1998).

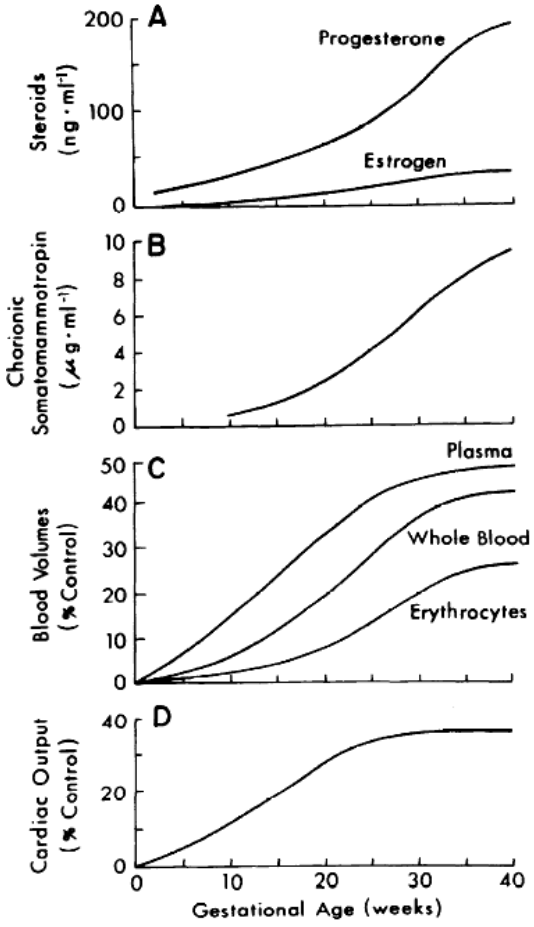

Figure 15 Increase in hormone levels, blood volume and cardiac output during the course of gestation in humans (Longo, 1983)

Of these hormones, experimental evidence has shown that progesterone, and more importantly metabolites of progesterone, such as 3α-hydroxy-5α-pregnan-20-one (3α-OH-DHP, allopregnanolone) and 5α-hydroxy-2α,21-diol-20-one (allotetrahydrodeoxycorticosterone), show potent positive modulatory action at $GABA_A$ receptors, particularly extrasynaptic $GABA_A$ receptors (Concas *et al.*, 1999; Maguire & Mody, 2009; Sanna *et al.*, 2009). Furthermore, administration of progesterone or its metabolites into autonomic centres of the brains of virgin female rats (such as the RVLM) has been shown to produce cardiovascular effects that mimic those observed in pregnancy (Heesch & Rogers, 1995; Storey & Kaufman, 2004).

Systemic adminstration of progesterone or its metabolites has been shown to produce profound anxiolytic, hypnotic or anticonvulsant effects, a trait shared by the $GABA_A$-receptor modulating benzodiazepine class of drugs (Concas *et al.*, 1999).

A seminal paper by Harrison and Simmonds (1984), showed that in rat brain slice preparations, application of alphaxalone, a synthetic, progesterone-based steroid anaesthetic, potentiated the depolarising effects of the $GABA_A$ receptor agonist muscimol. Furthermore, muscimol binding to $GABA_A$ receptors was also increased in the presence of alphaxalone. These effects were not repeatable when the inhibitory neurotransmitter glycine was added, suggesting a specificity for the $GABA_A$ receptor (Harrison & Simmonds, 1984). Given the steroid nature of alphaxolone, the authors of this study concluded that endogenously synthesised steroids could also potentiate GABAergic inhibition in a similar manner.

Indeed this has been shown through various studies. Callachan *et al* (1987), showed that in cultured bovine adrenomedullary chromaffin cells, application of 100μM GABA in the presence of 300nM of the progesterone metabolites 5β-pregnan-3α-ol-20-one (pregnanolone) or 5β-pregnane-3,20-dione (pregnanedione), had an augmented depolarising effect compared with application of 100μM GABA alone. An effect which was blocked by prior application of the $GABA_A$ receptor antagonist bicuculline (Callachan *et al.*, 1987). In addition, application of high concentrations of both pregnanolone and pregnanedione activated $GABA_A$ receptor-mediated membrane depolarisations in the absence of GABA, suggesting that in addition to their modulatory role, progesterone metabolites have the ability to act as GABA-mimetics (Callachan *et al.*, 1987). However, given the high concentrations of steroids required to achieve this effect (>1μM), it is not clear whether endogenous progesterone metabolites would be able to achieve the same effects.

In cultured hippocampal neurones, application of SKF 105111- 17β-17-[bis (1methylethyl) amino carbonyl] androstane-3,5-diene-3-carboxylic acid (SKF); a potent inhibitor of 5α-reductase, the enzyme involved in the breakdown of progesterone into allopregnanolone, amongst other metabolites - reduced the Cl^- current intensity evoked from exogenously applied GABA. These results were reversed with dual application of allopregnanolone with either GABA or the $GABA_A$ receptor agonist muscimol (Puia *et al.*, 2003).

Modulation of $GABA_A$ receptors by progesterone metabolites has been shown to be dependent on their subunit conformation. Recent evidence has shown that in *Drosophila melanogaster* RDL (resistant to dieldrin) $GABA_A$

receptors, which lack neurosteroidal sensitivity, incorporation of the murine TM1 and TM2 domains in the α1 and β2 subunits results in potentiated neurosteroidal sensitivity in α1 subunits, but not in β2 subunits (Hosie *et al.*, 2006). Further dissection of the neurosteroidal binding site at this subunit reveals regions Q241 of the TM1 region, and N407 and Y410 of the TM2 region to be important, sites which are conserved amongst the α subunit family (Hosie *et al.*, 2006; 2009).

Multiple studies have shown that incorporation of a δ subunit into the $GABA_A$ receptor complex further potentiates neurosteroidal modulation of these receptors.

Application of the progesterone metabolite tetrahydrodeoxycorticosterone (THDOC) on oocytes expressing either α1β2 or α1β2δ $GABA_A$ receptors significantly increased the depolarising effects of both receptor types by increasing the decay time constant and magnitude of the depolarisation. Application of 1μM GABA onto α1β2δ containing receptors did not induce membrane depolarisation. However, in the presence of THDOC, 1μM GABA did produce a significant depolarisation. In addition, application of 100μM GABA onto δ containing receptors did produce a modest depolarisation, which was significantly enhanced with the addition of THDOC (Figure 16**,** B/C). The degree of depolarisation was enhanced, but to a much lesser degree in $GABA_A$ receptors which lacked the δ subunit (Figure 16, A/C, Zheleznova *et al.*, 2008).

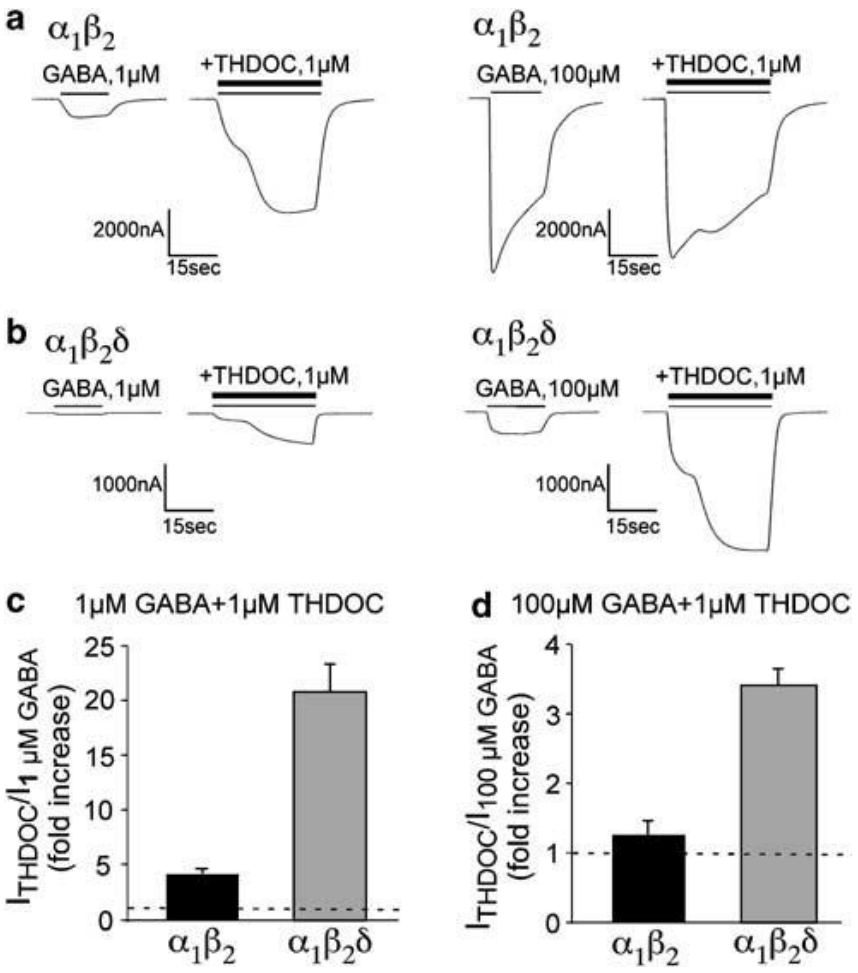

Figure 16 Effects of 1μM THDOC on GABA-induced inhibitory currents in oocytes expressing either α1β2 (A) or α1β2δ (B) GABAA-containing receptors. THDOC significantly increased the decay time and depolarising magnitude in both receptor subtypes. This effect was more profound in δ containing receptors (C). Application of 1μM GABA on δ containing receptors did not produce significant depolarising effects alone (B). Zheleznova *et al*, 2008.

The results of this study suggest that in the absence of neurosteroidal modulation, $GABA_A$ receptors comprising the δ subunit appear to be silent, and thus contribute very little to inhibition. However, in the presence of neurosteroids, their inhibitory potential is significantly enhanced. Additionally, the potentiating effects of neurosteroids are not dependent on the presence of a δ subunit, since THDOC enhanced the inhibitory potential of $GABA_A$ receptors which lacked the δ subunit; however their presence does confer significant

increases in their modulatory potential. This has been confirmed, since mutation of Q246 in the α4 subunit (analogous to Q241 in the α1 subunit) of α4β3δ-containing $GABA_A$ receptor blocked neurosteroid potentiation (Hosie *et al.*, 2009), suggesting that δ subunits are not required for the binding or actions of neurosteroids, but do confer distinct physiological properties to receptors which incorporate the δ subunit in the presence of neurosteroids.

Pregnancy and the accompanying increases in progesterone levels have also been shown to modulate the subunit expression of $GABA_A$ receptors in the brain. During late stage pregnancy in rats (P19), expression of the δ subunit in granule cells of the dentate gyrus (DGGC) significantly increases, as identified immunohistochemically (Sanna *et al.*, 2009). Concomitantly, there is a significant decrease in expression of the γ subunit in these same cells. These changes equate to an increase in the expression of extrasynaptic, and a decrease in the expression of synaptic $GABA_A$ receptors (Sanna *et al.*, 2009). Coupled with these receptor subunit changes, application of GABA onto DGGCs from rats in oestrus, P15 and P19 show a significant increase in GABA-mediated inhibitory currents in cells from rats at P19 compared with oestrus (Sanna *et al.*, 2009). These results suggest that in the presence of high levels of neurosteroids, $GABA_A$ receptors containing the δ subunit have greater inhibitory potentials than those containing the γ2 subunit. Furthermore, the changes in δ and γ2 subunit expression in rats at P19 were reversed following antagonism of the enzyme 5α-reductase with finasteride, suggesting that the observed changes are as a result of increased progesterone levels observed during pregnancy (Sanna *et al.*, 2009).

Conversely, in cultured hippocampal pyramidal cells from neonatal rats, exposure to 1μM progesterone for 6 days decreased mRNA and protein expression of the δ subunit by almost 50% compared with control levels. This was reversed following withdrawal of progesterone (Mostallino *et al.*, 2006). This effect was mimicked by application of allopregnanolone and blocked with finasteride, suggesting this effect was specific to progesterone application. In correlation with a decrease in δ containing $GABA_A$ receptors, application of 4,5,6,7-tetrahydroisoxazolo-[5,4-c]pyridine-3-ol (THIP), a $GABA_A$ receptor agonist with preference for δ-containing receptors over γ2-containing receptors, in conjunction with allopregnanolone resulted in a reduced potentiation of the Cl^- current following 6 days of allopregnanolone treatment compared with control (Mostallino *et al.*, 2006).

The significance of these conflicting results is interesting. Given that both progesterone levels and levels of its metabolites increase in the brain during pregnancy, it would be likely that chronic application of progesterone or allopregnanolone onto cultured hippocampal cells would produce similar effects on δ-subunit expression than those seen during pregnancy; however the opposite appears to be the case. It is possible to speculate that application of progesterone alone does not mimic pregnancy. Since many hormonal fluctuations occur during pregnancy, a convergence of these hormones may interact to produce complex changes, which ultimately manifest as those observed during *de facto* pregnancy. Alternatively, the differences observed in these two studies could be due to the difference in ages between the animals. The study by Sanna *et al* (2009) utilised adult rats (60-90 days old), whereas Mostallino *et al* (2006), used cultured hippocampal neurones from neonatal rats.

It is known that $GABA_A$ receptors behave differently in the neonatal rat compared with adults (Taketo & Yoshioka, 2000), indeed acting as an excitatory receptor (Ben-Ari *et al.*, 1994), and that endogenous neurosteroids produce differential responses in various populations of neurones (Lambert *et al.*, 2009). It is therefore possible that the differential effects seen between these two studies are due to the age differences of animals. Interestingly these two studies are the product of the same laboratory, yet the later study (Sanna *et al.*, 2009) does not correlate the results obtained *in vivo* with those obtained from the earlier *in vitro* study (Mostallino *et al.*, 2006). It is therefore possible to speculate that the authors also do not believe the *in vitro* methodology to be a reliable model for pregnancy.

In correlation with the observed decrease in γ2 expression in the hippocampus of late-stage pregnant rats (Sanna *et al.*, 2009), both mRNA and protein expression of the long isoform of the γ2 subunit (γ2L) was found to be significantly reduced in both the hippocampus and cerebral cortex at day 10 of pregnancy, peaking at day 19 in rats. Levels returned to control values at day 21 of pregnancy, just prior to delivery (Follesa *et al*, 1998; Concas *et al*, 1998, 1999). The altered levels of γ2L expression in the hippocampus and cerebral cortex were abolished following treatment with finasteride from days 12-18 of pregnancy (Concas *et al.*, 1999). Levels of mRNA for the α5 subunit were also significantly reduced in the cerebral cortex during pregnancy, reaching maximal reduction at day 21 (~25% decrease compared to oestrus rats). Levels of α5 expression returned to normal following delivery (Follesa *et al.*, 1998). Coupled with these decreases in expression of the γ2L and α5 subunits, muscimol-induced $^{36}Cl^-$ uptake in the cerebral cortex was significantly reduced at day 19

of pregnancy. In addition, the potentiating effects of allopregnanolone was also reduced at day 19 of pregnancy, and only returned to control levels 2 days following delivery (Follesa *et al.*, 1998).

XV. Neurosteroidal Modulation of Cardiovascular Homeostasis

The numerous studies described previously show that neurosteroids, particularly progesterone and progesterone metabolites, have significant potential to modulate the activity of $GABA_A$ receptors in the brain.

Synthesis of hormonal steroids typically takes place in peripheral tissues, such as the adrenal gland, liver, ovary, prostate and testis (Normington & Russell, 1992). However, evidence has also shown the 5α-reductase enzyme to be present in the brain of humans, monkeys, rabbits, rats, dogs, ferrets, guinea pigs and mice; specifically in the hypothalamus, amygdala, midbrain, thalamus, hippocampus, cerebellum, cerebral cortex and olfactory tubercle (reviewed by Lephart, 1993), suggesting that the brain has the capacity to synthesise neuroactive steroids *de novo*.

Of interest from this list are the hypothalamus and the midbrain, sites which play significant roles in modulating cardiovascular homeostasis through actions of the autonomic nervous system. Given that pregnancy induces alterations in cardiovascular homeostasis, mediated in part through changes in autonomic control, it is possible to speculate that progesterone metabolite modulation of $GABA_A$ receptors in these nuclei could play a significant role.

Previous evidence has shown that in late term pregnant rats subjected to balloon inflation of the right atrium, the normal responses - increased urine volume, sodium excretion and potassium excretion - are abolished (Kaufman & Deng, 1993). This is also accompanied by a reduction in the number of c-Fos positive neurones in the PVN, medial preoptic area and lateral septum (Deng & Kaufman, 1998), suggesting that pregnancy impairs the impact of

cardiovascular afferents entering regions of the brain known to influence plasma volume. From these experiments however, it was unclear whether the alterations were the result of central alterations to afferent input and/or alterations in the discharge properties of atrial volume receptors. In addition, it was unclear whether these changes were mediated through progesterone or through alternative influences.

Further experiments have demonstrated that the discharge properties of atrial volume receptors are indeed altered during pregnancy. Two subtypes of unmyelinated atrial C-fibres exist, termed low-frequency (LF) and high-frequency (HiF). Low-frequency type fibres produce bursts of activity, which is independent of the magnitude of the stretch. Conversely, HiF type fibres fire only when subjected to higher degrees of stretch than LF fibres (Hines & Hodgson, 2000; Storey & Kaufman, 2004). Two independent studies have concluded that pregnancy impairs the functioning of the HiF type fibre, whist conserving LF fibre function (Hines & Hodgson, 2000; Storey & Kaufman, 2004). Furthermore, this effect was mimicked in virgin female rats following chronic administration (2 days) of pregnan (2-hydroxy-β-cyclodextrin), but not acute (10s atrial infusion) pregnan administration (Storey & Kaufman, 2004), implying that the pregnancy-induced changes in atrial receptor discharge properties are mediated through the chronic increased levels of progesterone.

One of the main cardiovascular characteristics associated with pregnancy is an impairment of the arterial baroreflex. During pregnancy, the baroreflex curve is lowered and the midpoint shifted to the left, meaning that the baroreflex operates at a lower set point. Moreover, the sensitivity (gain) of the baroreflex curve at the most linear point is reduced, meaning that smaller

perturbations in blood pressure do not elicit as profound change in either heart rate or RSNA. Finally, maximal heart rate and RSNA are reduced, suggesting that the ability of the sympathetic nervous system to produce a sympathoexcitatory response in reaction to a hypotensive challenge is attenuated (Figure 17**;** Masilamani & Heesch, 1997; Brooks *et al.*, 2010b).

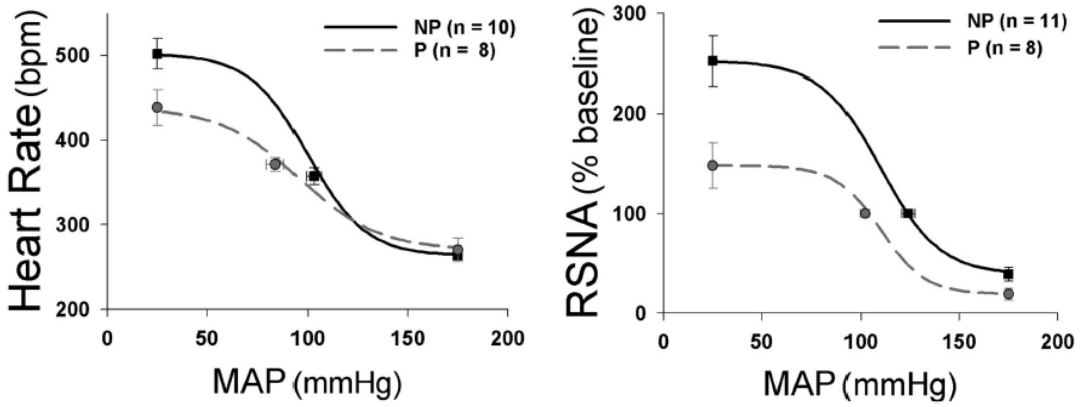

Figure 17 Pregnancy reduces baroreflex control of heart rate and RSNA in conscious rats. Blood pressure was increased and decreased with varying doses of phenylephrine and nitroprusside respectively. Pregnancy resulting in attenuated heart rate and sympathoexcitatory responses during baroreceptor unloading (hypotensive) stimuli only. Pregnancy also decreased the maximal heart rate, heart rate range and baroreflex gain. (Brooks *et al.*, 2010a)

The consequences of the attenuated baroreflex control of blood pressure can be profound. Pregnant women are prone to orthostatic hypotension and have a reduced ability to respond to haemorrhage, due to a depressed sympathoexcitatory response. It is estimated that between 11-22% of all maternal deaths are due to peripartum haemorrhage (Brooks *et al.*, 2010a). It is not completely clear as to the need for a blunted baroreflex during pregnancy. It is possible that it could act as a protective mechanism, preventing vasoconstriction in the presence of high blood volume and cardiac output.

Moreover, a decreased baroreflex, and the resulting hypotensive condition which arises, could prevent blood from being shunted to more low-resistant vascular beds, such as the uterine circulation, thereby protecting the maternal-foetal circulation barrier (Brooks *et al*, 2010a).

In the previous section (section 1.XIV), evidence was presented that neurosteroids, specifically metabolites of progesterone, have significant potential to modulate the physiological characteristics and subunit expression levels of $GABA_A$ receptors. The studies examined in section 1.VI show that GABA acting at central sites known to regulate efferent sympathetic outflow to the cardiovascular system; such as the RVLM and PVN, has profound effects on the level of sympathetic output and cardiovascular homeostasis. It is therefore possible to speculate that some of the cardiovascular characteristics observed in pregnancy are due to progesterone-mediated modulation of $GABA_A$ receptors in these brain areas.

To this effect, autoradiographic analysis of [^{125}I]Progestin and [^{3}H]-oestrodiol binding has shown expression of both progesterone and oestrogen nuclear receptors in areas of the brain involved in cardiovascular regulation, such as the PVN, RVLM and NTS, suggesting these neuroactive hormones have the ability to act at the nuclear level, and thus alter gene transcription at these sites (Stumpf, 1990). Furthermore, it has been previously shown that α1 containing $GABA_A$ receptors have a stronger capacity for modulation than α2 containing $GABA_A$ receptors (Orchinik *et al.*, 1995). Analysis of mRNA levels of the α1 and α2 subunits of the $GABA_A$ receptor in the RVLM of pregnant rats has shown that

their relative expression levels are unchanged in late-term pregnancy, suggesting that the RVLM retains the capacity for neurosteroidal modulation during pregnancy (Foley *et al.*, 2003).

This data suggests that the RVLM has the capacity for both genomic and non-genomic modulation by progesterone. To this effect, intravenous (i.v.) administration of allopregnanolone in virgin female rats produces a leftward shift in the baroreflex curve after just 15 minutes in SD rats, and 30 minutes in WKY rats (Heesch & Rogers, 1995). Although this particular experiment does not conclusively demonstrate that these actions are centrally mediated it is clear that progesterone metabolites also have the capacity to perform non-genomic modulation of the cardiovascular system, most likely through $GABA_A$ receptor potentiation, as described earlier.

To address the question regarding the cardiovascular effects of allopregnanolone administration being centrally mediated, Heesch (2011) microinjected the active isomer (3α-OH-DHP) into the RVLM of inactin-anaesthetised virgin female rats. Fifteen minutes following injection, RSNA had significantly decreased from baseline (82 ± 4.4% of control) with no effect on blood pressure. In addition, sympathoexcitatory responses to a hypotensive stimulus were attenuated resulting in a downward shift and reduced gain of the baroreflex curve, with no alteration of the midpoint (pressure set point). Moreover, microinjection of the inactive isomer of allopregnanolone (3β-OH-DHP) produced no significant effect, suggesting that the alterations observed were mediated through the active isomer of allopregnanolone and not a consequence of the surgical procedure or anaesthetic (Heesch, 2011).

In addition, the results of this experiment show that neurosteroidal hormones, which show a significant increase in circulating levels during pregnancy (Longo, 1983), have the potential to alter cardiovascular parameters at a central level. However, the results from the study performed by Heesch (2011) show that neurosteroidal modulation of the RVLM does not produce a direct representation of the baroreflex curve observed in pregnancy, in which the curve is shifted down and to the left, allowing the hypotensive setting to prevail (Heesch & Rogers, 1995; Masilamani & Heesch, 1997; Brooks *et al.*, 2010a). This therefore suggests that other factors must be important in resetting the baroreceptors to operate at a lower set point. Given the myriad of hormonal changes that occur in pregnancy, it is not surprising that a single hormonal influence fails to confer all the necessary changes to mimic pregnancy in the virgin rat. Furthermore, given the numerous brain nuclei which govern cardiovascular homeostasis, and the localisation of progesterone nuclear binding receptors (Stumpf, 1990), coupled with the physiological importance of GABAergic inhibition in these areas (discussed in 1.VI)**,** it is also possible to suggest that pregnancy-induced modulation of these sites, for example the CVLM and PVN, could account for some of the cardiovascular alterations observed.

An interesting observation when studying the baroreflex curve of the pregnant rat compared with virgin controls is that the alterations in sympathetic outflow are restricted to the hypotensive state, whereby reductions in blood pressure are met by an attenuated sympathoexcitation. When challenged with a hypertensive stimulus, the sympathoinhibitory responses are not significantly different to virgin controls (Heesch & Rogers, 1995; Masilamani & Heesch,

1997). It is well established that the RVLM receives a substantial baroreceptor-independent inhibition from the CVLM, since lesions of the rostral CVLM (known to receive baroreceptor inputs Cravo *et al.*, 1991) in sinoaortically denervated rats still results in tonic sympathoinhibition (Cravo & Morrison, 1993). Given that the attenuated sympathetically mediated responses to blood pressure fluctuations only manifest when baroreceptors are unloaded (i.e. during hypotension), it is possible that the RVLM is under increased baroreceptor-independent GABAergic inhibition.

This was acknowledged by Kvochina *et al* (2007), where the response to bilateral bicuculline injection into the RVLM of inactin anaesthetised, sinoaortic denervated late-term pregnant rats was measured. It was observed that the sympathoexcitatory and pressor effects following RVLM disinhibition were significantly greater in the pregnant compared with non-pregnant controls (Kvochina *et al.*, 2007). It is therefore possible that baroreceptor-independent inputs in late-term pregnant rats result in greater GABA release, increased $GABA_A$ receptor expression, $GABA_A$ receptor subunit alterations or increased GABAergic inputs, most likely originating from the caudal CVLM (Cravo *et al.*, 1991), which confer the observed increase in GABA-mediated inhibition.

Of the central sites involved in cardiovascular control, the RVLM is by far the most studied in relation to pregnancy. However, recent studies have also examined the role of the PVN in mediating the cardiovascular changes characteristic of pregnancy.

It has long been established that the PVN has a critical role in regulating blood volume homeostasis in the rat and rabbit (Lovick & Coote, 1988b; Deering &

Coote, 2000; Pyner *et al.*, 2002) and a contested role in blood pressure regulation (Kannan *et al.*, 1988; Coote *et al.*, 1998; Guyenet, 2006). Since pregnancy is associated with a 40% increase in blood volume (Atherton *et al.*, 1982) and a mild reduction in blood pressure, it is sensible to suggest that alterations in PVN activity could contribute to these observed cardiovascular changes, and perhaps surprising that little work has been undertaken to examine the role of the PVN in manifesting these changes.

Of the work that has examined the PVN in pregnancy; the main focus has been on alterations in GABAergic inhibition. Following unilateral microinjection of bicuculline into the PVN, late-term pregnant rats (P21) showed a significant sympathoexcitation, pressor and tachycardic response. However, this response was significantly attenuated compared with non-pregnant virgin controls (Kvochina *et al.*, 2009; Page *et al.*, 2011).

Moreover, following unilateral microinjection of bicuculline into the PVN of urethane anaesthetised late-term pregnant rats (P20), the heart rate baroreflex gain is increased. However this increase is significantly attenuated compared with non-pregnant virgin controls (0.9 ± 0.3bpm/mmHg compared with 1.9 ± 0.2bpm/mmHg; Page *et al.*, 2011). Furthermore, following blockade of $GABA_A$ receptors in the PVN of late-term pregnant rats, baroreflex function is only slightly elevated, while still remaining depressed compared with virgin controls (Figure 18). This result suggests that during pregnancy, the PVN control of baroreflex function is under reduced GABAergic influence, a result which is consistent with those of Kvochina *et al* (2009).

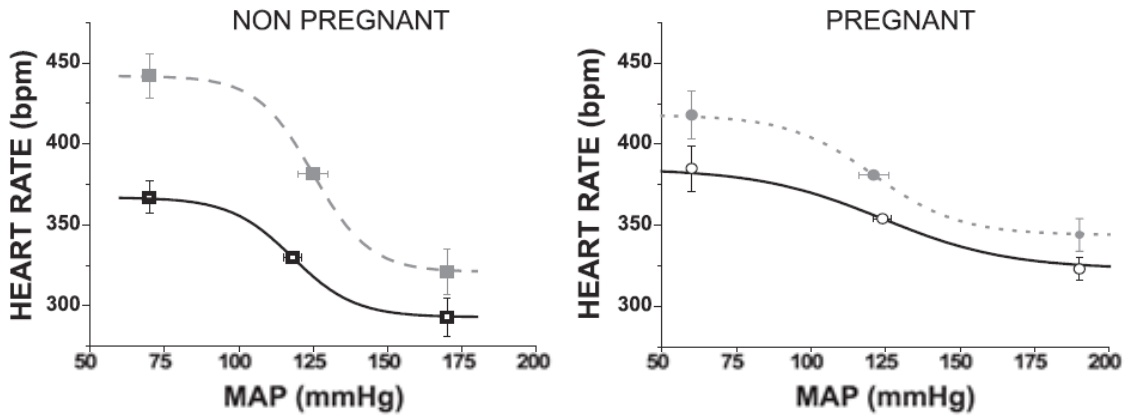

Figure 18 Microinjection of bicuculline into the PVN of non-pregnant and pregnant rats increases the heart rate baroreflex function and gain. This was significantly attenuated in the pregnant rat. Black lines represent control values. Dashed, grey lines represent bicuculline induced alterations in baroreflex (Page *et al.*, 2011)

This evidence for a decreased bicuculline-induced sympathoexcitation in the PVN of late-term pregnant rats correlates with the effects of bicuculline microinjection into the PVN of SHRs, however the results observed in the SHR following microinjection of comparable concentrations of bicuculline into the PVN (0.2nmol in Kvochina *et al*, 2009 compared with 0.15nmol in Li & Pan, 2007b) were significantly greater. For example, in the pregnant animal, microinjection of 2.0nmol bicuculline resulted in an increase in blood pressure by approximately 12mmHg, whereas in the SHR, microinjection of 1.5nmol bicuculline resulted in an increase of approximately 25mmHg (Li & Pan, 2007b). This discrepancy could be the result of differential methods for determining ABP. Kvochina *et al,* (2009) used cannulation of the femoral artery, whereas Li & Pan (2007a) measured ABP using a non-invasive tail cuff sphygmomanometer. Furthermore, these two experiments utilised different anaesthetics (Inactin (Kvochina *et al.*, 2009) and α-chloralose and urethane (Li & Pan, 2007b)), which could result in the differential response observed. Barbiturates, such as inactin, have previously been observed to decrease

cardiovascular parameters, such as cardiac output and blood pressure in dogs (MacCannell, 1969), whereas α-chloralose produces a mild sympathoexcitation, but is often preferred due to its non-significant effects on cardiovascular parameters (Balis & Monroe, 1964). This result could however be due to either a greater reduction in GABAergic inhibition in the pregnant rat compared with the SHR, or greater excitatory input to the PVN in the SHR.

The mechanisms involved in mediating the sympathoexcitation observed in pregnancy are poorly understood; especially given the potent modulatory action of neurosteroids on $GABA_A$ receptors it would be assumed that this would result in a decreased sympathetic drive.

Indeed, *in vitro* electrophysiological experiments on PVN slices from normotensive, non-pregnant rats show that bath application of the neuroactive steroid THDOC significantly decreases the firing rate of PVN-RVLM projecting neurones through potentiation of $GABA_A$ receptors (Figure 19; Womack *et al.*, 2006). This clearly shows that presympathetic neurones within the PVN have the capacity to be inhibited by neurosteroids associated with pregnancy, adding confusion to the emerging model of increased PVN activity during pregnancy.

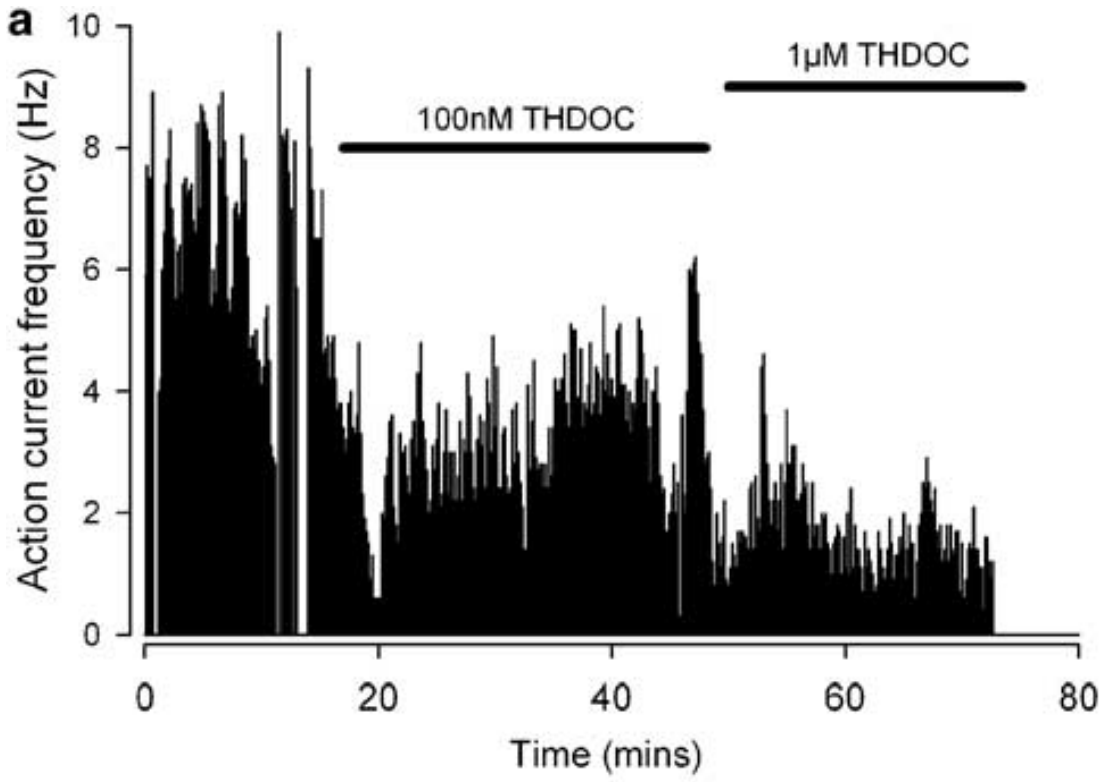

Figure 19 Action currents recorded from PVN-RVLM projecting neurones following application of THDOC (100nM and 1μM indicated by bars). Application of THDOC significantly reduced the firing activity of pre-autonomic neurones within the PVN of non-pregnant, normotensive rats (Womack *et al.*, 2006).

The reason for the increased sympathetic nerve activity and PVN activity observed in late-term pregnant rats could be as a result of increased circulating levels of angiotensin II (AngII), which is characteristic of pregnancy (Hanssens *et al.*, 1991). *In vitro* application of AngII increases the firing rate of PVN-RVLM projecting neurones and significantly decreases the presynaptic release of GABA (Li & Pan, 2005). Therefore the increased activity of PVN neurones observed in pregnancy could be a result of an AngII-mediated decrease in presynaptic GABA release, therefore negating any potentiating effects of pregnancy-associated neuroactive steroids on $GABA_A$ receptors. What remains unclear is whether this is also associated with a decrease in the expression of $GABA_A$ receptors.

This was further evidenced when *in vivo* microinjection of an AT_1 receptor antagonist into the PVN of non-pregnant and late-term pregnant rats significantly attenuated bicuculline-induced sympathoexcitation and pressor responses (Kvochina *et al.*, 2009). In the non-pregnant rat, further application of the excitatory amino acid antagonist Kyn further reduced the pressor response to bicuculline compared with AT_1 receptor blockade, however this was unchanged in the late-term pregnant rat, such that Kyn application was not significantly different to AT_1 receptor blockade (Kvochina *et al.*, 2009). The significance of this study is two-fold; firstly AngII, acting via AT_1 receptors, contributes to the sympathoexcitatory effect of $GABA_A$ receptor blockade in the PVN of both normotensive and pregnant rats, and secondly; the sympathoexcitation observed in pregnancy appears not to be driven by excitatory amino acids (i.e. glutamate), but primarily via angiotensin. This latter result is in contrast with the sympathoexcitation observed in hypertension, which is heavily governed by glutamatergic inputs in the PVN (Li & Pan, 2007a). However this does share a commonality with HF, where AT_1 receptor expression in the PVN is increased and angiotensin administration into the PVN of HF rats produces a potentiated sympathoexcitation compared with sham operated controls (Zheng *et al.*, 2009). This could therefore be an important mechanism whereby sympathetic control of blood pressure and blood volume is controlled, since both HF and pregnancy are conditions of hypervolaemia (Longo, 1983; Remes, 1994)

Furthermore, *in vitro* electrophysiological studies have revealed that neurosteroidal application onto PVN-RVLM projecting neurones results in an attenuated potentiation of GABAergic inhibition in late-term pregnant rats

compared with non-pregnant controls (Heesch *et al*, unpublished). This suggests that presympathetic neurones in the PVN of late-term pregnant rats either have a reduced sensitivity to neurosteroidal modulation, or the expression of $GABA_A$ receptors is reduced.

In conclusion, studies have shown that central control of the cardiovascular system plays a key role in mediating the cardiovascular changes that are vital to normal gestation in both humans and rodents. Furthermore, many of these alterations are as a result of neurosteroidal modulation of $GABA_A$ receptors, predominantly mediated through progesterone and its neuroactive metabolites, which have been shown to have potent actions on the sympathetic nervous system when administered centrally. The inhibitory role of GABA shows both an enhanced functioning; in relation to baroreceptor-insensitive neurones of the RVLM, and reduced functioning, in relation to the PVN. Furthermore, the sympathoexcitatory effects of $GABA_A$ receptor blockade within the PVN do not appear to be driven by glutamate; a result which is in contrast with the sympathoexcitation observed in hypertension, but do appear to be governed by angiotensin II; a trait which is shared with HF. What remains unclear is the mechanism behind this reduced $GABA_A$ receptor-mediated inhibition in the PVN of pregnant rats.

XVI. Aims of Project

The studies outlined indicate that both hypertension and pregnancy are conditions associated with significant increases in sympathetic nerve activity, and that the PVN has consistently been shown to contribute to this sympathoexcitation. In addition, the PVN of hypertensive, but not pregnant rats has been shown to have increased glutamatergic excitation (Li & Pan, 2007a; Li *et al.*, 2008a). However, both pregnancy and hypertension have a demonstrated decrease in GABAergic inhibition within the PVN (Li & Pan, 2006, 2007b; Kvochina *et al.*, 2009; Page *et al.*, 2011).

Although this decrease in GABAergic inhibition and increase in glutamatergic excitation have been demonstrated electrophysiologically, no study has so far identified the molecular mechanism which underpins this alteration.

We aim to do this by addressing the hypothesis that altered GABA and NMDA receptor subunit configurations contribute to the sympathoexcitation observed in hypertension and pregnancy. Given the electrophysiological experiments detailed above, we also hypothesise that these alterations will be different in nature, and that this may contribute to the chronicity of hypertension and the reversibility of the sympathoexcitation observed in pregnancy. We will do this by combining quantitative immunoblotting with immunohistochemistry to identify if any of the subunits which comprise the $GABA_A$ receptor and NMDA receptor show alterations in expression in the PVN of both hypertensive and late-term pregnant rats compared with the normotensive, non-pregnant Wistar rat. Furthermore, we aim to identify within which of the parvocellular subnuclei of the PVN any alteration occurs; so as to infer whether these alterations could

impact on sympathetic outflow. Finally we aim to identify whether any of the subunits for which we observe changes in expression are directly associated with spinally projecting, presympathetic neurones.

Any similarities or differences in subunit expression between the three physiological states observed from this study will be important in our understanding of the molecular mechanisms underpinning the different longevities of these two sympathoexcitatory states. Moreover, these changes have the potential to become novel therapeutic targets for the treatment of hypertension and pregnancy-induced cardiovascular insufficiency.

Chapter 2. Methods

Unless otherwise stated, all solutions used in this chapter are detailed in Appendix A

I. Animals

Experiments were carried out on age-matched (14 week) female Wistar (n=15) and spontaneously hypertensive rats (SHR n=15; Harlan Laboratories, Bicester, Oxon). Pregnant Wistar rats (n=15) were mated either by Harlan Laboratories or by the Durham University Life Sciences Support Unit (LSSU). The presence of a vaginal plug was deemed day 1 of pregnancy (Masilamani & Heesch, 1997; Kvochina *et al.*, 2007, 2009) and animals were sacrificed on day 19. All animals were given *ad libitum* access to food and water and housed on a 12 hour dark:light cycle (8am-8pm). All experiments were approved by the local ethics committee and conducted in accordance with the Animals (Scientific Procedures) Act 1986 under the PPL 40/3393 held by Dr Susan Pyner and the PIL 60/11867 held by the author.

Wistars were chosen as the control animal due to their closer genetic relationship with the SHR than the more commonly used Wistar Kyoto rat (WKY). This is evidenced through both transplant studies, where transplantation of skin from WKY to SHR and vice versa resulted in rejection (H'Doubler *et al.*, 1991) and behavioural studies, where behaviour of the SHR was closer related to the Wistar and SD rat compared with WKY (Sagvolden *et al.*, 1993). Furthermore, the incidence of spontaneous hypertension in the WKY strain limits their usefulness as a control for the SHR (Louis & Howes, 1990).

II. Antibody Production

Antibodies to the GluN1, GluN2A and GluN2B subunits of the NMDA receptor and the α1 and β3 subunits of the $GABA_A$ receptor were produced in the laboratory of Dr Paul Chazot (Durham University), a detailed method of which has been previously published (Chazot *et al.*, 1999). The peptide for GluN1 corresponded to regions 35-53 of the mouse GluN1 subunit (TRKHEQMFREAVNQANKRHC; Chazot *et al.*, 1995), the GluN2A peptide corresponded to region 1381-1394 (RCPSDPYKHSLPSQ) of the mouse GluN2A N-terminal (Hawkins *et al.*, 1999), the GluN2B peptide corresponded to regions 46-60 of the mouse C-domain (DEVAIKDAHEKDDKHC; Chazot & Stephenson, 1997a). The $GABA_A$α1 peptide corresponded to region 1-14 of the mouse C-terminal (Ives *et al*, 2002). The $GABA_A$β3 peptide corresponded to regions 345-408 of the N-terminal (Sperk *et al*, 1997).

Antibodies to the α2 (amino acids 416-424), α4 (amino acids 379-421), α5 (amino acids 2-10), β1 (amino acids 350-404) β2 (amino acids 351-405) and δ (amino acids 1-44) subunits of the $GABA_A$ receptor were produced and kindly donated by Prof. Werner Sieghart (Uni. Vienna; Sperk *et al*, 1997). A detailed method of their production has previously been published (Sperk *et al,* 1997; Pirker *et al*, 2000).

III. Preparation of Brain Tissue for Immunohistochemistry

Rats from each physiological state (i.e. normotensive, SHR and late-term pregnancy) were initially anaesthetised with Isoflurane (5% in 6L/min O_2). The level of anaesthesia was determined using absence of the pedal withdrawal reflex, with anaesthesia maintained at 2.5-3% Isoflurane in 6L/min O_2. An abdominal midline incision was made followed by isolation of the aorta from surrounding connective tissue. A thread was placed around the aorta just above the iliac bifurcation and securely tied. Anterior to this thread and just posterior to the left renal vasculature, an artery clip was placed on the aorta to occlude blood flow. A further thread was positioned posterior to artery clip, which was loosely tied. An incision was then made midway between the thread placed above the iliac bifurcation and artery clip, into which a cannula (Portex tubing 200/320/040), containing sodium pentobarbital (Dolethal, 60mg/kg, Vetoquinol, Buckingham, UK) was inserted (Figure 20). This was secured in place using the previously placed thread anterior to the incision. An incision just lateral to the midline was then made in the neck and the jugular vein was located and cut, as was the right renal vein, to allow the perfusate to flow freely. The animal was then perfused with 200ml ice-cold heparinised saline (0.9%) followed by 500ml 4% paraformaldehyde in 0.1M phosphate buffer (PB). Once fixation was complete, the whole brain was removed from the skull and placed into 4% paraformaldehyde for 24 hours at 4ºC, followed by cryoprotection in 10% and 20% sucrose.

Hearts were also taken from each animal by removal from the thoracic cavity, weighed and expressed as a percentage of whole animal body weight.

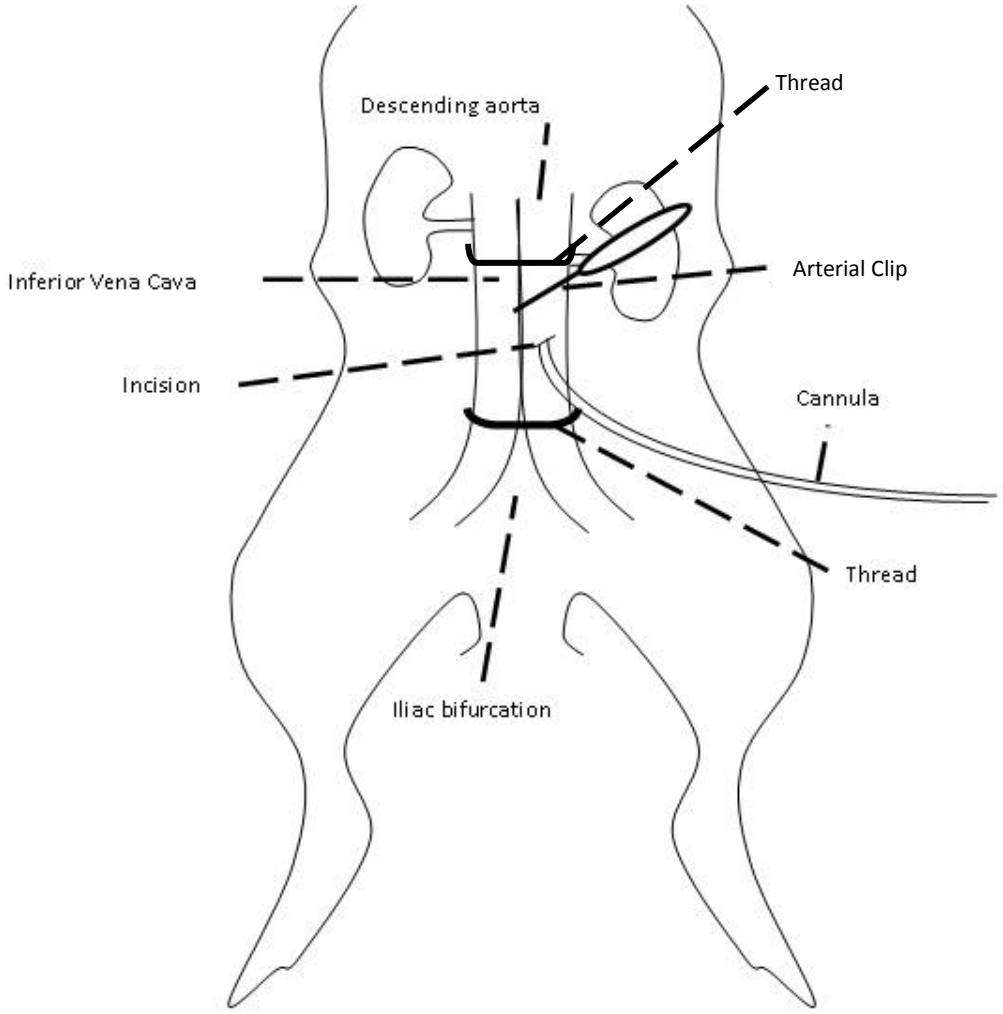

Figure 20 Schematic representation of surgical protocol as described in section 2.III. The descending aorta is removed from the surrounding tissue, around which a thread is tied dorsal to the iliac bifurcation. Anterior to this thread and posterior to the renal vasculature, an artery clip is placed. An incision is made midway between the thread and artery clip and a cannula inserted through which the perfusate flows.

IV. Measurement of Arterial Blood Pressure

A subset of rats (Wistar, SHR and pregnant Wistar, n=3 for each) undergoing procedure 2.III were used for blood pressure measurements. An aortic cannula was inserted as previously described and through this 1.5ml of anaesthetic (75mg/kg α-chloralose & 700mg/kg urethane) was administered. At this point, isoflurane anaesthetic was withdrawn. Animals were then connected to a blood pressure transducer (PowerLab 8/30; ADInstruments, Sydney, Aus.), and blood pressure recordings were obtained through LabChart software (version 7). Animals then underwent perfusion as detailed in section 2.III.

V. Immunohistochemistry of NMDA and $GABA_A$ Receptors

a. Sectioning of Brain Tissue

In order to access the PVN, the frontal lobe of the brain, rostral to the optic chiasm was removed using a razor blade, as was the hindbrain and cerebellum. Brains were then affixed to a freezing microtome on their coronal plane and allowed to fully freeze for around 10-15 minutes. Once fully frozen, coronal sections of 40µm were taken and placed free floating into wells containing 0.1M PB. Successive sections were taken and placed into a separate tray, which were then stained with 0.5% cresyl violet for neuroanatomical reference, as detailed later.

b. Peroxidase Labelling of NMDA and $GABA_A$ Receptor Subunits in PVN

After washing with PB, sections were incubated in 3% hydrogen peroxide (made in PB) for 5 minutes to quench any remaining endogenous peroxidise activity. This was removed and followed by 5 minute incubation with antigen retrieval solution 'Liberate Antibody Binding Solution' (L.A.B. Polysciences Inc, Philadelphia, USA). After removing the L.A.B. solution and washing in PB, sections were incubated in 0.4% Triton X-100 for 15 minutes, followed by blocking solution (0.4% Triton X-100, 10% normal goat serum) for 1 hour. Blocking solution was then removed and sections were incubated in primary antibody diluted in PB/1% normal serum over night at 4ºC (see Table I for concentrations).

After incubation, sections were allowed to reach room temperature before removal of the primary antibody and washing 3 times for 5 minutes each with PB-Tween (0.03% Tween-20 in PB). Primary antibody was then removed and sections were incubated in 1:200 dilution of biotinylated secondary antibody (Vector Labs, Peterborough, UK) diluted in PB/1% normal serum for 2 hours at room temperature.

Vectastain ABC Kit (Vector Labs, Peterborough, UK) was prepared following the manufacturers recommendations at least 30 minutes before use. After removing the secondary antibody and washing 3x5 minutes in PB-Tween, sections were incubated in the ABC solution for 1 hour at room temperature.

Sections were again washed for 3x5 minutes in PB-Tween before being incubated in 0.05% diaminobenzidine (DAB) and 0.0033% hydrogen peroxide diluted in PB until an adequate level of staining had been achieved, as determined by eye.

After staining, sections were washed twice in distilled water (dH_2O) before being mounted onto gelatinised slides and left to dry overnight.

When dry, slides were dehydrated through increasing concentrations of ethanol (70, 95 and 2x 100%) for 4 minutes each, then cleared in xylene for 4 minutes before being coverslipped using DPX mountant and left to dry in a fume hood.

c. Cresyl Violet Staining of Serial Sections

Sections which were to be counterstained were mounted onto gelatinised slides and left to dry before being stained with Cresyl Violet (0.5% w/v) for 25 minutes,

followed by dehydration and clearing through ethanol and xylene (as above). Sections were then coverslipped using DPX mountant and left to dry.

d. Table I. Concentration of Primary Antibodies used in Immunohistochemistry

	Antibody	Concentration (μg/ml)/Source
NMDA	GluN1	1.0 (Chazot)
	GluN2A	1.0 (Chazot)
	GluN2B	1.5(Chazot)
$GABA_A$	α1	1.0 (Chazot)
	α4	2.0 (Sieghart)
	α5	3.0 (Sieghart)
	β3	1.0 (Sieghart)

Table 1. Only subunits for which a change in expression had been identified through Western blotting of whole PVN micropunches were analysed using Immunohistochemistry. $GABA_A$α4 and $GABA_A$β3 were used as counting controls

e. Antibody Specificity

The specificity of GluN1, GluN2A, GluN2B, α1 and β3 antibodies was determined at the time of production as detailed in Chazot & Stephenson) (1997b). Briefly, human embryonic kidney cells were transfected with the appropriate subunit to which the antibody had been made. These were then

subjected to SDS-PAGE. The presence of a single band at the correct molecular weight was deemed specific.

The specificity of α2, α4, α5, β1, β2 and δ antibodies was determined at the time of production as detailed in Pirker *et al* (2000). Briefly, antibodies were pre-absorbed with their respective synthetic peptide for 24 hours before being subjected to immunohistochemical analysis. Using this approach, no staining was evident.

Furthermore, the pattern of expression that the antibodies produced when utilised for immunohistochemistry was compared with that expected from the literature (i.e. discrete staining pattern in the hippocampus and cortex).

During the current experiments, sections underwent staining in which the primary or secondary antibodies had been omitted. With this regimen, no staining was observed.

f. Quantification of Immunohistochemically Stained $GABA_A$ and NMDA Receptor Subunits

Immunohistochemically stained sections were examined using a Zeiss Axioskop 2 microscope under bright field illumination for the presence of $GABA_A$ and NMDA receptor subunits within the PVN. Digital images were captured using either a Hamamatsu Orca 285-CCD camera or Micropublisher 3.3 RTV camera controlled by Improvision Volocity software (v 6.0). The on-screen axis was calibrated against a photomicrographed 1mm graticule. Using this axis a 150μm x 150μm square was drawn. This was then placed indiscriminately within the anatomical boundaries of the PVN subnuclei, determined by analysis

of retrogradely traced CTB-labelled spinally projecting neurones (see Chapter 2.VI and Chapter 4), corresponding counter stained sections, and the Paxinos and Watson (1998) brain atlas. Although selected areas were not completely random (i.e. area of interest was not chosen by computer), bias was kept to a minimum by not consciously choosing areas with high or low cell densities. Cell counts were then performed using the on-screen counting tool with a numbered marker placed over each identified cell (Figure 21). Cell counts were subjected to a one way analysis of variance (ANOVA) test, with Bonferroni post-hoc test and are expressed ± SEM. Values with a P value <0.05 were considered statistically significant. No correction was made for double counting. Cells that expressed morphological characteristics of a neuron (soma or associated with identifiable projections) and were stained darker than background at x200 magnification were counted. A second individual, who was both independent from and ignorant of the conditions of the experiment counted a subset of sections. Counts obtained from this independent analysis, which were within 10% of the counts obtained by the original investigator, were deemed to be accurate. Using this regimen, all second counted sections were within 10% of those counted by the original investigator.

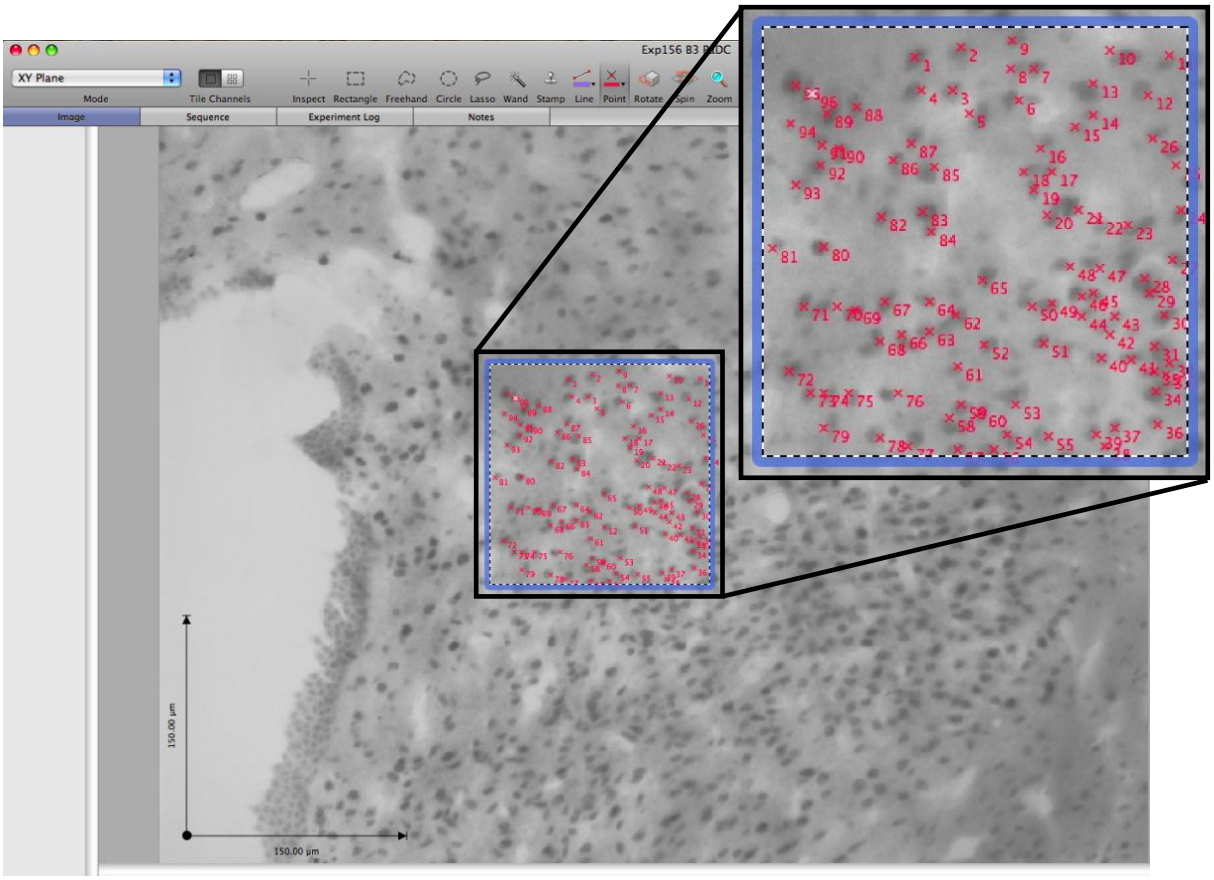

Figure 21 Example of immunohistochemistry quantification. A square measuring 150µm x 150µm was placed randomly on the image and the on-screen counting tool (red numbers) used to mark counted neurones within the boundaries of the box. Inset image shows a magnified view of the counting area.

VI. Identifying Areas of the PVN Containing Spinally Projecting Presympathetic Neurones in the PVN

a. Injection of Retrograde Tracers in the IML Region of the Spinal Cord

Normotensive female Wistar rats (n=7) were anaesthetised using an intraperitoneal injection of medetomindine (0.6mg/kg) and ketamine (30mg/kg) made up in 0.9% saline. Depth of anaesthesia was tested using absence of pedal withdrawal reflex. Once adequate anaesthesia was achieved, the animals were fixed into a stereotaxic frame (Stoelting, IL, USA); with heads fixed with ear bars for stability. A midline incision was made between the dorsal scapula and the vertebral process of T2 was located. Using this process as a guide, the musculature and soft tissue was dissected away to reveal the dorsal surface of the spinal column. To allow easy access to the spinal cord, a thread was inserted through the musculature at T2 and secured to the front of the stereotaxic frame and the tail was stretched and secured to the operating table with surgical tape. Using a hypodermic needle, an incision was made in the dura mater, and forceps were used to tease this away from the cord. A 33G nanofill syringe was then filled with 2µl of either 2% Fluorogold (Fluorochrome LLC, USA) or 0.5% Cholera Toxin-B (CTB; List Biologicals, USA) and mounted into the micromanipulator. Fluorogold (n=5) or CTB (n=2) was then slowly pressure injected into the IML region of the left spinal cord (300µm lateral to the posterior median sulcus, 500µm ventral to the dorsal surface; Figure 22).

The musculature and skin were then sutured and appropriate analgesic (buprenorphine; 0.01ml/100g intramuscular) was given. To prevent

hypothermia, animals were placed into an incubator preheated to 29ºC for around 2 hours until the anaesthetic was reversed with atipamezole (Antisedin, 0.2mg/kg i.p.). Animals were then left to recover for either 7 days (for Fluorogold) or 14 days (for CTB) to allow retrograde transport of the tracer to the PVN, until the perfusion protocol detailed in section 2.III was implemented.

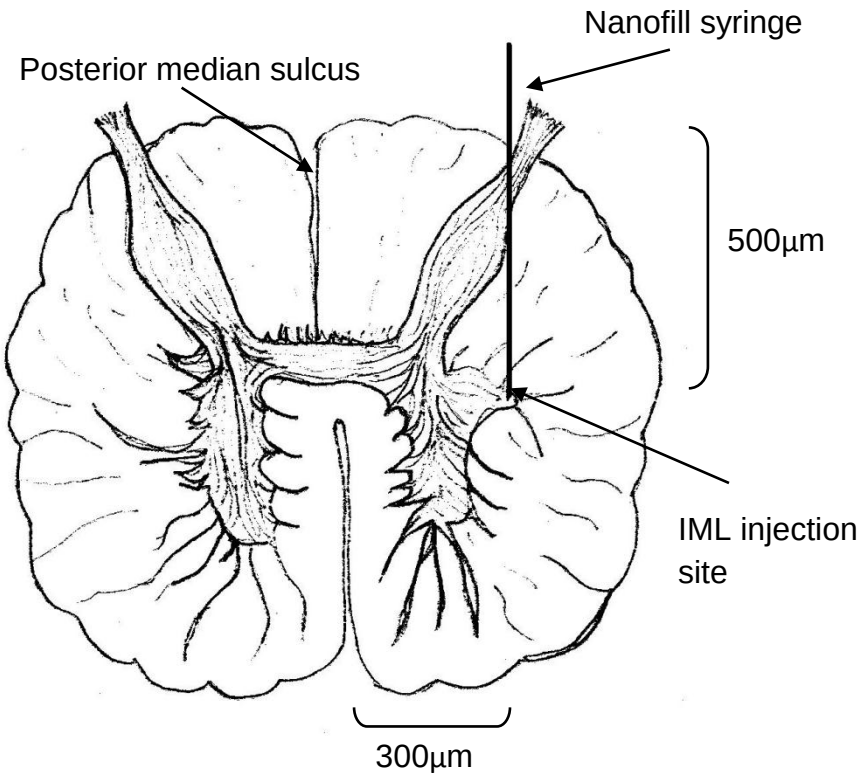

Figure 22 Schematic representation of T2 region of spinal cord. Nanofill syringe is represented as a line and shows the course through the spinal cord and site of injection into the IML region. Drawing courtesy of Mr J.P. Cork.

b. Peroxidase Labelling of CTB-Labelled Presympathetic Neurones in the PVN

Peroxidase labelling of CTB-labelled neurones was performed as previously published (Llewellyn-Smith *et al*, 2005).

Animals that had been subjected to CTB injection in the T2 region of the IML were perfused with 4% paraformaldehyde via the descending aorta as described in section 2.III. Whole brains were removed, post-fixed overnight in the same fixative and cryoprotected at 4°C in 20% sucrose.

Brains were sectioned to 40μm on a freezing microtome as described in section 2.Va; following which sections were placed in wells containing 0.1M PB (pH 7.4). Phosphate buffer was removed from the wells and sections were incubated in blocking buffer (0.4% Triton X-100, 10% normal horse serum) for 60 minutes at room temperature. Blocking buffer was removed and sections were incubated in goat anti-CTB (1:200,000 dilution; List Biologicals, USA) diluted in PB/1% normal serum for 48 hours at room temperature. Following incubation, primary antibody solution was removed and sections were rinsed 3 x 5 minutes in PB. Sections were then incubated with biotinylated donkey anti-goat secondary antibody (1:500 dilution; Vector Labs, Peterborough UK), diluted in PB/1% normal serum overnight at 4°C. Secondary antibody solution was then removed and sections rinsed 3 x 5 minutes in PB, following which sections were incubated in ExtrAvidin-HRP (1:1500 dilution, Sigma, St Louis MO, USA) for 4 hours at room temperature. Sections were again washed for 3x5 minutes in PB before being incubated in 0.05% diaminobenzidine (DAB) and 0.0033% hydrogen peroxide diluted in PB until an adequate level of

staining had been achieved, as determined by eye. Sections were washed in dH_2O and mounted onto gelatinised slides. Once air dried, slides were dehydrated by placing through increasing concentrations of ethanol (70%, 95%, 100%) before being cleared in xylene for 4 minutes. Slides were then coverslipped with DPX mountant and left to dry in a fume hood.

CTB-labelling was visualised using a Zeiss Axioskop 2 microscope under bright field illumination. Digital images were captured using a Micropublisher 3.3 RTV camera controlled by Improvision Volocity software (v 6.0). Images were exported to Adobe Photoshop (version CS3), where brightness and contrast were adjusted. Neurones were measured using the on-screen measuring tool. The pixel size was calibrated using a 1mm graticule and the measuring tool was used to measured neurones at their greatest diameter.

c. Identification of Fluorogold-labelled Spinally Projecting Neurones and their Co-localisation with $GABA_A$/NMDA Receptor Subunits

Animals which had been subjected to Fluorogold injection in the T2 region of the IML were perfused with 4% paraformaldehyde via the descending aorta as described in section 2.III. Whole brains were removed, post-fixed overnight in the same fixative and cryoprotected at 4°C in 20% sucrose.

Brains were sectioned to 40μm on a freezing microtome as described in section 2.Va; following which sections were placed in wells containing 0.1M PB (pH 7.4). Phosphate buffer was removed from the wells and sections were incubated in blocking buffer (0.4% Triton X-100, 10% normal goat serum) for 60

minutes at room temperature. Blocking buffer was then removed and sections were incubated in primary antibodies for either the α1 or α5 subunits of the $GABA_A$ receptor or the GluN2A subunit of the NMDA receptor (for antibody concentrations see Table 2.Vd), diluted in PB/1% normal serum overnight at 4°C. Following incubation, primary antibody solution was removed and sections were rinsed for 3 x 5 minutes in PB. Sections were then incubated in a fluorescently labelled secondary antibody (Texas Red-labelled goat anti-rabbit; 1:200 dilution; Jackson Immunoresearch Labs, USA) for 2 hours at room temperature. Following staining, sections were mounted onto gelatinised slides and air dried; following which slides were dehydrated through increasing concentrations of alcohol (70%, 95% and 100%), before being cleared in xylene. Slides were then coverslipped using DPX mountant and left to air dry in a fume hood.

d. Visualisation and Quantification of Fluorescent Labelling and 3D rendering of Neurones

Immunofluorescence was visualised using a Zeiss Axioskop 2 microscope equipped for epifluorescence with a motorised filter system. Fluorogold labelled neurones were readily detectible by illumination at 350nm. Texas-red labelled $GABA_A$α1, $GABA_A$α5 and GluN2A subunits were visualised by excitation at 594nm. Digital images were captured using a Hamamatsu Orca 285-CCD camera controlled by Improvision Volocity software (v 6.0). Images were exported to Adobe Photoshop (version CS3), where brightness and contrast were adjusted.

Acquisition of 3D rendered neurones was performed as previously described (Affleck *et al*, 2012). Briefly, a series of z-stack images at 0.3µm intervals collected full section thickness images. The acquired images were deconvolved using iterative restoration and the appropriate point spread function (PSF). PSF's model light behaviour and are based on Volocity specified parameters of widefield, numerical aperture, medium refractive index and emission wavelength, producing a confocal-like image. A single neurone of interest was cropped from the image and displayed as an isosurface image. This generates an opaque image of the surface elements. In this instance, this enables the relationship between Fluorogold and subunit immunoreactivity to be observed throughout the entirety of the neurone of interest in a single image.

In order to quantify the number of Fluorogold-labelled neurones expressing the subunit of interest, the number of Fluorogold-labelled neurones was counted per section, per PVN-subnuclei. The number of Fluorogold-labelled neurones which showed positive labelling for the subunit of interest was then counted in the same plane and expressed as a percentage of total Fluorogold-labelled neurones. Cell counts were then subjected to a one-way ANOVA test with Bonferroni post-hoc test and expressed ± SEM. Values with a P value <0.05 were considered statistically significant

VII. Acquisition of Brain Tissue for Western Blotting (Micropunches)

Rats of all physiological states were deeply anaesthetised with isoflurane (5%, 6L/min O_2) before being terminally anaesthetised with an intracardiac injection of sodium pentobarbitone. The dorsal surface of the skull was rapidly removed allowing for removal of the whole brain. This was placed straight into cold 20% sucrose before being stored at 4ºC. Brains were then frozen at between -20 and -30ºC for 3 minutes in iso-pentane before being stored at -20ºC until required.

Removing the cerebellum and sectioning the frontal lobe rostral to the optic chiasm accessed the region of interest. The caudal end of the remaining section was then mounted to a freezing microtome. Using the Paxinos and Watson (1998) brain atlas, the area of the brain containing the PVN was located using the third ventricle and hippocampus as anatomical landmarks, and two 600µm sections were taken. These were then stored at -20°C until required.

Bilateral micropunches from individual animals were taken using a 1-200µl pipette tip with an external diameter of 750µm and a dissecting microscope. Using the Paxinos & Watson (1998) brain atlas, the location of the PVN was lateral to the dorsal point of the third ventricle (Figures 23-24). Bilateral punches were then transferred to 70µl sample buffer containing 1:100 dilution of protease inhibitor cocktail type III (Calbiochem, Germany), vigorously vortexed for 10 minutes to solubilise protein and then frozen at -20ºC.

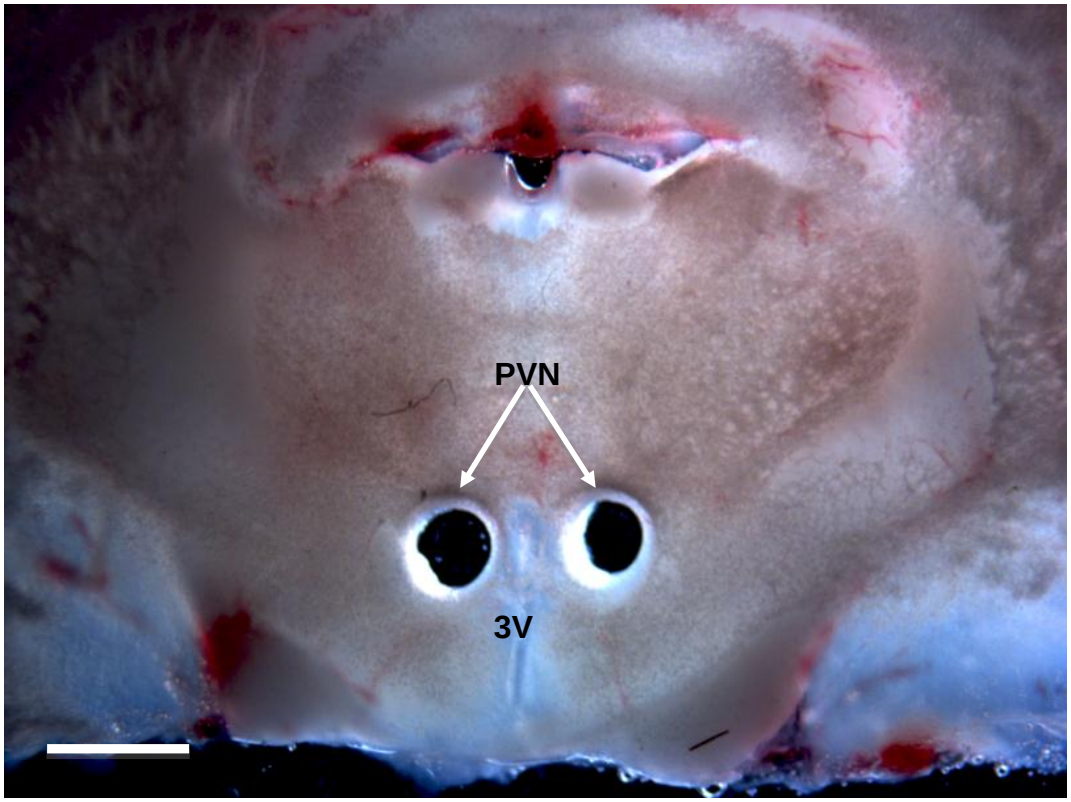

Figure 23 Photomicrograph of coronal section through rat brain showing location of PVN micropunches. The PVN was located using a brain atlas (Paxinos & Watson, 1998) and was determined to lie at the lateral aspect of the dorsal point of the 3rd ventricle (Shaded black in Figure 24). Scale = 3mm, 3V = 3rd ventricle

VIII. Isolation of Cortex Tissue

In order to ascertain whether any changes in NMDA or $GABA_A$ receptor subunit expression observed in the PVN were specific to this region, the level of protein expression for these subunits was analysed from cortex tissue from the same animals.

Following removal of the PVN; as detailed in section 2.VII, the cortex was removed from the same brain sections using a razor blade to detach the cortex dorsal to the corpus callosum (Figure 24). These were homogenised using a glass-glass dounce (VWR, PA USA) in homogenisation buffer (50mM Tris base, 5mM EDTA, 5mM EGTA, 150µM protease inhibitor cocktail (Calbiochem, Nottingham UK), pH 7.4), following which a Lowry assay was performed to assess protein concentrations.

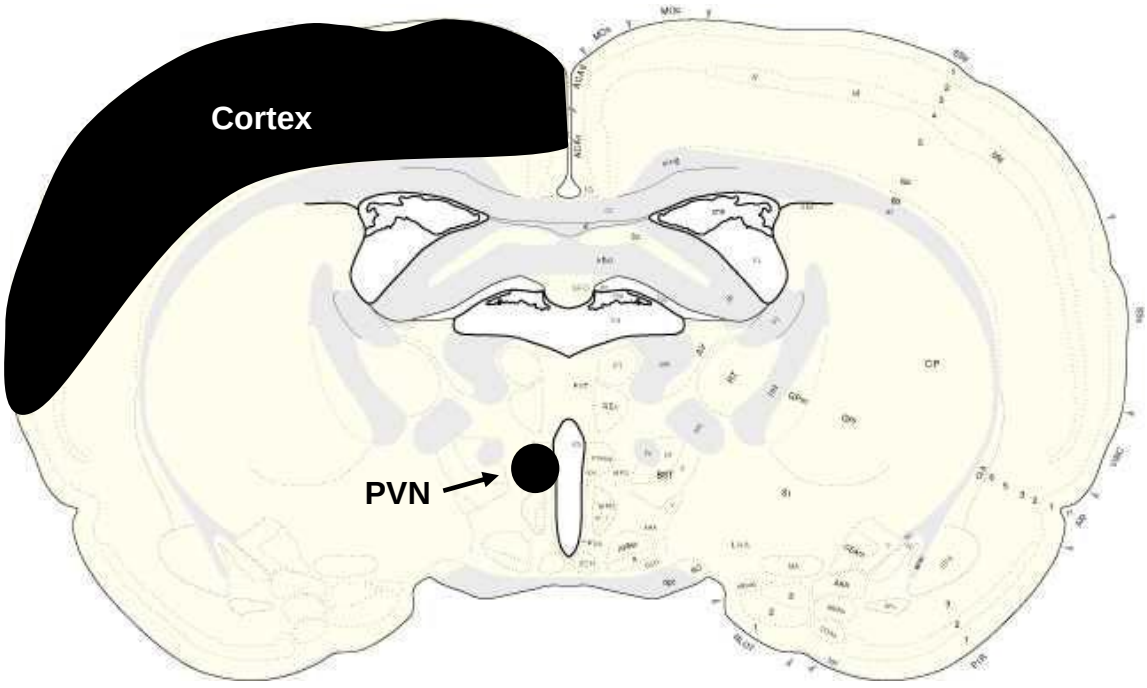

Figure 24 Schematic of brain slice through the PVN region, showing the area removed from the cortex and PVN. Unilateral regions are shown; however bilateral regions were removed from tissue. Schematic corresponds to the same level observed in Figure 23. Paxinos & Watson, 1998.

IX. Lowry Assay

A Lowry protein assay was performed on cortex samples as previously described (Lowry *et al.*, 1951). A protein standard was prepared using bovine serum albumin (BSA) from 0-100mg/ml diluted in dH_2O. Furthermore 5µl and 10µl aliquots of homogenised cortex sample were taken. All samples (standard and cortex) were made up in triplicate. Reagent D was prepared by combining 100ml Reagent A (2% Na_2CO_3; 0.1M NaOH; 0.5% SDS) to 1ml Reagent B (2% Na K Tartrate) and 1ml Reagent C (1% $CuSO_4$, 10% trichloroacetic acid). 0.5ml Reagent D was added to each sample, vortexed and left for 10 minutes. Following this, 50µl folin (1:1 dilution with dH_2O) was added to each solution, vortexed and left for 30 minutes in dark. 0.5ml dH_2O was then added to each sample, vortexed thoroughly and the absorbance read at 770nm using a Genova spectrophotometer (Jenway, Dunmow UK). Absorbance readings from the protein standards were plotted on a standard curve, which was used to determine the protein concentrations of the cortex samples.

X. Quantitative Immunoblotting of PVN and Cortex Homogenates

a. Sample Preparation

PVN homogenates, as obtained in section 2.VII, were separated into 10µl aliquots. Cortex homogenates were separated into 10µl aliquots. Added to this was 2µl dithiothreitol (DTT) and 3µl dH_2O to bring the total loading volume to 15µl. Samples were then briefly centrifuged (Microcentrifuge 5415R, Eppendorf, Germany) at 13000rpm and heated to 95°C for 5 minutes, before being centrifuged again at 13000rpm and vortexed thoroughly.

b. Quantitative Immunoblotting of PVN and Cortex Homogenates for NMDA and $GABA_A$ Receptor Subunits

PVN and cortex homogenates, as prepared in 2.VIIIa were subjected to SDS-PAGE as previously described (Bradford *et al.*, 2005). Briefly, loading wells were formed in a 6.5% SDS-PAGE stacking gel, which was set above a 10% acrylamide gel. Gels were inserted into a Hoefer Mighty small II SE260 vertical slab gel electrophoresis tank (Hoefer, Germany) and filled with electrode buffer. Samples were loaded in nine out of ten wells; the final well was loaded with a pre-stained standard (10-250kDa; Sigma St Louis, MO USA).

Electrophoresis was conducted at 180mV and 15mA until the sample buffer-stained protein front was at the bottom of the gel. The gel was removed from the tank and transferred to nitrocellulose (Fisher Scientific, Hampton UK) using a Hoefer TE series transfer unit (Hoefer, Germany), set to 50V, <200mA for 2-2.5 hours in transfer buffer.

The nitrocellulose was removed from the transfer tank and incubated in blocking buffer (5% (w/v) skimmed milk powder, 0.2% Tween-20, made up in tris-buffered saline (TBS)) for at least 1 hour at room temperature, or overnight at 4°C. Primary antibodies were diluted in incubation solution (2.5% (w/v) skimmed milk powder, made up in TBS) and incubated at 4°C overnight (see Table II for concentrations).

Nitrocellulose blots were moved back to room temperature and a series of 4 x 6 minute washes was implemented using wash buffer (2.5% (w/v) skimmed milk powder, 0.2% Tween-20 made up in TBS), followed by secondary antibody incubation (1:2000 dilution in incubation buffer; Fisher Scientific, Hampton UK) for 1 hour at room temperature. A further set of 4 x 6 minute washes was implemented after which the blot was stored in TBS to remove any excess wash buffer.

The nitrocellulose was then incubated with luminol solution (Solution A:Solution B 1:1 (Solution A = 100mM Tris-base pH8.5, 25mM luminol, 396µM p-Courmaric acid. Solution B = 100mM Tris-base pH8.5, 6.27mM H_2O_2)) for 1 minute and exposed to ECF hyperfilm (Amersham) at differing exposure times. The hyperfilm was developed manually using Kodak GBX fixer and developer solutions.

Nitrocellulose was then incubated again in blocking solution for 1 hour at room temperature, followed by overnight incubation in mouse anti-β-actin (1:3000; Sigma, St Louis MO) at 4°C. This was then removed and 4x6 minute washes were implemented, followed by incubation in HRP linked anti-mouse secondary (1:2000; Fisher Scientific, Hampton UK) antibody for 1 hour at room

temperature. This was then removed and further 4x6 minute washes were implemented. Nitrocellulose blots were then developed as described above.

c. Protein Expression Quantification

Exposed hyperfilm were scanned (Dell, USA) into a desktop PC and analysed using ImageJ (NIH). Optical density of each band was analysed and normalised against β-actin and background levels. Values were subjected to a one-way ANOVA with Bonferroni post-hoc test and expressed ± SEM. Values with a P value <0.05 were considered statistically significant. In blots where a second band appeared in addition to the band at the expected molecular weight, the density of the second band was also measured. The density of both bands was then averaged to produce the final value. These second bands were often believed to be the result of glycosylation or degradation of the original protein of interest.

d. Table II. Primary Antibody Concentrations Used in Quantitative Immunoblotting

	Antibody	Concentration (μg/ml)
NMDA	GluN1	1.0
	GluN2A	1.0
	GluN2B	1.5
GABA	α1	1.0
	α2	1.0
	α5	1.0
	β1	1.0
	β2	0.5
	β3	1.0
	δ	3.0

Chapter 3. Physiological Parameters of Animals Used

I. Animal Weights

A total of 50 animals were used in this study. Female Wistar control rats (n = 20) weighed 199 ± 2g (range 186 - 215g), female spontaneously hypertensive rats (SHR, n = 15) weighed 178 ± 2g (range 160 - 198g) and pregnant Wistars weighed 299 ± 7g (range 262 - 330g, n = 15). Pregnant rats had 10 ± 0.7 (range 6 - 14) foetuses weighing 2.1 ± 0.15g (range 1.2 - 3.2g), placing them between P19 and P20 (Schneidereit, 1985).

II. Blood Pressure

Female SHR's had a significantly higher blood pressure (150 ± 5mmHg; range 140 – 160mmHg) than both Wistar control (72 ± 5mmHg; range 65 – 83mmHg) and late-term pregnant rats (90 ± 2mmHg; range 85 – 95mmHg). Late term pregnant rats also had a slight but significantly higher mean arterial blood pressure than non-pregnant controls ($P<0.05$; Figure 25).

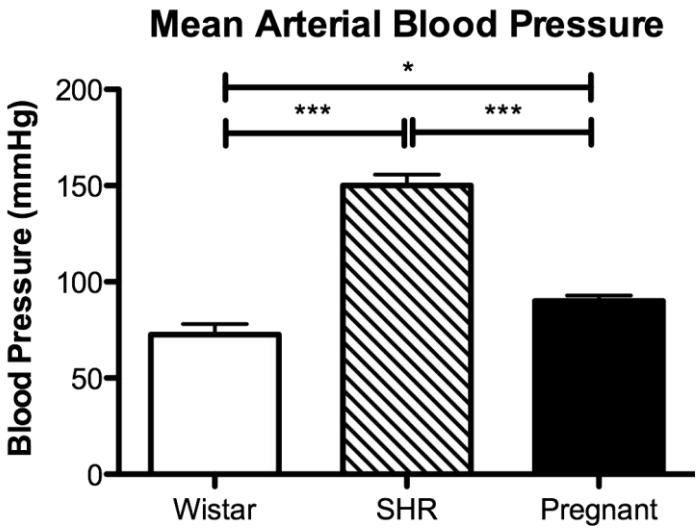

Figure 25 Mean arterial blood pressure of non-pregnant Wistar control, female SHR and late-term pregnant rats, measured by intra-aortic cannula. SHRs had a significantly higher blood pressure than both Wistar (P<0.001) and Pregnant (P<0.001) rats. Pregnant Wistars also had a slightly higher BP than non-pregnant (P<0.05). n = 3 for each biological group.

III. Heart Weights

SHR's had a significantly higher heart weight/body weight ratio (1.05 ± 0.06%; range 0.9 – 1.2%) than both normotensive (0.68 ± 0.05%; range 0.6 – 0.7%; P<0.01) and pregnant (0.57 ± 0.04%; range 0.5 – 0.6%; P<0.001) Wistars (Figure 26). The heart weight/body weight ratio of the pregnant rat was not significantly different to that of the non-pregnant Wistar.

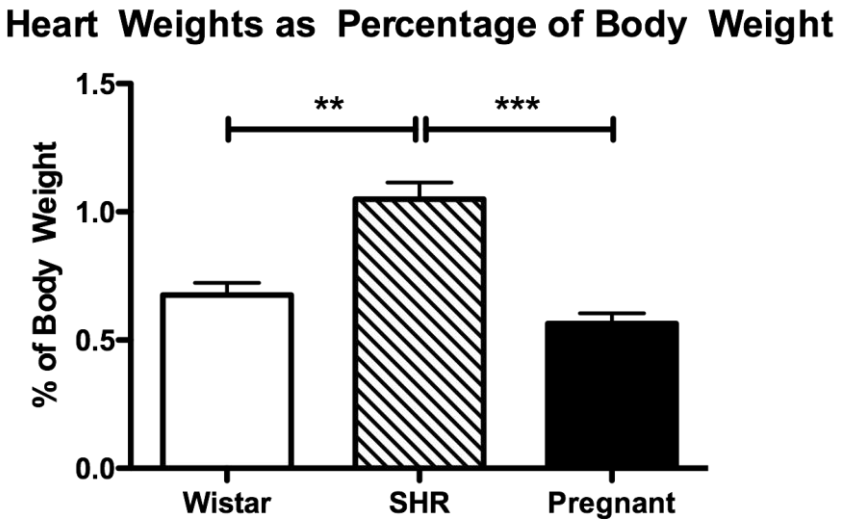

Figure 26 Heart weights expressed as percentage of overall body weight. SHR had a significantly higher Heart weight/body weight than both normotensive (P<0.01) and pregnant (P<0.001) Wistars. N = 7 for each biological group.

Chapter 4. CTB Labelling of Spinally Projecting Neurones

I. Introduction

The distribution of spinally projecting neurones within the PVN has been extensively studied before (Swanson *et al*, 1980; Strack *et al*, 1989; Ranson *et al*, 1998; Pyner & Coote, 2000; Oldfield *et al*, 2001). However, these studies have largely been carried out on male SD rats, with little or no information on the distribution of spinally projecting neurones in the female Wistar rat.

This study aims to assess whether changes in the expression of specific $GABA_A$ and NMDA receptor subunits are associated with changes in the expression of immunoreactive cells in parvocellular subnuclei of the PVN. It is therefore important to assess whether the anatomical boundaries of parvocellular subnuclei described previously in other species of rat match those observed in the female Wistar rat.

The aim of this chapter was to map the distribution of spinally projecting neurones in the PVN of the female Wistar rat, and to identify subnuclei boundaries to assist in later cell count analysis.

II. Identification of spinally projecting neurones from the PVN of the female Wistar rat

CTB injection into the T2 region of the spinal cord of two normotensive female Wistar rats labelled 1090 ± 92 (range 998 – 1182) neurones throughout the rostrocaudal extent of the PVN. CTB injection into the spinal cord labelled neurones in five distinct nuclei in the ipsilateral PVN (Figure 27) with a small amount of labelling present in the contralateral PVN.

Labelling was confined to the PVN, with no identifiable neurones present in other hypothalamic nuclei (Figure 27 Ai-Ci).

Spinally projecting neurones were mainly located in the mid- to caudal levels of the PVN (Bregma -1.80mm to -2.12mm) and showed both somatic and projection labelling.

PVN-IML projecting neurones were found in the anterior parvocellular (A), dorsal cap and ventral parvocellular (B), medial and posterior parvocellular subnuclei (C). The somata of neurones in the anterior, medial, dorsal cap and ventral parvocellular regions were similar in size (23.33 ± 0.87μm; range 19.8 – 26.9μm), but significantly smaller than those in the posterior parvocellular subnucleus (45.85 ± 3.02μm; range 40.5 – 54.5μm; $P<0.0001$) when measured at their greatest diameter. Some labelled neurones were observed in magnocellular subnuclei, as has previously been reported (Pyner & Coote, 2000; Oldfield *et al*, 2001).

CTB-labelling was present in both soma (indicated by * on inset images of Figure 27 Ai-Ci) and projections (indicated by arrow head on inset images of

Figure 27) in all subnuclei. Neurones in the posterior parvocellular subnuclei had a flattened appearance and were orientated such that the apical points of the soma were lying horizontal to the vertical midline (Figure 27 Ci plus inset). Neurones in the remaining parvocellular subnuclei had no such level of organisation (Figure 27 Ai/Bi).

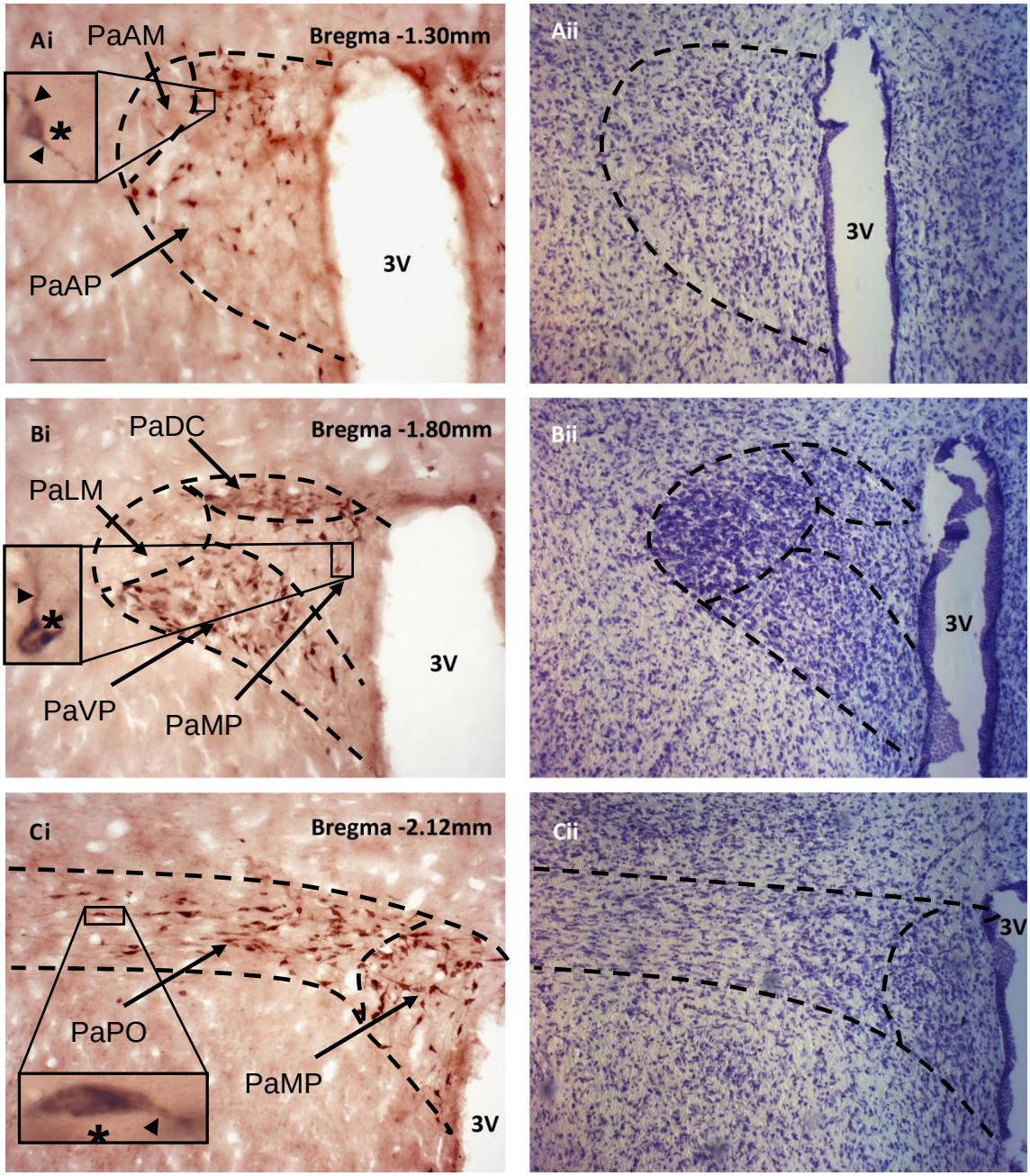

Figure 27 Photomicrographs of CTB-labelled spinally projecting PVN neurones (Ai-Ci) and corresponding Cresyl violet stained countersections (Aii-Cii). Inset images show magnified views of highlighted neurones. Arrowheads = labelled projections, * = labelled soma. PaAP = Anterior Parvocellular; PaAM = Anterior Magnocellular PaDC = Dorsal Cap; PaVP = Ventral Parvocellular; PaLM = Lateral Magnocellular; PaMP = Medial Parvocellular; PaPO = Posterior Parvocellular; 3V = 3rd Ventricle. Scale Bar = 200µm

Chapter 5. Localisation of NMDA Receptor Subunits in the PVN

I. Introduction

Electrophysiological studies in normotensive rats have shown that application of glutamate into the PVN consistently increases sympathetic outflow, heart rate and blood pressure (Li *et al.*, 2006). In addition, endogenous glutamate appears to be heavily inhibited by GABAergic inhibitory networks under normotensive conditions (Chen *et al.*, 2003; Li *et al.*, 2006).

Studies examining the role of the PVN in the aetiology of hypertension have identified that glutamatergic activity appears to be increased. To this effect, application of NMDA directly onto PVN-IML projecting neurones *in vitro* produces a greater inward current in SHR rats than in age matched WKY controls (Li *et al.*, 2008a). Furthermore, antagonism of NMDA receptors in the PVN of SHR significantly decreased LSNA, ABP and HR; a response, which was not observed in age matched WKY controls.

In vitro electrophysiological studies have identified that the GluN2A subunit of the NMDA receptor appears to be up-regulated in the PVN of male SHR compared to age matched WKY controls (Ye *et al.*, 2012b). This up-regulation of the GluN2A subunit was also observed to contribute to the sympathoexcitation observed in these animals and normalisation of GluN2A levels returned NMDA receptor currents to control levels (Ye *et al.*, 2012b).

Pregnancy is a physiological condition that has also been shown to display increased sympathetic outflow controlled in part from the PVN (Kvochina *et al.*, 2009; Page *et al.*, 2011). However blockade of NMDA receptors in the PVN of

late-term pregnant rats did not significantly decrease the level of sympathetic outflow compared to when AT_1 receptors alone were blocked, suggesting that NMDA receptors do not play a significant role in mediating the sympathoexcitation observed in pregnancy (Kvochina *et al.*, 2009).

The aim of this chapter was to identify whether the increase in GluN2A subunit expression observed in the PVN of the male SHR were also observed in the PVN of female SHRs, as well as identifying whether pregnancy was associated with any molecular changes in NMDA receptor subunit expression. Furthermore, this was combined with immunohistochemical identification of the distribution and quantification of cell immunoreactivity to assess within which subnuclei of the PVN any of the identified changes occurred.

II. Determination of NMDA Receptor Subunit Expression by Quantitative Immunoblotting

a. PVN

Expression levels of NMDA subunits in the PVN were analysed from PVN micropunches from non-pregnant normotensive Wistar rats, 14 week old SHR and late-term pregnant Wistar rats as described in section 2.X. The level of GluN1 subunit expression was not significantly changed in either normotensive, SHR or pregnant rats (Figure 28). There was a slight, but non-significant decrease in expression of the GluN2A subunit in the late-term pregnant rat compared with Wistar controls (Figure 29); however there was an 85 ± 23% increase in expression in the SHR (Figure 29). There was also a significant increase in GluN2B expression in the PVN of late-term pregnant rats compared with normotensive and SHR (fig. 30), but no significant change observed in the SHR compared with normotensive controls.

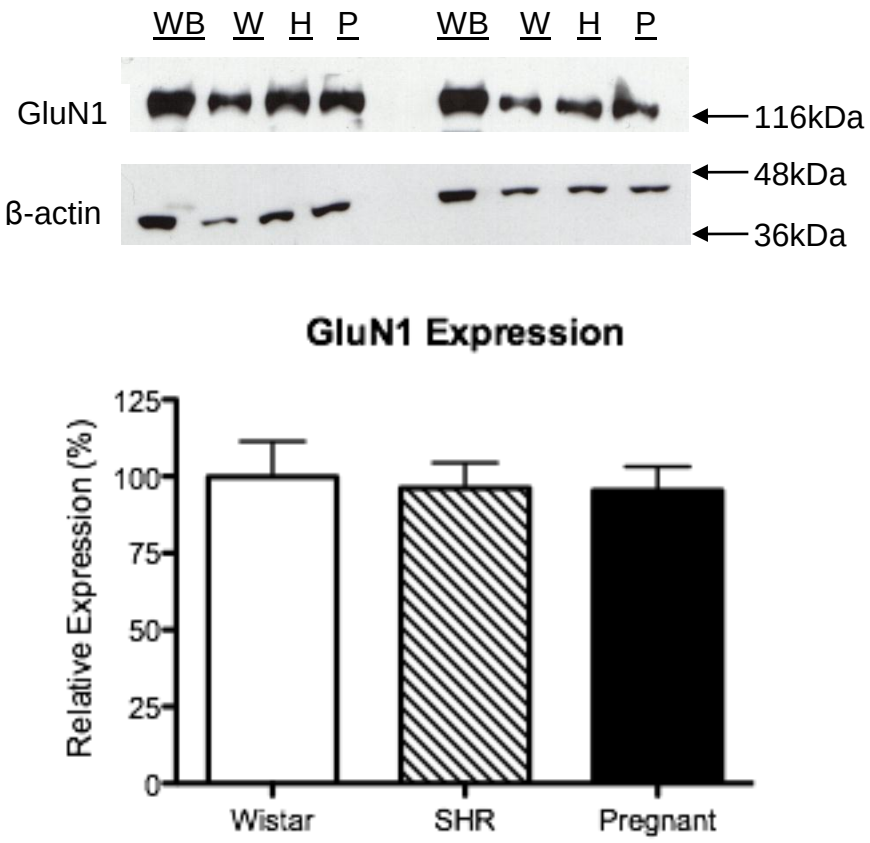

Figure 28 Expression of the GluN1 subunit of the NMDA receptor in the PVN of normotensive, SHR and late-term pregnant rats, expressed as a percentage relative to the Wistar control value. Analysis shows no significant change in expression between any of the physiological states. Whole brain homogenate from normotensive Wistar rats was probed to act as a positive control. WB = Whole brain, W = Wistar, H = SHR, P = Pregnant. N = 6 biological replicates. Molecular weight of GluN1 band = 120kDa. Molecular weight of β-actin band = 42kDa

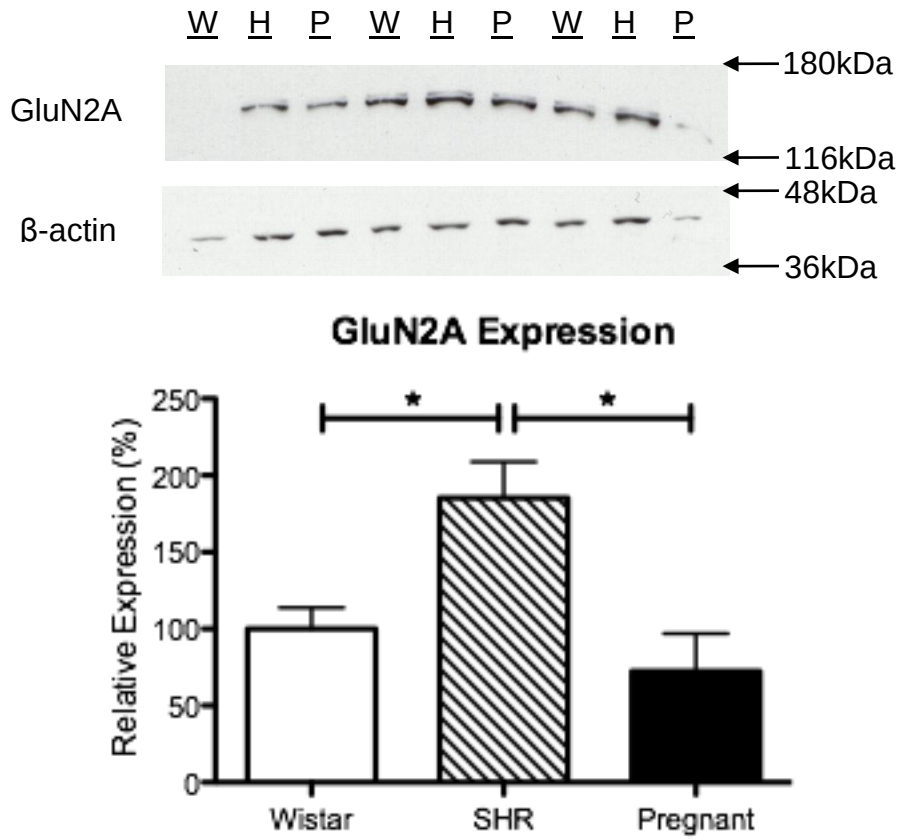

Figure 29 Expression of the GluN2A subunit of the NMDA receptor in the PVN of normotensive controls, SHR and late-term pregnant Wistar rats, expressed as a percentage relative to Wistar. Analysis shows a significant increase in expression in the SHR compared to both normotensive ($P<0.05$) and late-term pregnant ($P<0.05$) rats. W = Wistar, H = SHR, P = Pregnant. N=7 biological replicates. Molecular weight of GluN2A band = 170kDa. Molecular weight of β-actin band = 42kDa.

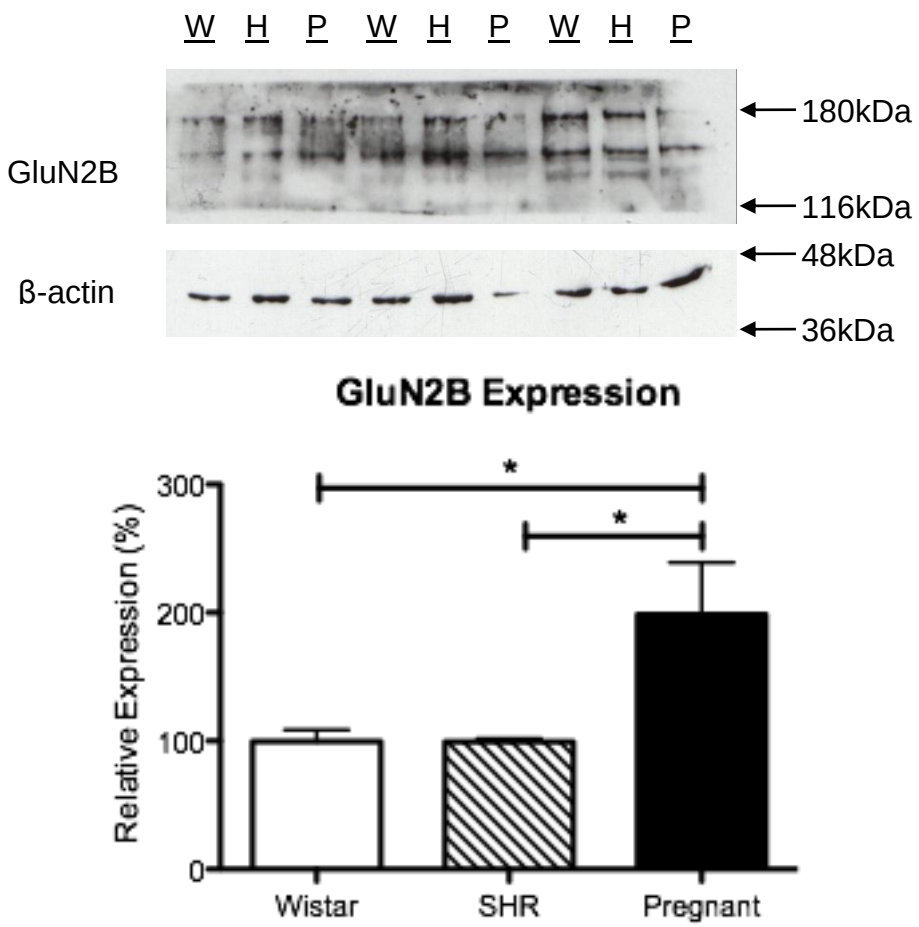

Figure 30 Expression of the GluN2B subunit of the NMDA receptor in the PVN of normotensive controls, SHR and late-term pregnant rats, expressed as a percentage relative to Wistar. Analysis shows a significant increase in expression in the pregnant rat compared with normotensive, non-pregnant ($P<0.05$) and SHR ($P<0.05$). W = Wistar, H = SHR, P = Pregnant. N = 3 biological replicates. The lower band of the GluN2B subunit blot represents the expected molecular weight of the GluN2B subunit (166kDa). The higher band represents the expected molecular weight of the phosphorylated GluN2B subunit (180kDa). For this reason, the density of both bands was measured. The molecular weight of the β-actin band was 42kDa.

b. GluN2A Levels in Cortex

To identify whether the increase in GluN2A subunit expression observed in the SHR was specific to the PVN, the level of GluN2A expression was measured from samples of cortex taken from the same animals. The level of GluN2A subunit expression in the cortex of SHR and pregnant Wistars was significantly decreased compared with normotensive Wistars (37±0.5% and 47±6.5% decrease respectively; Figure 31).

Western blotting of the GluN2A subunit in the cortex revealed a second, smaller band with a molecular weight of around 140kDa. This band is believed to be a proteolytic fragment possibly caused by the serine protease plasmin (Yuan *et al*, 2009). We hypothesise that this was not observed in the PVN due to the potentially lower protein expression observed.

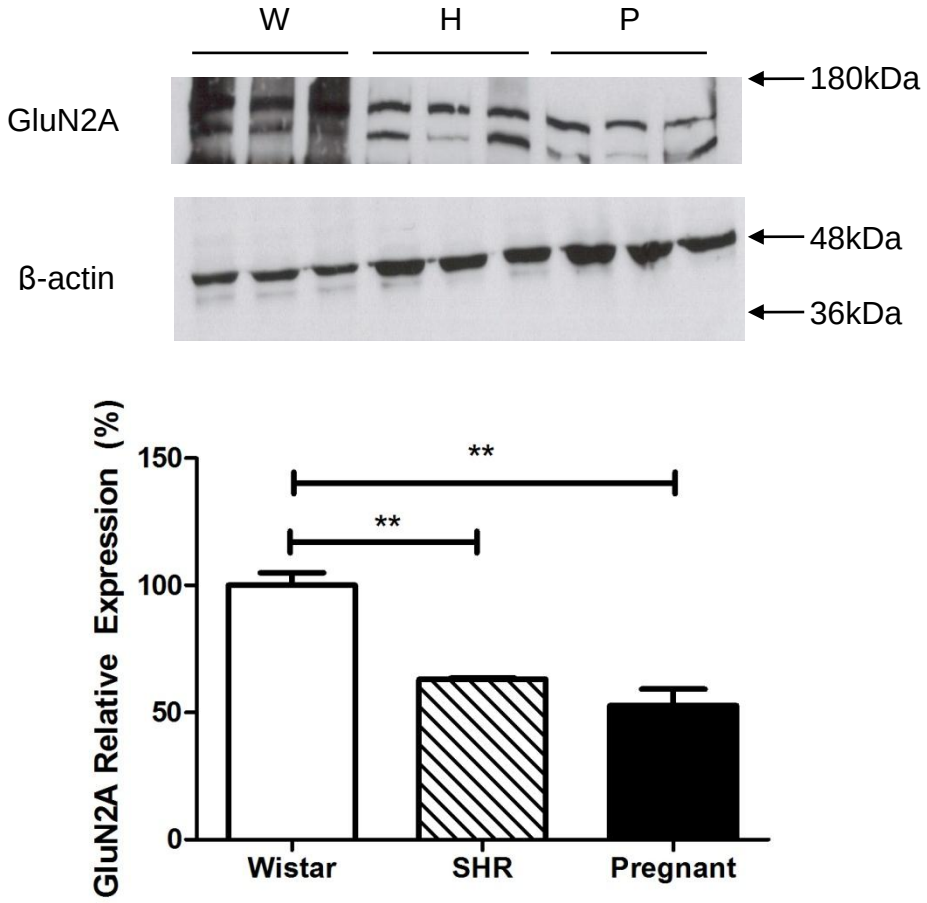

Figure 31 Expression of GluN2A subunit expression in the cortex of normotensive controls, SHR and late-term pregnant rats; expressed as a percentage relative to normotensive controls. Analysis shows a significant reduction in expression in both SHR (P<0.01) and late-term pregnant rats (P<0.01) relative to normotensive controls. W = Wistar, H = SHR, P = Pregnant. N = 3 biological replicates. The higher band on the GluN2A subunit blot represents the expected molecular weight of the GluN2A subunit (170kDa). The lower band is believed to be a proteolytic fragment with a molecular weight of around 140kDa. For this reason the density of both bands were measured.

III. NMDA Receptor Subunit Expression Revealed by Immunohistochemical Analysis

Cells immunoreactive (IR) for the GluN1, -2A and -2B subunits of the NMDA receptor were found throughout the rostrocaudal extent of the PVN and within all five parvocellular subnuclei in normotensive (Figure 32), SHR (Figure 33) and late-term pregnant rats (Figure 34).

a. GluN1

GluN1 immunoreactivity was confined to the soma of neurones with no projections labelled (Figures 31-33 B,D,F). Cells in the anterior (Figures 31-33 A/B), medial, ventral and dorsal (Figures 32-34 C/D) subnuclei showed dark uniform staining (an example of which is identified by * in images B & D of Figure 32-34), whereas labelling in cells of the posterior subnucleus was confined to the lateral edges of each cell (an example of which is identified by an ‡ in image F of Figure 32-34).

GluN1-IR cells within the posterior subnucleus have a flattened appearance and are orientated in the same plane, such that their apical points are lying horizontally to the vertical midline. GluN1-IR cells within the subsequent four parvocellular subnuclei appear to have no such level of organised orientation.

Semi-quantitative analysis of immunohistochemical staining of the GluN1 subunit showed the highest density of GluN1-IR cells were located in the dorsal cap region in both normotensive (23 ± 1.8; range 20-26) and late-term pregnant rats (22 ± 2.6; range 17 – 26) Figure 35). SHR showed a higher proportion of GluN1 staining in the ventral parvocellular subnuclei (24 ± 2; range 20 – 26;

Figure 35), although there was no statistically significant difference between any of the subnuclei. No significant change in expression was found in any subnuclei of the PVN between normotensive and SHR or late-term pregnant rats. A small but significant reduction was observed between SHR and late-term pregnant rats in the medial parvocellular subnuclei (SHR = 21.6 ± 0.8; range 20 – 24. Late-term pregnancy = 16 ± 1.8; range 14 – 18), but this was not significant when compared against normotensive controls (Figure 35).

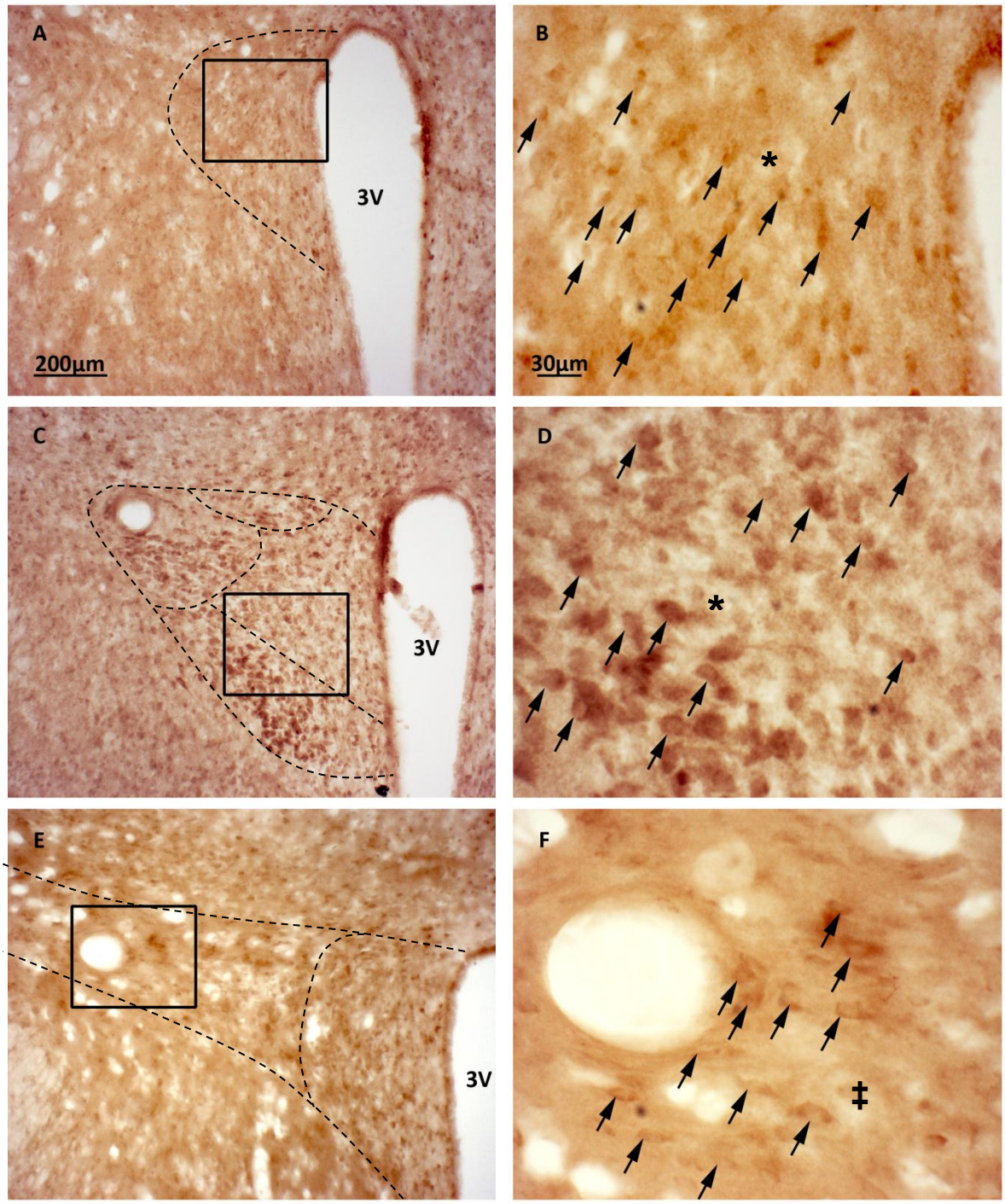

Figure 32 Photomicrographs showing expression of the GluN1 subunit throughout the rostrocaudal extent of the PVN of normotensive rats. Neurones immunoreactive for GluN1 (GluN1-IR) were found in the anterior (A-B), medial, ventral, dorsal cap (C-D) and posterior (E-F) parvocellular subdivisions. Neurones show somatic labelling (arrows) with no identifiable projections observed. Somatic labelling was mainly observed around the periphery of each neurone in the posterior (F) subnuclei. Neurones in the anterior (A/B) medial, ventral and dorsal cap subnuclei (C/D) show full-somatic labelling with no apparent anatomical bias. Boxed regions in A, C & E represent images B, D & F respectively. 3V = 3rd ventricle. Scale bar 200µm A, C & E. 30µm B, D & F. * = example of neurone showing uniform staining throughout soma. ‡ = example of neurone showing staining confined to lateral aspects of soma. Arrows = example of identified neurones

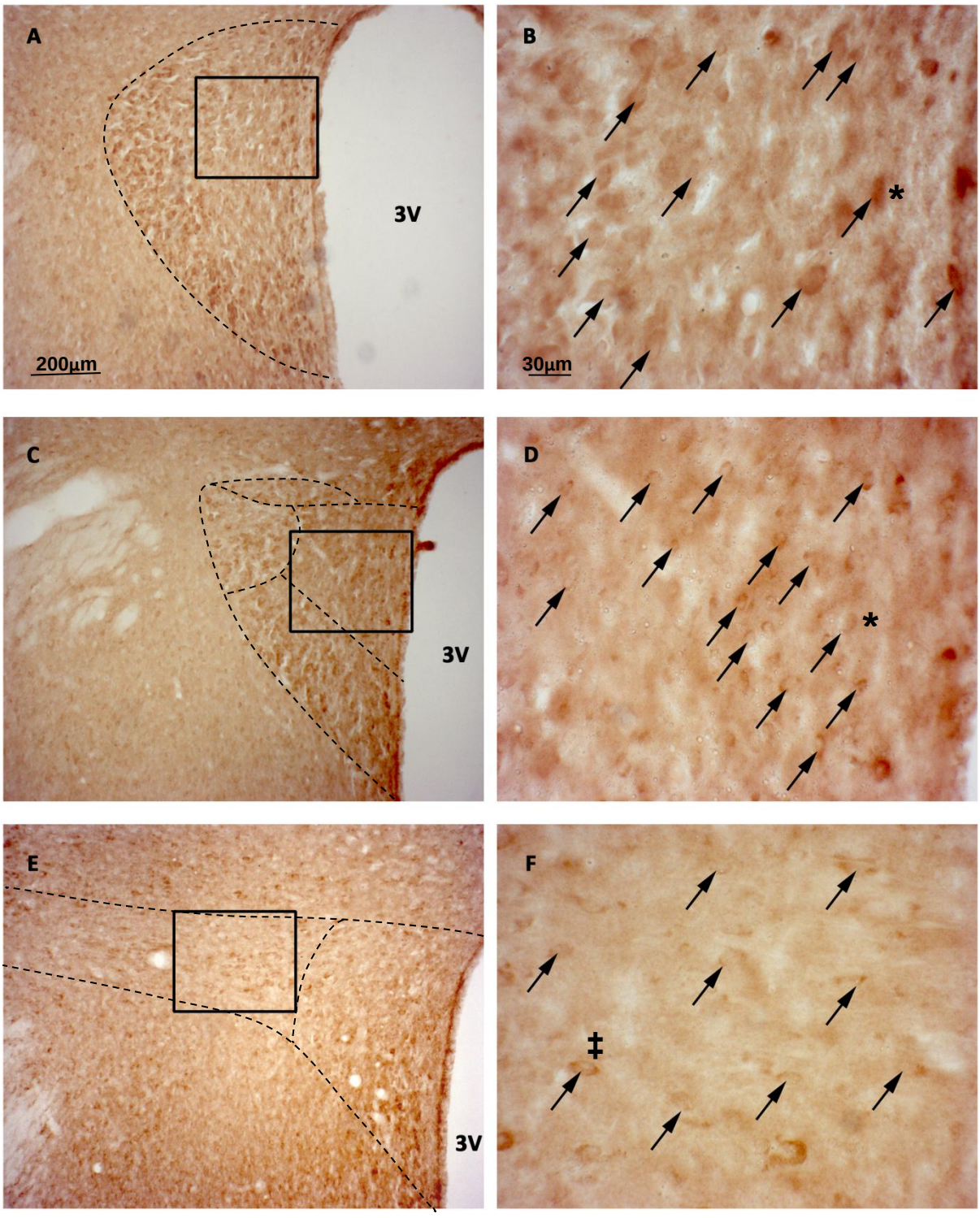

Figure 33 Photomicrographs showing expression of the GluN1 subunit throughout the rostrocaudal extent of the PVN of SHR. Neurones immunoreactive for GluN1 (GluN1-IR) were found in the anterior (A-B), medial, ventral, dorsal cap (C-D) and posterior (E-F) parvocellular subdivisions. Neurones show somatic labelling (arrows) with no identifiable projections observed. Somatic labelling was mainly confined to the periphery of each neurone in all subnuclei. Boxed regions in A, C & E represent images B, D & F respectively. 3V = 3rd ventricle. Scale bar 200µm A, C & E. 30µm B, D & F. * = example of neurone showing uniform staining throughout soma. ‡ = example of neurone showing staining confined to lateral aspects of soma. Arrows = example of identified neurones

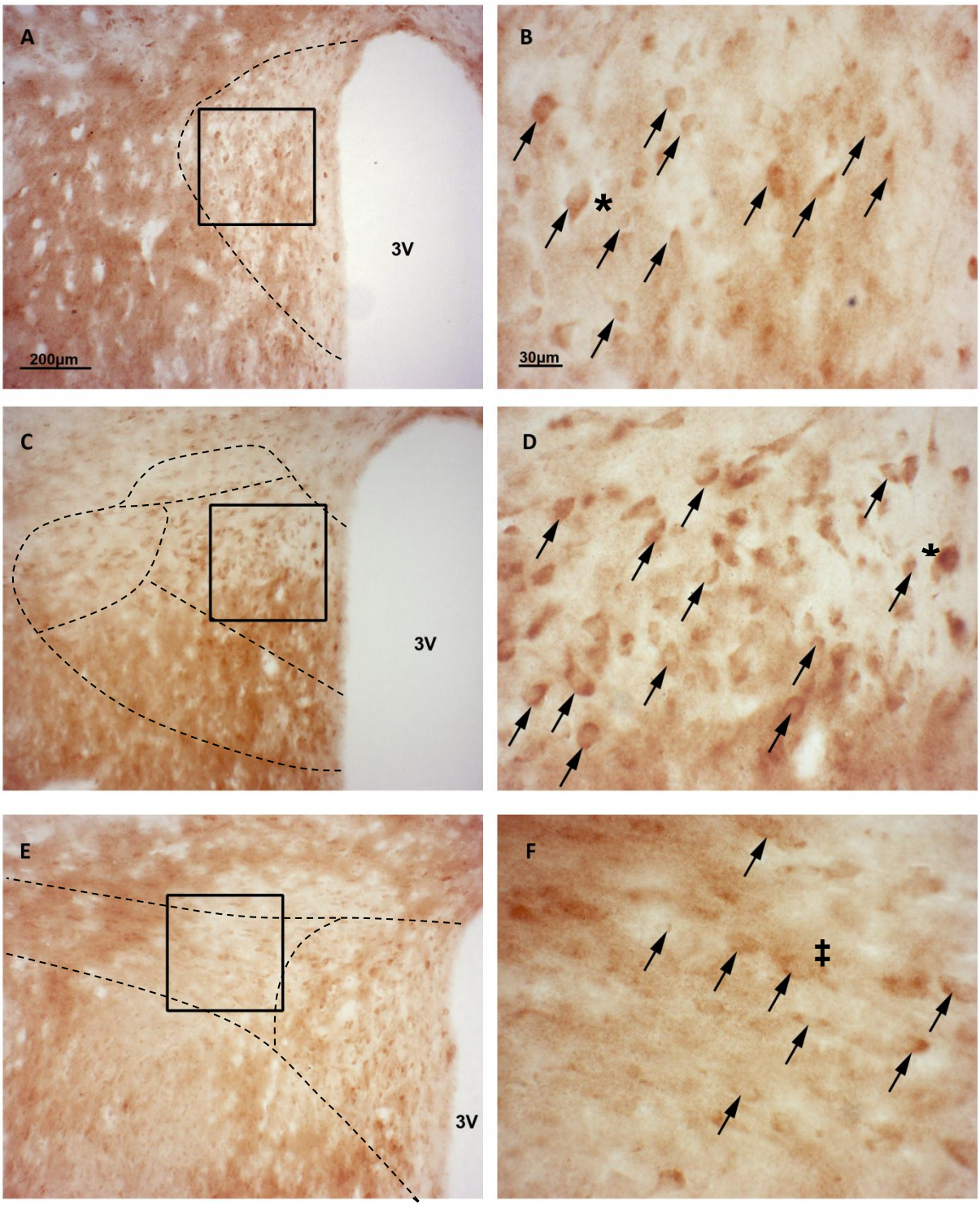

Figure 34 Photomicrographs showing expression of the GluN1 subunit throughout the rostrocaudal extent of the PVN of late-term pregnant rats. Neurones immunoreactive for GluN1 (GluN1-IR) were found in the anterior (A-B), medial, ventral, dorsal cap (C-D) and posterior (E-F) parvocellular subdivisions. Neurones show somatic labelling (arrows) with no identifiable projections observed. Somatic labelling was mainly confined to the periphery of each neurone in all subnuclei. Boxed regions in A, C & E represent images B, D & F respectively. 3V = 3rd ventricle. Scale bar 200µm A, C & E. 30µm B, D & F. * = example of neurone showing uniform staining throughout soma. ‡ = example of neurone showing staining confined to lateral aspects of soma. Arrows = example of identified neurones

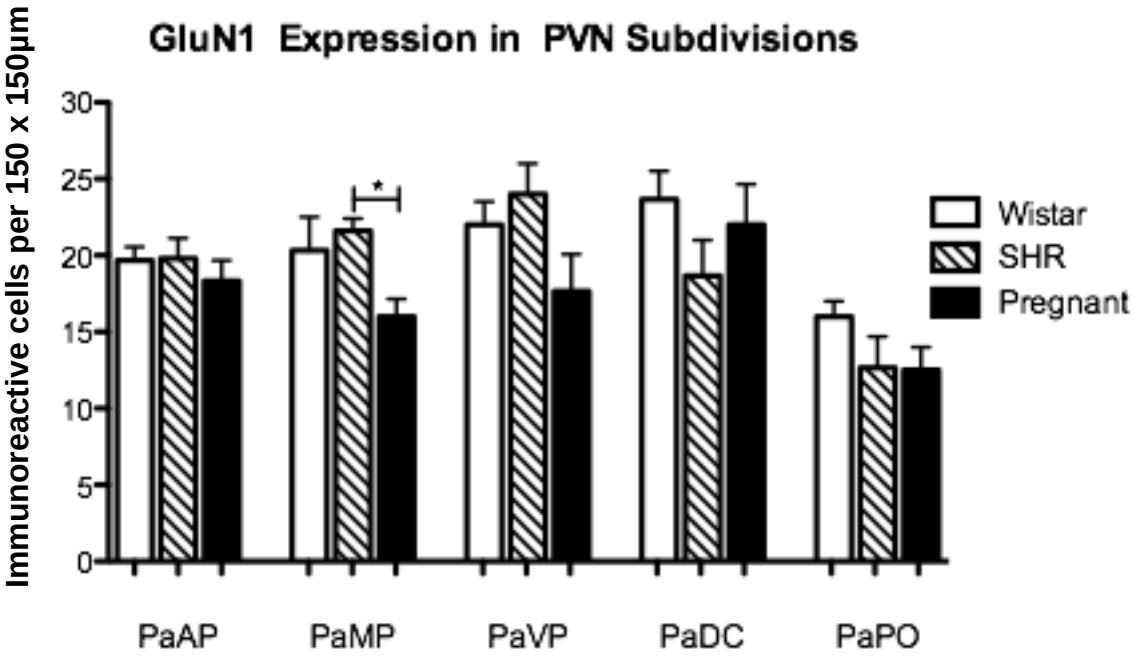

Figure 35 Mean GluN1-IR cells per 150µm x 150µm in the five-parvocellular subnuclei of the PVN in normotensive, SHR and late-term pregnant rats. Analysis shows no significant change in GluN1 subunit expression in either hypertension or late-term pregnancy compared with normotensive controls. A small, but significant decrease in expression was noted between SHR and late-term pregnancy in the PaMP. The highest density of staining was observed in the dorsal cap in both non-pregnant and late-term pregnant rats and the ventral parvocellular subnuclei in the SHR. *Abbr. = PaAP = Anterior Parvocellular, PaMP = Medial Parvocellular, PaVP = Ventral Parvocellular, PaDC = Dorsal Cap, PaPO = Posterior Parvocellular*. Values are ± SEM. Significance Values: * = P<0.05. N=4 biological replicates for each subnucleus.

b. GluN2A

Cells which were immunoreactive for the GluN2A subunit of the NMDA receptor were found throughout the rostrocaudal extent of the PVN and in all subnuclei for each physiological state (Figures 36-38). Both somatic (indicated by * in Figures 36-38) and projection labelling (identified by arrowhead in Figures 36-38) was identified throughout all five parvocellular subnuclei.

Neurones in all parvocellular subnuclei had uniform staining throughout the soma, with no apparent anatomical bias observed (Figures 36-38 B/D/F). GluN2A-IR cells within the posterior subnucleus have a flattened appearance and are orientated in the same plane, such that their apical points are lying horizontally to the vertical midline (Figure 36-38 F). GluN2A-IR cells within the subsequent four parvocellular subnuclei appear to have no such level of organised orientation (Figure 36-38 B/D).

Semi-quantitative analysis of GluN2A-IR cells shows the highest proportion to be within the dorsal cap region of the normotensive animal (37 ± 1.3; range 35 – 39), and the anterior and ventral parvocellular subnuclei of the late-term pregnant rat (AP = 35 ± 2.8; range 28 – 45. VP = 35 ± 2.8; range 32 – 41). There was no statistical significance in any of the parvocellular subnuclei between non-pregnant and pregnant rats. Conversely however, GluN2A-IR staining was significantly increased in the medial (48 ± 2.8; range 45 – 54. 32 ± 7.8% increase compared with control), dorsal cap (45 ± 1.7; range 42 – 48. 19 ± 4% increase compared with control) and posterior (37.5 ± 2.5; range 35 – 40. 57 ± 10% increase compared with control) parvocellular regions in the SHR (Figure 39).

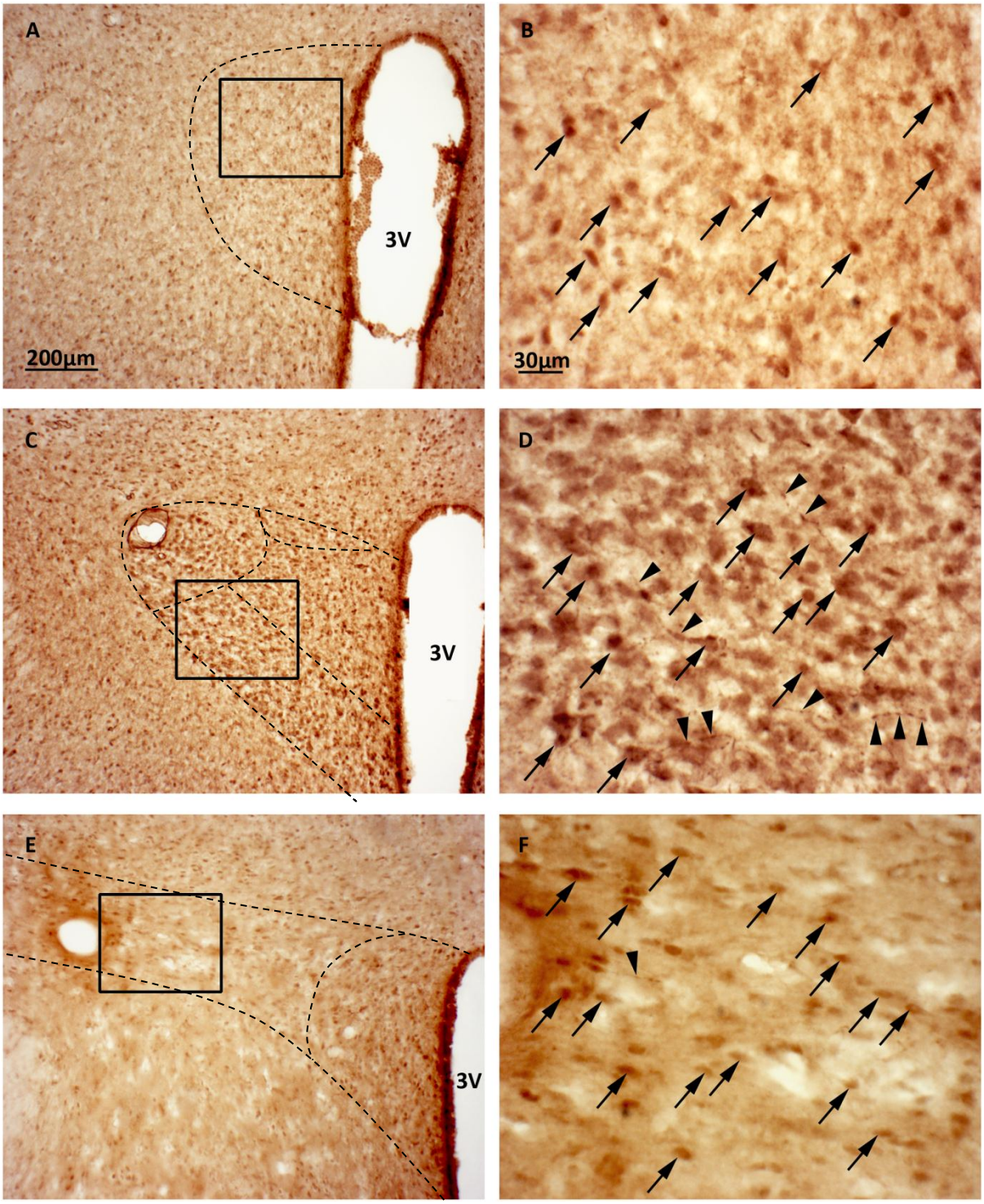

Figure 36 Photomicrographs showing expression of the GluN2A subunit throughout the rostrocaudal extent of the PVN of normotensive rats. GluN2A-IR neurones were found in the anterior (A-B), medial, ventral, dorsal cap (C-D) and posterior (E-F) parvocellular subdivisions. Neurones show both somatic labelling (arrows) and projection labelling (arrowheads). Somatic labelling was confined to the periphery in a subset of neurones in all subnuclei, however the majority of neurones in the medial, ventral and dorsal cap (D), as well as some in the anterior (A) and posterior (F) show uniform labelling with no apparent sub-cellular bias. Boxed regions in A, C & E represent images B, D & F respectively. 3V = 3rd ventricle. Scale bar 200µm A, C & E. 30µm B, D & F. * = example of neurone showing uniform staining throughout soma. Arrows = example of identified neurones

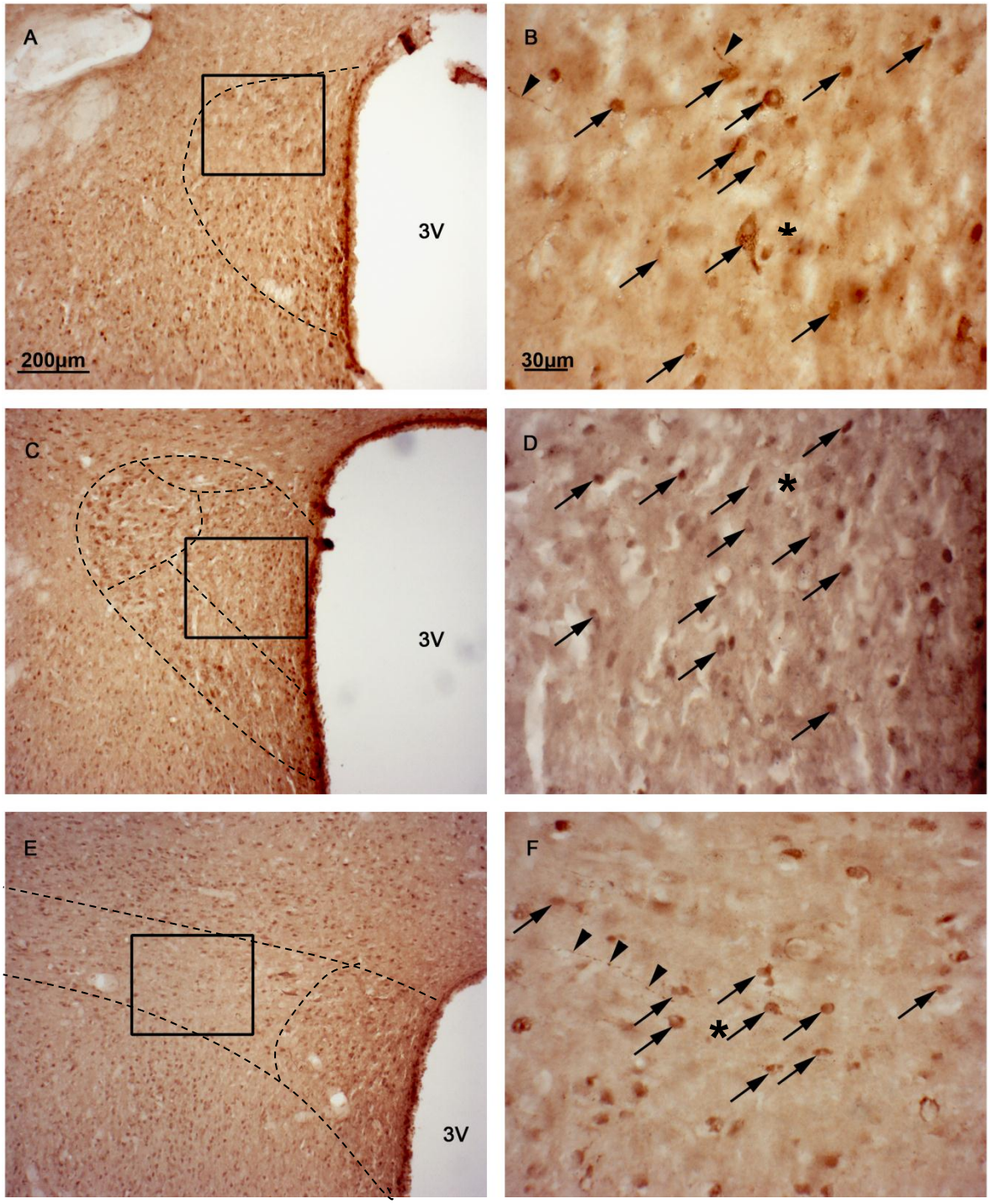

Figure 37 Photomicrograph showing expression of the GluN2A subunit throughout the rostrocaudal extent of the PVN of the SHR. GluN2A-IR neurones were found in the anterior (A-B), medial, ventral, dorsal cap (C-D) and posterior (E-F) parvocellular subdivisions. Neurones show predominantly somatic labelling (arrows) with a few labelled projections (arrowheads). All subnuclei display neurones which show staining localised to the periphery of the cell as well as neurones that show uniform cell labelling throughout the soma. Boxed regions in A, C & E refer to the magnified areas in B, D & F respectively. 3V = 3rd ventricle. Scale bar in A refers to C & E also. Scale bar in B refers to D & F also. * = example of neurone showing uniform staining throughout soma. Arrows = example of identified neurones

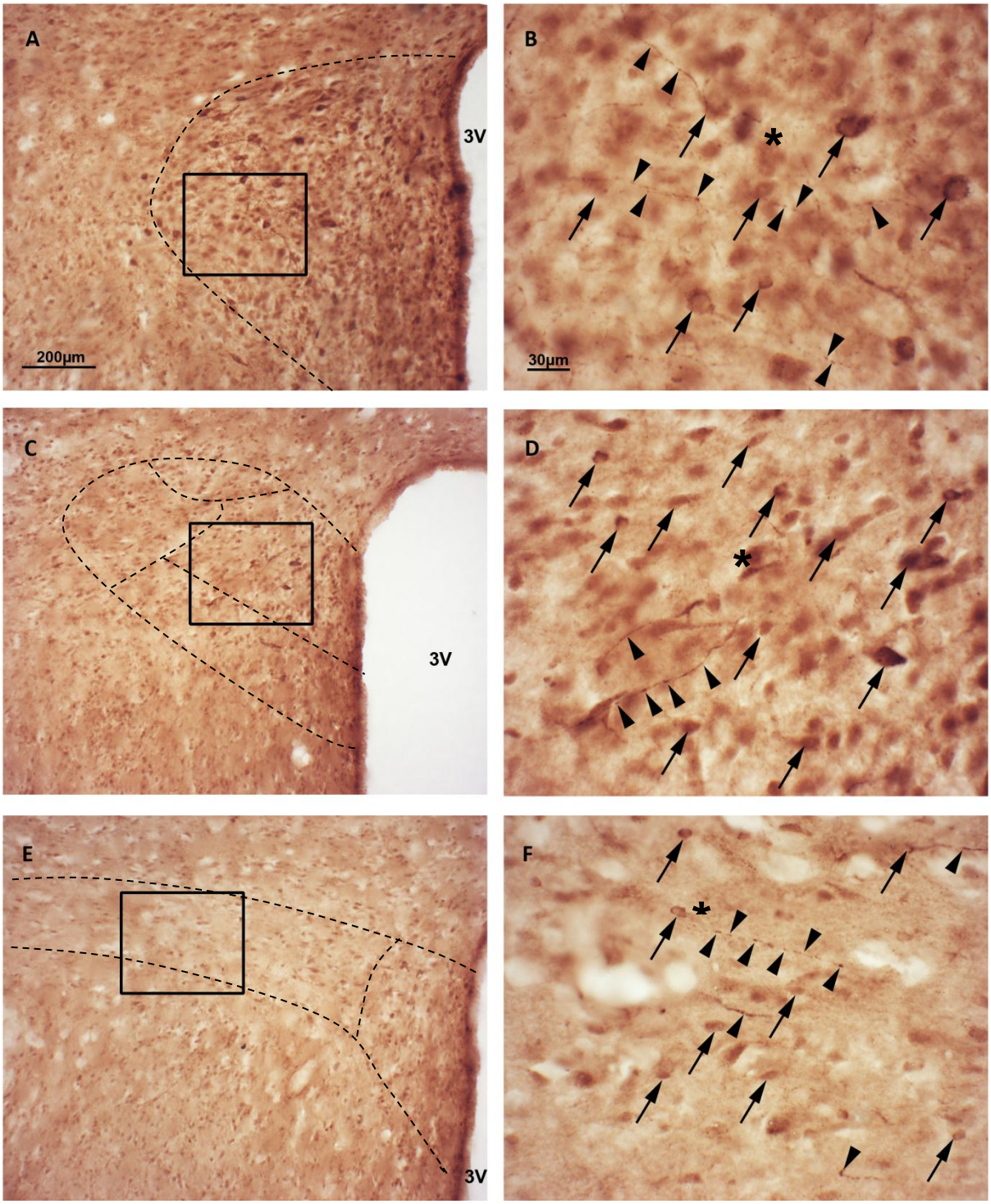

Figure 38 Photomicrographs showing expression of the GluN2A subunit throughout the rostrocaudal extent of the PVN of late-term pregnant rats. GluN2A-IR neurones were found in the anterior (A-B), medial, ventral, dorsal cap (C-D) and posterior (E-F) parvocellular subdivisions. Neurones show both somatic (arrows) and projection labelling (arrowheads). All subnuclei display neurones where labelling is confined to the periphery of the cell as well as neurones where labelling is uniform throughout. Boxed regions in A, C & E represent images B, D & F respectively. 3V = 3rd ventricle. Scale bar 200µm A, C & E. 30µm B, D & F. * = example of neurone showing uniform staining throughout soma. Arrows = example of identified neurones

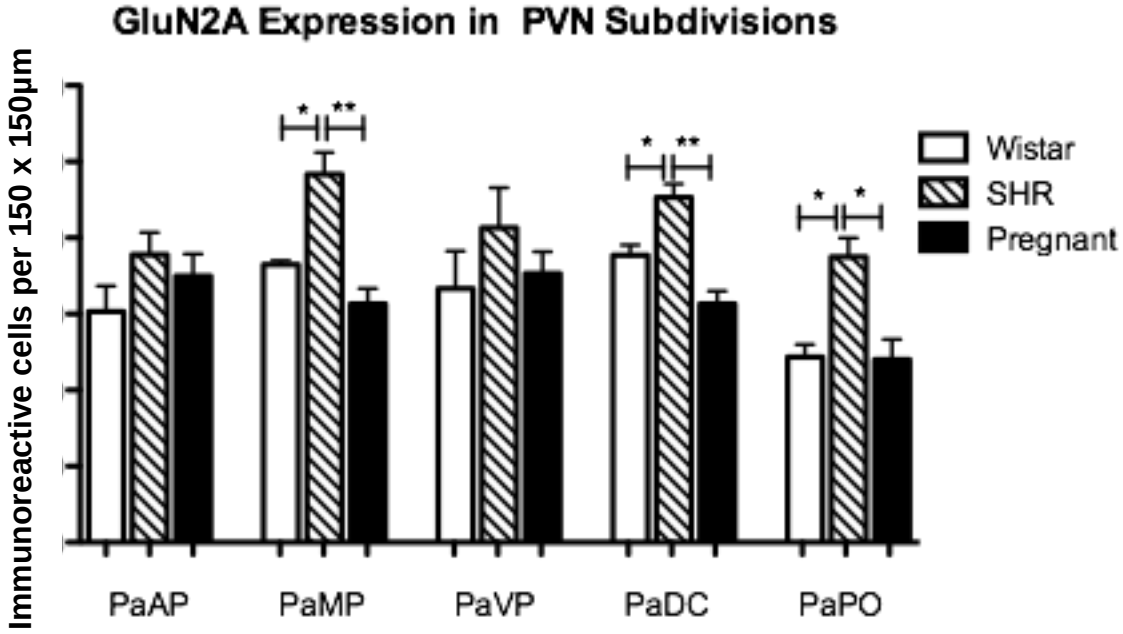

Figure 39 Mean number of GluN2A-IR cells per 150µm x 150µm in each subnuclei of the PVN in normotensive, SHR and late-term pregnant rats. A significant increase in expression was observed in the PaMP, PaDC and PaPO in the SHR compared with both normotensive and late-term pregnant rats.. *Abbr: PaAP = Anterior Parvocellular, PaMP = Medial Parvocellular, PaVP = Ventral Parvocellular, PaDC = Dorsal Cap, PaPO = Posterior Parvocellular*. Values are ± SEM. Significance values: * = P<0.05, ** = P<0.01. N=4 biological replicates for each subnucleus.

c. GluN2B

GluN2B subunits were found throughout the rostrocaudal extent of the PVN and in each subnucleus (Figure 40-42 A-F). GluN2B subunits were present in parvocellular subdivisions of the PVN; however they appeared to be more prominent in the magnocellular subdivisions, where immunoreactive cells were larger and stained darker (Figure 42 C). A proportion of cells in the ventral parvocellular subnuclei appear to have magnocellular morphology. However retrograde tracing methods (Chapter 4), have shown there to be the presence of spinally-projecting cells within this area. For this reason, all immunoreactive cells within this region have been counted.

GluN2B-IR stained cells were generally somatic in morphology (identified by * in Figures 40-42, with no projections observed. Staining appeared uniform in the anterior, medial, ventral and dorsal cap (Figure 40-42 B/D), with staining appearing to be confined to the lateral edges of each cell in the posterior subnucleus (Figure 40-42 F).

GluN2B-IR cells within the posterior subnucleus have a flattened appearance and are orientated in the same plane, such that their apical points are lying horizontally to the vertical midline (Figure 40-42 F). GluN2B-IR cells within the subsequent four parvocellular subnuclei appear to have no such level of organised orientation (Figure 40-42 B/D).

Semi-quantitative analysis of GluN2B-IR cells showed no significant change in expression amongst any of the parvocellular subnuclei in either normotensive non-pregnant, SHR or late-term pregnant rats (Figure 43). Analysis shows that the highest degree of GluN2B-IR cells are located in the anterior (Wistar = 21 ±

1.7; range 18 – 24. SHR = 22 ± 1.3; range 17 – 24. Pregnant = 22 ± 1.7; range 20 – 26) and ventral (Wistar = 27 ± 5; range 20 – 38. SHR = 22 ± 0.5; range 22 – 23. Pregnant = 26 ± 0.5; range 26 – 27) parvocellular subnuclei in all three physiological states (Figure 43).

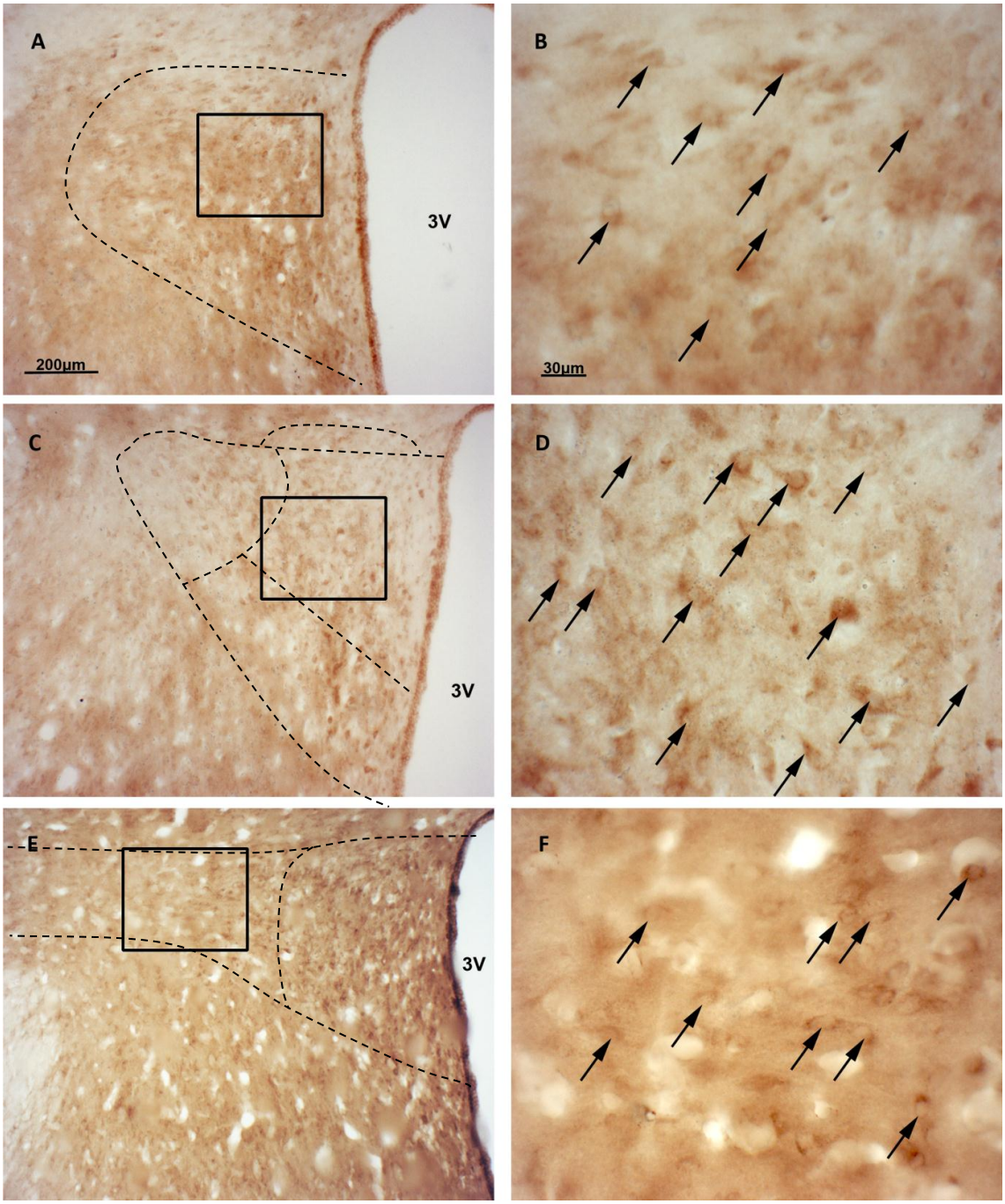

Figure 40 Photomicrographs showing expression of the GluN2B subunit throughout the rostrocaudal extent of the PVN of normotensive rats. GluN2B-IR neurones were found in the anterior (A-B), medial, ventral, dorsal cap (C-D) and posterior (E-F) parvocellular subdivisions. Neurones show somatic labelling only (arrows). In all subnuclei, staining was almost exclusively confined to the peripheral edge of the cell. Boxed regions in A, C & E represent images B, D & F respectively. 3V = 3rd ventricle. Scale bar 200µm A, C & E. 30µm B, D & F.

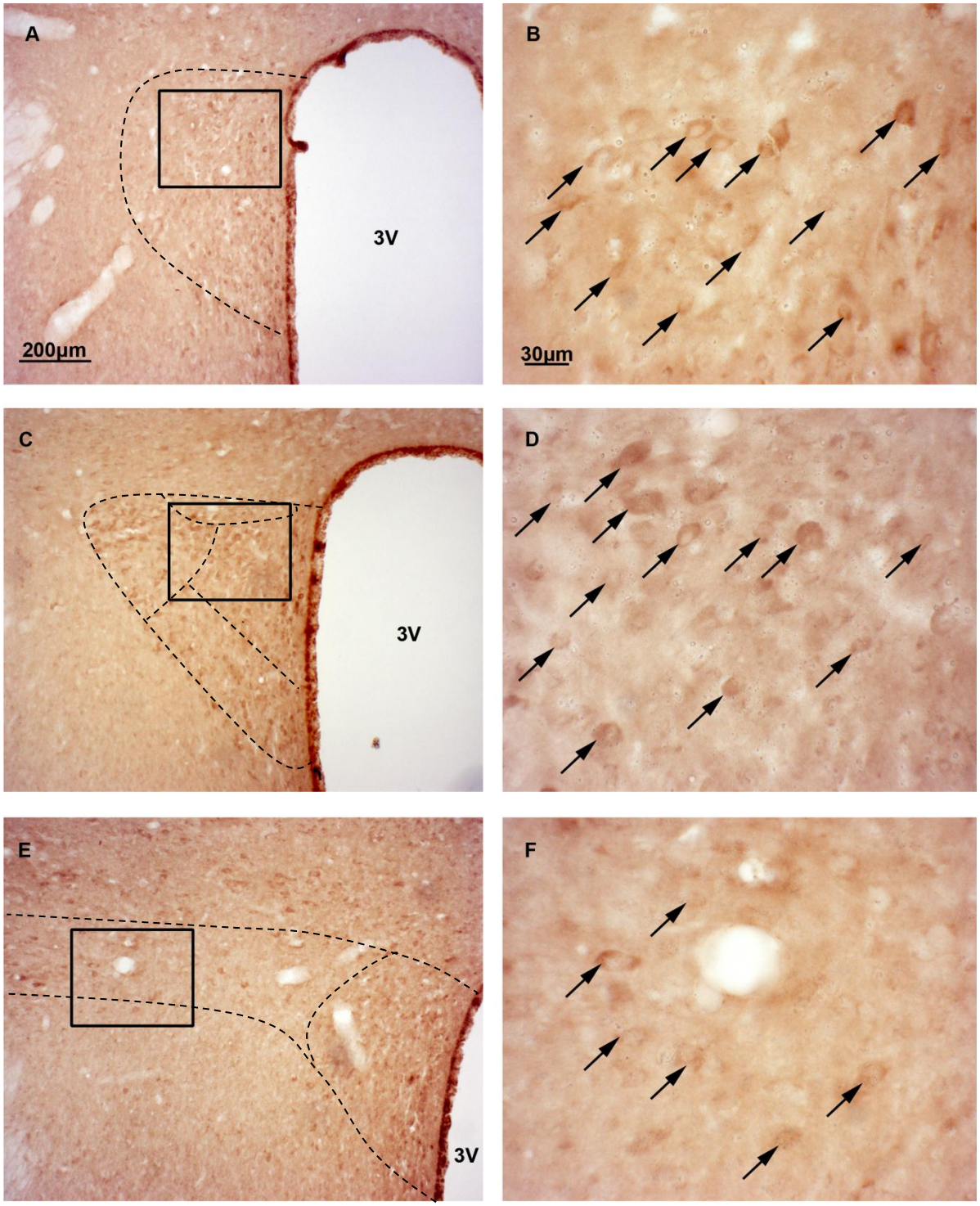

Figure 41 Photomicrographs showing expression of the GluN2B subunit throughout the rostrocaudal extent of the PVN of SHR. GluN2B-IR neurones were found in the anterior (A-B), medial, ventral, dorsal cap (C-D) and posterior (E-F) parvocellular subdivisions. Neurones show somatic labelling only (arrows). In all subnuclei, staining was almost exclusively confined to the peripheral edge of the cell. Boxed regions in A, C & E represent images B, D & F respectively. 3V = 3rd ventricle. Scale bar 200µm A, C & E. 30µm B, D & F.

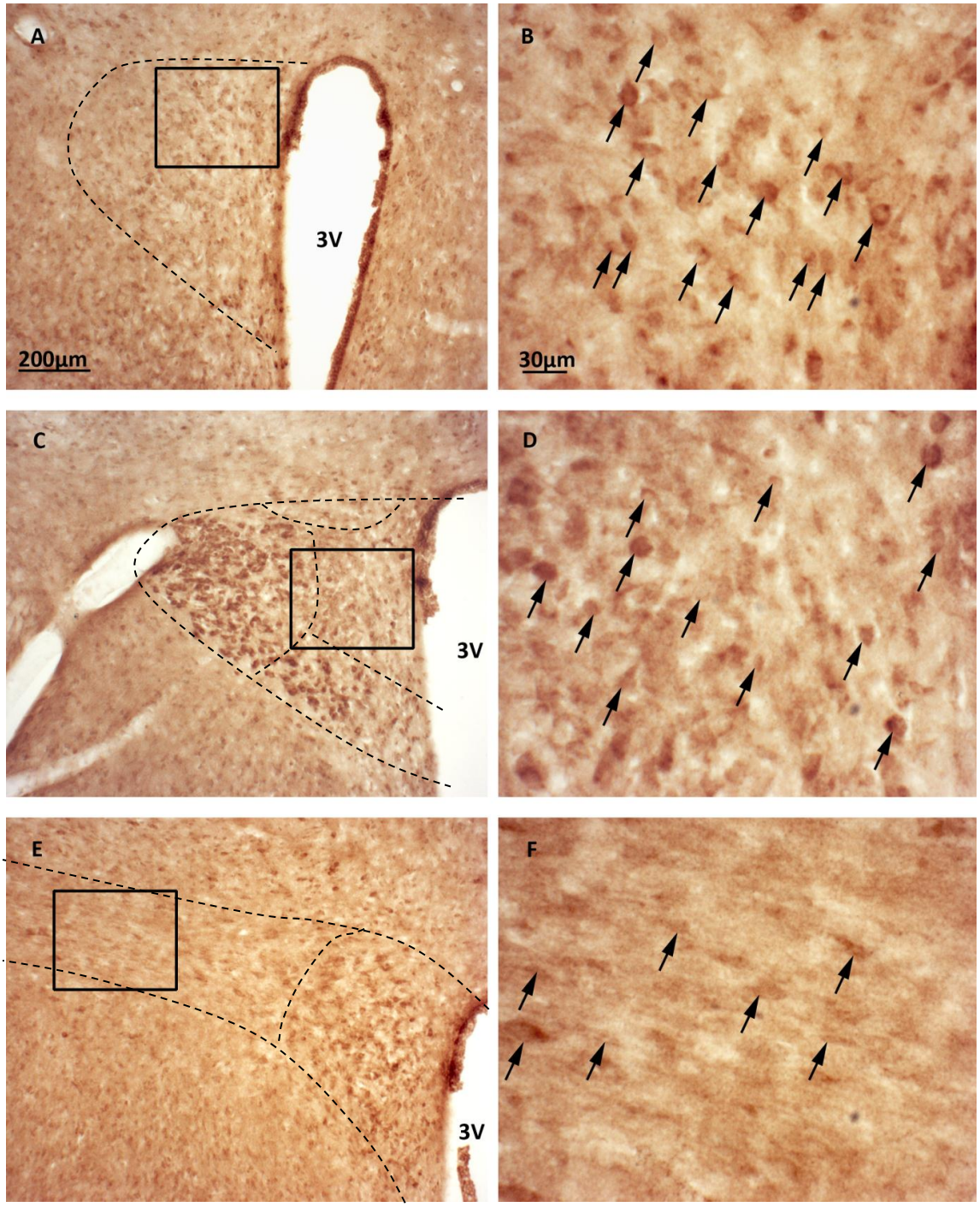

Figure 42 Photomicrographs showing expression of the GluN2B subunit throughout the rostrocaudal extent of the PVN of late-term pregnant rats. GluN2B-IR neurones were found in the anterior (A-B), medial, ventral, dorsal cap (C-D) and posterior (E-F) parvocellular subdivisions. Neurones show both somatic labelling (arrows), with no projections observed. Labelling in neurones located in the posterior parvocellular subnuclei (E/F) was confined to the periphery of the cell. In all other subnuclei, staining was uniform throughout the soma. Staining in magnocellular subnuclei was darker and more dense than in parvocellular subnuclei. Boxed regions in A, C & E represent images B, D & F respectively. 3V = 3rd ventricle. Scale bar 200µm A, C & E. 30µm B, D & F.

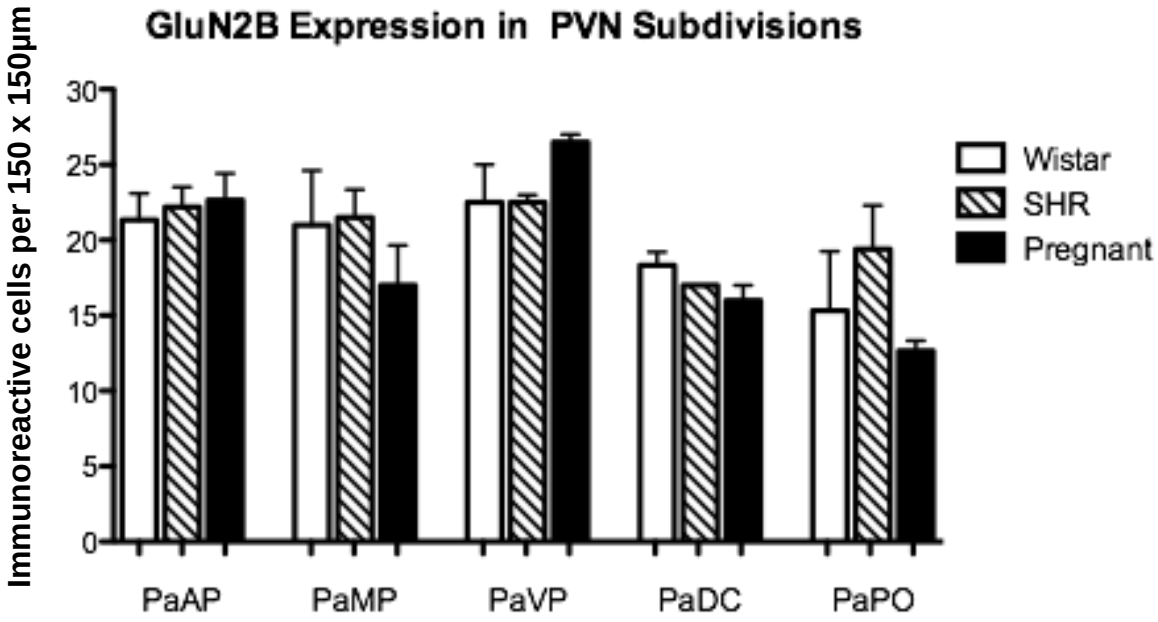

Figure 43 Mean number of GluN2B-IR cells per 150µm x 150µm in each subnuclei of the PVN in normotensive, SHR and late-term pregnant rats. No significant change in expression was observed across any of the subnuclei in either of the physiological states, in accordance with Western blot analysis. *Abbr: PaAP = Anterior Parvocellular, PaMP = Medial Parvocellular, PaVP = Ventral Parvocellular, PaDC = Dorsal Cap, PaPO = Posterior Parvocellular*. Values are ± SEM. N=4 biological replicates for each subnucleus.

Chapter 6. Localisation of $GABA_A$ Receptors in the PVN

I. Introduction

Around half of all synapses in the hypothalamus are GABAergic (Decavel & Van den Pol, 1990). Multiple i*n vivo* electrophysiological studies have shown that microinjection of GABA or $GABA_A$ receptor agonists into the PVN of normotensive rats produces profound depressor, bradycardic and sympathoinhibitory effects (Li & Pan, 2007b; Wang *et al.*, 2009). Furthermore, *in vitro* electrophysiological studies have shown that application of $GABA_A$ receptor antagonists dose dependently increases the firing activity of presympathetic neurones in the PVN (Li & Pan, 2006).

Both *in vivo* and *in vitro* electrophysiological studies have been utilised to explore the role of GABA and $GABA_A$ receptors in the PVN in the aetiology of sympathoexcitation in hypertension and pregnancy.

Studies in the SHR have revealed that microinjection of GABA or $GABA_A$ receptor agonists produce a blunted (Li & Pan, 2007b) or exaggerated (Allen, 2002; Akine *et al.*, 2003) sympathoinhibitory, depressor and bradycardic effect. *In vitro* electrophysiological studies however have shown that application of GABA onto PVN-RVLM projecting neurones produced a significantly blunted peak amplitude of GABA current compared with normotensive WKY and SD controls (Li & Pan, 2006).

Seldom work has been carried out to explore the role of the PVN in contributing to the sympathoexcitation observed in late-term pregnant rats. However of the work performed, blockade of $GABA_A$ receptors with the antagonist bicuculline produced significantly attenuated sympathoexcitatory, pressor and tachycardic

effects compared with non-pregnant controls (Kvochina *et al.*, 2009; Page *et al.*, 2011).

Given that both hypertension and late-term pregnancy appear to be associated with decreased GABAergic inhibition in the PVN, the purpose of this chapter was to examine whether these electrophysiological changes were associated with changes in the expression of specific $GABA_A$ receptor subunits. Furthermore, this was combined with immunohistochemical identification of $GABA_A$ receptor subunits to assess within which subnuclei of the PVN these changes occurred.

II. Determination of $GABA_A$ Receptor Subunit Expression by Quantitative Immunoblotting

a. PVN

Expression levels of the $GABA_A$ α1, α2, α5, β1, β2 and β3 subunits were analysed from bilateral whole PVN micropunches acquired from normotensive Wistar, SHR and late-term pregnant rats, as described in 2.X.

Expression of the α1 subunit was significantly reduced in both SHR (48 ± 6.5%; $P<0.01$) and late-term pregnant rats (43 ± 1.2%; $P<0.01$) compared with normotensive Wistars (Figure 44).

Expression of the α5 subunit was significantly reduced in both SHR (97 ± 2% decrease; $P<0.001$) and late-term pregnant rats (38 ± 8% decrease; $P<0.05$) compared to normotensive Wistar controls (Figure 46).

The expression of the α2 (Figure 45), β1 (Figure 47), β2 (Figure 48) and β3 (Figure 49) subunits was not significantly altered in the PVN of SHR or late-term pregnant rats compared with Wistar controls ($P>0.05$).

Quantitative immunoblotting failed to reveal any expression of the δ-subunit in normotensive, SHR and late-term pregnant rats (results not shown).

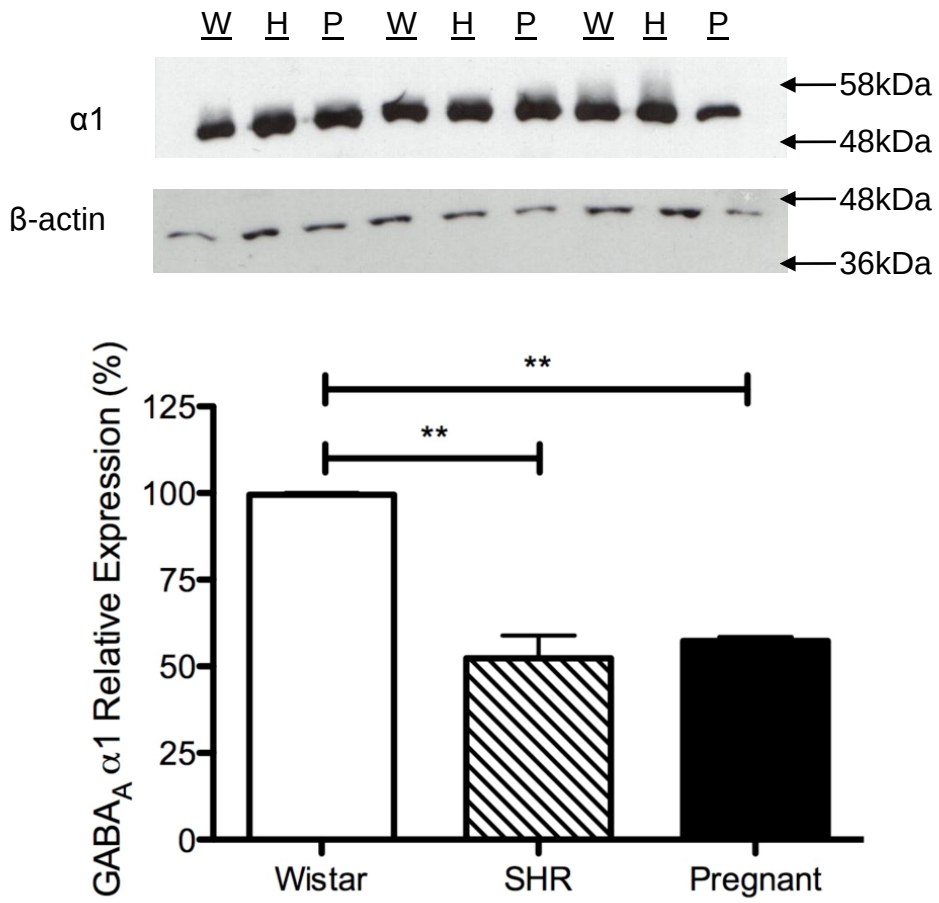

Figure 44 Expression of the $GABA_A$ α1 subunit in the PVN of normotensive, SHR and late-term pregnant rats expressed as a percentage relative to Wistar. Expression is 48 ± 6.5% lower in the SHR than Wistar controls (P<0.01). Expression is 43 ± 1.2% lower in the late-term pregnant rat compared with Wistar control (P<0.01). W = Wistar, H = SHR, P = Pregnant. n =3 biological replicates

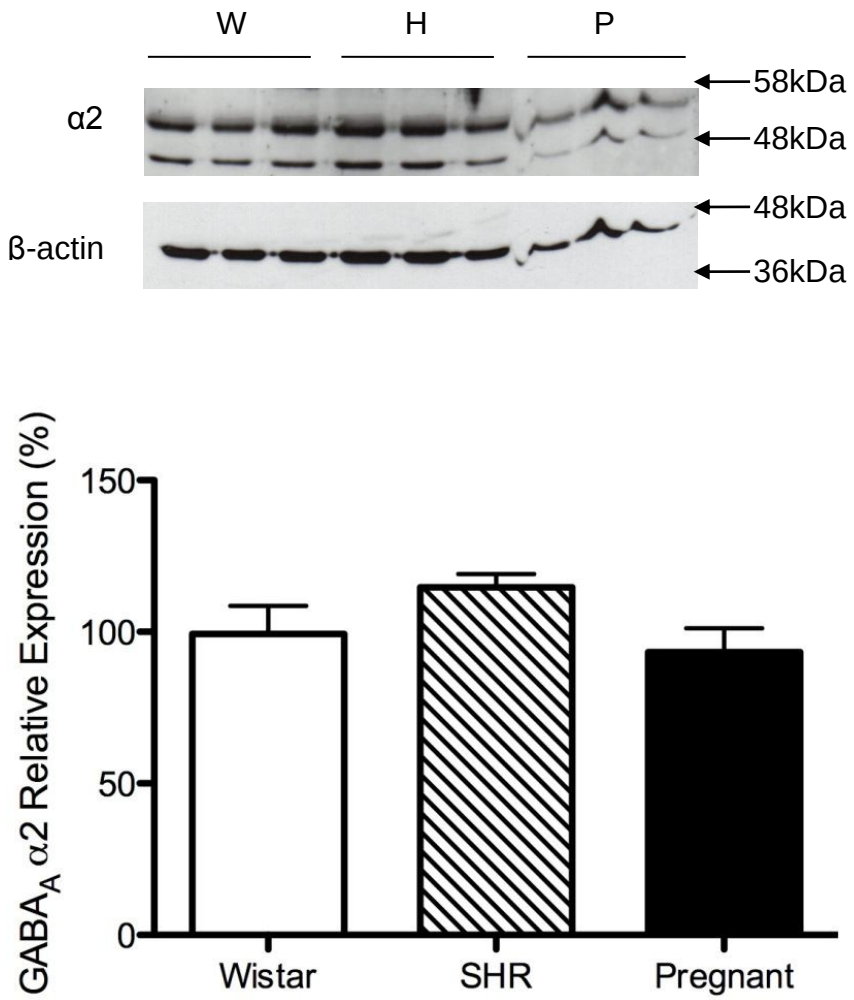

Figure 45 Expression of the GABA$_A$ α2 subunit in the PVN of normotensive, SHR and late-term pregnant rats expressed as a percentage relative to Wistar. Probing of PVN tissue with anti-α2 antibody produced two bands; only the top band was analysed. Analysis shows no significant change in expression between either SHR or late-term pregnant rats and Wistar controls (P>0.05). W = Wistar, H = SHR, P = Pregnant. n = 3 biological replicates. In the GABA$_A$α2 blot, the higher band represents the expected molecular weight of the GABA$_A$α2 subunit (51kDa). The identity of the lower band, with a molecular weight of around 45kDa was unknown, and for this reason was not analysed.

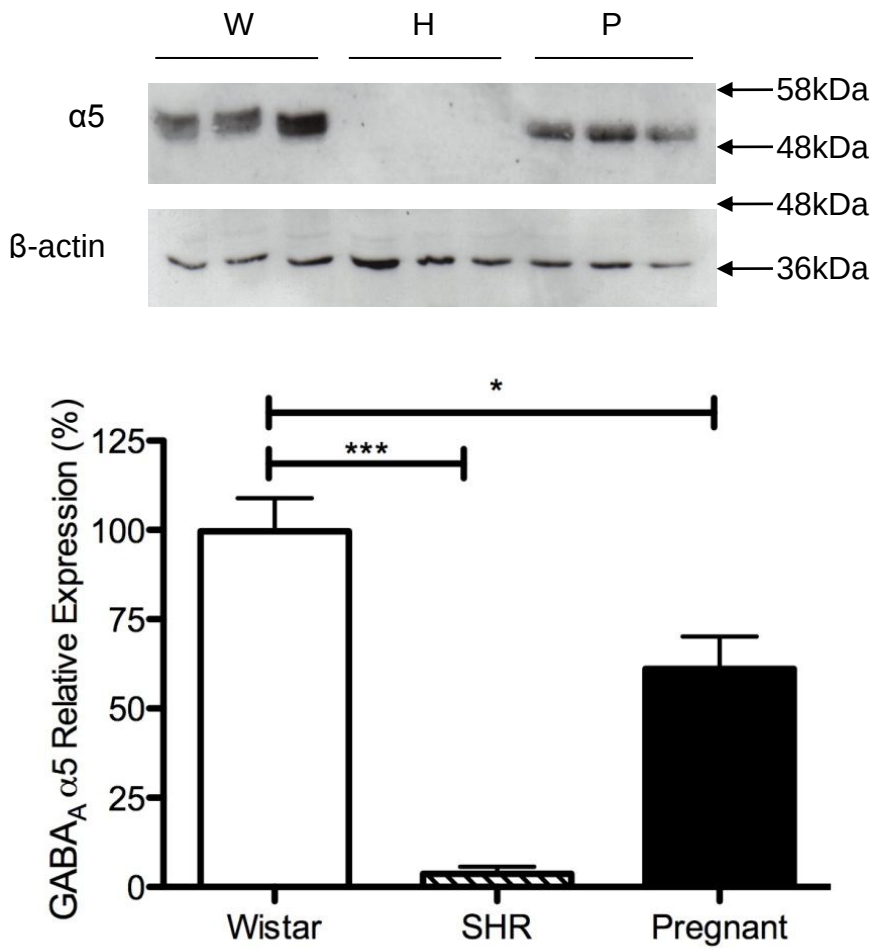

Figure 46 Expression of the GABA$_A$ α5 subunit in the PVN of normotensive, SHR and late-term pregnant rats expressed as a percentage relative to Wistar. Expression was 97 ± 2% lower in SHR compared with Wistar controls (P<0.001). Expression in the late-term pregnant rat was 38 ± 8% compared with Wistar controls (P<0.05). W = Wistar, H = SHR, P = Pregnant. n = 6 biological replicates

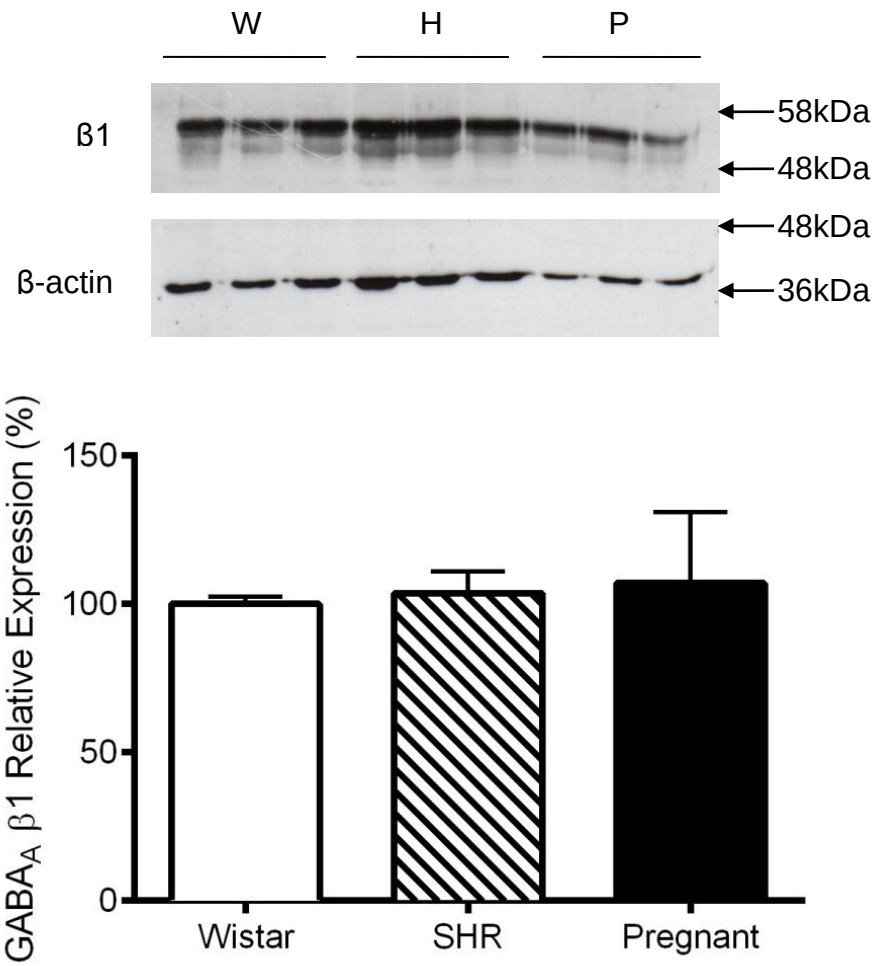

Figure 47 Expression of the GABAA β1 subunit in the PVN of normotensive, SHR and late-term pregnant rats expressed as a percentage relative to Wistar. Analysis shows no significant change in expression between either SHR or late-term pregnant rats compared with Wistar controls (P>0.05). W = Wistar, H = SHR, P = Pregnant. n = 3 biological replicates

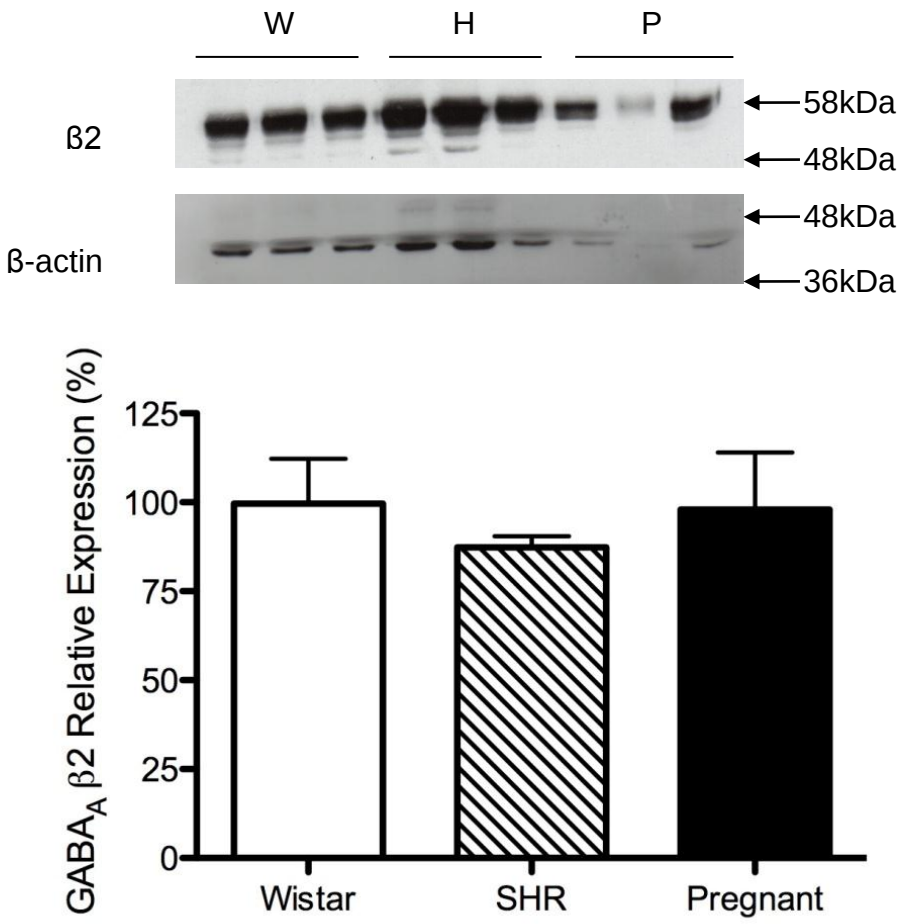

Figure 48 Expression of the GABAA β2 subunit in the PVN of normotensive, SHR and late-term pregnant rats expressed as a percentage relative to Wistar. Analysis shows no significant change in expression between either SHR or late-term pregnant rats compared with Wistar controls (P>0.05). W = Wistar, H = SHR, P = Pregnant. n = 3 biological replicates

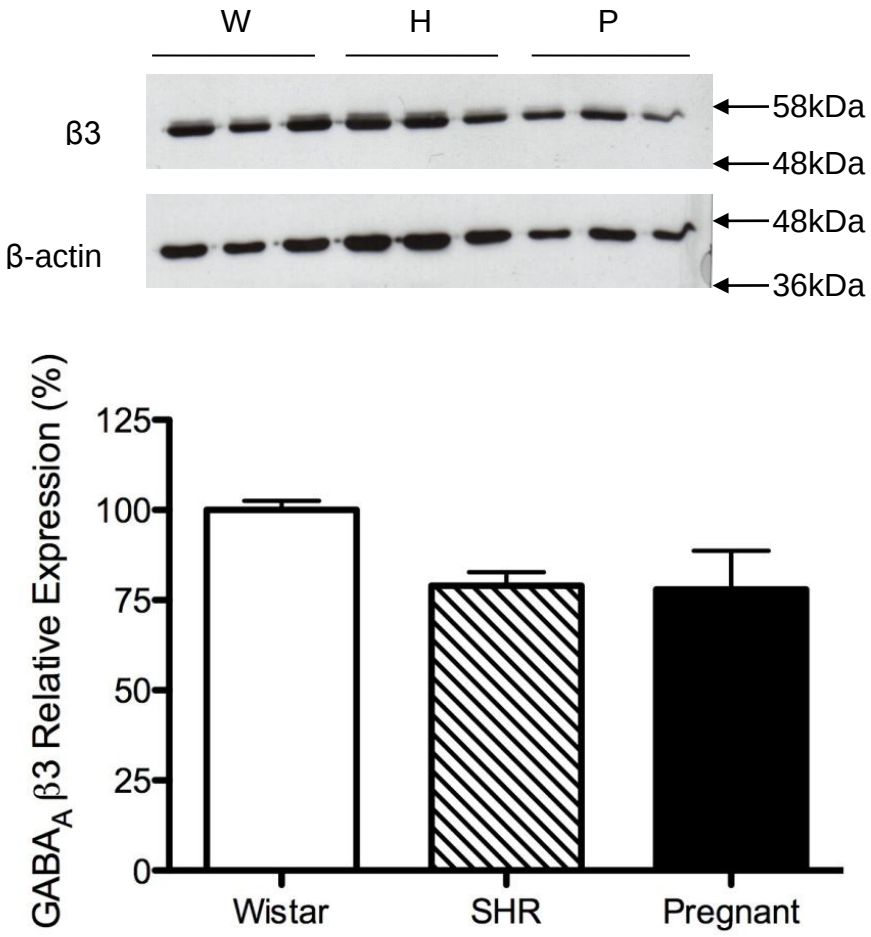

Figure 49 Expression of the GABAA β3 subunit in the PVN of normotensive, SHR and late-term pregnant rats expressed as a percentage relative to Wistar. Analysis shows no significant change in expression between either SHR or late-term pregnant rats compared with Wistar controls (P>0.05). W = Wistar, H = SHR, P = Pregnant. n = 3 biological replicates

b. Cortex

Expression of the α1 subunit in the cortex was not significantly different between SHR and late-term pregnant rats compared with Wistar controls (Figure 50). Expression of the α5 subunit was significantly reduced in the cortex of SHR (65 ± 10% decrease; $P<0.01$) and late-term pregnant rat (71 ± 3.5% decrease; $P<0.01$) compared with Wistar control (Figure 51). The percentage decrease in α5 expression observed in the cortex of the SHR was significant compared to the PVN ($P<0.05$). There was no significant difference between the decrease in expression observed in the cortex and PVN of the late-term pregnant rat ($P>0.05$).

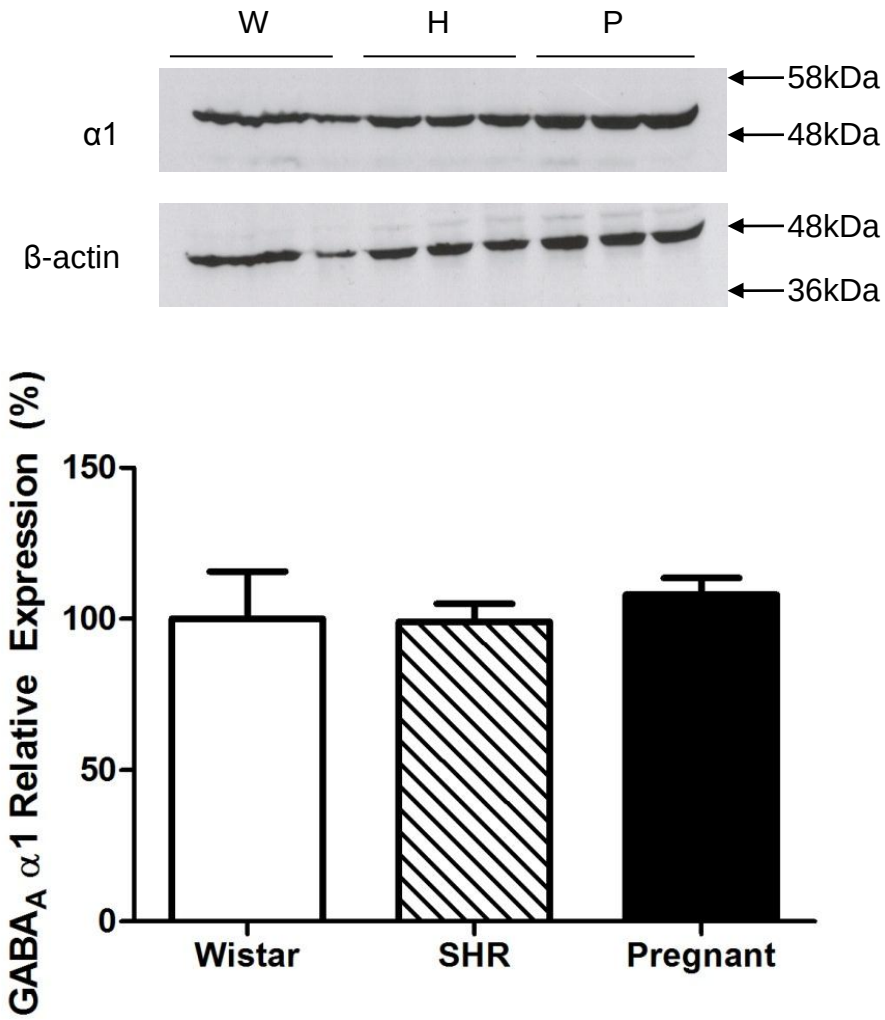

Figure 50 GABA$_A$ α1 expression in the cortex of Wistar, SHR and late-term pregnant rats expressed as a percentage of Wistar control. Analysis shows no significant change in expression between any state (P>0.05). W = Wistar, H = SHR, P = Pregnant. n = 3 biological replicates

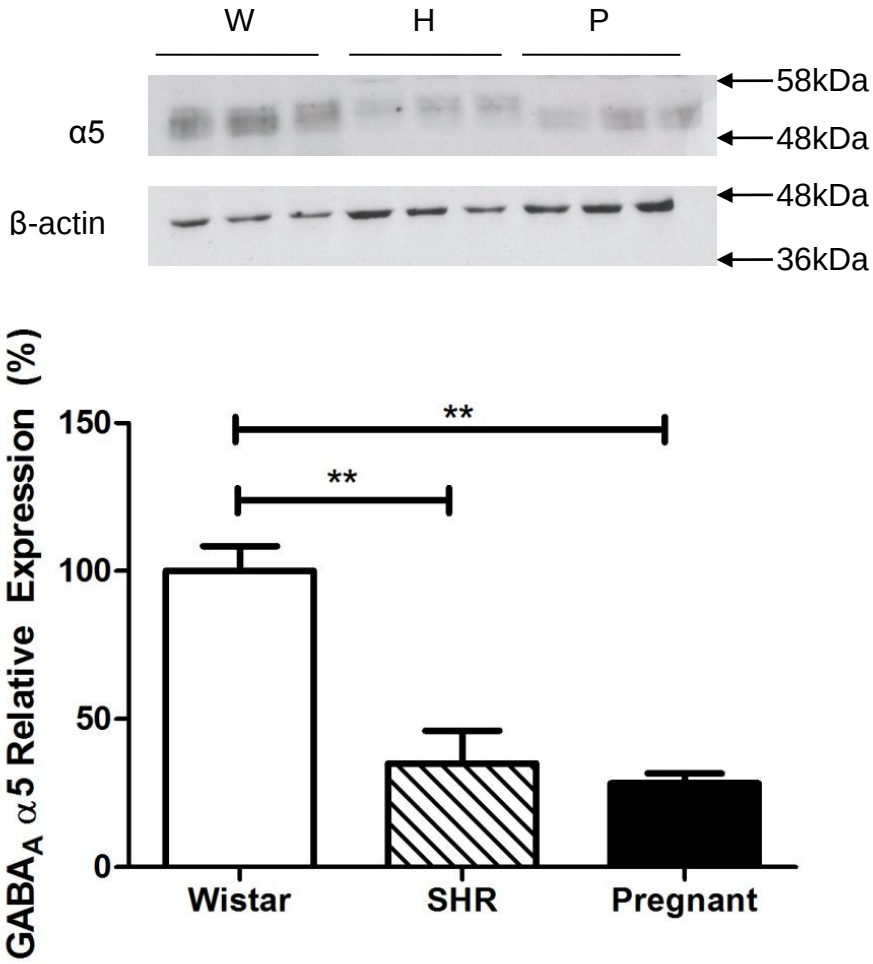

Figure 51 GABA$_A$ α5 expression in the cortex of Wistar, SHR and late-term pregnant rats, expressed as a relative percentage of Wistar. Analysis shows a significant decrease in expression in the cortex of SHR (P<0.01) and late-term pregnant rats (P<0.01). W = Wistar, H = SHR, P = Pregnant. n = 3 biological replicates

III. $GABA_A$ Receptor Subunit Expression Revealed by Immunohistochemical Analysis

Cells immunoreactive for α1 (Figures 52, 54, 55), α4 (Figures 56, 58, 59), α5 (Figures 60, 62, 63) and β3 (Figures 64, 66, 67) were found throughout the rostrocaudal extent of the PVN of normotensive and late-term pregnant rats. Expression of the α1 (Figures 53, 55), α4 (Figures 57, 59) and β3 (Figures 65, 67) subunit was observed throughout the rostrocaudal extent of the SHR, but there was no evidence of staining for the α5 subunit (Figure 61, 63).

a. $GABA_A$α1

$GABA_A$α1 immunoreactivity had a somatic morphology (identified by arrows in Figures 52-54), with no observable projections (Figure 54-55). Neurones appeared round and uniform in staining with little variation in morphology or size (16.19 ± 0.8μm). It is possible that this is labelling of the cell nucleus, since no nucleus can be identified in these neurones. However, previous studies using this antibody have proven its specificity by subjecting HEK cells both positive and negative for the $GABA_A$α1 subunit to SDS-PAGE. Using this regimen, no staining appeared in HEK-ve cells and a single band with the expected molecular weight was observed in HEK+ve cells (Chazot & Stephenson, 1997b).

Semi-quantitative analysis of α1-immunoreactive cells showed the highest density of staining to be in the anterior parvocellular subnucleus of the normotensive (98 ± 2.5; range 93 – 106) and SHR (117 ± 10.5; range 107 – 128) and ventral parvocellular subnucleus of the late-term pregnant rat (70 ± 2;

range 65 – 74). However, there was no significant change in expression in any parvocellular subnuclei of the SHR compared with normotensive controls (Figure 55). However α1-IR was significantly decreased in the anterior (66 ± 2.3; range 59 – 70. 34 ± 2% decrease compared with non-pregnant controls), medial (72 ± 3; range 67 – 80. 19 ± 3% decrease compared with non-pregnant controls), ventral (70 ± 2; range 65 – 74. 26 ± 5% decrease compared to normotensive Wistar) and posterior (44 ± 5; range 36 – 55. 39 ± 7% decrease compared with non-pregnant controls) parvocellular subdivisions of the late-term pregnant rat compared with non-pregnant controls (Figure 55).

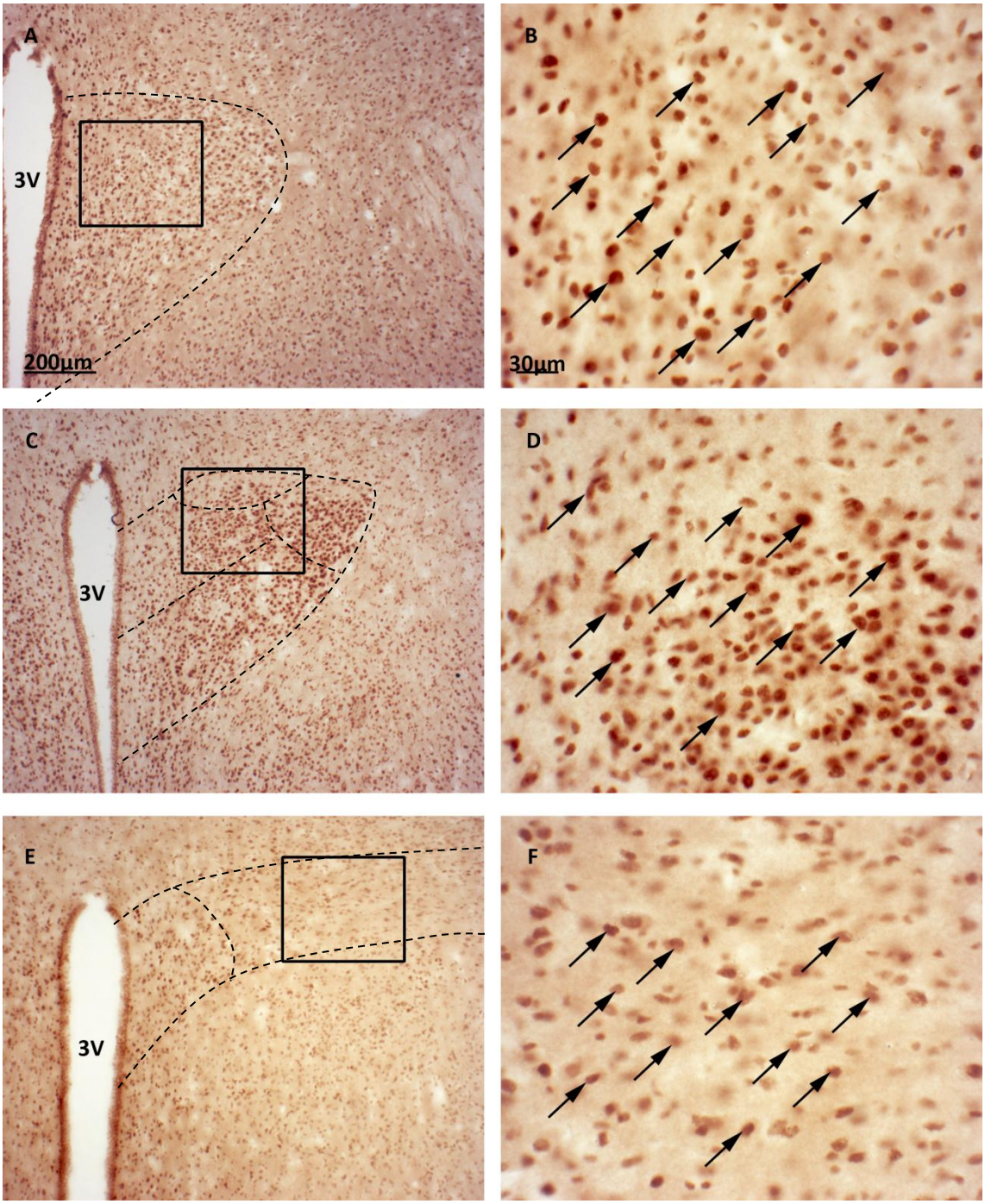

Figure 52 Photomicrographs showing expression of the α1 subunit throughout the rostrocaudal extent of the PVN of normotensive Wistar rats. Neurones immunoreactive for α1 (α1-IR) were found in the anterior (A-B), ventral, dorsal cap (C-D), medial and posterior (E-F) parvocellular subdivisions. Neurones show somatic labelling (arrows) with no identifiable projections observed. Somatic labelling was uniform throughout each neurone in all subnuclei. Boxed regions in A, C & E represent images B, D & F respectively. 3V = 3rd ventricle. Scale bar 200µm A, C & E. 30µm B, D & F.

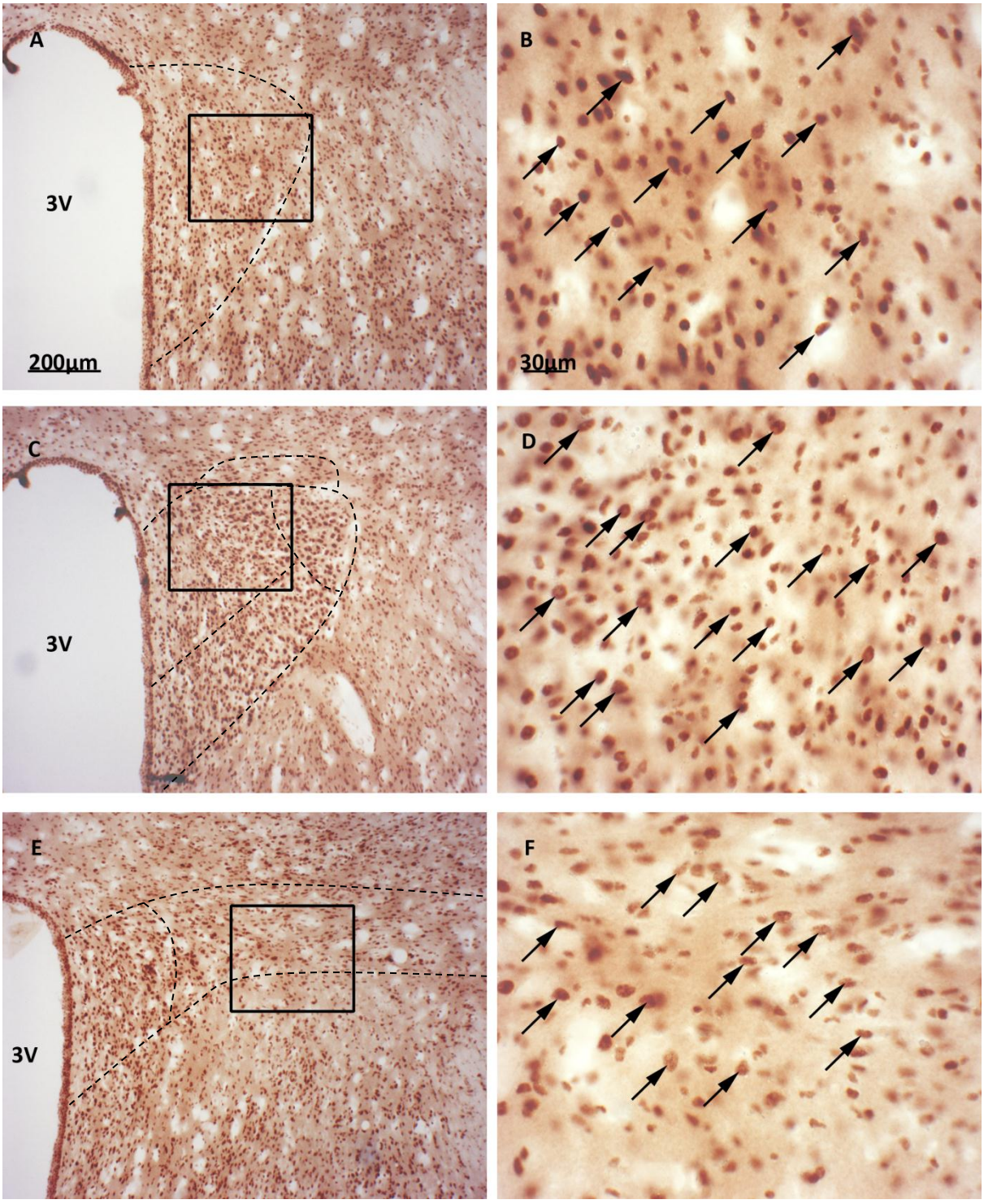

Figure 53 Photomicrographs showing expression of the α1 subunit throughout the rostrocaudal extent of the PVN of SHR. Neurones immunoreactive for α1 (α1-IR) were found in the anterior (A-B), ventral, dorsal cap (C-D), medial and posterior (E-F) parvocellular subdivisions. Neurones show somatic labelling (arrows) with no identifiable projections observed. Somatic labelling was uniform throughout each neurone in all subnuclei. No significant difference in cell number was observed in any parvocellular subnuclei compared with normotensive Wistars. Boxed regions in A, C & E represent images B, D & F respectively. 3V = 3rd ventricle. Scale bar 200µm A, C & E. 30µm B, D & F.

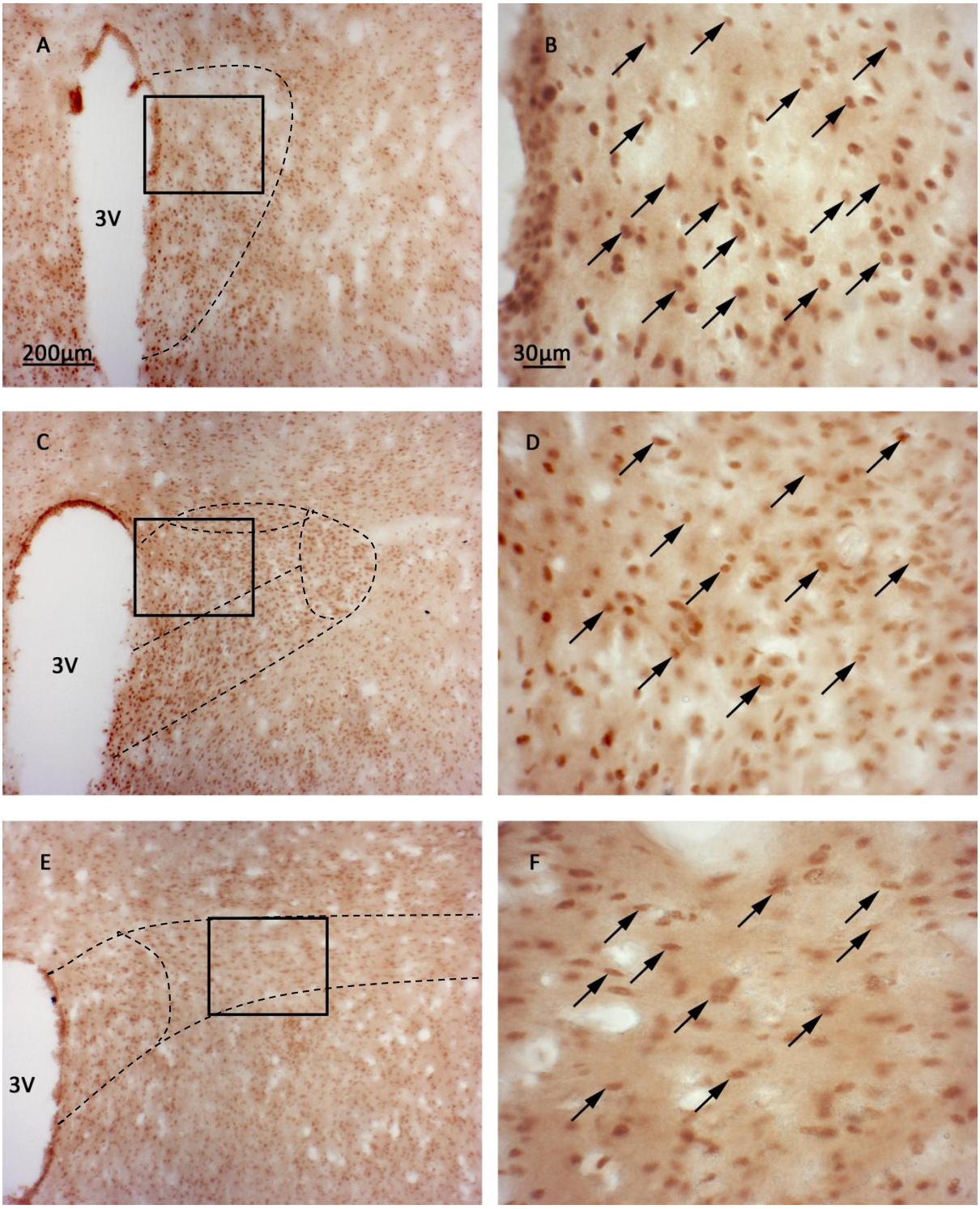

Figure 54 Photomicrographs showing expression of the α1 subunit throughout the rostrocaudal extent of the PVN of late-term pregnant Wistar rats. Neurones immunoreactive for α1 (α1-IR) were found in the anterior (A-B), ventral, dorsal cap (C-D), medial and posterior (E-F) parvocellular subdivisions. Neurones show somatic labelling (arrows) with no identifiable projections observed. Somatic labelling was uniform throughout each neurone in all subnuclei. A significant decrease in cell number was observed in the anterior, medial, ventral, dorsal cap and posterior parvocellular subnuclei compared with non-pregnant Wistars. Boxed regions in A, C & E represent images B, D & F respectively. 3V = 3rd ventricle. Scale bar 200µm A, C & E. 30µm B, D & F.

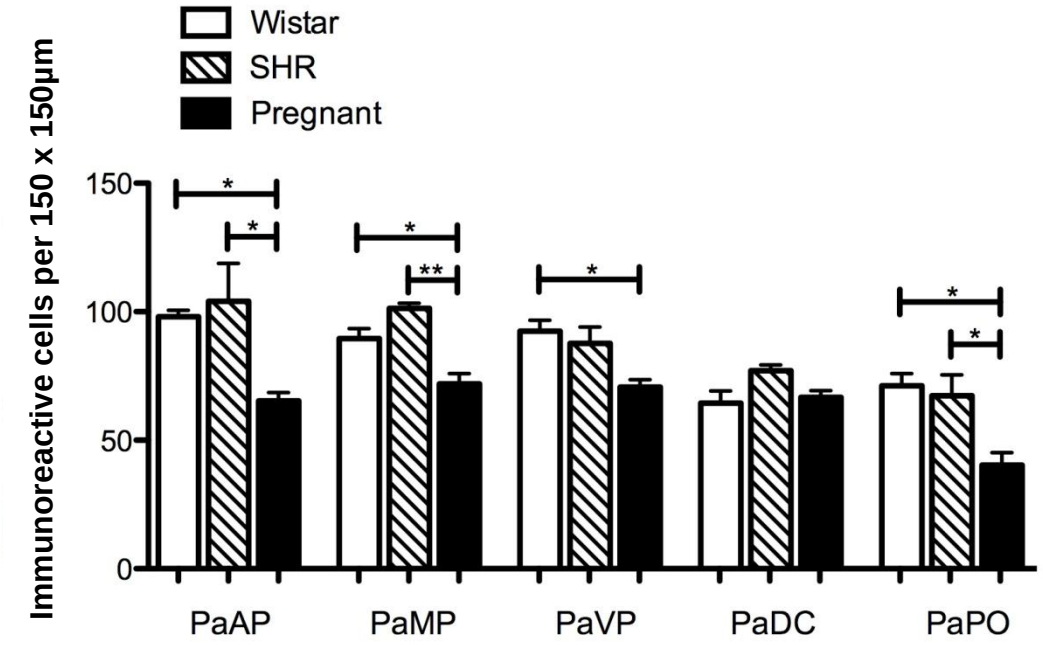

Figure 55 Mean number of α1-IR cells per 150µm x 150µm in each subnucleus of the PVN in normotensive, SHR and late-term pregnant rats. No significant change in cell number was observed between SHR and normotensive Wistar in any parvocellular subnuclei. A significant decrease in expression was observed in the anterior, medial, ventral and posterior parvocellular subnuclei of the late-term pregnant rat compared with non-pregnant Wistar and SHR. *Abbr: PaAP = Anterior Parvocellular, PaMP = Medial Parvocellular, PaVP = Ventral Parvocellular, PaDC = Dorsal Cap, PaPO = Posterior Parvocellular*. Values are ± SEM. * = P<0.05; ** = P<0.01. N=4 biological replicates for each subnucleus.

b. $\underline{GABA_A\alpha4}$

Cells immunoreactive for the α4 subunit of the $GABA_A$ receptor were found throughout the rostrocaudal extent of the PVN and in all parvocellular subnuclei of Wistar (Figure 56), SHR (Figure 57) and late-term pregnant (Figure 58) rats.

Staining was confined to the soma (identified with arrows in Figures 56-58), with no projections observed. Qualitative analysis shows that in late-term pregnant rats, the density of staining was increased in the periventricular area of the anterior parvocellular subnucleus (Figure 58 A).

The somata of neurones immunoreactive for the α4 subunit were significantly larger than those stained for the α1, α5 and β3 subunit, measured at their longest axis (α1 = 16.19 ± 0.8μm; α4 = 24.13 ± 2.4μm; α5 = 16.51 ± 0.6μm; β3 = 15.56 ± 1.1μm).

In all physiological states, α4-IR neurones in the posterior parvocellular subnucleus had a flattened appearance and were orientated in the same plane, such that their apical points were lying horizontal to the vertical midline (Figure 56-58 F). Cells in the subsequent four parvocellular subnuclei had no such level of orientation (Figure 56-58 B/D). Furthermore, in the non-pregnant, normotensive Wistar rat staining within cells of the posterior parvocellular subnucleus was confined to the lateral edges (identified by ‡ in Figure 56F); whereas staining in other parvocellular subnuclei was more uniform throughout the cell (identified by arrows in Figure 56 B/D). No such pattern of staining was observed in the posterior subnucleus of the SHR or late-term pregnant rat (Figure 57-58 F). The highest degree of staining was observed in the medial parvocellular subnucleus for the normotensive Wistar (26 ± 4; range 19 – 38)

and late-term pregnant rat (20 ± 2.6; range 14 – 27) and the ventral parvocellular subnucleus for the SHR (24 ± 4.3; range 17 – 32). However there was no significant difference between any parvocellular subnuclei between any of the different physiological states (Figure 59).

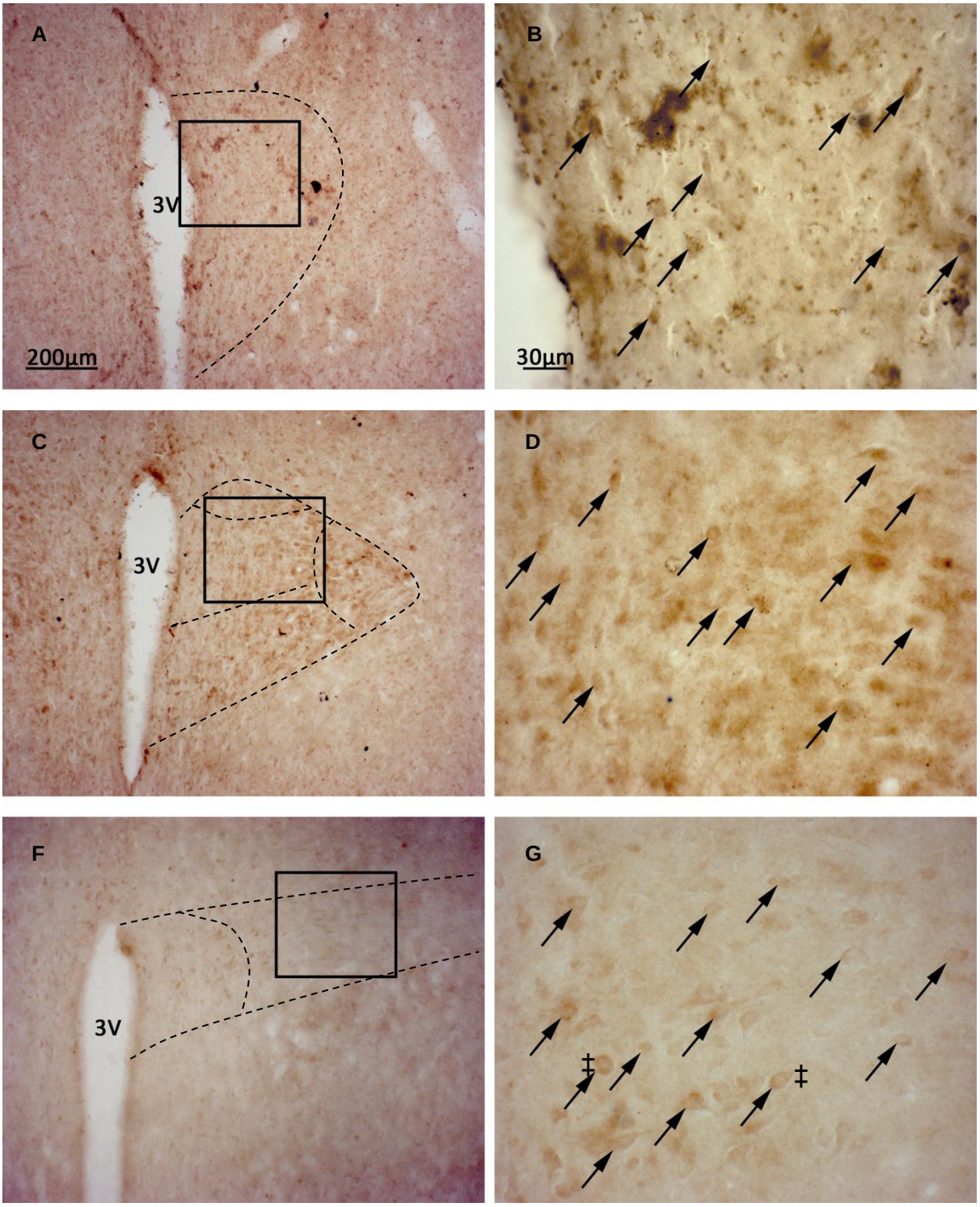

Figure 56 Photomicrographs showing expression of the α4 subunit throughout the rostrocaudal extent of the PVN of Wistar rats. Neurones immunoreactive for α4 (α4-IR) were found in the anterior (A-B), ventral, dorsal cap (C-D), medial and posterior (E-F) parvocellular subdivisions. Neurones show somatic labelling (arrows) with few identifiable projections observed. Somatic labelling was uniform throughout each neurone in the mid- to rostral levels. In the posterior parvocellular subnuclei, staining was somatic with few projections; however the somatic staining was confined to the periphery of each neurone. Boxed regions in A, C & E represent images B, D & F respectively. 3V = 3rd ventricle. Scale bar 200µm A, C & E. 30µm B, D & F. ‡ = example of neurone were staining is confined to lateral edges. Darker stained patches on Figure A-B are non-specific artefacts and were not considered when acquiring data.

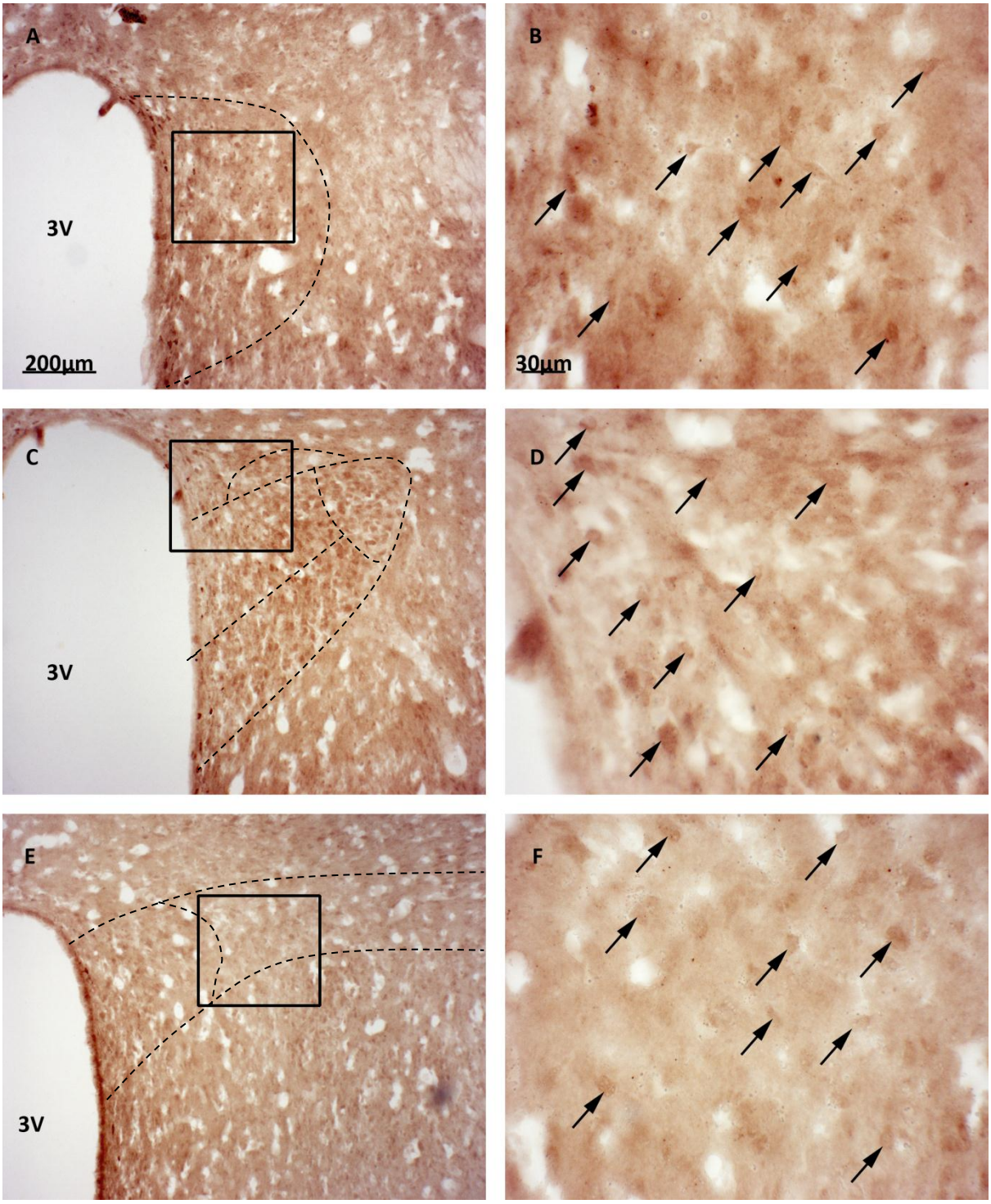

Figure 57 Photomicrographs showing expression of the α4 subunit throughout the rostrocaudal extent of the PVN of SHR. Neurones immunoreactive for α4 (α4-IR) were found in the anterior (A-B), ventral, dorsal cap (C-D), medial and posterior (E-F) parvocellular subdivisions. Neurones show somatic labelling (arrows) with no identifiable projections observed. Somatic labelling was uniform throughout each neurone in the mid- to rostral levels. In the posterior parvocellular subnuclei, staining was somatic with few projections; however the somatic staining was confined to the periphery of each neurone. No significant change in expression was observed between SHR and normotensive Wistar. Boxed regions in A, C & E represent images B, D & F respectively. 3V = 3rd ventricle. Scale bar 200µm A, C & E. 30µm B, D & F. Arrows represent examples of immunoreactive neurones.

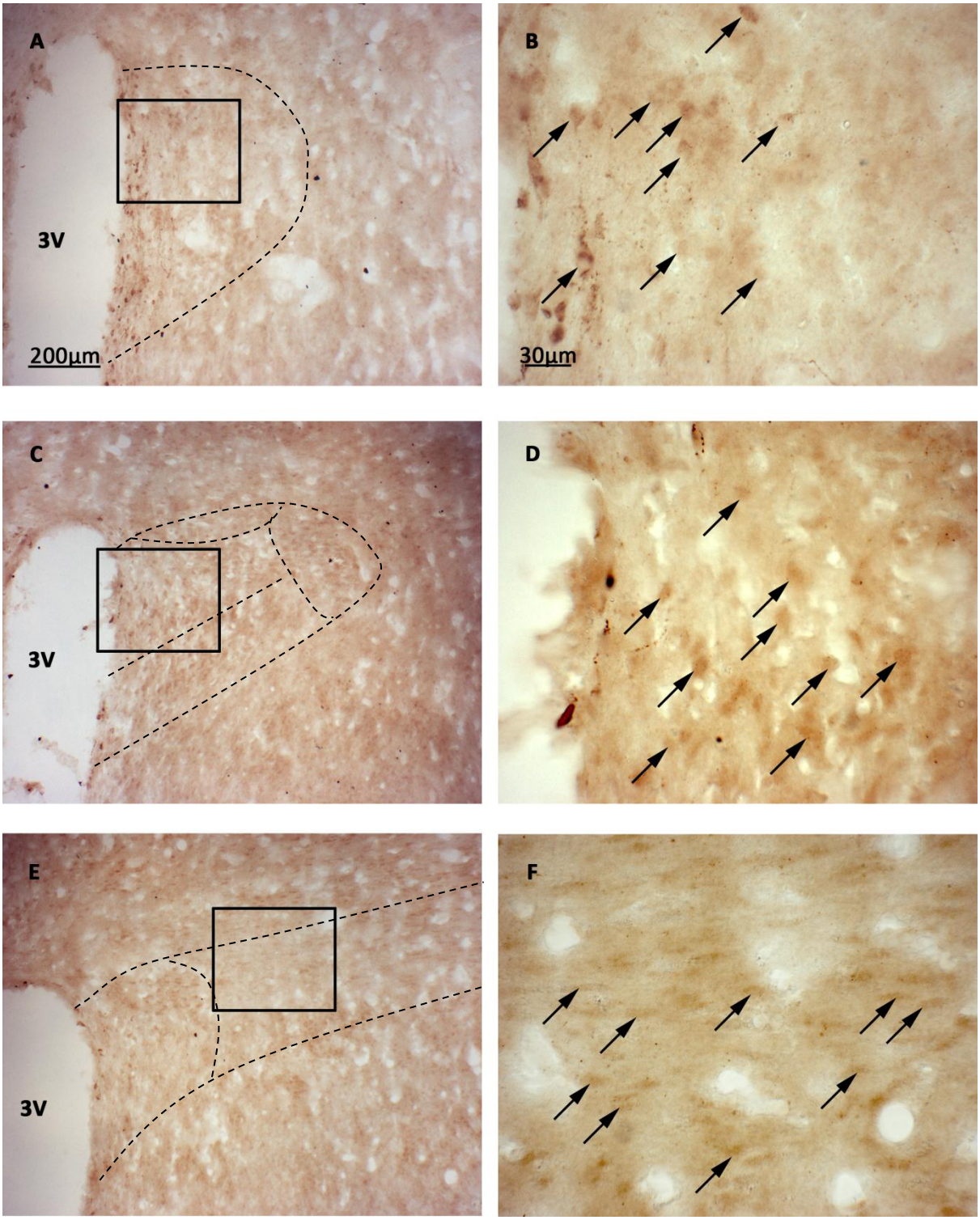

Figure 58 Photomicrographs showing expression of the α4 subunit throughout the rostrocaudal extent of the PVN of late-term pregnant Wistar rats. Neurones immunoreactive for α4 (α4-IR) were found in the anterior (A-B), ventral, dorsal cap (C-D), medial and posterior (E-F) parvocellular subdivisions. Neurones show somatic labelling (arrows) with few identifiable projections observed. Somatic labelling was uniform throughout each neurone in all subnuclei. Qualitative analysis suggests α4-IR neurones showed a higher level of expression in the periventricular area. Boxed regions in A, C & E represent images B, D & F respectively. 3V = 3rd ventricle. Scale bar 200µm A, C & E. 30µm B, D & F. Arrows represent examples of immunoreactive neurones.

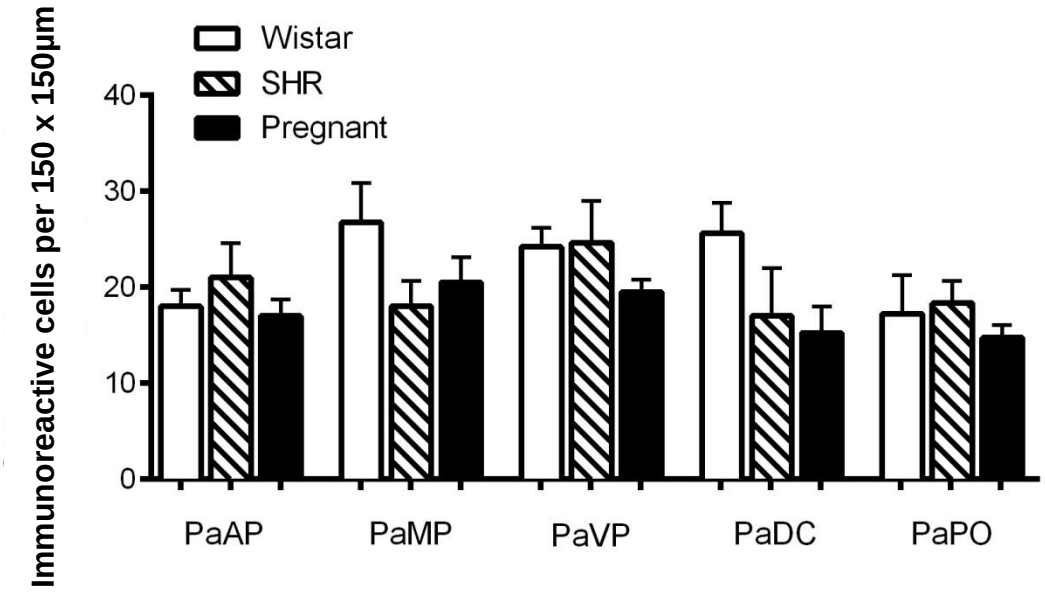

Figure 59 Mean number of α4-IR cells per 150µm x 150µm in each subnucleus of the PVN in normotensive, SHR and late-term pregnant rats. No significant change in cell number was observed between any physiological state. *Abbr: PaAP = Anterior Parvocellular, PaMP = Medial Parvocellular, PaVP = Ventral Parvocellular, PaDC = Dorsal Cap, PaPO = Posterior Parvocellular*. Values are ± SEM. N=4 biological replicates for each subnucleus.

c. $GABA_A\alpha5$

Cells immunoreactive for the α5 subunit of the $GABA_A$ receptor were found throughout the rostrocaudal extent of the PVN of normotensive and late-term pregnant rats (Figure 60 & 62). No expression was observed in any parvocellular subnuclei of the SHR PVN (Figure 61). Furthermore, late-term pregnancy was associated with a significant decrease in α5-IR neurones in the medial (12 ± 1.2; range 11 – 15. 56 ± 4% decrease compared to non-pregnant controls), ventral (12 ± 0.6; range 11 – 13. 60 ± 2% decrease compared to non-pregnant controls) and dorsal cap (12 ± 1.4; range 10 – 15. 52 ± 6% decrease compared to non-pregnant controls) parvocellular regions of the PVN (Figure 63). There was a slight but non-significant decrease in the number of α5-IR neurones in the anterior subnucleus (14 ± 2.3; range 10 – 18. 30 ± 12% decrease) compared with non-pregnant Wistars (Figure 63). There was no significant difference in the number of α5-IR neurones in the posterior parvocellular subnucleus in the late-term pregnant rat compared with normotensive controls (31 ± 1.5 α5-IR neurones/150μm^2 (range 29 – 34) vs. 29.5 ± 0.5 α5-IR neurones/150μm^2 (range 29 – 30) respectively; Figure 63).

Qualitative analysis of α5-IR neurones in the PVN of late-term pregnant rat's shows that the density of staining is reduced compared with non-pregnant Wistars (Figure 60 & 62). This appears more prominent in mid- to rostral levels of the PVN (Figure 60 & 62 D/F).

Cells immunoreactive for the α5 subunit in non-pregnant, normotensive and late-term pregnant rats showed somatic labelling with no obvious projections

observed. Staining was uniform in density in all parvocellular subnuclei (illustrated by arrows in Figure 60 & 62 B/D/F).

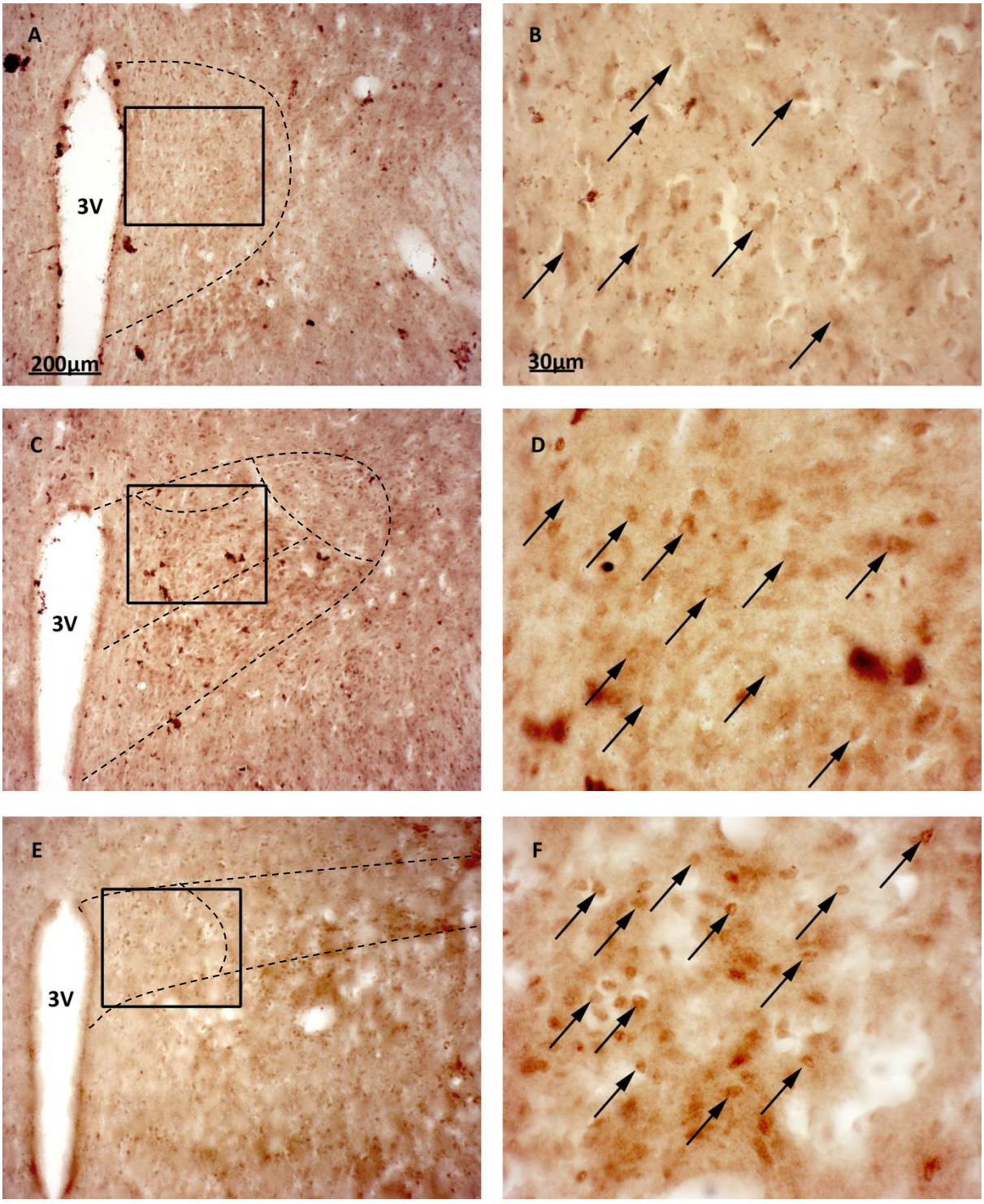

Figure 60 Photomicrographs showing expression of the α5 subunit throughout the rostrocaudal extent of the PVN of Wistar rats. Neurones immunoreactive for α5 (α5-IR) were found in the anterior (A-B), ventral, dorsal cap (C-D), medial and posterior (E-F) parvocellular subdivisions. Neurones show somatic labelling (arrows) with no identifiable projections observed. Somatic labelling was uniform throughout each neurone in all subnuclei. Boxed regions in A, C & E represent images B, D & F respectively. 3V = 3rd ventricle. Scale bar 200µm A, C & E. 30µm B, D & F. Darker stained patches on Figure A-D are non-specific artefacts and were not considered when acquiring data.

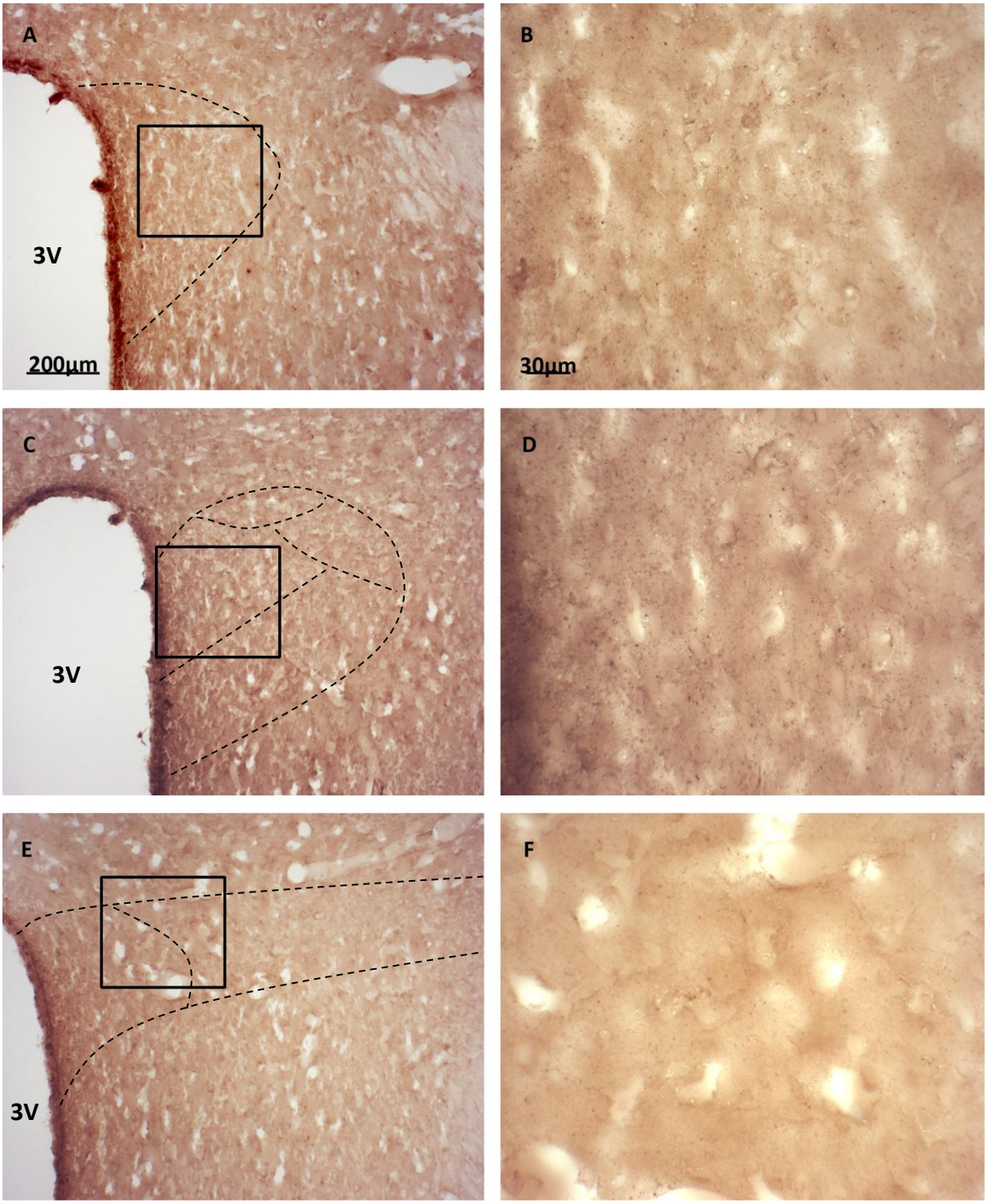

Figure 61 Photomicrographs showing expression of the α5 subunit throughout the rostrocaudal extent of the PVN of SHR. No identifiable neurones were observed in any of the parvocellular subnuclei. Boxed regions in A, C & E represent images B, D & F respectively. 3V = 3rd ventricle. Scale bar 200µm A, C & E. 30µm B, D & F.

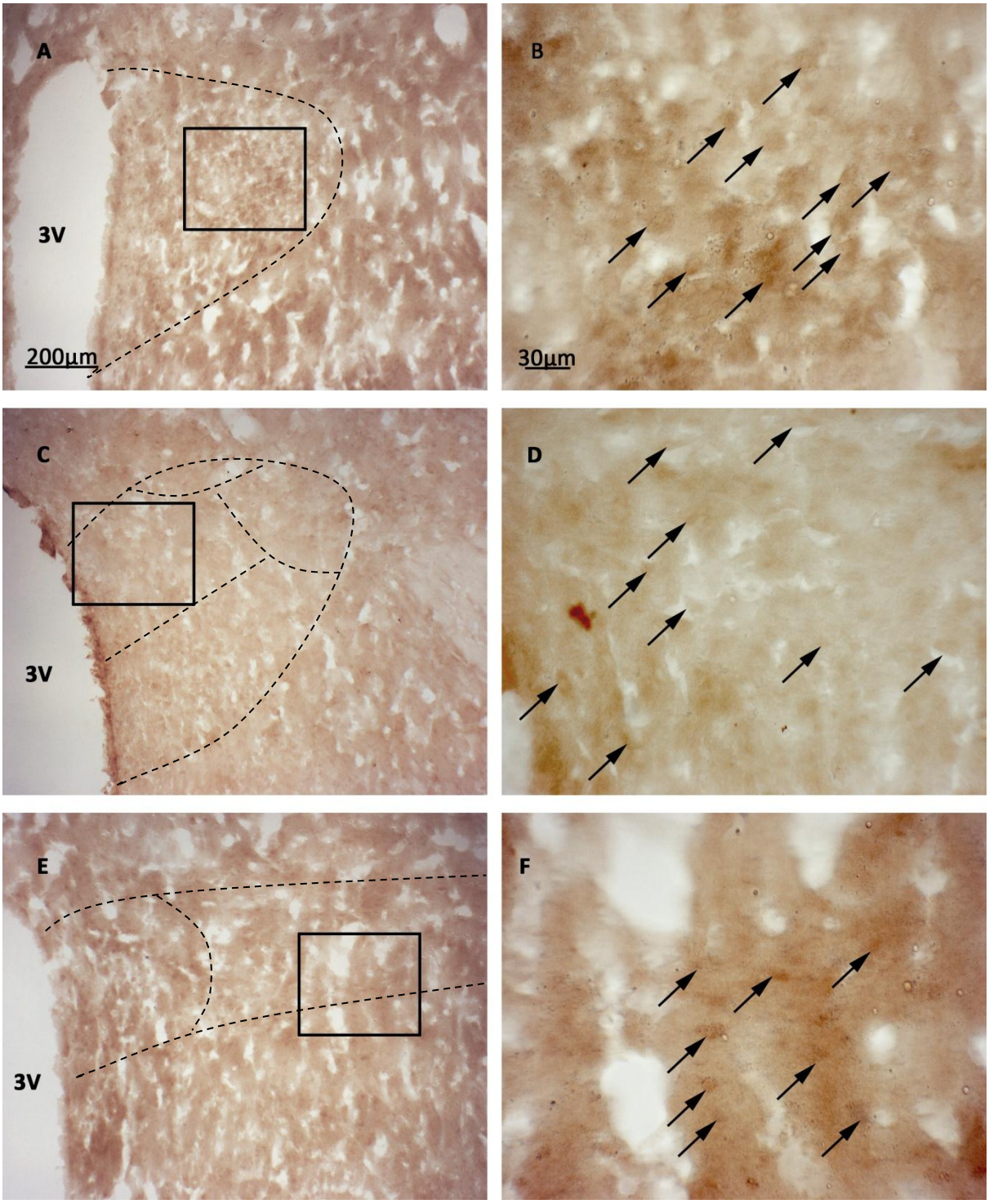

Figure 62 Photomicrographs showing expression of the α5 subunit throughout the rostrocaudal extent of the PVN of late-term pregnant Wistar rats. Neurones immunoreactive for α5 (α5-IR) were found in the anterior (A-B), ventral, dorsal cap (C-D), medial and posterior (E-F) parvocellular subdivisions. Neurones show somatic labelling (arrows) with no identifiable projections observed. Somatic labelling was uniform throughout each neurone in all subnuclei. Qualitative analysis suggests that the staining density was reduced in α5-IR neurones compared with non-pregnant Wistar rats. Boxed regions in A, C & E represent images B, D & F respectively. 3V = 3rd ventricle. Scale bar 200µm A, C & E. 30µm B, D & F.

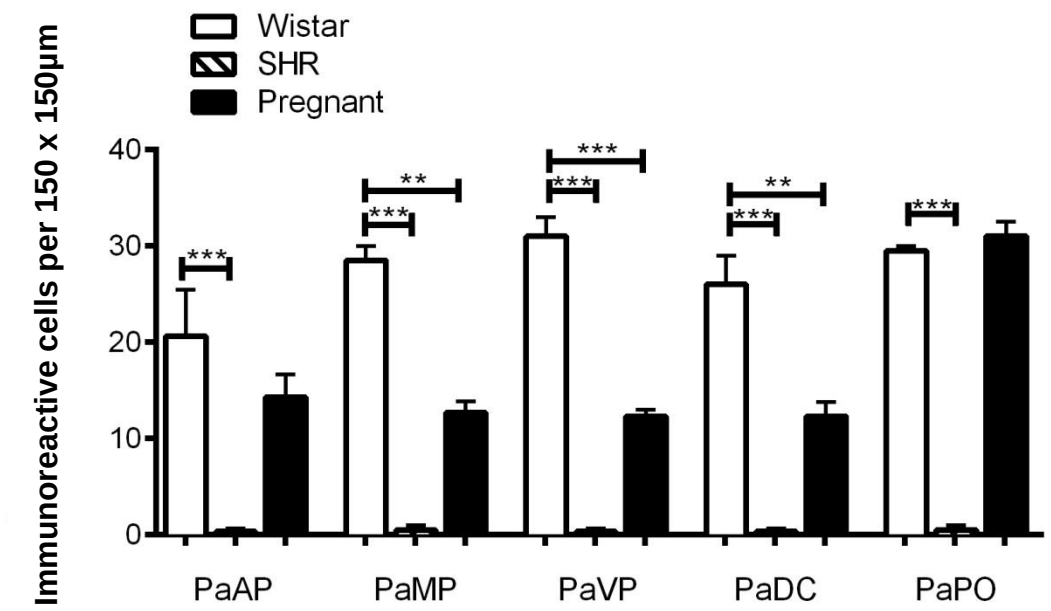

Figure 63 Mean number of α5-IR cells per 150µm x 150µm in each subnucleus of the PVN in normotensive, SHR and late-term pregnant rats. A significant decrease in the number of α5-IR neurones was observed in all parvocellular subnuclei of the PVN. Furthermore, a significant decrease in the number of α5-IR neurones was observed in the medial, ventral, dorsal cap and posterior parvocellular subnuclei of the PVN in the late-term pregnant rat. A slight but non-significant decrease was observed in the anterior parvocellular subnucleus of the late-term pregnant rat. Interestingly, there was no change in the number of α5-IR neurones in the posterior subnucleus in the late-term pregnant rat. *Abbr: PaAP = Anterior Parvocellular, PaMP = Medial Parvocellular, PaVP = Ventral Parvocellular, PaDC = Dorsal Cap, PaPO = Posterior Parvocellular*. Values are ± SEM. N=4 biological replicates for each subnucleus.

d. $GABA_A\beta3$

Cells immunoreactive for the β3 subunit of the $GABA_A$ receptor were found throughout the rostrocaudal extent of the PVN and in all parvocellular subnuclei in the Wistar (Figure 64), SHR (Figure 65) and late-term pregnant rat (Figure 66).

$GABA_A\beta3$-IR neurones had a somatic morphology with no evidence of projection labelling. Staining density appeared uniform throughout the neurone (illustrated by arrows in Figures 64-66 B/D/F). Neurones appeared round and uniform in staining with little variation in morphology or size (16.19 ± 0.8μm). It is possible that this is labelling of the cell nucleus, since no nucleus can be identified in these neurones. However, previous studies using this antibody have proven its specificity by subjecting HEK cells both positive and negative for the $GABA_A\alpha1$ subunit to SDS-PAGE. Using this regimen, no staining appeared in HEK-ve cells and a single band with the expected molecular weight was observed in HEK+ve cells (Chazot & Stephenson, 1997b).

In all physiological states, neurones within the posterior subnucleus had a flattened appearance and were orientated in the same plane; such that their apical points were lying horizontal to the vertical midline (Figures 64-66 F). Neurones in the remaining four parvocellular subnuclei had no such level of orientation (Figures 64-66 B/D).

Semi-quantitative analysis shows the highest density of staining to be in the anterior parvocellular subnucleus of the normotensive Wistar (91 ± 3.3; range 85 – 104); medial parvocellular subnucleus of the SHR (100 ± 0.5; range 100 – 101) and ventral parvocellular subnucleus of the late-term pregnant rat (89 ±

2.9; range 81 – 94). However, no significant change in the number of β3-IR neurones was observed in any parvocellular subnuclei between any of the physiological states (Figure 67).

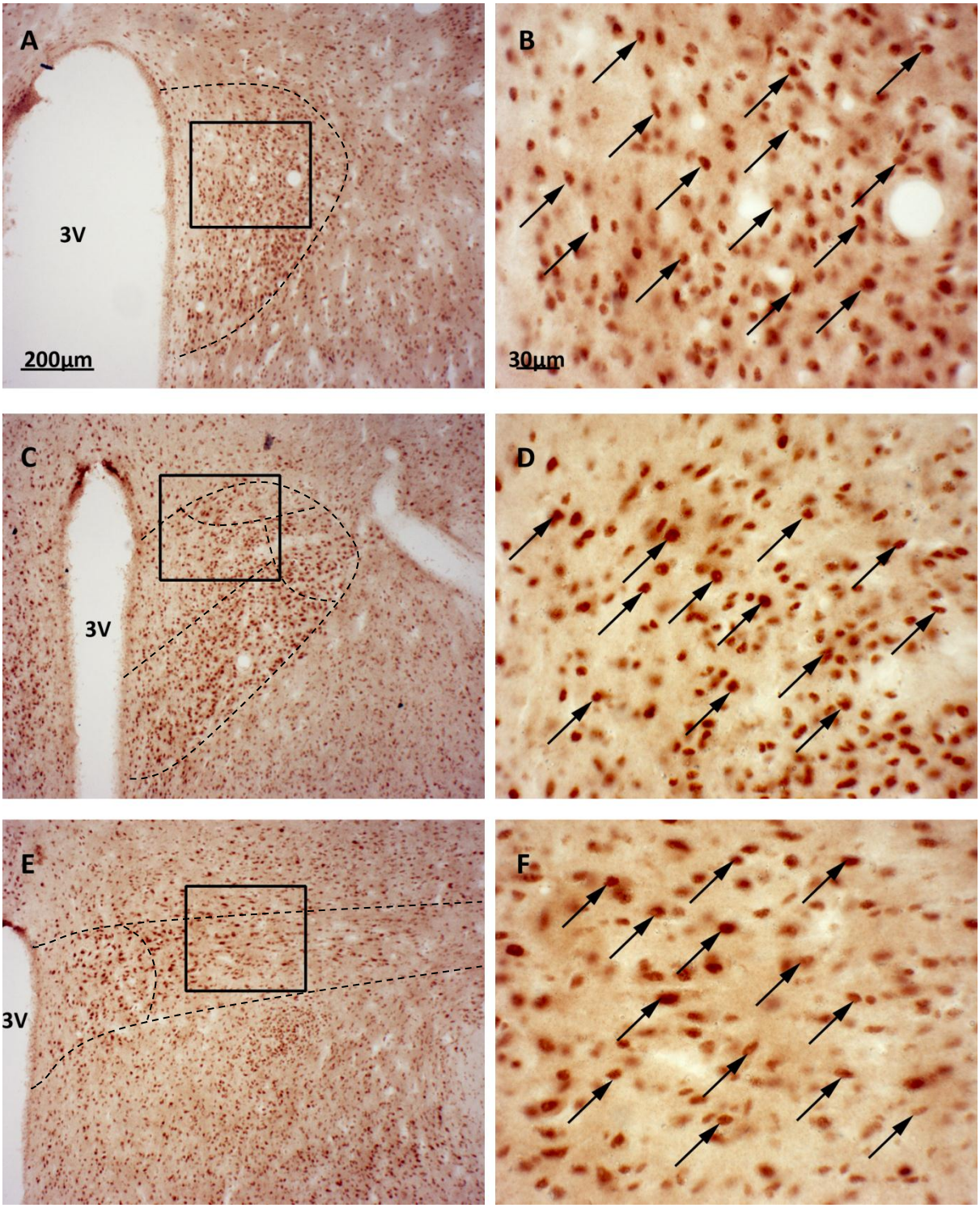

Figure 64 Photomicrographs showing expression of the β3 subunit throughout the rostrocaudal extent of the PVN of Wistar rats. Neurones immunoreactive for β3 (β3-IR) were found in the anterior (A-B), ventral, dorsal cap (C-D), medial and posterior (E-F) parvocellular subdivisions. Neurones show somatic labelling (arrows) with no identifiable projections observed. Somatic labelling was uniform throughout each neurone in all subnuclei. Boxed regions in A, C & E represent images B, D & F respectively. 3V = 3rd ventricle. Scale bar 200µm A, C & E. 30µm B, D & F.

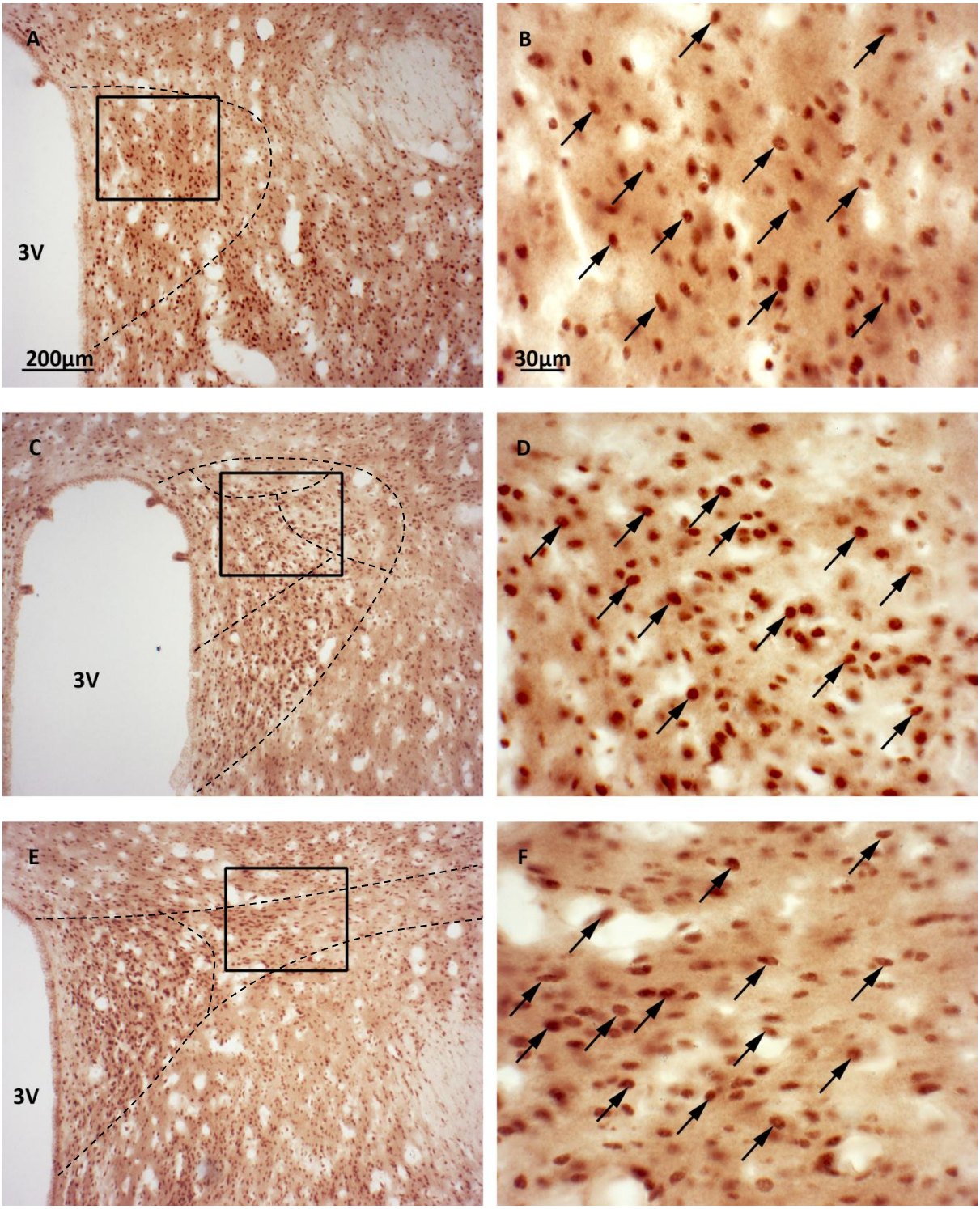

Figure 65 Photomicrographs showing expression of the β3 subunit throughout the rostrocaudal extent of the PVN of SHR. Neurones immunoreactive for β3 (β3-IR) were found in the anterior (A-B), ventral, dorsal cap (C-D), medial and posterior (E-F) parvocellular subdivisions. Neurones show somatic labelling (arrows) with no identifiable projections observed. Somatic labelling was uniform throughout each neurone in all subnuclei. No significant change in β3-IR neurones was observed between SHR and normotensive Wistar. Boxed regions in A, C & E represent images B, D & F respectively. 3V = 3rd ventricle. Scale bar 200µm A, C & E. 30µm B, D & F.

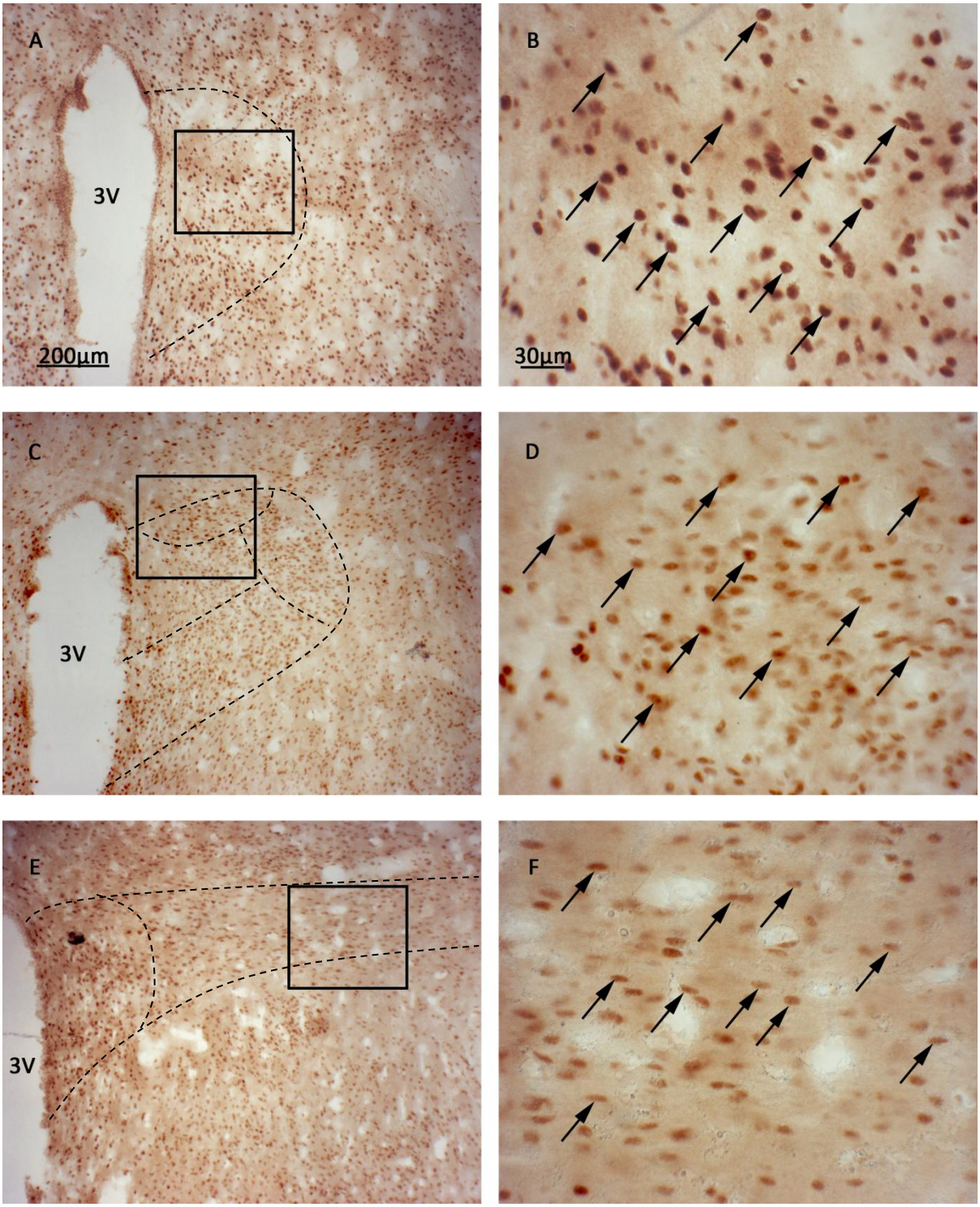

Figure 66 Photomicrographs showing expression of the β3 subunit throughout the rostrocaudal extent of the PVN of late-term pregnant Wistar. Neurones immunoreactive for β3 (β3-IR) were found in the anterior (A-B), ventral, dorsal cap (C-D), medial and posterior (E-F) parvocellular subdivisions. Neurones show somatic labelling (arrows) with no identifiable projections observed. Somatic labelling was uniform throughout each neurone in all subnuclei. No significant change in β3-IR neurones was observed between late-term pregnant rat and non-pregnant Wistar. Boxed regions in A, C & E represent images B, D & F respectively. 3V = 3rd ventricle. Scale bar 200µm A, C & E. 30µm B, D & F.

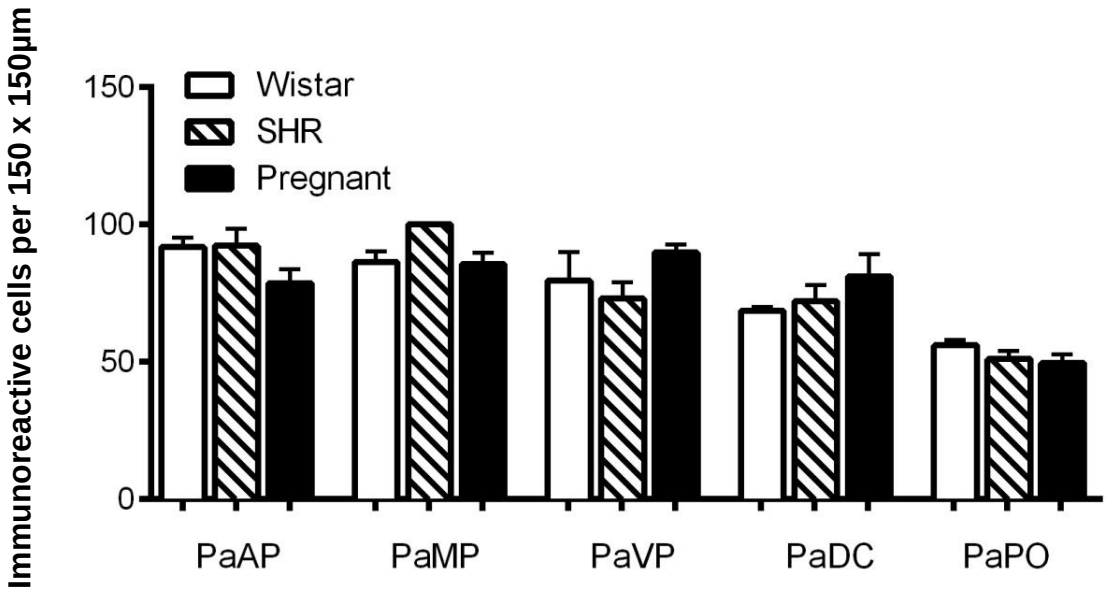

Figure 67 Mean number of β3-IR cells per 150µm x 150µm in each subnucleus of the PVN in normotensive, SHR and late-term pregnant rats. No significant change in cell number was observed between any state. *Abbr: PaAP = Anterior Parvocellular, PaMP = Medial Parvocellular, PaVP = Ventral Parvocellular, PaDC = Dorsal Cap, PaPO = Posterior Parvocellular*. Values are ± SEM. N=4 biological replicates for each subnucleus.

IV. Summary of Changes Observed in the Number of Immunoreactive Cells in the PVN of Hypertensive and Pregnant Rats

The results presented in the previous two chapters detail the changes in expression of specific $GABA_A$ and NMDA receptor subunits in the PVN of hypertensive and late-term pregnant rats.

Hypertension was associated with a significant decrease in the number of α5-IR neurones in all five parvocellular subnuclei (Figure 68; black circles) as well as a significant increase in the number of GluN2A-IR neurones in the dorsal cap, medial and posterior parvocellular subnuclei of the PVN (Figure 68; red squares). Concomitant changes were also observed in the dorsal cap, medial and posterior subnuclei of the PVN (Figure 68).

Late-term pregnancy was associated with a significant decrease in the number of α1-IR neurones in the anterior, ventral, medial and posterior parvocellular subnuclei (Figure 69; red triangles) as well as a significant decrease in the number of α5-IR neurones in the dorsal cap, ventral and medial parvocellular subnuclei (Figure 69; black circles). Concomitant decreases were therefore observed in the ventral and medial parvocellular subnuclei of the PVN (Figure 69).

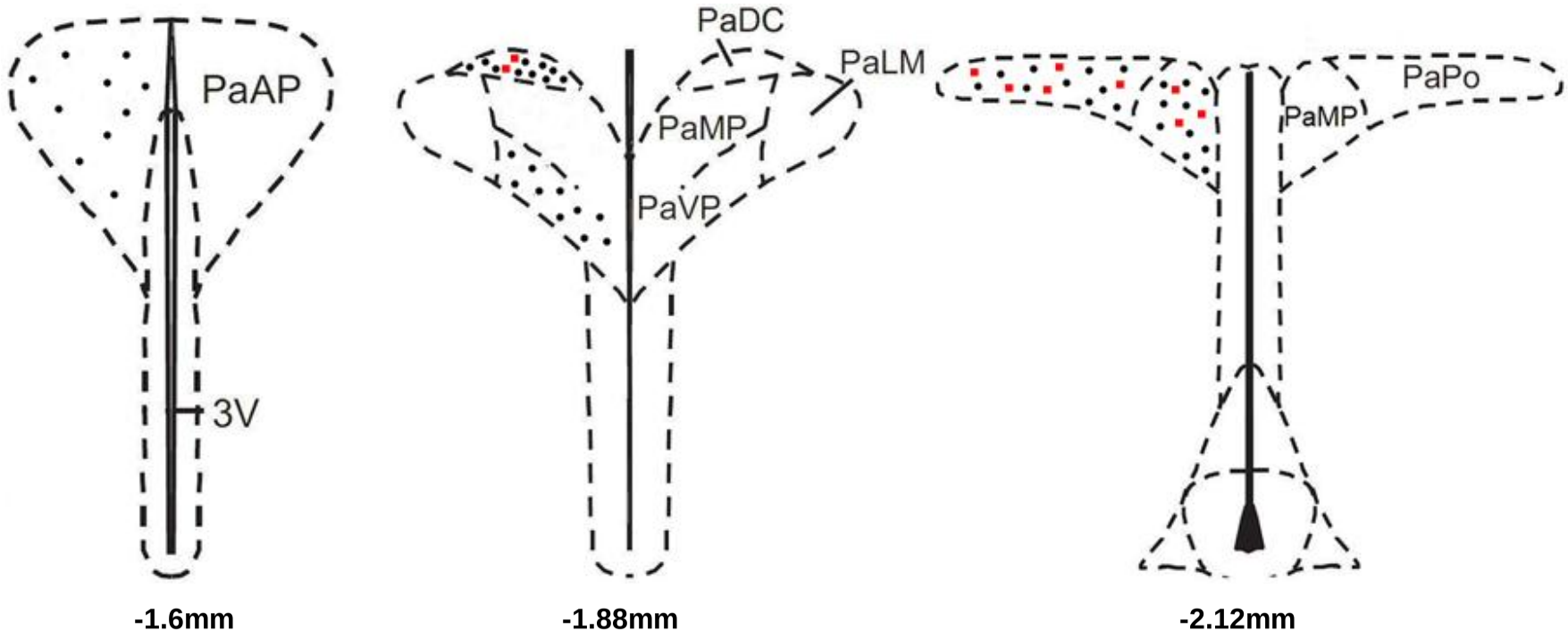

Figure 68 Plots of the positions of immunoreactivity changes for the $GABA_A$ α5 subunit (black circles) and NMDA GluN2A subunit (red squares) for the SHR compared to normotensive controls. Each symbol represents either a 10% decrease (α5) or a 10% increase (GluN2A) in immunoreactivity. Concomitant changes were observed in the dorsal cap, medial and posterior parvocellular. PaAP = anterior parvocellular, PaMP = medial parvocellular, PaDC = dorsal cap, PaVP = ventral parvocellular, PaLM = lateral magnocellular, PaPO = posterior parvocellular, 3V = 3rd ventricle. Coordinates refer to bregma levels.

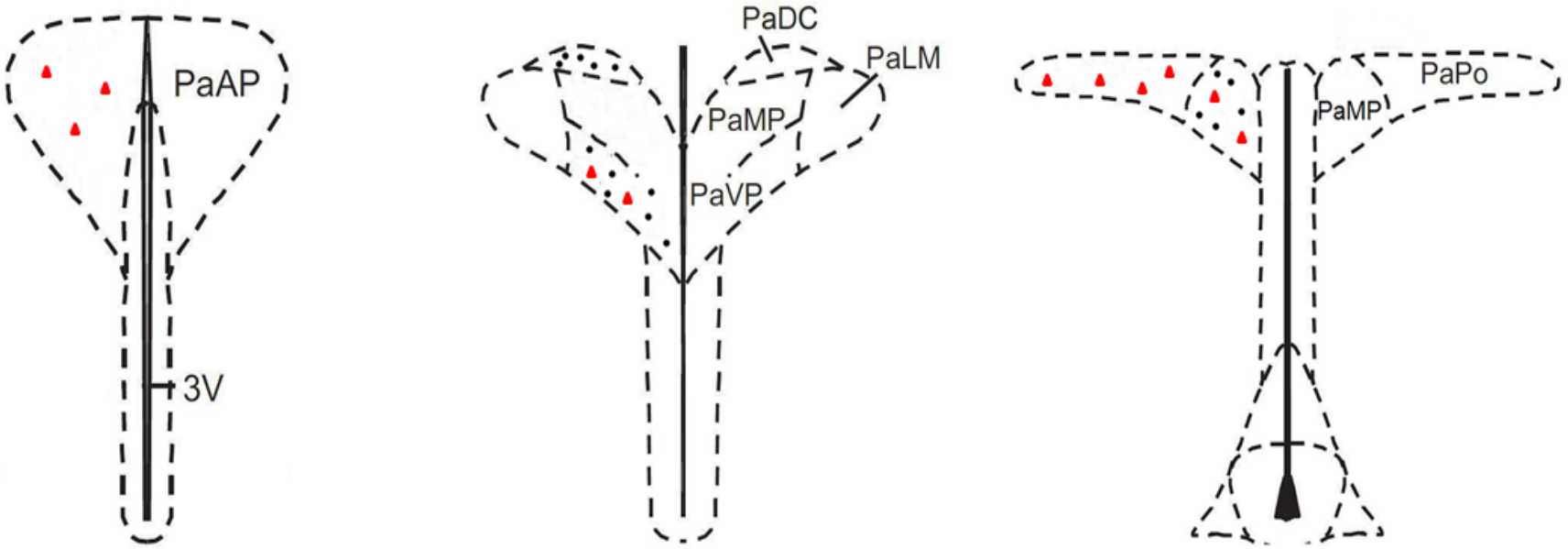

Figure 69 Plots of positions of immunoreactivity changes for the $GABA_A$ α1 (red triangles) and α5 (black circles) subunit for the late-term pregnant rat compared to non-pregnant controls. Each symbol represents a 10% decrease in immunoreactivity. Concomitant changes were observed in the ventral and medial parvocellular subnuclei. PaAP = anterior parvocellular, PaMP = medial parvocellular, PaDC = dorsal cap, PaVP = ventral parvocellular, PaLM = lateral magnocellular, PaPO = posterior parvocellular, 3V = 3rd ventricle. Coordinates refer to bregma levels.

Chapter 7. Co-localisation of $GABA_A$ and NMDA Receptors with Presympathetic Spinally Projecting PVN Neurones

I. Introduction

It is reasonable to suggest that the most direct way for GABA and glutamate to exert their effects on sympathetic outflow from the PVN is to synapse directly onto presympathetic neurones. A significant population of presympathetic neurones emanating from the PVN and known to influence cardiovascular homeostasis project to the IML region of the spinal cord (Pyner & Coote, 2000), and are one of the final sites for modulation of sympathetic outflows (Ranson *et al.*, 1998).

Electron microscopic analysis has revealed that glutamate makes direct synaptic contact onto parvocellular neurones of the PVN (van den Pol, 1991). However this study did not ascertain the nature of these parvocellular neurones (i.e. whether they were interneurone or presympathetic neurone). Furthermore, glutamate was used to identify the synapse, and so the identity of the postsynaptic receptor to which glutamate in these synapses targets remains unclear.

Electrophysiological studies have revealed that PVN-IML projecting neurones are responsive to pharmacological modulation of $GABA_A$ and NMDA receptors (Li *et al.*, 2008a; Han *et al.*, 2010). Interestingly blockade of $GABA_A$ receptors with bicuculline failed to significantly alter the firing rate of the majority of PVN-IML neurones; suggesting that most of these neurones are unresponsive to GABA acting through $GABA_A$ receptors (Han *et al.*, 2010).

What remains unclear from these studies is the identity of the subunits, which compose the $GABA_A$ and NMDA receptors that this population of neurones express. The purpose of this chapter was to assess whether the subunits for which changes have been observed in this thesis (Chapters 5 & 6) were directly associated with PVN-IML projecting neurones in the normotensive rat.

II. Results

a. $GABA_A\alpha1$

Fluorogold (FG) labelling was present in the somata of the spinally projecting neurones as well as projections arising from the somata (Figure 70 A & A'). An isosurface view (indirect rendering) selected from a 3D opacity image, revealed $GABA_A\alpha1$ immunofluorescence to be encapsulating cytoplasmic labelled FG fluorescence. This suggests that $GABA_A\alpha1$ immunofluorescence is potentially membrane bound.

Cells immunoreactive for the $GABA_A\alpha1$ subunit were found throughout the rostrocaudal extent of the PVN with an identical pattern of staining to that described in Chapter 6.III.a.

Quantitative analysis of the number of FG positive (FG+ve) neurones expressing the $GABA_A\alpha1$ subunit revealed 55.15 ± 2.5% (range 41 - 74%) of the FG+ve neurones were also positive for the $GABA_A\alpha1$ subunit. The highest proportion of double labelled neurones were observed in the posterior parvocellular subnuclei (59.5 ± 7.2%; range 43 – 74%) and the lowest proportion found in the anterior parvocellular subnuclei (50.25 ± 4.2%; range 41 – 58%; Figure 71). Fluorogold positive neurones that were not immunoreactive for the $GABA_A\alpha1$ subunit were often lying in close apposition to $GABA_A\alpha1$+ve neurones (Figure 70 C' inset).

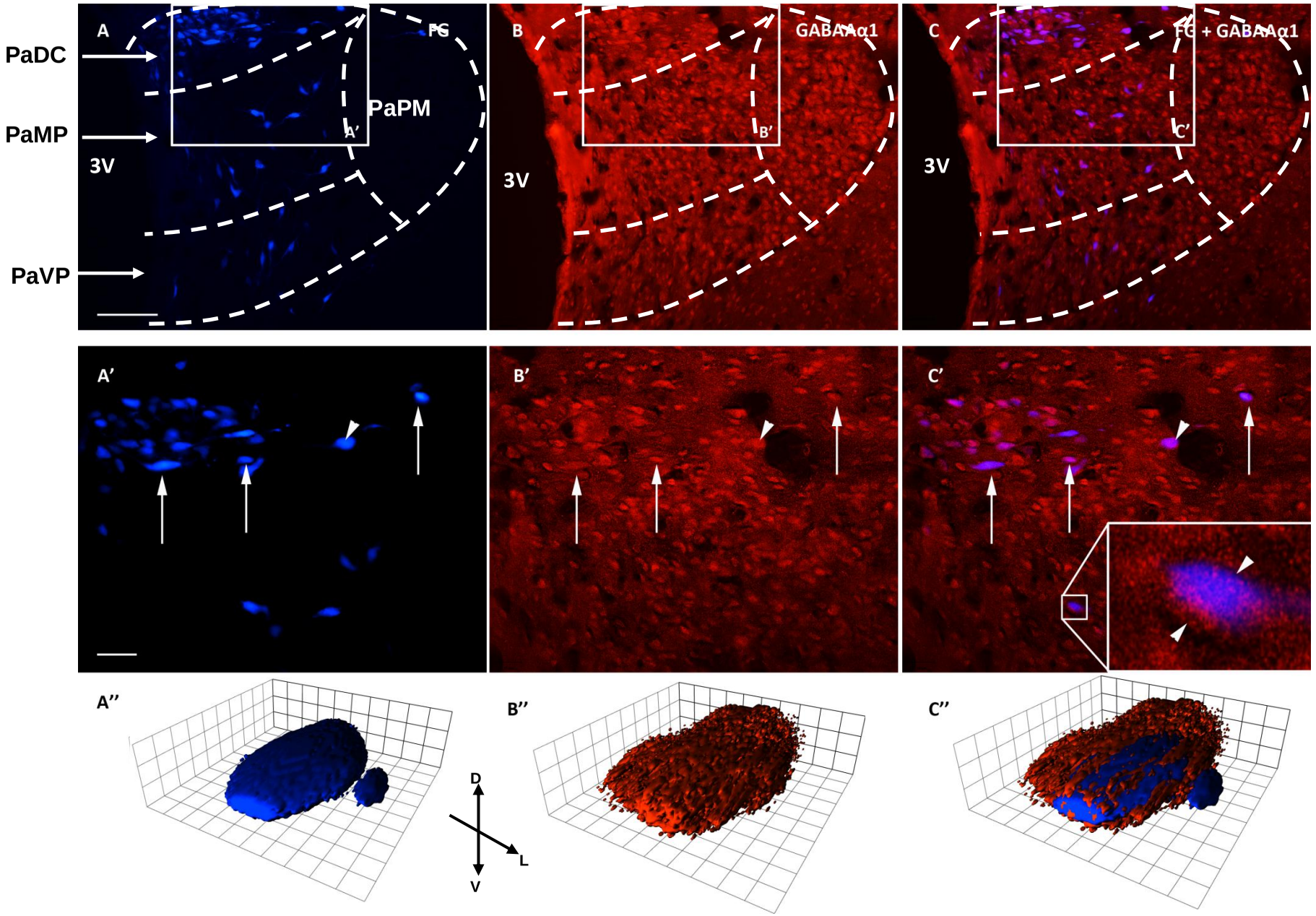
A
FG
PaDC
PaPM
PaMP
A′
3V
PaVP
B
GABAAα1
B′
3V
C
FG + GABAAα1
C′
3V
A′
B′
C′
A″
B″
C″
D
L
V

Figure 70 Photomicrographs showing relationship between spinally projecting PVN neurones and the $GABA_A\alpha1$ subunit in the normotensive, non-pregnant Wistar. Neurones labelled with FG (FG+ve) were found throughout the rostrocaudal extent of the PVN (A). The pattern of $GABA_A\alpha1$ ($GABA_A\alpha1$+ve) staining was as described previously (Chapter 6.III.a) for the PVN. Quantitative analysis shows 55.15 ± 2.5% of FG neurones express the $GABA_A\alpha1$ subunit (large arrows A'-C'). FG+ve neurones that did not express the $GABA_A\alpha1$ subunit lay in close apposition to FG-ve/$GABA_A\alpha1$+ve neurones (inset image C'). Isosurface rendering view revealed the $GABA_A\alpha1$ subunit to surround the FG labelled spinally projecting neurones (A''-C''). Scale bars: A-C = 100μm, A'-C' = 30μm, A''-C'' = 2.7μm^2. 3V = 3rd ventricle. PaDC = Dorsal Cap, PaMP = Medial Parvocellular, PaVP = Ventral Parvocellular, PaPM = Posterior Magnocellular. Orientation Marker for 3D rendered image - D = Dorsal, V = Ventral, L = Lateral. n = 5 biological replicates

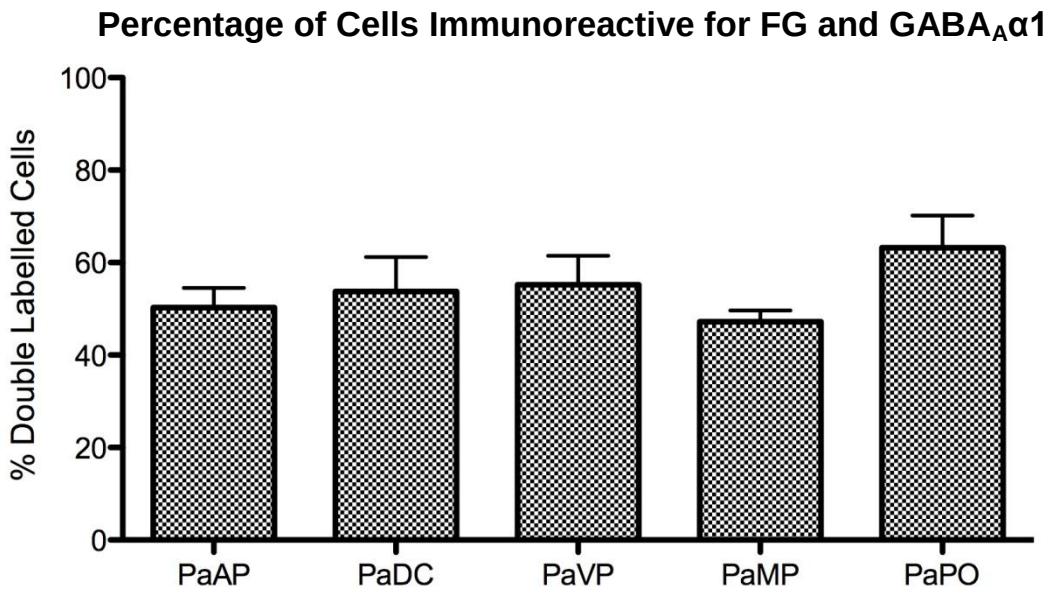

Figure 71 Quantitative analysis of the relationship between FG+ve neurones and $GABA_A\alpha1$+ve neurones in the five parvocellular subnuclei of the PVN, expressed as a percentage of total FG neurones immunoreactive for $GABA_A\alpha1$. Analysis reveals a mean total of 55.15 ± 2.5% of FG+ve neurones to be immunopositive for $GABA_A\alpha1$, with no statistical difference observed between individual subnuclei. n = 5 biological replicates for each subnuclei

b. $\underline{GABA_A\alpha5}$

Cells immunoreactive for the $GABA_A\alpha5$ subunit were found throughout the rostrocaudal extent of the PVN with an identical pattern of staining to that described in Chapter 6.III.c.

Immunoreactivity for the $GABA_A\alpha5$ subunit was confined to the somata (Figure 72 B – B'), in contrast to FG labelling which was observed in both soma and projections (Figure 72 A – A'). An isosurface view (indirect rendering) selected from a 3D opacity image, revealed $GABA_A\alpha5$ immunofluorescence to be encapsulating cytoplasmic labelled FG fluorescence. This suggests that $GABA_A\alpha5$ immunofluorescence is potentially membrane bound. (Figure 72 A''-C'').

Quantitative analysis of the number of FG+ve neurones which were also immunopositive for the $GABA_A\alpha5$ subunit revealed an average of 73.29 ± 3.2% (range 44 - 89%) of FG+ve neurones expressed the $GABA_A\alpha5$ subunit, with the highest proportion observed in the ventral parvocellular subnuclei (81 ± 4%; range 77 – 85%) and the lowest observed in the posterior parvocellular subnuclei (61 ± 9.2%; range 44 – 76%; Figure 73).

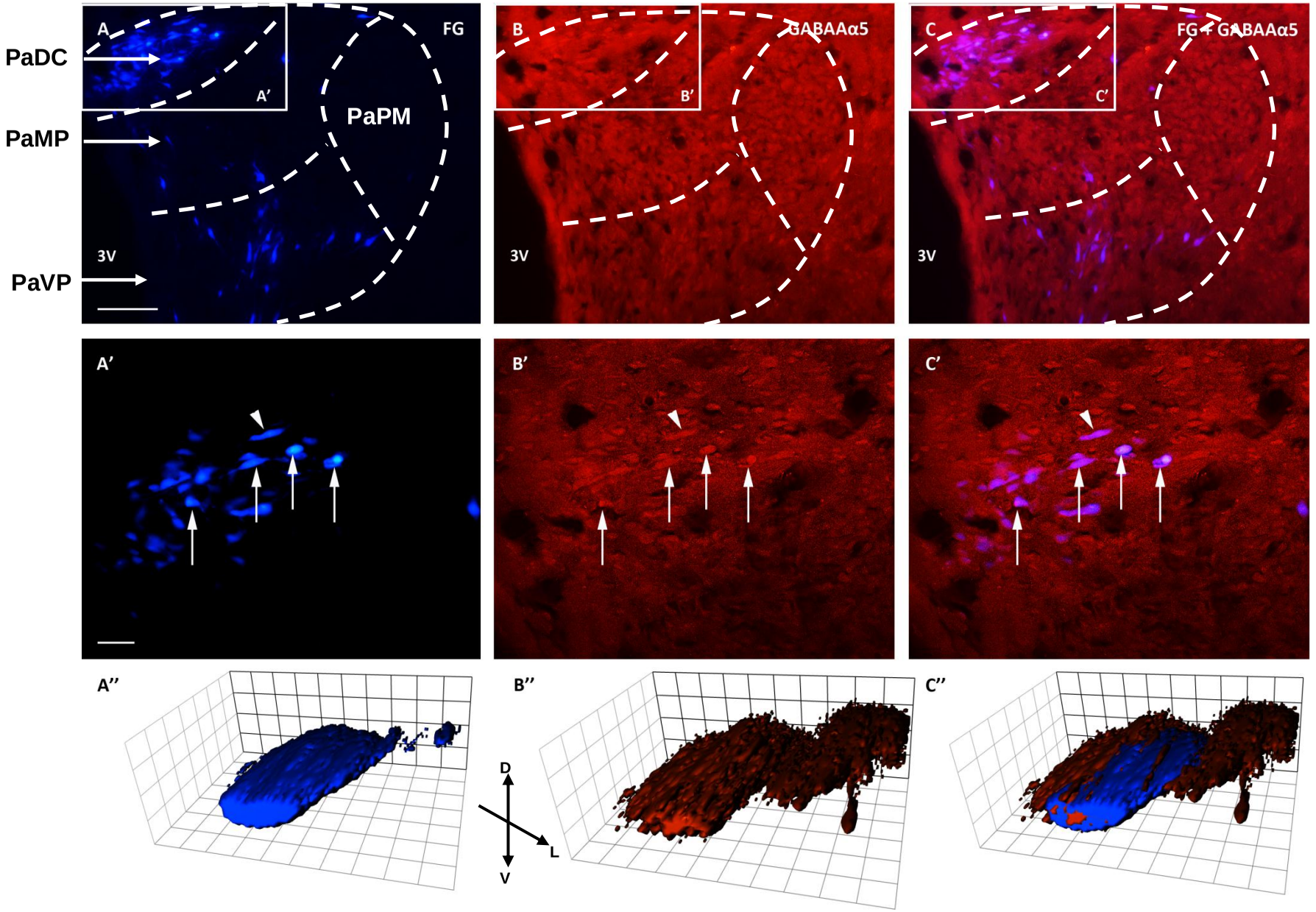
PaDC
PaMP
PaVP
A
FG
A'
PaPM
3V
B
GABAAα5
B'
3V
C
FG + GABAAα5
C'
3V
A'
B'
C'
A''
B''
C''
D
L
V

Figure 72 Photomicrographs showing relationship between spinally projecting PVN neurones and the $GABA_A\alpha5$ subunit in the normotensive, non-pregnant Wistar. Neurones labelled with FG (FG+ve) were found throughout the rostrocaudal extent of the PVN (A). The pattern of $GABA_A\alpha5$ ($GABA_A\alpha5$+ve) staining was as described previously (Chapter 6.III.c) for the PVN. Quantitative analysis shows 73.29 ± 3.2% of FG neurones express the $GABA_A\alpha5$ subunit (large arrows A'-C'). Isosurface rendering view revealed the $GABA_A\alpha5$ subunit to surround the FG labelled spinally projecting neurones (A''-C''). Scale bars: A-C = 100µm, A'-C' = 30µm, A''-C'' = 2.6µm^2. 3V = 3rd ventricle, PaDC = Dorsal Cap, PaMP = Medial Parvocellular, PaVP = Ventral Parvocellular, PaPM = Posterior Magnocellular. Orientation Marker for 3D rendered image - D = Dorsal, V = Ventral, L = Lateral. n = 5 biological replicates.

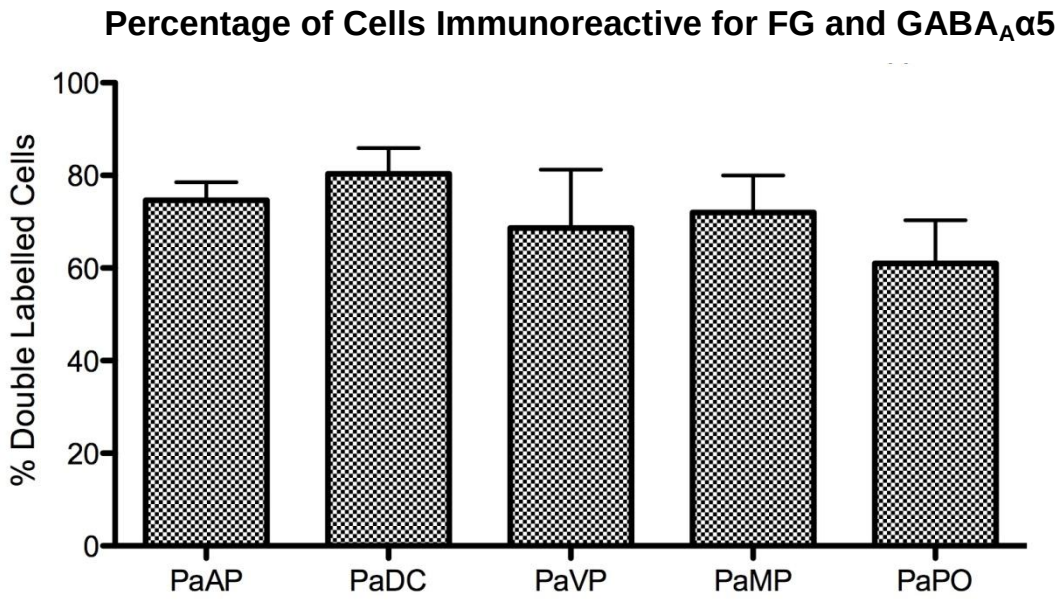

Figure 73 Quantitative analysis of the relationship between FG+ve neurones and $GABA_A\alpha5$+ve neurones in the five parvocellular subnuclei of the PVN, expressed as a percentage of total FG neurones immunoreactive for $GABA_A\alpha5$. Analysis reveals a mean total of 73.29 ± 3.2% of FG+ve neurones to be immunopositive for $GABA_A\alpha5$, with no statistical difference observed between individual subnuclei. n = 5 biological replicates for each subnuclei

c. GluN2A

Expression of the GluN2A subunit of the NMDA receptor was found throughout the rostrocaudal extent of the PVN, with a pattern of expression as described previously (Chapter 5.III.b).

Staining for the GluN2A subunit was found in both soma and projections (Figure 74 B – B'). Although FG labelling was found in both soma and projections (Figure 74 A – A'), double labelling of FG/GluN2A was predominantly localised to the soma (Figure 74 C – C'). Isosurface rendered viewing of an FG+ve/GluN2A+ve neurone revealed GluN2A subunit immunoreactivity surrounds FG labelled spinally projecting neurone (Figure 74 A''- C'').

Quantitative analysis of the number of FG+ve neurones which express the GluN2A subunit of the NMDA receptor revealed 54.95 ± 2.8% (range 40 – 88%) of FG+ve neurones to express the GluN2A subunit, with the highest proportion of double labelled neurones in the posterior parvocellular subnuclei (69.75 ± 7.1%; range 53 – 88%) and the lowest proportion observed in the ventral parvocellular subnuclei (43.75 ± 1.9%; range 40 – 49%; Figure 75). Fluorogold positive neurones which were not immunoreactive for the GluN2A subunit were often lying in close apposition to GluN2A+ve neurones (Figure 74 C' inset).

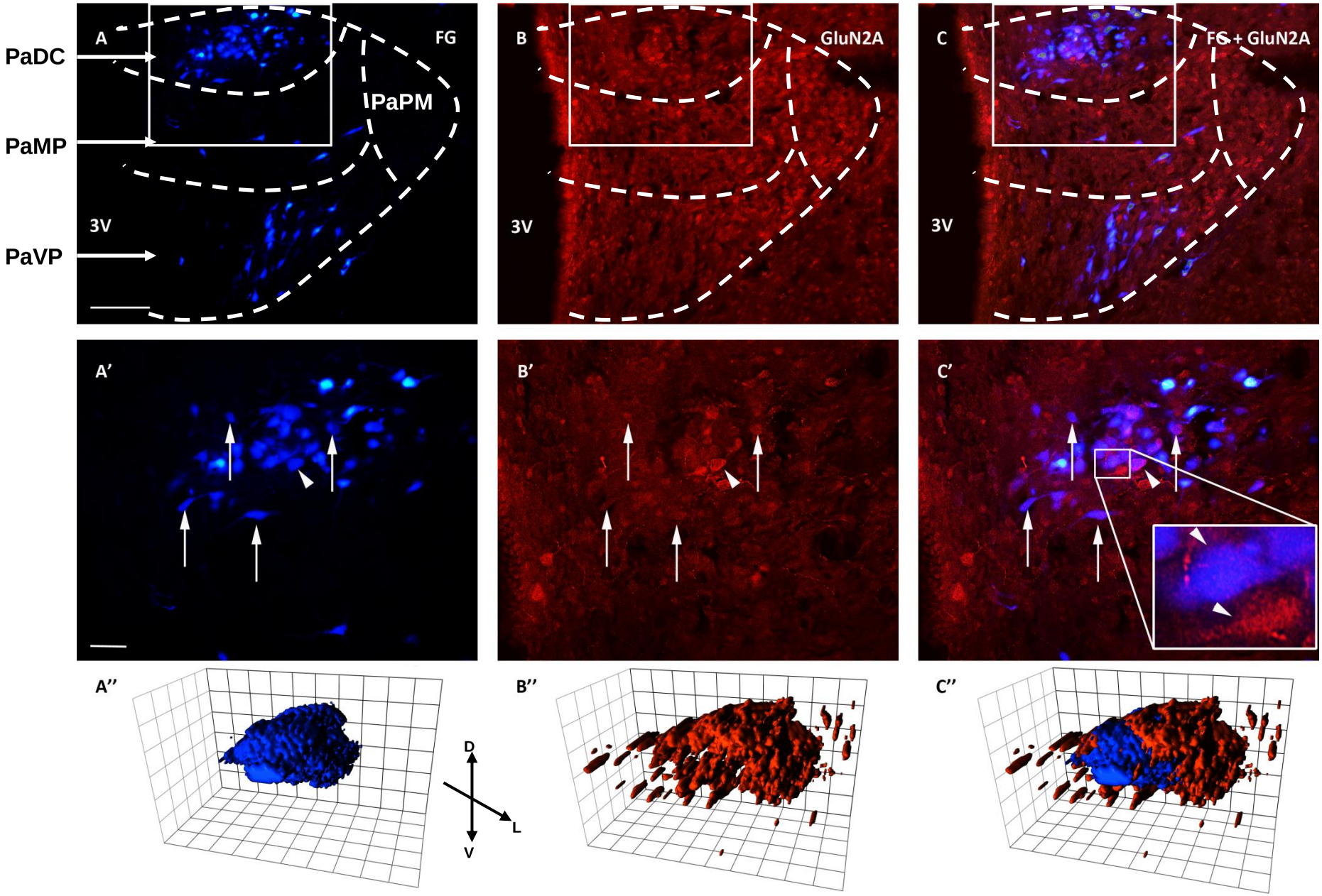
A
FG
PaDC
PaMP
PaVP
PaPM
3V
B
GluN2A
3V
C
FG + GluN2A
3V
A'
B'
C'
A''
B''
C''
D
L
V

Figure 74 Photomicrographs showing relationship between spinally projecting PVN neurones and the GluN2A subunit of the NMDA receptor in the normotensive, non-pregnant Wistar. Neurones labelled with FG (FG+ve) were found throughout the rostrocaudal extent of the PVN (A). The pattern of GluN2A (GluN2A+ve) staining was as described previously (Chapter 5.III.b) for the PVN. Quantitative analysis shows 54.95 ± 2.8% of FG neurones express the GluN2A subunit (large arrows A'-C'). FG+ve neurones that did not express the GluN2A subunit lay in close opposition to FG-ve/GluN2A+ve neurones (inset image C'). Isosurface rendering view revealed the GluN2A subunit to surround the FG labelled spinally projecting neurones (A''-C''). Scale bars: A-C = 100μm, A'-C' = 30μm, A''-C'' = 1.5μm^2. 3V = 3rd ventricle, PaDC = Dorsal Cap, PaMP = Medial Parvocellular, PaVP = Ventral Parvocellular, PaPM = Posterior Magnocellular. Orientation Marker for 3D rendered image - D = Dorsal, V = Ventral, L = Lateral.. n = 5 biological replicates

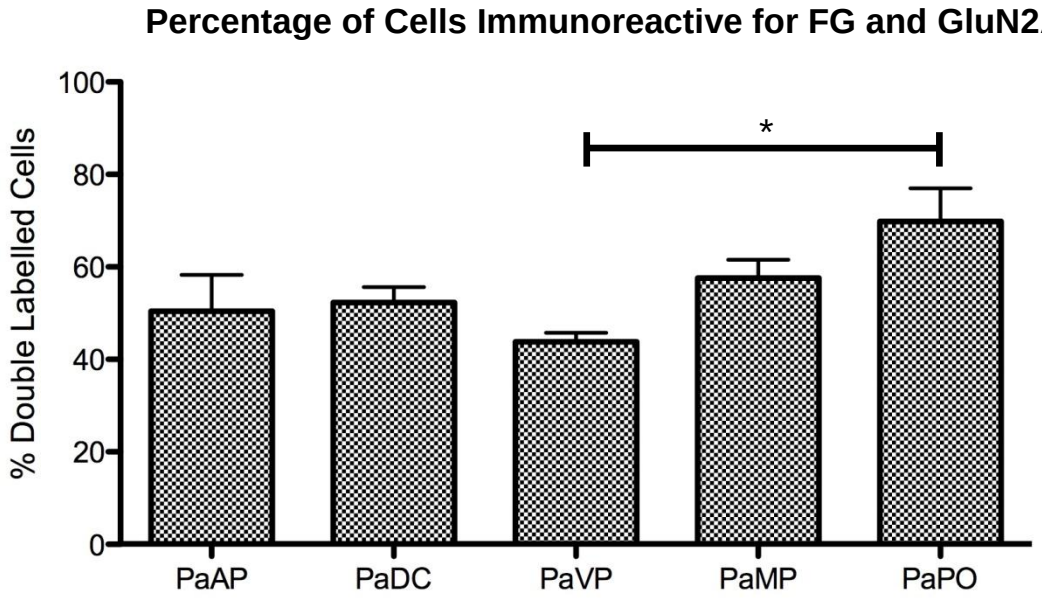

Figure 75 Quantitative analysis of the relationship between FG+ve neurones and GluN2A+ve neurones in the five parvocellular subnuclei of the PVN, expressed as a percentage of total FG neurones immunoreactive for GluN2A. Analysis reveals a mean total of 54 ± 2.8% of FG+ve neurones to be immunopositive for GluN2A. Significantly more double labelled neurones were observed in the PaPO compared with the PaVP (P<0.05), however no other statistically significant differences were observed. n = 5 biological replicates for each subnuclei. * = P<0.05

Chapter 8. Discussion

I. Overview of Results

This study aims to address whether hypertension and pregnancy are associated with changes in the subunit expression of the $GABA_A$ and NMDA receptors in the hypothalamic paraventricular nucleus (PVN). These changes may underpin the sympathoexcitation which is characteristic of these two physiological states.

A decrease in the expression of the α1 and α5 subunit of the $GABA_A$ receptor was found in the PVN of both hypertensive and late-term pregnant rats. In the late-term pregnant rat, the decrease in α1 expression was also associated with a significant decrease in the number of immunoreactive cells in parvocellular subnuclei of the PVN. However, a decrease in immunoreactive cells was not observed in the PVN of the hypertensive rat.

Conversely, both hypertension and pregnancy were associated with significant decreases in the number of α5-IR neurones in parvocellular subnuclei of the PVN.

Hypertension was associated with a significant increase in the expression of the GluN2A subunit of the NMDA receptor, which was associated with significant increases in the number of immunoreactive cells in parvocellular subnuclei of the PVN. Late-term pregnancy on the other hand was associated with a significant increase in the GluN2B subunit of the NMDA receptor, although this was not associated with any increase in cell immunoreactivity.

Furthermore, spinally projecting neurones in the PVN of normotensive rats were associated with the $GABA_A$α1, $GABA_A$α5 and GluN2A subunit of the NMDA

receptor, suggesting that any changes observed in these subunits is likely to influence the discharge properties of these neurones.

Both hypertension and late-term pregnancy were not associated with significant changes in the expression of the α2, α4, β1, β2 or β3 subunit of the $GABA_A$ receptor or the GluN1 subunit of the NMDA receptor.

These results would therefore suggest that normal cardiovascular control requires the contribution of the α1 and α5 subunits of the $GABA_A$ receptor as well as a balance of GluN2A and GluN2B subunits, whereas hypertension and pregnancy exhibiting sympathoexcitation possess different receptor confirmations from the normal state. Furthermore, the changes observed in late-term pregnancy differ from that which is observed in hypertension and may reflect the plasticity of this state such that sympathetic nerve activity can revert to normal post-partum.

Sympathoexcitation is a characteristic feature of both hypertension and pregnancy. This sympathoexcitation is critically involved in the pathogenesis of hypertension, chronically elevating blood pressure by directly increasing vascular resistance and myocardial contractility (Esler, 2000). Conversely the sympathoexcitation observed in pregnancy is a necessity for normal foetal development. Pregnancy-induced sympathoexcitation results in a significant increase in blood volume and cardiac output (40% and 30% increases respectively; Longo, 1983; Jarvis *et al.*, 2012) and a positive correlation exists between maternal blood volume and foetal birth weight (Salas *et al.*, 1993). Crucially, as mentioned above, the sympathoexcitation apparent in late-term pregnancy refers to normal post-partum; therefore the neurochemical changes

which underpin this sympathoexcitation maintains plasticity within the system; in contrast to that which is observed in hypertension.

Interestingly, previous studies have shown that pregnancy in rats is associated with a slight but significant reduction in MAP (Kvochina *et al*, 2009; Page *et al*, 2011). However in this study, late-term pregnancy was associated with a slight but significant increase in blood pressure. The reasons for this are unclear, but could be due to differences in measurement protocol. For example, in this study MAP was measured by catheterisation of the aorta, whereas previous studies (Kvochina *et al*, 2009; Page *et al,* 2011) measured MAP from the femoral artery. It is possible that given the increase in plasma volume and cardiac output observed in pregnancy (Longo *et al*, 1983) that this is manifested as a slight increase in aortic pressure.

Previous studies have provided compelling evidence that the PVN is a key central nucleus involved in the aetiology of sympathoexcitation observed in both of these physiological states (Guyenet, 2006; Page *et al*, 2011). *In vivo* electrophysiological studies have shown that both hypertension and pregnancy appear to be associated with a decrease in the activity of the GABAergic system within the PVN (Li & Pan, 2006; Kvochina *et al.*, 2009; Page *et al.*, 2011; Ye *et al.*, 2012a). However, the molecular mechanisms that govern this increased sympathetic nerve activity are not fully understood.

II. Changes in $GABA_A$ Receptor Subunit Expression Observed in the PVN of Hypertensive and Late-Term Pregnant Rats

In hypertension, bilateral microinjection of the $GABA_A$ receptor agonist muscimol into the PVN produced an attenuated depressor, bradycardic and sympathoinhibitory response in the SHR compared to age matched WKY controls (Li & Pan, 2007b). Furthermore, blockade of the GABAergic system, with bilateral microinjections of the $GABA_A$ receptor antagonist bicuculline produced attenuated pressor, tachycardic and sympathoexcitatory effects in SHR compared with WKY controls (Li & Pan, 2007b). *In vitro* analysis of PVN neurones from both SHR and WKY rats showed that PVN-RVLM projecting neurones in the SHR had a significantly higher baseline firing rate than those in age-matched WKY controls (Li & Pan, 2006). Direct application of bicuculline increased the firing rate of all rhodamine-labelled neurones in 6 week SHR and 13 week old WKY rats, but only increased the firing rate of 48.9% of these neurones in 13 week old SHR (Li & Pan, 2006). Furthermore, the concentration of endogenous GABA in the hypothalamus has also been shown to be reduced in 10- and 17-week old SHR compared with age matched WKY controls (Hambley *et al.*, 1984). Taken together, these results suggest that the GABAergic inhibition in the PVN of the SHR is attenuated compared with normotensive rats.

This study has shown that hypertension is accompanied by a 48 ± 6.5% decrease in expression of the α1 subunit as well as a 97 ± 2% decrease in expression of the α5 subunit of the $GABA_A$ receptor compared with normotensive Wistar controls. Furthermore, this is accompanied by a complete reduction in α5-IR neurones in all parvocellular subdivisions of the PVN in the

SHR (Figure 63). This is the first demonstration that the PVN of hypertensive animals are associated with decreases in specific $GABA_A$ receptor subunits. Furthermore, this is the first study to show that the PVN of the hypertensive rat is associated with a highly significant decrease in expression of the α5 subunit of the $GABA_A$ receptor. The α5 knockout mice ($gabra5^{-/-}$) shows that removal of this subunit from the $GABA_A$ receptor results in significant increases in the basal firing rate of hippocampal neurones (Glykys *et al*, 2008). Therefore it is highly likely that the complete decrease in expression observed in the PVN of the hypertensive rat will significantly increase the basal firing rate of these neurones, as well as contributing to the decreased GABAergic influence observed in this state. We also have evidence that there is decreased α5 expression in the spinal cord of the SHR; albeit to a lesser extent (unpublished results).

Interestingly, the reduction in α1 subunit expression observed in the SHR is not accompanied by a reduction in the number of immunoreactive cells in any of the parvocellular subnuclei of the PVN. Possible explanations for this are twofold. First, the cell counts were confined to the parvocellular subdivisions only, whereas the quantitative immunoblotting was performed on PVN micropunches incorporating both the parvocellular and magnocellular subdivisions. Since $GABA_A$α1 subunits were expressed in both magno- and parvocellular subnuclei of the PVN, it is possible that the decrease in α1 expression is confined to the magnocellular subdivisions and not associated with any parvocellular subnuclei. Secondly, a decrease in cell immunoreactivity suggests that neurones which would have previously expressed the α1 subunit of the $GABA_A$ receptor now lack this subunit. It is possible that no neurone fully

loses expression of the α1 subunit, but may express it at a decreased level. The methodological approach taken in this study did not allow for quantification of cell staining density; which could have alluded to the relative expression of subunits within individual cells.

A reduced GABAergic inhibition has also been observed in the PVN of late-term pregnant rats. To this effect, unilateral microinjection of bicuculline into the PVN of late-term pregnant rats (P21) produced an attenuated pressor, tachycardic and sympathoexcitatory effect compared with non-pregnant animals (Kvochina *et al.*, 2009; Page *et al.*, 2011). At present, little work has been undertaken to further examine the contribution the PVN makes to sympathoexcitation observed in pregnancy. However the studies detailed above, suggest that overall GABAergic inhibition is reduced in the PVN of late-term pregnant rats.

Here we show that late-term pregnancy (P19) is associated with a decrease in the expression of the α1 and α5 subunits in the PVN. The decrease in α1 subunit expression is similar in degree to that observed in the SHR (43 ± 1.2% vs. 48 ± 6.5% respectively). However, the decrease in expression for the α5 subunit was not as pronounced in the late-term pregnant rat as for the SHR (38 ± 8% vs. 97 ± 2% respectively). Furthermore, the decrease in α1 expression was associated with a significant decrease in the number of α1-IR neurones in the anterior (34 ± 2%), medial (19 ± 3%), ventral (26 ± 5%) and posterior (39 ± 7%) parvocellular subdivisions compared with non-pregnant controls (Figure 55). The decrease in α5 expression was also associated with a significant

decrease in the number of α5-IR neurones in the medial (56 ± 4%), ventral (60 ± 2%) and dorsal cap (52 ± 6%) regions (Figure 63).

Cell counts of α1-IR neurones in the PVN show a differential response between SHR and late-term pregnant rats, despite showing similar decreases in overall expression. Late-term pregnancy is associated with a 29.5 ± 4% decrease in the number of α1-IR neurones across all parvocellular subnuclei compared with normotensive controls, whereas the SHR shows no significant difference. This suggests that while the expression of the α1 subunit within individual neurones in the PVN of SHR may be reduced, in late-term pregnant rats, this is associated with a total loss of immunoreactivity in almost 30% of neurones.

Furthermore, both hypertension and late-term pregnancy are associated with a significant reduction in the expression of the α5 subunit of the $GABA_A$ receptor, which in both physiological states is associated with a decrease in the number of α5-IR neurones within the PVN. In agreement with the Western blot analysis, the number of α5-IR neurones in the SHR is significantly less than is observed in the late-term pregnant rat. Indeed, no α5-IR neurone was identified in any parvocellular subnuclei in the PVN of the SHR, whereas late-term pregnancy was associated with an averaged 56 ± 2% decrease across all parvocellular subnuclei compared with non-pregnant controls.

III. Changes in NMDA Receptor Subunit Expression Observed in the PVN of Hypertensive and Late-Term Pregnant Rats

The PVN of hypertensive rats has been found to be associated with increased activity of NMDA receptors, such that blockade of NMDA receptors in the PVN of the SHR produces a significantly greater decrease in LSNA, HR and ABP than in normotensive controls (Li & Pan, 2007a). Furthermore, application of NMDA onto PVN-IML projecting neurones produced a significantly augmented inward current compared with normotensive controls (Li *et al.*, 2008a).

This study also presents data to show that the decrease in $GABA_A$ receptors observed in the hypertensive rat is also accompanied by an increase in expression of the GluN2A subunit of the NMDA receptor. Analysis of whole PVN micropunches shows an 85 ± 23% increase in GluN2A expression in the PVN of the SHR compared with normotensive controls. Furthermore, this is accompanied by an increase in the number of GluN2A-IR neurones in the medial (32 ± 7.8%), dorsal cap (19 ± 4%) and posterior (57 ± 10%) parvocellular subnuclei of the PVN compared with normotensive controls (Figure 39). Hypertension was not associated with a significant increase in expression of the GluN1 or GluN2B subunits from either whole PVN micropunches or analysis of immunoreactive cells. This is in contrast to results obtained by Ye *et al* (2012b), who observed that the PVN of the SHR was associated with an increase in GluN2B subunit expression, although this was not associated with an increase at the level of the synapse.

Results from *in vivo* electrophysiological studies in late-term pregnant rats suggest that the sympathoexcitation observed in this state is not mediated by glutamatergic inputs, but is instead dependent upon AngII inputs (Kvochina *et al.*, 2009).

In this study, we show that late-term pregnancy was associated with a 98.5 ± 40% increase in GluN2B expression in whole-PVN micropunches. This was not associated with any increase in the number of immunoreactive cells in any of the parvocellular subnuclei. However, qualitative analysis of immunohistochemical staining for this subunit showed that staining density was more pronounced in the magnocellular subnuclei of the PVN, suggesting that this increased expression may contribute to the increased neurohumoral component associated with pregnancy. Further evidence that this increase is not associated with autonomic controlling parvocellular neurones was presented in a study by Kvochina *et al* (2009) where blockade of NMDA receptors in the PVN of late-term pregnant rats did not significantly attenuate the sympathoexcitatory or pressor effects of prior bicuculline microinjection (Kvochina *et al.*, 2009).

IV. Distribution of Presympathetic Spinally Projecting Neurone from the PVN and their Subunit Immunoreactivity

To our knowledge, this is the first study to examine the distribution of presympathetic spinally projecting neurones in the PVN of the female Wistar rat. Previous neuroanatomical studies have focussed their studies on the male Wistar (Portillo *et al.*, 1998) or Sprague Dawley rat (Shafton *et al.*, 1998; Pyner & Coote, 2000; Hallbeck *et al.*, 2001).

The pattern of distribution observed in this study labelled with both CTB (Chapter 4) and FG (Chapter 7) was similar to that previously reported (Portillo *et al.*, 1998; Shafton *et al.*, 1998), with labelling observed in the five parvocellular subnuclei as described by Paxinos and Watson (1998).

Results from this study also show that presympathetic neurones in the PVN of normotensive female Wistar rats express subunits of the $GABA_A$ and NMDA receptor. In the normotensive female Wistar rat, quantitative analysis of the number of FG labelled presympathetic neurones show that 55.15 ± 2.5% express the α1 subunit of the $GABA_A$ receptor, whereas 73.29 ± 3.2% express the α5 subunit of the $GABA_A$ receptor. Furthermore, 54.95 ± 2.8% of presympathetic spinally projecting neurones express the GluN2A subunit of the NMDA receptor.

These results suggest that at least a proportion of spinally projecting neurones in the PVN of the normotensive female Wistar rat have the potential to be directly influenced by the decrease in $GABA_A$ α1 and α5 subunit expression, a

characteristic of both hypertension and late-term pregnancy and previously reported in this study.

The observation that 54.95 ± 2.8% of PVN-IML projecting presympathetic neurones express the GluN2A subunit of the NMDA receptor in the normotensive Wistar reveals that there is a significant proportion of this population which are not directly influenced by GluN2A-containing NMDA receptor activity. Given that the increase in GluN2A subunit expression observed in the SHR was associated with significant increases in the number of GluN2A-IR neurones in the medial, dorsal cap and posterior parvocellular subnuclei; areas which contain the majority of PVN-IML presympathetic neurones (Pyner & Coote, 2000), it is possible to speculate that at least part of this increase in GluN2A-IR is attributable to this population of presympathetic neurones.

A number of neurones expressed the α1 or α5 subunit of the $GABA_A$ receptor or the GluN2A subunit of the NMDA receptor and are putatively identified as non-spinally projecting given their absence of FG; however it is feasible that not all spinally-projecting neurones were labelled in this study. This suggests that populations of neurones other than PVN-IML projecting presympathetic neurones have the capacity to respond to the changes in expression that these subunits show in both hypertension and pregnancy. The identity of these neurones remains unclear, but given the high level of interneurones and neurones projecting to other central nuclei within the PVN (i.e. RVLM, NTS; Oldfield *et al.*, 2001), it is possible that these populations of

neurones may also be susceptible to fluctuations in the expression of these subunits.

Interestingly, in the case of the $GABA_A$α1 and GluN2A subunits, those FG+ve neurones which did not express either of these subunits were often found to be lying in close apposition to $GABA_A$α1 or GluN2A positive neurones. This suggests a potential indirect mechanism; possibly through an interneurone, by which these neurones respond to receptors containing these subunits. This also provides another mechanism by which these presympathetic neurones may be able to respond to fluctuations in the expression of these subunits observed during hypertension and pregnancy.

V. Physiological Implications of Results

a. Implications of the Decrease in $GABA_A$ Receptor Expression on Neuronal Excitability in the PVN

$GABA_A$ receptors containing either the α1 or the α5 subunits display distinct physiological characteristics as well as subcellular localisation. $GABA_A$ receptors containing the α1 subunit comprise the most common $GABA_A$ receptor subunit conformation, together with the β2 and γ2 subunits, and confirms a synaptic localisation (Somogyi *et al.*, 1996). As such, these receptors play an important role in mediating phasic inhibition (Prenosil *et al.*, 2006). Although a reduction in the expression of the α1 subunit was observed, there was no alteration observed in β2 expression, suggesting that this subunit may complex with other subunits to form receptors with physiologically distinct characteristics.

Conversely, the presence of the α5 subunit within $GABA_A$ receptors (most often in combination with the β3 and γ2 subunits) overrides the ability of the γ2 subunit to promote synaptic localisation and targets the receptor to the extrasynaptic membrane (Farrant & Nusser, 2005; Serwanski *et al.*, 2006). $GABA_A$ receptors comprising the α5 subunit have a higher sensitivity to GABA and are able to respond to lower concentrations that are constantly present in the extrasynaptic space, thereby mediating a constant tonic form of inhibition (Farrant & Nusser, 2005). This allows extrasynaptic receptors to act as a brake, preventing over excitation of neuronal membranes.

Hippocampal neurones from α5 knock-out mice show an increased basal firing rate compared with wild type controls. This level of baseline activity is of a

similar magnitude to wild type neurones subjected to the α5 inverse agonist L655,708 (Glykys *et al.*, 2008). Furthermore, PVN-RVLM projecting neurones from normotensive rats have been found to be under a heavy tonic inhibitory influence from extrasynaptic receptors (Park *et al.*, 2007). To this effect, blockade of extrasynaptic receptors significantly increased the basal firing rate of these neurones when compared with control or when synaptic receptors only were blocked (Park *et al.*, 2007), suggesting that tonic inhibition is critical in controlling the level of firing of these PVN neurones. Furthermore, results described in this thesis have shown that an average of 73.6 ± 5.9% of PVN-IML projecting neurones express the α5 subunit, suggesting that this population of neurones has the potential to be influenced by activity of α5-containing $GABA_A$ receptors.

Although tonic inhibition is largely believed to be controlled by δ-containing $GABA_A$ receptors, due to its high sensitivity for GABA (Zheleznova *et al.*, 2009), recent *in vitro* studies on magnocellular neurosecretory neurones of the supraoptic nucleus (SON) have shown that tonic inhibition in this population of neurones is governed by α5 containing $GABA_A$ receptors more-so than δ-containing $GABA_A$ receptors (Jo *et al.*, 2011). Moreover, the expression of α5-subunit mRNA in the SON was 400% greater than the δ subunit (Jo *et al.*, 2011). Given that the PVN and SON are similar in their neurochemistry and function (Swanson & Sawchenko, 1983), it is reasonable to suggest that tonic inhibition in the PVN is controlled by a similar manner, and could explain the relative difficulty in probing for the δ subunit in the PVN in this study. This suggestion is further evidenced in this study by the high number of PVN-IML projecting presympathetic neurones which express the α5 subunit.

Given the results obtained, and in conjunction with the electrophysiological studies described above, it is possible to speculate that both the complete loss of expression of the α5 subunit observed in hypertension and the partial reduction in expression in late-term pregnancy would significantly increase the basal firing rate of neurones within the PVN. Furthermore, given that α1 containing receptors are concentrated at synapses (Somogyi *et al.*, 1996), it is possible to speculate that the similar reduction in expression observed in both hypertension and late-term pregnancy would also reduce the capacity for phasic inhibition.

Physiologically, this reduction in both phasic and tonic inhibition would be important in mediating the sympathoexcitation observed in both hypertension and pregnancy. The causes of this decrease in inhibition are not clear; however multiple previous studies give some indication.

First, the PVN of both hypertensive and pregnant rats has been found to have an increased sensitivity to angiotensin administration (Kvochina *et al.*, 2009; Gabor & Leenen, 2012). To this effect blockade of angiotensin receptors by the angiotensin receptor antagonist candesartan into the PVN of hypertensive rats significantly decreased arterial blood pressure in Dahl salt sensitive rats fed a high salt diet, but not those fed a low salt diet (Gabor & Leenen, 2012). Furthermore, infusion of the AT1 receptor antagonist L158, 809 into the PVN of late-term pregnant rats significantly attenuated the sympathoexcitatory and pressor effects of bicuculline injection (Kvochina *et al.*, 2009). Previous studies have shown that the sympathoexcitatory effects of angiotensin II within the PVN are achieved through inhibition of presynaptic GABA release (Li & Pan, 2005). Taken together, the sympathoexcitation in both hypertension and pregnancy

may be mediated; at least in part, through an AngII mediated disinhibition through attenuation of GABA release. Since reduced GABA activity in cell culture lines has been shown to decrease the cell surface expression of $GABA_A$ receptors (Saliba *et al.*, 2009), it is possible that reduced presynaptic GABA release in the PVN could reduce the number of postsynaptic $GABA_A$ receptors. This would be true for both synaptic and extrasynaptic $GABA_A$ receptors, since it has been shown that the activity of extrasynaptic $GABA_A$ receptors within the PVN is dependent upon presynaptic GABA release (Park *et al.*, 2007)

Angiotensin may not be the only candidate for the loss of presynaptic GABA release. Studies have shown that both hypertension and pregnancy are associated with a reduced baroreceptor input. In hypertension, this is believed to be due to either arterial stiffening, reducing the capacity for arterial distension and therefore baroreceptor activation, and/or “resetting” of baroreceptors to operate at a higher set point (Head, 1995; Kougias *et al.*, 2010). In pregnancy, progesterone has been shown to reduce the activity of high frequency atrial volume receptors (Hines & Hodgson, 2000; Storey & Kaufman, 2004). In rats, baroreceptor inputs synapse onto second order neurones in the NTS (Andresen & Kunze, 1994; Kougias *et al.*, 2010). A recent neuroanatomical study from our laboratory has provided evidence that a subpopulation of these second order neurones project to and make a putative glutamatergic synapse with GABAergic interneurones surrounding the PVN (Affleck *et al.*, 2012); which previous evidence has shown to synapse with spinally projecting presympathetic neurones (Watkins *et al.*, 2009). Since hypertension and pregnancy are associated with reduced baroreceptor input, this would likely reduce glutamatergic input on GABAergic neurones in the PVN; in turn reducing

presynaptic GABA release, and therefore reducing the density of postsynaptic $GABA_A$ receptors.

Thirdly, electrophysiological data has shown that NMDA receptor activation can suppress $GABA_A$ receptor function. Electrical stimulation of CA1 neurones in a hippocampal slice preparation from adult guinea pigs produces an NMDA receptor dependent excitation. Continued stimulation of these neurones results in an increased sensitivity to applied NMDA, and a reduced sensitivity to GABA (Stelzer *et al.*, 1987). This was also observed in isolated CA1 neurones from adult guinea pigs, in which continued application of NMDA reduced the peak amplitude of evoked GABA currents to around 15% of control levels (Figure 76**;** Stelzer & Shi, 1994). Furthermore, the decreased sensitivity to GABA and increased NMDA sensitivity were blocked by prior application of the NMDA receptor antagonist AP5. Moreover, application of NMDA to cultured mouse cortical neurones reduced the expression of GAD65/67 as well as reducing dendrite growth (Monnerie & Le Roux, 2007); an effect, which was blocked by prior antagonism of GluN1/2A/2B containing receptors, but not GluN1/2B containing receptors (Monnerie *et al.*, 2010). This suggests that GluN2A containing receptors may be important in mediating the NMDA-mediated decrease in GAD expression. Indeed a decrease in GAD activity has been previously observed in the hypothalamus of SHR (Czyzewska-Szafran & Wutkiewicz, 1986). This decrease in GAD activity and the resulting decrease in presynaptic GABA release could ultimately drive a decrease in postsynaptic $GABA_A$ receptor density.

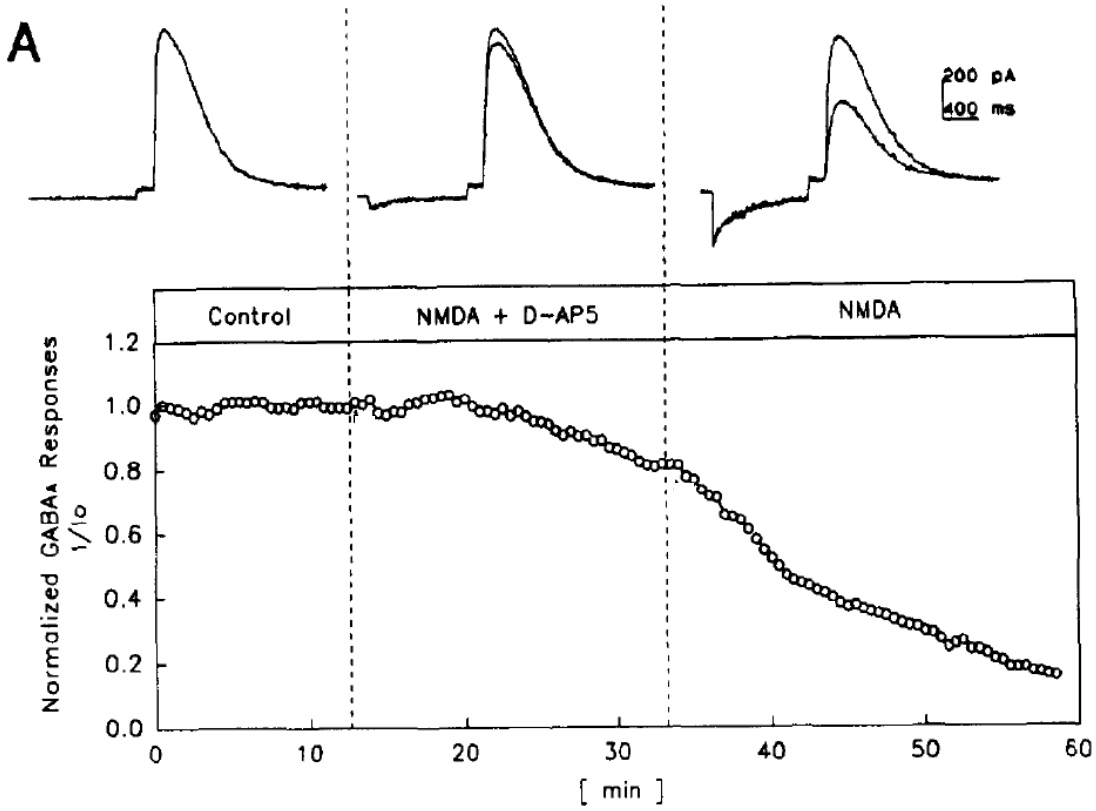

Figure 76 Normalised $GABA_A$ receptor responses following NMDA receptor activation. NMDA receptor activation reduces $GABA_A$ receptor activity in a time-dependent fashion (right), culminating in a response which is 75% lower than control levels. Application of NMDA in the presence of the NMDA receptor antagonist AP5 fails to significantly alter peak responses (centre), suggesting a NMDA-specific mechanism (Stelzer & Shi, 1994).

Previous studies have shown that activation of NMDA receptors maintains sympathetic tone in hypertension (Li & Pan, 2007a; Li *et al.*, 2008a), and that this is coupled with a decrease in $GABA_A$ receptor activity (Li & Pan, 2006, 2007b). Furthermore, results from this study and from a recently published study by another group (Ye *et al.*, 2012b) show that hypertension is associated with a significant up-regulation of the GluN2A subunit of the NMDA receptor in the PVN. Taken together, it is possible to speculate that NMDA receptor activation in the PVN of hypertensive rats results in $GABA_A$ receptor endocytosis, thereby reducing the activity of $GABA_A$ receptors and resulting in the reduced expression of the α1 and α5 subunits observed in this study.

However this is unlikely since pregnancy has been shown to be associated with a decrease in GABAergic inhibition of autonomic neurones (Kvochina *et al.*, 2009; Page *et al.*, 2011) independent of an increase in both NMDA receptor activity (Kvochina *et al.*, 2009) and increase in NMDA receptor subunit expression in parvocellular subnuclei.

It is more likely that since NMDA receptors are under heavy $GABA_A$ receptor mediated inhibition in the PVN of normotensive rats (Chen *et al.*, 2003); that the down regulation of the α1 and α5 subunits of the $GABA_A$ receptor in hypertensive and pregnant rats precedes the up-regulation of NMDA receptor activity. This is evidenced by studies showing that the sympathoinhibitory actions of NMDA receptor blockade in the PVN of normotensive rats requires the prior removal of $GABA_A$ receptor mediated inhibition (Chen *et al.*, 2003). Furthermore, GluN2A subunit trafficking to the synapse is dependent on activation of synaptic NMDA receptors (Barria & Malinow, 2002; Storey *et al.*, 2011). Therefore, the removal of $GABA_A$ receptors in the PVN of hypertensive rats would allow for an increase in the activity of glutamatergic synapses, thereby increasing GluN2A subunit expression.

Irrespective of whether the decrease in $GABA_A$ receptor expression precedes the increase in NMDA receptor expression or vice versa; it is possible that the two are self-perpetuating; such that the reduction in GABAergic inhibition resulting from the decreased $GABA_A$ receptor expression allows for NMDA-mediated excitation to dominate. This in turn may further propagate the decrease in GABAergic inhibition, either through decreasing $GABA_A$ receptor expression and/or decreasing GAD67 expression.

b. Implications of the Increase in NMDA Receptor Expression on Neuronal Excitability in the PVN

Although we show an increase in GluN2B subunit expression in the whole PVN of late-term pregnant rats, it is unclear what physiological effect this has, since this was not associated with changes in immunoreactivity in parvocellular subnuclei. In a previous study examining the role of NMDA receptors in maintaining sympathetic tone in late-term pregnancy, blockade of NMDA receptors with kynurenic acid failed to significantly blunt the sympathoexcitatory and pressor effects of bicuculline microinjection when compared to blockade of angiotensin receptors (Kvochina *et al.*, 2009). This suggests that NMDA receptors do not play a significant role in controlling the sympathoexcitation observed in pregnancy. Furthermore, given the activity-dependent nature of GluN2A subunit entry into synapses, it would be expected that any increase in glutamatergic activity would result in an increase in GluN2A subunit expression, since these are activity-dependent (Gambrill *et al.*, 2011). However, it was noted that expression of the GluN2B subunit was more prominent in magnocellular subnuclei. It is therefore possible that the increase in GluN2B subunit expression mediates an increase in the neurohumoral component of pregnancy and has little effect on autonomic control.

This is consistent with previous experiments examining plasma osmolality. Non-pregnant rats that consumed a 2% saline solution for 4-10 days showed a significant increase in plasma osmolality as well as a decrease in GluN2B subunit expression in both the PVN and SON (Curras-Collazo & Dao, 1999). Since pregnancy is associated with a decrease in plasma osmolality of around 10mOsm/kg (Heesch *et al.*, 2009), it is possible to speculate that this may

cause an increase in GluN2B subunit expression, opposing that observed following an increase in osmolality. This is further supported by a study from Davison *et al* (1989) showing that vasopressin secretion is increased in late term pregnancy, consistent with an increase in excitatory input to hypothalamic neurosecretory cells (although metabolic clearance of vasopressin is increased, resulting in normalised serum levels).

Analysis of GluN1 subunit expression in whole PVN micropunches as well as immunohistochemistry revealed no significant increase in expression in either SHR or late-term pregnant rats. This is in contrast to results obtained from HF rats; where GluN1 subunit expression was found to increase in the PVN (Li *et al.*, 2003).

Since the GluN1 subunit is an obligatory subunit, required for binding of the co-agonist glycine (Kohr, 2006), it would be expected that any increase in GluN2 subunit expression should be met with a concomitant increase in GluN1 immunoreactivity. Furthermore, a recent electrophysiological study has demonstrated that the increase in GluN2A subunit expression in the PVN of SHR confers physiologically relevant properties to PVN neurones (Ye *et al.*, 2012b); suggesting that the increase in GluN2A subunit expression is contributing to an increase in functional receptors.

We hypothesise that this discrepancy may be the result of intracellular pools of unassembled GluN1 subunits, located within the endoplasmic reticulum (Chazot & Stephenson, 1997b). Expression of GluN1 subunits alone in cultured cells results in the accumulation of intracellular GluN1 subunits, with no cell surface expression (McIlhinney *et al.*, 1998). This pool of unassembled intracellular

GluN1 subunits has also been identified in the brain of mice (Chazot & Stephenson, 1997b). Co-expression of the GluN1 subunit in cell cultures with the GluN2A subunit promotes cell surface trafficking of these receptors (McIlhinney *et al.*, 1998), suggesting that the intracellular GluN1 subunits require a GluN2 subunit for surface trafficking. In the PVN of hypertensive or late-term pregnant rats, the increase in GluN2A and GluN2B which are seen respectively in the absence of any GluN1 subunits could be due to cell surface promotion of intracellular GluN1 subunits by the increased level of GluN2 subunits observed in both of these physiological states (Figure 77). The methodology used in this study to investigate whole PVN protein expression as well as immunohistochemistry incorporated both intracellular and extracellular populations of GluN1 receptor subunits.

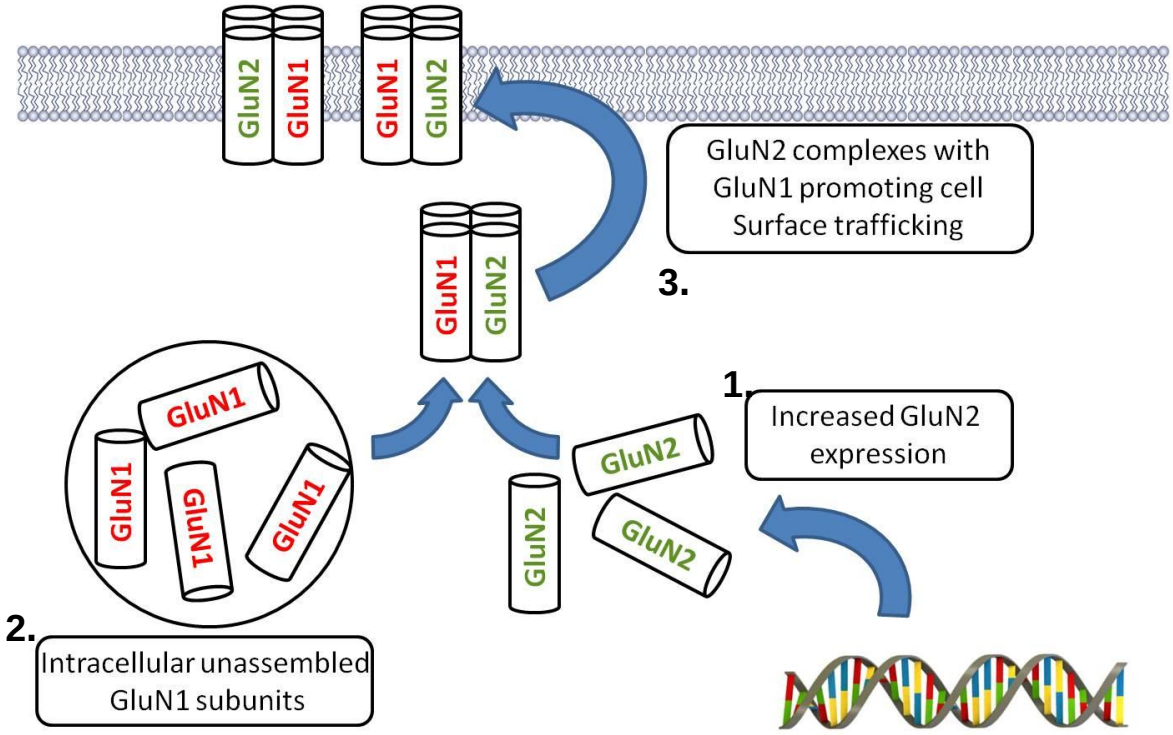

Figure 77 Schematic representation of possible mechanism mediating the increase in GluN2 subunit expression without increasing overall GluN1 subunit expression. Increased GluN2 expression (1); as observed in the PVN of SHR and late-term pregnant rats, recruits unassembled intracellular GluN1 (2) subunits for cell surface trafficking (3).

Alternatively, the GluN1 subunit undergoes alternative splicing to produce eight variants; GluN1-1a/b-GluN1-4a/b (Stephenson, 2001). The antibody used in this study encompassed all GluN1 isoforms. It was therefore not possible to assess whether an increase in one isoform resulted in the decrease of another, thereby creating the impression of no change.

c. Effect of Decreased $GABA_A$ and Increased NMDA Receptor Expression on Sympathetic Outflow and Pathophysiology

Both hypertension and pregnancy show marked elevations in sympathetic nerve activity (Greenwood *et al.*, 1999; Greenwood *et al.*, 2001); however in pregnancy this is known to return to pre-pregnancy levels post-partum (Greenwood *et al.*, 2001). Moreover, the level of sympathetic activation observed in pregnancy is significantly lower than in hypertension. Single-unit muscle sympathetic nerve activity (s-MSNA) in 35 week-pregnant humans, as measured through microneurographic measurement of the right peroneal nerve, was 30 ± 2.0 impulses per 100 cardiac beats, reducing to 21 ± 1.1 impulses per 100 cardiac beats post-partum (Greenwood *et al.*, 2001). In contrast, measurement of s-MSNA in established hypertensive humans by the same research group utilising the same methodology showed s-MSNA to be 63 ± 5.6 impulses per 100 cardiac beats (Greenwood *et al.*, 1999). Collectively, this suggests that the sympathoexcitation observed in hypertension and pregnancy is likely to be differentially controlled, such that pregnancy-induced sympathoexcitation is not as pronounced as hypertension, and is also reversible post-partum.

The results presented indicate that both hypertension and pregnancy show similar decreases in expression of the α1 subunit of the $GABA_A$ receptor (48 ± 6.5% vs. 43 ± 1.2% respectively). Similarly, both hypertension and pregnancy also show a reduction in expression of the α5 subunit, however to a much greater extent in the SHR than in the pregnant rat (97 ± 2% vs. 38 ± 8% respectively). Neither hypertension nor late-term pregnancy was associated

with any alterations in the expression of the α2, β1, β2 or β3 subunit. This suggests that the α1 and α5 subunits could be critically involved in contributing to the sympathoexcitation observed in both of these physiological states. The greater decrease observed in α5 subunit expression in the SHR compared with late-term pregnancy could contribute to the greater sympathoexcitation observed in this state by removal of tonic inhibition.

Furthermore, hypertension was associated with an 85 ± 23% increase in whole-PVN GluN2A subunit expression; as well as an average 36 ± 7.2% increase in GluN2A-IR cells in parvocellular subnuclei of the PVN. This increase in GluN2A subunit expression was not observed in the PVN of late-term pregnant rats. Moreover, *in vivo* electrophysiological studies have demonstrated that antagonism of NMDA receptors in the PVN of late-term pregnant rats does not significantly reduce renal sympathetic nerve activity or blood pressure (Kvochina *et al.*, 2009). It is therefore possible that coupled with the more pronounced decrease in α5 subunit expression, the increase in GluN2A subunit expression also contributes to maintaining an increased sympathetic tone in hypertension. Late-term pregnancy was associated with a significant increase in GluN2B subunit immunoreactivity; however this was not associated with an increase in cell immunoreactivity in any of the parvocellular subnuclei. Given that expression of the GluN2B subunit was more pronounced in magnocellular subnuclei, coupled with previous studies showing plasma osmolality influences GluN2B subunit expression in hypothalamic magnocellular subnuclei (Curras-Collazo & Dao, 1999), it is possible that this increase modulates the increased neurohumoral aspect of pregnancy and is more associated with altered plasma osmolality than the increased sympathetic nerve activity.

Immunohistochemical analysis allowed us to assess whether the changes observed from whole-PVN micropunches were associated with changes in the number of immunoreactive cells. This also allowed us to assess within which parvocellular subnuclei any changes occur, and from this speculate which neuronal pathways this could potentially influence.

The increase in GluN2A subunit expression in the PVN of the SHR was associated with a significant increase in immunoreactive cells in the medial, dorsal cap and posterior parvocellular subnuclei. Neuronal tract tracing of PVN-IML projecting neurones presented in this thesis and previously (Swanson *et al.*, 1980; Portillo *et al.*, 1998; Ranson *et al.*, 1998; Shafton *et al.*, 1998; Pyner & Coote, 2000; Oldfield *et al.*, 2001; Watkins *et al.*, 2009) have shown that all of these subnuclei contain neurones projecting to SPN in the spinal cord. Moreover, these subnuclei of the PVN also send projections to the NTS (Oldfield *et al.*, 2001), as well as containing high densities of RVLM projecting neurones (Shafton *et al.*, 1998; Pyner & Coote, 1999, 2000; Oldfield *et al.*, 2001; Stocker *et al.*, 2006; Chen & Toney, 2010) and branching projections to both the RVLM and IML (Shafton *et al.*, 1998; Pyner & Coote, 2000; Chen & Toney, 2010). Moreover, we have shown that around 54% of PVN-IML projecting neurones in the normotensive rat express the GluN2A subunit. This suggests that any alteration in excitatory transmission occurring in these subnuclei, as a result of the increased GluN2A subunit expression, is likely to increase the firing activity of neurones projecting to both the IML and RVLM; both sites of cardiovascular control. Furthermore, hypertension was also associated with a significant decrease in expression of the α5 subunit of the $GABA_A$ receptor in the same regions; as well as the anterior and ventral

parvocellular subnuclei. A reduction in α5 subunit expression in the absence of increased NMDA receptor expression has been shown to significantly increase the spontaneous firing activity of neurones (Glykys *et al.*, 2008). Therefore the concomitant increase in GluN2A expression and decrease in α5 expression in the same subnuclei is likely to significantly increase the firing rate of these neurones.

Furthermore, we have preliminary evidence that α5 expression is also reduced in whole spinal cord homogenate from SHR compared with normotensive controls (unpublished data). Moreover, this was associated with a significant reduction in α5-IR neurones in the IML region of the spinal cord (unpublished data). Sympathetic preganglionic neurones in the IML region of the spinal cord have been found to be under heavy α5-mediated tonic inhibition (Wang *et al.*, 2008). We have also provided evidence for a decrease in the expression of the α5 subunit in the cortex of the SHR. This decrease in α5 expression in the three central areas studied here suggests that this decrease may not only be a significantly important mechanism behind the increased sympathetic outflow, but may be a characteristic feature of this animal.

Pregnancy was associated with a significant decrease in expression of the α1 subunit in the anterior, medial, ventral and posterior parvocellular subnuclei; as well as a significant decrease in α5 cell immunoreactivity in the medial, ventral and dorsal cap subnuclei. A reduction in expression of these $GABA_A$ receptor subunits is likely to increase the spontaneous activity of neurones within these regions, however given the absence of any increase in NMDA receptor subunit expression in any of the parvocellular subdivisions, this is likely to be to a lesser extent than is observed in hypertension, and could

contribute to the lower level of sympathoexcitation observed in pregnancy compared with hypertension (Greenwood *et al.*, 1999; Greenwood *et al.*, 2001).

Given that the decrease in α5 subunit expression observed in the SHR occurred in subnuclei which did not show a significant increase in GluN2A expression (i.e. anterior and ventral parvocellular subnuclei), this suggests that the reduction in $GABA_A$ receptor expression may not be a consequence of increased NMDA receptor activation. However we cannot conclusively rule out the possibility that GluN2A expression has increased in these regions in the absence of *de novo* cell expression.

This is further evidenced in pregnancy, where the α1 and α5 subunits of the $GABA_A$ receptor show decreased cell immunoreactivity in the absence of increased NMDA receptor expression in any parvocellular subnuclei, again suggesting that $GABA_A$ receptor decreases may precede NMDA receptor activation.

VI. Methodological Considerations

The micropunch method of tissue isolation allows for the measurement of protein levels accurately and consistently in the PVN of animals from all three physiological states. However, it is possible that anatomical variation could result in regions other than the PVN from being acquired. Since there was not a substantial difference in weight between both normotensive and SHR animals and pre-pregnant Wistars, it is unlikely that differences in brain sizes would be a confounding factor in identifying the PVN region. The use of the third ventricle as an anatomical landmark to identify the region containing the PVN was also a factor reducing this risk.

Combining results obtained from quantitative immunoblotting with cells immunohistochemically stained for the respective subunits means that results obtained from the whole PVN micropunches can be determined at a subnuclear level. Based on neuroanatomical studies described in this thesis and previously, changes observed in discrete parvocellular subnuclei can then be translated into a possible physiological role. Identification of subnuclei was based on five parvocellular subnuclei identified through retrograde labelling of PVN-IML projecting neurones (Chapter 4), coupled with the Paxinos & Watson (1998) brain atlas.

Although retrograde labelled PVN-IML projecting neurones labelled five discrete parvocellular subnuclei (Swanson *et al.*, 1980), immunohistochemical staining for subunits of the $GABA_A$ or NMDA receptor in the absence of retrogradely labelled PVN-IML neurones produced more diffuse staining patterns, with no anatomical bias of parvocellular subnuclei. This was more pronounced at rostral-mid levels of the PVN, where absolute identification of the boundaries of

the anterior, dorsal cap and ventral parvocellular regions were often difficult to fully discern. The chance of misidentifying a subnucleus was minimised through the use of serial counter-stained sections, which in conjunction with the Paxinos and Watson brain atlas allowed for the identification of the specific parvocellular subnuclei.

The use of antibodies in scientific research provides a potential area of error, given the possibility of non-specific labelling. In this study, the specificity of all antibodies used had been tested at the point of production (as detailed in Chapter 2Ve). However the "gold standard" in the checking of antibody specificity is through the use of knock-out mice, whereby the protein of interest is removed from the genome and therefore not expressed. Since this has not been done with the antibodies used in this study, the possibility that the antibodies labelled non-specific proteins is possible.

In this study, semi-quantitative analysis of immunohistochemically stained brain sections was achieved by counting the number of stained neurones in a given area. Although the area selected to count was not chosen based on any criteria other than it lie within the subnuclear boundaries, the possibility of bias arises from the fact that the area was not chosen by random generation, and could be considered a limitation to the study.

Previous studies have shown that certain subunits of the $GABA_A$ receptor, specifically the α4, β1, γ2 and δ subunits, show fluctuating expression levels manifested by hormones related to the oestrous cycle (Griffiths & Lovick, 2005; Lovick, 2008). Studies in the periaqueductal grey region (PAG) have found that the number of α4, β1 and δ immunoreactive cells almost double in

number at the late diestrus stage compared with proestrus (Griffiths & Lovick, 2005). Furthermore, expression of the γ2 and δ subunits are shown to fluctuate in an opposing manner, such that high levels of δ during the diestrus phase are accompanied by low levels of γ2, and vice versa in oestrus (Maguire *et al.*, 2005). A possible methodological limitation to this study is that the stage of oestrous for the normotensive and SHR rats was not taken into consideration. Although fluctuations in the oestrous cycle of the normotensive and SHR animals may have masked alterations in some $GABA_A$ receptor subunits from being identified, multiple arguments can be made which validate the results obtained for the α1 and the α5 subunit.

First, there is no evidence in the literature to show that the oestrous cycle has any effect on the expression of the α5 subunit. Studies examining oestrous-related changes in tonic activity concentrate on expression of the δ subunit. Incorporation of a δ subunit into a $GABA_A$ receptor significantly increases its sensitivity to neurosteroids (Hosie *et al.*, 2009; Zheleznova *et al.*, 2009) and studies have shown that expression of the δ subunit is directly related to the stage of oestrus (Griffiths & Lovick, 2005; Lovick, 2008). Although accurate analysis of δ subunit expression could not be made in this study (due to the stage of oestrus cycle not being taken into account), attempts were made to determine δ subunit levels from PVN micropunches, but failed to detect the subunit. This is in accordance with results from the SON, where δ subunit mRNA expression was 400% lower than α5 subunit mRNA expression, and was barely detectable (Jo *et al.*, 2011).

A study by Follesa *et al* (1998) examined pregnancy-induced changes in expression of multiple $GABA_A$ receptor subunits in the cortex and hippocampus

of rats. This study observed that pregnancy was associated with a significant decrease in the expression of the α5 but not α1 subunit in the cortex, reaching a minimum around 25% lower than pre-pregnant levels at day 21 of pregnancy. Based on this study, it is apparent that the expression of $GABA_A$ α5 subunits may be susceptible to neurosteroidal modulation. If so, then given the substantially higher concentrations of progesterone observed in pregnancy compared with those observed during the oestrus cycle (263.7±12.1 nmol/L vs. 53.1±5.4 nmol/L respectively; Kobayashi *et al.*, 1999), we would expect to see substantially greater changes in α5 expression in the PVN of late-term pregnant rats compared with SHR. The results from this study show that expression of the α5 subunit in the SHR is 59% lower than that observed in the late-term pregnant rat (97.2±2% vs. 38 ± 8% respectively).

There is also no evidence in the literature that the α1 subunit of the $GABA_A$ receptor is susceptible to fluctuations in hormones associated with the oestrous cycle. Although studies have shown that the γ2 subunit of the $GABA_A$ receptor, which frequently complexes with the α1 subunit at synapses (Somogyi *et al.*, 1996), has an expression pattern which fluctuates in accordance with the stage of oestrous, no study has examined whether this is associated with a down-regulation of the α1 subunit. Indeed a recent paper by Maguire *et al* (2005) suggest that the oestrus cycle affects only the expression of the γ2 and δ subunits, since the kinetics or frequency of spontaneous IPSCs in hippocampal neurones were not altered during the cycle.

Further evidence that the changes we observed in expression of the α1 and α5 subunits in the SHR were independent of oestrous come from our own study. We performed semi-quantitative analysis of expression levels of the α4

subunit, which previous studies have found to be susceptible to fluctuations in oestrous-related hormone levels in regions of cardiovascular control (Griffiths & Lovick, 2005; Lovick, 2008). In this, we observed greater variation within the data observed for both normotensive and SHR than was observed for the other $GABA_A$ receptor subunits examined, suggesting changing expression levels amongst the different animals sampled, possibly associated with oestrous cycling. Furthermore, the results displaying a significant decrease in α1 and α5 subunit expression are consistent across normotensive and SHR animals taken from random periods of the oestrous cycle.

If the changes that we have observed in the expression of the α1 and α5 subunits were caused by an oestrous-related hormonal influence, we would expect the effect to be widespread throughout the brain. In this study, we measured the expression of the α1 and α5 subunits in the cortex of the same animals. From this, we observed that the level of α1 subunit expression was not significantly different between SHR or late-term pregnant rats compared with normotensive controls. Expression of the α5 subunit was significantly decreased in the cortex of the SHR and late-term pregnant rat; however the levels observed in the cortex were different from those observed in the PVN of the same animals. Expression of the α5 subunit in the cortex of SHR was 75% lower than control; significantly higher than the 97% observed in the PVN ($P<0.05$). Furthermore, expression of the α5 subunit was 72% lower in the cortex of late-term pregnant rats compared with control, significantly lower than the 38% decrease observed in the PVN. Changes in α5 expression in the cortex of pregnant rats have previously been observed in Sprague Dawley rats, where the decrease in α5 expression peaked at 25% on day 21 of pregnancy

(Follesa *et al.*, 1998). The larger decrease observed in this study could be the result of species variation.

It is not surprising that levels of the α5 subunit are decreased in the cortex of the SHR compared with normotensive controls. Studies have shown that GABAergic inhibition in the hippocampus of SHR is significantly reduced compared with normotensive controls (Ichida *et al.*, 1996) and may be related to its behavioural characteristics of attention deficit hyperactivity disorder (ADHD), where these animals show hyperkinesic and hyperactive tendencies compared with multiple control animals (Sagvolden *et al.*, 1993). Since there are dense reciprocal connections between the cortex and the hippocampus (Irle & Markowitsch, 1982; Rolls, 2000), it is possible that the down-regulation of GABAergic inhibition in the hippocampus results in altered neurotransmission of the cortex. Furthermore, the increased level of motor activity associated with the SHR (Sagvolden *et al.*, 1993) may be the result of decreased inhibition of cortical motor centres. Since results presented here show decreased α5 levels in the PVN, cortex and spinal cord of the SHR, a lower α5 subunit expression may be a characteristic feature of this animal.

Irrespective of the decreased cortical levels of α5, the evidence presented here showing the substantial difference in expression levels between the cortex and PVN of the SHR and late-term pregnant rat, coupled with the number of biological replicates within which the almost complete absence of α5 in the PVN of the SHR has been observed; strongly suggest that the decrease in α5 observed in the PVN of the SHR is specific to the PVN and could ultimately play a significant role in mediating the sympathoexcitation observed in this animal.

VII. Therapeutic Potential

The number of confirmed hypertensive cases in the Western world is rising year on year (Carretero & Oparil, 2000). Furthermore, two-thirds of patients who are prescribed anti-hypertensive medication fail to reach adequate blood pressure levels of lower than 140/90mmHg (Chobanian *et al.*, 2003). Pregnant women are at a higher risk of postural hypotension resulting in syncope, as well as a decreased ability to respond to haemorrhage; responsible for around 22% of all maternal deaths (Brooks *et al.*, 2010a). The need for novel treatments for both hypertension as well as for emergency obstetrics is therefore of a high priority for governments and health systems.

Current therapies aimed at reducing sympathetic nerve activity in various cardiovascular diseases, whether through pharmacological or mechanical means, have produced conflicting results.

Prolonged activation of the carotid sinus has been shown to reduce mean arterial blood pressure through reduction of sympathetic nerve activity in dogs (Lohmeier *et al.*, 2009; Lohmeier *et al.*, 2010). However results show that once stimulation ceases, ABP rose back to control levels, suggesting that the effects are not long lasting (Lohmeier *et al.*, 2009).

Renal denervation has provided an exciting prospect for reducing renal nerve activity in hypertensive patients. Clinical studies have found that patients who have undergone bilateral renal denervation observed a decrease in systolic blood pressure of 33mmHg and a decrease in diastolic blood pressure of 11mmHg at 6 months post-operative, compared with control groups (Esler *et al.*, 2010). In addition, blood pressure continued to decrease at 24 months post-operative (Schlaich *et al.*, 2012). Promising as these results may be, renal

denervation is an invasive and irreversible procedure, and is not applicable to all patients.

Pharmacological reduction of sympathetic nerve activity has been attempted in patients with heart failure. Treatment with the imidazoline receptor antagonist monoxidine significantly reduced plasma noradrenaline levels by 18.8% compared with pre-treatment levels (Cohn *et al.*, 2003). However a significantly higher mortality rate in the treatment compared with placebo group resulted in this trial being halted. This suggests that although a pharmacological reduction in sympathetic nerve activity in cardiovascular disease states is possible, much is still unknown about its effectiveness and tolerability.

The results presented in this thesis provide novel therapeutic targets for the treatment of hypertension, as well as targets for potential manipulation of the cardiovascular system during pregnancy.

Many clinically used neuroactive drugs act by targeting either the glutamatergic or GABAergic systems within the brain. Benzodiazepines are a classic example and have been widely used for the treatment of insomnia and anxiety disorders (Lader, 2008). Benzodiazepines are modulators of $GABA_A$ receptor function, and act either to potentiate (positive modulators) or attenuate (negative modulators) GABAergic transmission (Johnston, 1996; Rudolph & Knoflach, 2011). Furthermore, many of the drugs which come under the umbrella of benzodiazepines are subunit specific. It is therefore possible to speculate that, based on the results presented in this thesis, therapies which act as positive modulators specifically targeted at either the α1 or α5 subtype of the

$GABA_A$ receptor may be useful in the treatment of essential hypertension and pregnancy-induced baroreflex suppression. Indeed clinically available drugs, which act at $GABA_A$ receptors comprising either the α1 or the α5 subunit, do exist (Rudolph & Mohler, 2006).

Currently however, these drugs have significant undesirable side effects. Zolpidem is a benzodiazepine that preferentially binds to α1 containing $GABA_A$ receptors. Its primary therapeutic role is in the treatment of insomnia, since potentiation of α1 containing $GABA_A$ receptors results in sedation (Rudolph & Knoflach, 2011). Given its high degree of sedation, α1 based therapies pose significant side effects using currently available drugs.

Pharmacological modulation of α5 containing $GABA_A$ receptors has recently attracted a great deal of attention. Studies have shown that mice lacking the α5 subunit show greater hippocampus-dependent learning than wild-type mice (Martin *et al.*, 2009). Furthermore, wild-type mice administered with an inverse agonist to α5 containing $GABA_A$ receptors also show greater hippocampus-dependent learning (Chambers *et al.*, 2003; Martin *et al.*, 2009). The α5 subunit therefore provides an enticing therapeutic target for cognitive enhancement. However, the results presented here suggest that a removal or down-regulation of the α5 subunit in the PVN may contribute to the sympathoexcitation observed in hypertension and pregnancy. At present, none of the studies employing inverse agonists to the α5 subunit have measured sympathetic nerve activity or blood pressure to assess whether positive inverse modulation of these receptors has a sympathoexcitatory or pressor effect.

Currently, no drug that specifically and positively modulates α5 containing $GABA_A$ receptors exists. L-838417 is a partial agonist of $GABA_A$ receptors, which contain α2, α3 or α5 subunits, but is an antagonist to α1 containing receptors (Rudolph & Knoflach, 2011). Since it does not positively modulate α1 containing receptors, this drug does not display the sedative properties associated with zolpidem, but does have unfavourable pharmacokinetic properties, such as variable absorption and bioavailability that limit its clinical use (Scott-Stevens *et al.*, 2005; Rudolph & Knoflach, 2011). Given its more restricted expression compared with the α1 subunit, as well as its non-sedative properties and significant reduction in expression in the PVN of hypertensive and pregnant rats, positive pharmacological modulation of the α5 subunit may prove an important therapeutic target that offers fewer side effects.

Pharmacological antagonism of the NMDA receptor with the uncompetitive antagonist memantine has proved an important therapeutic target in the treatment of Alzheimer's disease, where it is prescribed for its cognitive enhancement properties (Tricco *et al.*, 2012). The efficacy of this drug in the treatment of hypertension has not yet been established; however memantine appears to be generally well tolerated with few side effects (Areosa *et al.*, 2005), suggesting its use as a therapeutic may be beneficial over the benzodiazepines described previously. The actions of memantine are not dependent upon the subunit conformation of the NMDA receptor therefore its actions would not be a specific antagonism of GluN2A containing receptors, for which we observed an increase in the PVN of SHR. However given that NMDA receptor activity is increased in the PVN of SHR, antagonism of NMDA receptors with non-selective drugs provides a possible therapeutic target for the

treatment of hypertension. Future pharmaceutical advances may provide clinically relevant drugs, which would allow for the specific antagonism of GluN2A-containing NMDA receptors.

VIII. Future Perspectives

The results from this study provide a potential molecular basis to explain the sympathoexcitation observed in hypertensive and late-term pregnant rats. However this needs to be confirmed by combining relevant pharmacological tools with *in vivo* and *in vitro* electrophysiology to assess the contribution these receptor subunit changes make to both PVN neuronal excitability and cardiovascular physiology.

The results described here have also shown that the alterations observed in expression of the α1 and α5 subunit of the $GABA_A$ receptor and GluN2A subunit of the NMDA receptor is specific to the PVN. However what remains unclear is the order in which these subunit changes occur. The hypertensive animals used in this study were at a stage of established hypertension; what these results fail to answer is whether the alterations indeed precede the onset of hypertension; i.e. are these alterations in $GABA_A$ and NMDA expression a cause or result of hypertension. Assessing when these changes occur in pre- and/or early hypertensive animals could have profound implications for future drug therapy regimens.

Moreover, oestrus-related changes in the expression of certain $GABA_A$ receptor subunits has prevented us from being able to assess the expression levels of all components of the $GABA_A$ receptor; specifically the γ2 and δ subunits. These two subunits are known to mediate profound effects on both phasic and tonic inhibition within the CNS respectively, and potential alterations in these subunits would allow for a more complete assessment of all potential mechanisms underlying reduced GABAergic control in the PVN.

IX. General Discussion

The results presented in this thesis provide evidence that the PVN of both hypertensive and late-term pregnant rats are associated with changes in specific subunits of the $GABA_A$ and NMDA receptor. Furthermore, both hypertension and late-term pregnancy were associated with changes in the same subunits of the $GABA_A$ receptors, suggesting that these may be crucial in mediating the sympathoexcitation observed in these two states. Whereas hypertension was associated with an increase in the expression of the GluN2A subunit of the NMDA receptor, this was not observed in the PVN of late-term pregnant animals and this may be a critical component underpinning the chronicity of hypertension.

What remains unclear from this study is the nature of these changes throughout the course of hypertension or pregnancy. In the case of hypertension, assessing when the decrease in α1 and α5 subunit expression occurs could be crucial for the implementation of future therapeutic regimens. Determining whether these changes occur prior to the increase in GluN2A subunit expression may also be critical in maintaining reversibility in the neurochemical imbalance observed in the PVN of these animals.

Therefore, we have provided some insight into the neurochemical changes that could underpin the sympathoexcitation observed in both hypertension and pregnancy; however this is by no means a complete picture. Future work will determine whether these changes can be exploited therapeutically.

Appendix 1 - Recipes

0.1M Phosphate Buffer (PB): 0.05M sodium dihydrogen orthophosphate, 0.05M disodium hydrogen orthophosphate, made up in distilled water (dH_2O). pH 7.4

4% Paraformaldehyde (PFA): 1 litre 0.1M PB, heated to 60ºC (not exceeding). 40g paraformaldehyde added and left until dissolved. Once cooled, pH adjusted to 7.4 and then stored at 4ºC.

Transfer Buffer: 0.025M Tris, 0.4M glycine, 20% (v/v) methanol, made to final volume with dH_2O

Electrode Buffer: 5mM Tris, 0.38mM glycine, 2mM EDTA, pH 8.8. Made to final volume with dH_2O.

Blocking buffer for immunoblotting: 5% (w/v) skimmed milk powder, 0.2% Tween-20, made up in TBS

Incubation buffer for immunoblotting: 2.5% (w/v) skimmed milk powder, made up in TBS

Wash buffer for immunoblotting: 2.5% (w/v) skimmed milk powder, 0.2% Tween-20 made up in TBS

Tris-buffered Saline (TBS): 50mM Tris, 0.9% (w/v) sodium chloride, pH 7.4. Made up in dH_2O

Sucrose for Cryoprotection: 10% or 20% (w/v) sucrose made up in 0.1M PB

Sample Buffer: 30mM NaH_2PO_4, 30% (v/v) glycerol, 0.05% (w/v) Bromophenol blue, 7.5% (w/v) sodium dodecyl sulphate (SDS) made up in dH_2O

SDS-PAGE Stacking Gel: 56.9% (v/v) dH_2O, 24.7% (v/v) stacking gel buffer (1M Tris, 1% (w/v) SDS), 16.1% (v/v) acrylamide (40%), 2% ammonium persulphate (APS, 1mM stock) and 0.25% TEMED

SDS-PAGE Running Gel (10%): 47.6% (v/v) dH_2O, 23.8% (v/v) acrylamide (40% stock), 23.8% running gel buffer (0.5M Tris, 8mM EDTA, pH6.8, 0.4% SDS (w/v), pH8.8), 4.8% APS, and 0.8% TEMED

Luminol: Solution A:Solution B 1:1 (Solution A = 100mM Tris-base pH8.5, 25mM luminol, 396µM p-Courmaric acid. Solution B = 100mM Tris-base pH8.5, 6.27mM H_2O_2)

Bibliography

AFFLECK, V. S., COOTE, J. H. & PYNER, S. (2012). The projection and synaptic organisation of NTS afferent connections with presympathetic neurons, GABA and nNOS neurons in the paraventricular nucleus of the hypothalamus. *Neuroscience,* 219**,** 48-61.

AKINE, A., MONTANARO, M. & ALLEN, A. M. (2003). Hypothalamic paraventricular nucleus inhibition decreases renal sympathetic nerve activity in hypertensive and normotensive rats. *Auton Neurosci,* 108**,** 17-21.

ALLEN, A. M. (2002). Inhibition of the hypothalamic paraventricular nucleus in spontaneously hypertensive rats dramatically reduces sympathetic vasomotor tone. *Hypertension,* 39**,** 275-280.

ANDRESEN, M. C. & KUNZE, D. L. (1994). Nucleus tractus solitarius--gateway to neural circulatory control. *Annu Rev Physiol,* 56**,** 93-116.

ARANCIBIA-CARCAMO, I. L. & KITTLER, J. T. (2009). Regulation of GABA(A) receptor membrane trafficking and synaptic localization. *Pharmacol Ther,* 123**,** 17-31.

AREOSA, S. A., SHERRIFF, F. & MCSHANE, R. (2005). Memantine for dementia. *Cochrane Database Syst Rev***,** CD003154.

ASHWELL, K. W., LAJEVARDI, S. E., CHENG, G. & PAXINOS, G. (2006). The hypothalamic supraoptic and paraventricular nuclei of the echidna and platypus. *Brain Behav Evol,* 68**,** 197-217.

ATHERTON, J. C., DARK, J. M., GARLAND, H. O., MORGAN, M. R., PIDGEON, J. & SONI, S. (1982). Changes in water and electrolyte balance, plasma volume and composition during pregnancy in the rat. *J Physiol,* 330**,** 81-93.

BADOER, E., MCKINLEY, M. J., OLDFIELD, B. J. & MCALLEN, R. M. (1993). A comparison of hypotensive and non-hypotensive hemorrhage on Fos expression in spinally projecting neurons of the paraventricular nucleus and rostral ventrolateral medulla. *Brain Res,* 610**,** 216-223.

BAILEY, T. W., HERMES, S. M., ANDRESEN, M. C. & AICHER, S. A. (2006). Cranial visceral afferent pathways through the nucleus of the solitary tract to caudal ventrolateral medulla or paraventricular hypothalamus: target-specific synaptic reliability and convergence patterns. *J Neurosci,* 26**,** 11893-11902.

BALIS, G. U. & MONROE, R. R. (1964). The pharmacology of chloralose. A review. *Psychopharmacologia,* 6**,** 1-30.

BARRIA, A. & MALINOW, R. (2002). Subunit-specific NMDA receptor trafficking to synapses. *Neuron,* 35**,** 345-353.

BEN-ARI, Y., TSEEB, V., RAGGOZZINO, D., KHAZIPOV, R. & GAIARSA, J. L. (1994). gamma-Aminobutyric acid (GABA): a fast excitatory transmitter which may regulate the development of hippocampal neurones in early postnatal life. *Prog Brain Res,* 102**,** 261-273.

BENKE, D., MERTENS, S., TRZECIAK, A., GILLESSEN, D. & MOHLER, H. (1991). GABAA receptors display association of gamma 2-subunit with alpha 1- and beta 2/3-subunits. *J Biol Chem,* 266**,** 4478-4483.

BERGAMASCHI, C., CAMPOS, R. R., SCHOR, N. & LOPES, O. U. (1995). Role of the rostral ventrolateral medulla in maintenance of blood pressure in rats with Goldblatt hypertension. *Hypertension,* 26**,** 1117-1120.

BETTLER, B. & TIAO, J. Y. (2006). Molecular diversity, trafficking and subcellular localization of GABAB receptors. *Pharmacol Ther,* 110**,** 533-543.

BIANCARDI, V. C., CAMPOS, R. R. & STERN, J. E. (2010). Altered balance of gamma-aminobutyric acidergic and glutamatergic afferent inputs in rostral ventrolateral medulla-projecting neurons in the paraventricular nucleus of the hypothalamus of renovascular hypertensive rats. *J Comp Neurol,* 518**,** 567-585.

BINGHAM, B., WILLIAMSON, M. & VIAU, V. (2006). Androgen and estrogen receptor-beta distribution within spinal-projecting and neurosecretory neurons in the paraventricular nucleus of the male rat. *J Comp Neurol,* 499**,** 911-923.

BRADFORD, A., BARLOW, A. & CHAZOT, P. L. (2005). Probing the differential effects of infrared light sources IR1072 and IR880 on human lymphocytes: evidence of selective cytoprotection by IR1072. *J Photochem Photobiol B,* 81**,** 9-14.

BRAMBILLA, P., PEREZ, J., BARALE, F., SCHETTINI, G. & SOARES, J. C. (2003). GABAergic dysfunction in mood disorders. *Mol Psychiatry,* 8**,** 721-737, 715.

BROOKS, V. L., DAMPNEY, R. A. & HEESCH, C. M. (2010a). Pregnancy and the endocrine regulation of the baroreceptor reflex. *Am J Physiol Regul Integr Comp Physiol,* 299**,** R439-451.

BROOKS, V. L., MULVANEY, J. M., AZAR, A. S., ZHAO, D. & GOLDMAN, R. K. (2010b). Pregnancy impairs baroreflex control of heart rate in rats: role of insulin sensitivity. *Am J Physiol Regul Integr Comp Physiol,* 298**,** R419-426.

BUSNARDO, C., TAVARES, R. F. & CORREA, F. M. (2009). Role of N-methyl-D-aspartate and non-N-methyl-D-aspartate receptors in the cardiovascular effects of L-glutamate microinjection into the hypothalamic paraventricular nucleus of unanesthetized rats. *J Neurosci Res,* 87**,** 2066-2077.

CALLACHAN, H., COTTRELL, G. A., HATHER, N. Y., LAMBERT, J. J., NOONEY, J. M. & PETERS, J. A. (1987). Modulation of the GABAA receptor by progesterone metabolites. *Proc R Soc Lond B Biol Sci,* 231**,** 359-369.

CARRETERO, O. A. & OPARIL, S. (2000). Essential hypertension. Part I: definition and etiology. *Circulation,* 101**,** 329-335.

CARVALHO, A. L., DUARTE, C. B. & CARVALHO, A. P. (2000). Regulation of AMPA receptors by phosphorylation. *Neurochem Res,* 25**,** 1245-1255.

CECHETTO, D. F. & SAPER, C. B. (1988). Neurochemical organization of the hypothalamic projection to the spinal cord in the rat. *J Comp Neurol,* 272**,** 579-604.

CHAMBERS, M. S., ATACK, J. R., BROUGHTON, H. B., COLLINSON, N., COOK, S., DAWSON, G. R., HOBBS, S. C., MARSHALL, G., MAUBACH, K. A., PILLAI, G. V., REEVE, A. J. & MACLEOD, A. M. (2003). Identification of a novel, selective GABA(A) alpha5 receptor inverse agonist which enhances cognition. *J Med Chem,* 46**,** 2227-2240.

CHARKOUDIAN, N. & RABBITTS, J. A. (2009). Sympathetic neural mechanisms in human cardiovascular health and disease. *Mayo Clin Proc,* 84**,** 822-830.

CHAZOT, P. L., COLEMAN, S. K., CIK, M. & STEPHENSON, F. A. (1994). Molecular characterization of N-methyl-D-aspartate receptors expressed in mammalian cells yields evidence for the coexistence of three subunit types within a discrete receptor molecule. *J Biol Chem,* 269**,** 24403-24409.

CHAZOT, P. L., CIK, M. & STEPHENSON, F. A. (1995). An investigation into the role of N-glycosylation in the functional expression of a recombinant heteromeric NMDA receptor. *Mol Membr Biol,* 12**,** 331-337.

CHAZOT, P. L. & STEPHENSON, F. A. (1997a). Molecular dissection of native mammalian forebrain NMDA receptors containing the NR1 C2 exon: direct demonstration of NMDA receptors comprising NR1, NR2A, and NR2B subunits within the same complex. *J Neurochem,* 69**,** 2138-2144.

CHAZOT, P. L. & STEPHENSON, F. A. (1997b). Biochemical evidence for the existence of a pool of unassembled C2 exon-containing NR1 subunits of the mammalian forebrain NMDA receptor. *J Neurochem,* 68**,** 507-516.

CHAZOT, P. L., POLLARD, S. & STEPHENSON, F. A. (1999). Immunoprecipitation of Receptors. BOULTON, A. A., BAKER, G. B. & BATESON, A. N. *In Vitro Neurochemical Techniques.* Humana Press.

CHEBIB, M. & JOHNSTON, G. A. (1999). The 'ABC' of GABA receptors: a brief review. *Clin Exp Pharmacol Physiol,* 26**,** 937-940.

CHEN, Q. H., HAYWOOD, J. R. & TONEY, G. M. (2003). Sympathoexcitation by PVN-injected bicuculline requires activation of excitatory amino acid receptors. *Hypertension,* 42**,** 725-731.

CHEN, Q. H. & TONEY, G. M. (2010). In vivo discharge properties of hypothalamic paraventricular nucleus neurons with axonal projections to the rostral ventrolateral medulla. *J Neurophysiol,* 103**,** 4-15.

CHERUBINI, E. (2012). Phasic GABAA-Mediated Inhibition. NOEBELS, J. L., AVOLI, M., ROGAWSKI, M. A., OLSEN, R. W. & DELGADO-ESCUETA, A. V. *Jasper's Basic Mechanisms of the Epilepsies.* 4 ed. Oxford University Press.

CHOBANIAN, A. V., BAKRIS, G. L., BLACK, H. R., CUSHMAN, W. C., GREEN, L. A., IZZO, J. L., JR., JONES, D. W., MATERSON, B. J., OPARIL, S., WRIGHT, J. T., JR. & ROCCELLA, E. J. (2003). Seventh report of the Joint National Committee on Prevention, Detection, Evaluation, and Treatment of High Blood Pressure. *Hypertension,* 42**,** 1206-1252.

CIRIELLO, J., KLINE, R. L., ZHANG, T. X. & CAVERSON, M. M. (1984). Lesions of the paraventricular nucleus alter the development of spontaneous hypertension in the rat. *Brain Res,* 310**,** 355-359.

COCHRANE, K. L. & NATHAN, M. A. (1989). Normotension in conscious rats after placement of bilateral electrolytic lesions in the rostral ventrolateral medulla. *J Auton Nerv Syst,* 26**,** 199-211.

COCHRANE, K. L. & NATHAN, M. A. (1993). Cardiovascular effects of lesions of the rostral ventrolateral medulla and the nucleus reticularis parvocellularis in rats. *J Auton Nerv Syst,* 43**,** 69-81.

COHN, J. N., PFEFFER, M. A., ROULEAU, J., SHARPE, N., SWEDBERG, K., STRAUB, M., WILTSE, C. & WRIGHT, T. J. (2003). Adverse mortality effect of central sympathetic inhibition with sustained-release moxonidine in patients with heart failure (MOXCON). *Eur J Heart Fail,* 5**,** 659-667.

COLOMBARI, E., BONAGAMBA, L. G. & MACHADO, B. H. (1994). Mechanisms of pressor and bradycardic responses to L-glutamate microinjected into the NTS of conscious rats. *Am J Physiol,* 266**,** R730-738.

CONCAS, A., MOSTALLINO, M. C., PORCU, P., FOLLESA, P., BARBACCIA, M. L., TRABUCCHI, M., PURDY, R. H., GRISENTI, P. & BIGGIO, G. (1998). Role of brain allopregnanolone in the plasticity of gamma-aminobutyric acid type A receptor in rat brain during pregnancy and after delivery. *Proc Natl Acad Sci U S A,* 95**,** 13284-13289.

CONCAS, A., FOLLESA, P., BARBACCIA, M. L., PURDY, R. H. & BIGGIO, G. (1999). Physiological modulation of GABA(A) receptor plasticity by progesterone metabolites. *Eur J Pharmacol,* 375**,** 225-235.

COOTE, J. H., YANG, Z., PYNER, S. & DEERING, J. (1998). Control of sympathetic outflows by the hypothalamic paraventricular nucleus. *Clin Exp Pharmacol Physiol,* 25**,** 461-463.

CRANDALL, M. E. & HEESCH, C. M. (1990). Baroreflex control of sympathetic outflow in pregnant rats: effects of captopril. *Am J Physiol,* 258**,** R1417-1423.

CRAVO, S. L., MORRISON, S. F. & REIS, D. J. (1991). Differentiation of two cardiovascular regions within caudal ventrolateral medulla. *Am J Physiol,* 261**,** R985-994.

CRAVO, S. L. & MORRISON, S. F. (1993). The caudal ventrolateral medulla is a source of tonic sympathoinhibition. *Brain Res,* 621**,** 133-136.

CSAKI, A., KOCSIS, K., HALASZ, B. & KISS, J. (2000). Localization of glutamatergic/aspartatergic neurons projecting to the hypothalamic paraventricular nucleus studied by retrograde transport of [3H]D-aspartate autoradiography. *Neuroscience,* 101**,** 637-655.

CURRAS-COLLAZO, M. C. & DAO, J. (1999). Osmotic activation of the hypothalamo-neurohypophysial system reversibly downregulates the NMDA receptor subunit, NR2B, in the supraoptic nucleus of the hypothalamus. *Brain Res Mol Brain Res,* 70**,** 187-196.

CZYZEWSKA-SZAFRAN, H. & WUTKIEWICZ, M. (1986). The activity of glutamate decarboxylase and the turnover of gamma-aminobutyric acid in spontaneously hypertensive rats. *Pol J Pharmacol Pharm,* 38**,** 135-141.

DAVISON, J. M., SHEILLS, E. A., BARRON, W. M., ROBINSON, A. G. & LINDHEIMER, M. D. (1989). Changes in the metabolic clearance of vasopressin and in plasma vasopressinase throughout human pregnancy. *J Clin Invest,* 83**,** 1313-1318.

DE ANDRADE, T. U., ABREU, G. R., MOYSES, M. R., DE MELO CABRAL, A. & BISSOLI, N. S. (2008). Role of cardiac hypertrophy in reducing the sensitivity of cardiopulmonary reflex control of renal sympathetic nerve activity in spontaneously hypertensive rats. *Clin Exp Pharmacol Physiol,* 35**,** 1104-1108.

DECAVEL, C. & VAN DEN POL, A. N. (1990). GABA: a dominant neurotransmitter in the hypothalamus. *J Comp Neurol,* 302**,** 1019-1037.

DEERING, J. & COOTE, J. H. (2000). Paraventricular neurones elicit a volume expansion-like change of activity in sympathetic nerves to the heart and kidney in the rabbit. *Exp Physiol,* 85**,** 177-186.

DENG, Y. & KAUFMAN, S. (1998). Pregnancy-induced changes in central response to atrial distension mimicked by progesterone metabolite. *Am J Physiol,* 275**,** R1875-1877.

DINGLEDINE, R., BORGES, K., BOWIE, D. & TRAYNELIS, S. F. (1999). The glutamate receptor ion channels. *Pharmacol Rev,* 51**,** 7-61.

EILAM, R., MALACH, R., BERGMANN, F. & SEGAL, M. (1991). Hypertension induced by hypothalamic transplantation from genetically hypertensive to normotensive rats. *J Neurosci,* 11**,** 401-411.

ENZ, R. & CUTTING, G. R. (1998). Molecular composition of GABAC receptors. *Vision Res,* 38**,** 1431-1441.

ERNSBERGER, P., AZAR, S. & AZAR, P. (1985). The role of the anteromedial hypothalamus in Dahl hypertension. *Brain Res Bull,* 15**,** 651-656.

ESLER, M. D. (2000). The sympathetic system and hypertension. *Am J Hypertens,* 13**,** 99S-105S.

ESLER, M. D., KRUM, H., SOBOTKA, P. A., SCHLAICH, M. P., SCHMIEDER, R. E. & BOHM, M. (2010). Renal sympathetic denervation in patients with treatment-resistant hypertension (The Symplicity HTN-2 Trial): a randomised controlled trial. *Lancet,* 376**,** 1903-1909.

FARRANT, M. & NUSSER, Z. (2005). Variations on an inhibitory theme: phasic and tonic activation of GABA(A) receptors. *Nat Rev Neurosci,* 6**,** 215-229.

FLORAS, J. S. (2009). Sympathetic nervous system activation in human heart failure: clinical implications of an updated model. *J Am Coll Cardiol,* 54**,** 375-385.

FOLEY, C. M., STANTON, J. J., PRICE, E. M., CUNNINGHAM, J. T., HASSER, E. M. & HEESCH, C. M. (2003). GABA(A) alpha1 and alpha2 receptor subunit expression in rostral ventrolateral medulla in nonpregnant and pregnant rats. *Brain Res,* 975**,** 196-206.

FOLLESA, P., FLORIS, S., TULIGI, G., MOSTALLINO, M. C., CONCAS, A. & BIGGIO, G. (1998). Molecular and functional adaptation of the GABA(A) receptor complex during pregnancy and after delivery in the rat brain. *Eur J Neurosci,* 10**,** 2905-2912.

GABOR, A. & LEENEN, F. H. (2012). Cardiovascular effects of angiotensin II and glutamate in the PVN of Dahl salt-sensitive rats. *Brain Res,* 1447**,** 28-37.

GAMBRILL, A. C., STOREY, G. P. & BARRIA, A. (2011). Dynamic regulation of NMDA receptor transmission. *J Neurophysiol,* 105**,** 162-171.

GLYKYS, J. & MODY, I. (2006). Hippocampal network hyperactivity after selective reduction of tonic inhibition in GABA A receptor alpha5 subunit-deficient mice. *J Neurophysiol,* 95**,** 2796-2807.

GLYKYS, J., MANN, E. O. & MODY, I. (2008). Which GABA(A) receptor subunits are necessary for tonic inhibition in the hippocampus? *J Neurosci,* 28**,** 1421-1426.

GOODWIN, J. E. & GELLER, D. S. (2012). Glucocorticoid-induced hypertension. *Pediatr Nephrol,* 27**,** 1059-1066.

GRASSI, G., CATTANEO, B. M., SERAVALLE, G., LANFRANCHI, A. & MANCIA, G. (1998). Baroreflex control of sympathetic nerve activity in essential and secondary hypertension. *Hypertension,* 31**,** 68-72.

GRASSI, G., ARENARE, F., PIERUZZI, F., BRAMBILLA, G. & MANCIA, G. (2009). Sympathetic activation in cardiovascular and renal disease. *J Nephrol,* 22**,** 190-195.

GREENWOOD, J. P., STOKER, J. B. & MARY, D. A. (1999). Single-unit sympathetic discharge : quantitative assessment in human hypertensive disease. *Circulation,* 100**,** 1305-1310.

GREENWOOD, J. P., SCOTT, E. M., STOKER, J. B., WALKER, J. J. & MARY, D. A. (2001). Sympathetic neural mechanisms in normal and hypertensive pregnancy in humans. *Circulation,* 104**,** 2200-2204.

GRIFFITHS, J. L. & LOVICK, T. A. (2005). GABAergic neurones in the rat periaqueductal grey matter express alpha4, beta1 and delta GABAA receptor subunits: plasticity of expression during the estrous cycle. *Neuroscience,* 136**,** 457-466.

GUYENET, P. G. (2006). The sympathetic control of blood pressure. *Nat Rev Neurosci,* 7**,** 335-346.

H'DOUBLER, P. B., JR., PETERSON, M., SHEK, W., AUCHINCLOSS, H., ABBOTT, W. M. & ORKIN, R. W. (1991). Spontaneously hypertensive and Wistar Kyoto rats are genetically disparate. *Lab Anim Sci,* 41**,** 471-473.

HALLBECK, M., LARHAMMAR, D. & BLOMQVIST, A. (2001). Neuropeptide expression in rat paraventricular hypothalamic neurons that project to the spinal cord. *J Comp Neurol,* 433**,** 222-238.

HAMBLEY, J. W., JOHNSTON, G. A. & SHAW, J. (1984). Alterations in a hypothalamic GABA system in the spontaneously hypertensive rat. *Neurochem Int,* 6**,** 813-821.

HAN, T. H., LEE, K., PARK, J. B., AHN, D., PARK, J. H., KIM, D. Y., STERN, J. E., LEE, S. Y. & RYU, P. D. (2010). Reduction in synaptic GABA release contributes to target-selective elevation of PVN neuronal activity in rats with myocardial infarction. *Am J Physiol Regul Integr Comp Physiol,* 299**,** R129-139.

HANSSENS, M., KEIRSE, M. J., SPITZ, B. & VAN ASSCHE, F. A. (1991). Angiotensin II levels in hypertensive and normotensive pregnancies. *Br J Obstet Gynaecol,* 98**,** 155-161.

HARDY, S. G. (2001). Hypothalamic projections to cardiovascular centers of the medulla. *Brain Res,* 894**,** 233-240.

HARRISON, N. L. & SIMMONDS, M. A. (1984). Modulation of the GABA receptor complex by a steroid anaesthetic. *Brain Res,* 323**,** 287-292.

HASELTON, J. R., GOERING, J. & PATEL, K. P. (1994). Parvocellular neurons of the paraventricular nucleus are involved in the reduction in renal nerve discharge during isotonic volume expansion. *J Auton Nerv Syst,* 50**,** 1-11.

HAWKINS, L. M., CHAZOT, P. L. & STEPHENSON, F. A. (1999). Biochemical evidence for the co-association of three N-methyl-D-aspartate (NMDA) R2 subunits in recombinant NMDA receptors. *J Biol Chem,* 274**,** 27211-27218.

HAYWOOD, J. R., MIFFLIN, S. W., CRAIG, T., CALDERON, A., HENSLER, J. G. & HINOJOSA-LABORDE, C. (2001). gamma-Aminobutyric acid (GABA)--A function and binding in the paraventricular nucleus of the hypothalamus in chronic renal-wrap hypertension. *Hypertension,* 37**,** 614-618.

HEAD, G. A. (1995). Baroreflexes and cardiovascular regulation in hypertension. *J Cardiovasc Pharmacol,* 26 Suppl 2**,** S7-16.

HEESCH, C. M. & ROGERS, R. C. (1995). Effects of pregnancy and progesterone metabolites on regulation of sympathetic outflow. *Clin Exp Pharmacol Physiol,* 22**,** 136-142.

HEESCH, C. M. (1999). Reflexes that control cardiovascular function. *Am J Physiol,* 277**,** S234-243.

HEESCH, C. M., ZHENG, H., FOLEY, C. M., MUELLER, P. J., HASSER, E. M. & PATEL, K. P. (2009). Nitric oxide synthase activity and expression are decreased in the paraventricular nucleus of pregnant rats. *Brain Res,* 1251**,** 140-150.

HEESCH, C. M. (2011). Neurosteroid modulation of arterial baroreflex function in the rostral ventrolateral medulla. *Auton Neurosci,* 161**,** 28-33.

HERMAN, J. P., EYIGOR, O., ZIEGLER, D. R. & JENNES, L. (2000). Expression of ionotropic glutamate receptor subunit mRNAs in the hypothalamic paraventricular nucleus of the rat. *J Comp Neurol,* 422**,** 352-362.

HERZIG, T. C., BUCHHOLZ, R. A. & HAYWOOD, J. R. (1991). Effects of paraventricular nucleus lesions on chronic renal hypertension. *Am J Physiol,* 261**,** H860-867.

HINES, T. & HODGSON, T. M. (2000). Pregnancy alters cardiac receptor afferent discharge in rats. *Am J Physiol Regul Integr Comp Physiol,* 278**,** R149-156.

HORN, T., SMITH, P. M., MCLAUGHLIN, B. E., BAUCE, L., MARKS, G. S., PITTMAN, Q. J. & FERGUSON, A. V. (1994). Nitric oxide actions in paraventricular nucleus: cardiovascular and neurochemical implications. *Am J Physiol,* 266**,** R306-313.

HOSIE, A. M., WILKINS, M. E., DA SILVA, H. M. & SMART, T. G. (2006). Endogenous neurosteroids regulate GABAA receptors through two discrete transmembrane sites. *Nature,* 444**,** 486-489.

HOSIE, A. M., CLARKE, L., DA SILVA, H. & SMART, T. G. (2009). Conserved site for neurosteroid modulation of GABA A receptors. *Neuropharmacology,* 56**,** 149-154.

HOSOYA, Y. (1980). The distribution of spinal projection neurons in the hypothalamus of the rat, studied with the HRP method. *Exp Brain Res,* 40**,** 79-87.

ICHIDA, T., TAKEDA, K., SASAKI, S., NAKAGAWA, M., HASHIMOTO, T. & KURIYAMA, K. (1996). Age-related decrease of gamma-aminobutyric acid (GABA) release in brain of spontaneously hypertensive rats. *Life Sci,* 58**,** 209-215.

IRLE, E. & MARKOWITSCH, H. J. (1982). Widespread cortical projections of the hippocampal formation in the cat. *Neuroscience,* 7**,** 2637-2647.

ITO, S., KOMATSU, K., TSUKAMOTO, K. & SVED, A. F. (2000). Excitatory amino acids in the rostral ventrolateral medulla support blood pressure in spontaneously hypertensive rats. *Hypertension,* 35**,** 413-417.

ITO, S., KOMATSU, K., TSUKAMOTO, K., KANMATSUSE, K. & SVED, A. F. (2002). Ventrolateral medulla AT1 receptors support blood pressure in hypertensive rats. *Hypertension,* 40**,** 552-559.

JANEWAY, T. C. (1913). A Clinical Study of Hypertensive Cardiovascular Disease. *Arch Intern Med,* 12**,** 755-798.

JARVIS, S. S., SHIBATA, S., BIVENS, T. B., OKADA, Y., CASEY, B. M., LEVINE, B. D. & FU, Q. (2012). Sympathetic activation during early pregnancy in humans. *J Physiol,* 590**,** 3535-3543.

JO, J. Y., JEONG, J. A., PANDIT, S., STERN, J. E., LEE, S. K., RYU, P. D., LEE, S. Y., HAN, S. K., CHO, C. H., KIM, H. W., JEON, B. H. & PARK, J. B. (2011). Neurosteroid modulation of benzodiazepine-sensitive GABAA tonic inhibition in supraoptic magnocellular neurons. *Am J Physiol Regul Integr Comp Physiol,* 300**,** R1578-1587.

JOHNSTON, G. A. (1996). GABAA receptor pharmacology. *Pharmacol Ther,* 69**,** 173-198.

JUDY, W. V. & FARRELL, S. K. (1979). Arterial baroreceptor reflex control of sympathetic nerve activity in the spontaneously hypertensive rat. *Hypertension,* 1**,** 605-614.

KADAR, A., SANCHEZ, E., WITTMANN, G., SINGRU, P. S., FUZESI, T., MARSILI, A., LARSEN, P. R., LIPOSITS, Z., LECHAN, R. M. & FEKETE, C. (2010). Distribution of hypophysiotropic thyrotropin-releasing hormone (TRH)-synthesizing neurons in the hypothalamic paraventricular nucleus of the mouse. *J Comp Neurol,* 518**,** 3948-3961.

KANNAN, H., YAMASHITA, H. & OSAKA, T. (1984). Paraventricular neurosecretory neurons: synaptic inputs from the ventrolateral medulla in rats. *Neurosci Lett,* 51**,** 183-188.

KANNAN, H., NIIJIMA, A. & YAMASHITA, H. (1988). Effects of stimulation of the hypothalamic paraventricular nucleus on blood pressure and renal sympathetic nerve activity. *Brain Res Bull,* 20**,** 779-783.

KANNAN, H., HAYASHIDA, Y. & YAMASHITA, H. (1989). Increase in sympathetic outflow by paraventricular nucleus stimulation in awake rats. *Am J Physiol,* 256**,** R1325-1330.

KARIM, F., KIDD, C., MALPUS, C. M. & PENNA, P. E. (1972). The effects of stimulation of the left atrial receptors on sympathetic efferent nerve activity. *J Physiol,* 227**,** 243-260.

KAUFMAN, S. & DENG, Y. (1993). Renal response to atrial stretch during pregnancy in conscious rats. *Am J Physiol,* 265**,** R902-906.

KENNEY, M. J., WEISS, M. L. & HAYWOOD, J. R. (2003). The paraventricular nucleus: an important component of the central neurocircuitry regulating sympathetic nerve outflow. *Acta Physiol Scand,* 177**,** 7-15.

KLEIBER, A. C., ZHENG, H., SHARMA, N. M. & PATEL, K. P. (2010). Chronic AT1 receptor blockade normalizes NMDA-mediated changes in renal sympathetic nerve activity and NR1 expression within the PVN in rats with heart failure. *Am J Physiol Heart Circ Physiol,* 298**,** H1546-1555.

KOBAYASHI, M., AKAHANE, M., MINAMI, K., MORO, M., AJISAWA, Y., INOUE, Y. & KAWARABAYASHI, T. (1999). Role of oxytocin in the initiation of term and preterm labor in rats: changes in oxytocin receptor density and plasma oxytocin concentration and the effect of an oxytocin antagonist, L-366,509. *Am J Obstet Gynecol,* 180**,** 621-627.

KOHR, G. (2006). NMDA receptor function: subunit composition versus spatial distribution. *Cell Tissue Res,* 326**,** 439-446.

KOUGIAS, P., WEAKLEY, S. M., YAO, Q., LIN, P. H. & CHEN, C. (2010). Arterial baroreceptors in the management of systemic hypertension. *Med Sci Monit,* 16**,** RA1-8.

KOUTCHEROV, Y., MAI, J. K., ASHWELL, K. W. & PAXINOS, G. (2000). Organization of the human paraventricular hypothalamic nucleus. *J Comp Neurol,* 423**,** 299-318.

KUMAGAI, H., OSHIMA, N., MATSUURA, T., IIGAYA, K., IMAI, M., ONIMARU, H., SAKATA, K., OSAKA, M., ONAMI, T., TAKIMOTO, C., KAMAYACHI, T., ITOH, H. & SARUTA, T. (2012). Importance of rostral ventrolateral medulla neurons in determining efferent sympathetic nerve activity and blood pressure. *Hypertens Res,* 35**,** 132-141.

KUNKLER, P. E. & HWANG, B. H. (1995). Lower GABAA receptor binding in the amygdala and hypothalamus of spontaneously hypertensive rats. *Brain Res Bull,* 36**,** 57-61.

KVOCHINA, L., HASSER, E. M. & HEESCH, C. M. (2007). Pregnancy increases baroreflex-independent GABAergic inhibition of the RVLM in rats. *Am J Physiol Regul Integr Comp Physiol,* 293**,** R2295-2305.

KVOCHINA, L., HASSER, E. M. & HEESCH, C. M. (2009). Pregnancy decreases GABAergic inhibition of the hypothalamic paraventricular nucleus. *Physiol Behav,* 97**,** 171-179.

LADER, M. (2008). Effectiveness of benzodiazepines: do they work or not? *Expert Rev Neurother,* 8**,** 1189-1191.

LAMBERT, J. J., COOPER, M. A., SIMMONS, R. D., WEIR, C. J. & BELELLI, D. (2009). Neurosteroids: endogenous allosteric modulators of GABA(A) receptors. *Psychoneuroendocrinology,* 34 Suppl 1**,** S48-58.

LENKEI, Z., CORVOL, P. & LLORENS-CORTES, C. (1995). Comparative expression of vasopressin and angiotensin type-1 receptor mRNA in rat hypothalamic nuclei: a double in situ hybridization study. *Brain Res Mol Brain Res,* 34**,** 135-142.

LEPHART, E. D. (1993). Brain 5alpha-reductase: cellular, enzymatic, and molecular perspectives and implications for biological function. *Mol Cell Neurosci,* 4**,** 473-484.

LI, D. P. & PAN, H. L. (2005). Angiotensin II attenuates synaptic GABA release and excites paraventricular-rostral ventrolateral medulla output neurons. *J Pharmacol Exp Ther,* 313**,** 1035-1045.

LI, D. P. & PAN, H. L. (2006). Plasticity of GABAergic control of hypothalamic presympathetic neurons in hypertension. *Am J Physiol Heart Circ Physiol,* 290**,** H1110-1119.

LI, D. P. & PAN, H. L. (2007a). Glutamatergic inputs in the hypothalamic paraventricular nucleus maintain sympathetic vasomotor tone in hypertension. *Hypertension,* 49**,** 916-925.

LI, D. P. & PAN, H. L. (2007b). Role of gamma-aminobutyric acid (GABA)A and GABAB receptors in paraventricular nucleus in control of sympathetic vasomotor tone in hypertension. *J Pharmacol Exp Ther,* 320**,** 615-626.

LI, D. P., YANG, Q., PAN, H. M. & PAN, H. L. (2008a). Pre- and postsynaptic plasticity underlying augmented glutamatergic inputs to hypothalamic presympathetic neurons in spontaneously hypertensive rats. *J Physiol,* 586**,** 1637-1647.

LI, D. P., YANG, Q., PAN, H. M. & PAN, H. L. (2008b). Plasticity of pre- and postsynaptic GABAB receptor function in the paraventricular nucleus in spontaneously hypertensive rats. *Am J Physiol Heart Circ Physiol,* 295**,** H807-815.

LI, D. P. & PAN, H. L. (2010). Role of GABAB receptors in autonomic control of systemic blood pressure. *Adv Pharmacol,* 58**,** 257-286.

LI, Y. F., MAYHAN, W. G. & PATEL, K. P. (2001). NMDA-mediated increase in renal sympathetic nerve discharge within the PVN: role of nitric oxide. *Am J Physiol Heart Circ Physiol,* 281**,** H2328-2336.

LI, Y. F., CORNISH, K. G. & PATEL, K. P. (2003). Alteration of NMDA NR1 receptors within the paraventricular nucleus of hypothalamus in rats with heart failure. *Circ Res,* 93**,** 990-997.

LI, Y. F., JACKSON, K. L., STERN, J. E., RABELER, B. & PATEL, K. P. (2006). Interaction between glutamate and GABA systems in the integration of sympathetic outflow by the paraventricular nucleus of the hypothalamus. *Am J Physiol Heart Circ Physiol,* 291**,** H2847-2856.

LI, Y. W. & DAMPNEY, R. A. (1994). Expression of Fos-like protein in brain following sustained hypertension and hypotension in conscious rabbits. *Neuroscience,* 61**,** 613-634.

LLEWELLYN-SMITH, I. J., DICARLO, S. E., COLLINS, H. I. & KEAST, J. R. (2005). Enkephalin-immunoreactive interneurones extensively innervate sympathetic preganglionic neurones regulating the pelvic viscera. *J Comp Neurol*, 488, 278-289.

LOHMEIER, T. E., HILDEBRANDT, D. A., DWYER, T. M., ILIESCU, R., IRWIN, E. D., CATES, A. W. & ROSSING, M. A. (2009). Prolonged activation of the baroreflex decreases arterial pressure even during chronic adrenergic blockade. *Hypertension,* 53**,** 833-838.

LOHMEIER, T. E., ILIESCU, R., DWYER, T. M., IRWIN, E. D., CATES, A. W. & ROSSING, M. A. (2010). Sustained suppression of sympathetic activity and arterial pressure during chronic activation of the carotid baroreflex. *Am J Physiol Heart Circ Physiol,* 299**,** H402-409.

LONGO, L. D. (1983). Maternal blood volume and cardiac output during pregnancy: a hypothesis of endocrinologic control. *Am J Physiol,* 245**,** R720-729.

LOUIS, W. J. & HOWES, L. G. (1990). Geneology of the spontaneously hypertensive rat and Wistar Kyoto rat strains: Implications for studies of inherited disease. *J Cardio Pharma*, 16(S7), S1-S5

LOVICK, T. A. & COOTE, J. H. (1988a). Electrophysiological properties of paraventriculo-spinal neurones in the rat. *Brain Res,* 454**,** 123-130.

LOVICK, T. A. & COOTE, J. H. (1988b). Effects of volume loading on paraventriculo-spinal neurones in the rat. *J Auton Nerv Syst,* 25**,** 135-140.

LOVICK, T. A., MALPAS, S. & MAHONY, M. T. (1993). Renal vasodilatation in response to acute volume load is attenuated following lesions of parvocellular neurones in the paraventricular nucleus in rats. *J Auton Nerv Syst,* 43**,** 247-255.

LOVICK, T. A. (2008). GABA in the female brain -- oestrous cycle-related changes in GABAergic function in the periaqueductal grey matter. *Pharmacol Biochem Behav,* 90**,** 43-50.

LOWRY, O. H., ROSEBROUGH, N. J., FARR, A. L. & RANDALL, R. J. (1951). Protein measurement with the Folin phenol reagent. *J Biol Chem,* 193**,** 265-275.

MACCANNELL, K. L. (1969). The effect of barbiturates on regional blood flows. *Can Anaesth Soc J,* 16**,** 1-6.

MACDONALD, R. L. & TWYMAN, R. E. (1991). Biophysical properties and regulation of GABAA receptor channels. *The Neurosciences,* 3**,** 219-235.

MACDONALD, R. L. & OLSEN, R. W. (1994). GABAA receptor channels. *Annu Rev Neurosci,* 17**,** 569-602.

MAGUIRE, J. L., STELL, B. M., RAFIZADEH, M. & MODY, I. (2005). Ovarian cycle-linked changes in GABA(A) receptors mediating tonic inhibition alter seizure susceptibility and anxiety. *Nat Neurosci,* 8**,** 797-804.

MAGUIRE, J. L. & MODY, I. (2009). Steroid hormone fluctuations and GABA(A)R plasticity. *Psychoneuroendocrinology,* 34 Suppl 1**,** S84-90.

MARTIN, D. S., SEGURA, T. & HAYWOOD, J. R. (1991). Cardiovascular responses to bicuculline in the paraventricular nucleus of the rat. *Hypertension,* 18**,** 48-55.

MARTIN, D. S. & HAYWOOD, J. R. (1998). Reduced GABA inhibition of sympathetic function in renal-wrapped hypertensive rats. *Am J Physiol,* 275**,** R1523-1529.

MARTIN, L. J., BONIN, R. P. & ORSER, B. A. (2009). The physiological properties and therapeutic potential of alpha5-GABAA receptors. *Biochem Soc Trans,* 37**,** 1334-1337.

MASILAMANI, S. & HEESCH, C. M. (1997). Effects of pregnancy and progesterone metabolites on arterial baroreflex in conscious rats. *Am J Physiol,* 272**,** R924-934.

MCILHINNEY, R. A., LE BOURDELLES, B., MOLNAR, E., TRICAUD, N., STREIT, P. & WHITING, P. J. (1998). Assembly intracellular targeting and cell surface expression of the human N-methyl-D-aspartate receptor subunits NR1a and NR2A in transfected cells. *Neuropharmacology,* 37**,** 1355-1367.

MEHTA, A. K. & TICKU, M. K. (1999). An update on GABAA receptors. *Brain Res Brain Res Rev,* 29**,** 196-217.

MODY, I. & PEARCE, R. A. (2004). Diversity of inhibitory neurotransmission through GABA(A) receptors. *Trends Neurosci,* 27**,** 569-575.

MONNERIE, H. & LE ROUX, P. D. (2007). Reduced dendrite growth and altered glutamic acid decarboxylase (GAD) 65- and 67-kDa isoform protein expression from mouse cortical GABAergic neurons following excitotoxic injury in vitro. *Exp Neurol,* 205**,** 367-382.

MONNERIE, H., HSU, F. C., COULTER, D. A. & LE ROUX, P. D. (2010). Role of the NR2A/2B subunits of the N-methyl-D-aspartate receptor in glutamate-induced glutamic acid decarboxylase alteration in cortical GABAergic neurons in vitro. *Neuroscience,* 171**,** 1075-1090.

MONYER, H., BURNASHEV, N., LAURIE, D. J., SAKMANN, B. & SEEBURG, P. H. (1994). Developmental and regional expression in the rat brain and functional properties of four NMDA receptors. *Neuron,* 12**,** 529-540.

MOSTALLINO, M. C., MURA, M. L., MACIOCCO, E., MURRU, L., SANNA, E. & BIGGIO, G. (2006). Changes in expression of the delta subunit of the GABA (A) receptor and in receptor function induced by progesterone exposure and withdrawal. *J Neurochem,* 99**,** 321-332.

MOTAWEI, K., PYNER, S., RANSON, R. N., KAMEL, M. & COOTE, J. H. (1999). Terminals of paraventricular spinal neurones are closely associated with adrenal medullary sympathetic preganglionic neurones: immunocytochemical evidence for vasopressin as a possible neurotransmitter in this pathway. *Exp Brain Res,* 126**,** 68-76.

NORMINGTON, K. & RUSSELL, D. W. (1992). Tissue distribution and kinetic characteristics of rat steroid 5 alpha-reductase isozymes. Evidence for distinct physiological functions. *J Biol Chem,* 267**,** 19548-19554.

OLDFIELD, B. J., DAVERN, P. J., GILES, M. E., ALLEN, A. M., BADOER, E. & MCKINLEY, M. J. (2001). Efferent neural projections of angiotensin receptor (AT1) expressing neurones in the hypothalamic paraventricular nucleus of the rat. *J Neuroendocrinol,* 13**,** 139-146.

ORCHINIK, M., WEILAND, N. G. & MCEWEN, B. S. (1995). Chronic exposure to stress levels of corticosterone alters GABAA receptor subunit mRNA levels in rat hippocampus. *Brain Res Mol Brain Res,* 34**,** 29-37.

PAGE, M. C., CASSAGLIA, P. A. & BROOKS, V. L. (2011). GABA in the paraventricular nucleus tonically suppresses baroreflex function: alterations during pregnancy. *Am J Physiol Regul Integr Comp Physiol,* 300**,** R1452-1458.

PAOLETTI, P. & NEYTON, J. (2007). NMDA receptor subunits: function and pharmacology. *Curr Opin Pharmacol,* 7**,** 39-47.

PARK, J. B., SKALSKA, S., SON, S. & STERN, J. E. (2007). Dual GABAA receptor-mediated inhibition in rat presympathetic paraventricular nucleus neurons. *J Physiol,* 582**,** 539-551.

PAXINOS, G. & WATSON, C. (1998). *The rat brain in stereotaxic coordinates,* San Diego ; London, Academic.

PAYNE, J. A., RIVERA, C., VOIPIO, J. & KAILA, K. (2003). Cation-chloride co-transporters in neuronal communication, development and trauma. *Trends Neurosci,* 26**,** 199-206.

PETROFF, O. A. (2002). GABA and glutamate in the human brain. *Neuroscientist,* 8**,** 562-573.

PINTO, Y. M., PAUL, M. & GANTEN, D. (1998). Lessons from rat models of hypertension: from Goldblatt to genetic engineering. *Cardiovasc Res,* 39**,** 77-88.

PIRKER, S., SCHWARZER, C., WIESELTHALER, A., SIEGHART, W. & SPERK, G. (2000). GABA(A) receptors: immunocytochemical distribution of 13 subunits in the adult rat brain. *Neuroscience,* 101**,** 815-850.

PORTILLO, F., CARRASCO, M. & VALLO, J. J. (1998). Separate populations of neurons within the paraventricular hypothalamic nucleus of the rat project to vagal and thoracic autonomic preganglionic levels and express c-Fos protein induced by lithium chloride. *J Chem Neuroanat,* 14**,** 95-102.

PRENOSIL, G. A., SCHNEIDER GASSER, E. M., RUDOLPH, U., KEIST, R., FRITSCHY, J. M. & VOGT, K. E. (2006). Specific subtypes of GABAA receptors mediate phasic and tonic forms of inhibition in hippocampal pyramidal neurons. *J Neurophysiol,* 96**,** 846-857.

PUIA, G., MIENVILLE, J. M., MATSUMOTO, K., TAKAHATA, H., WATANABE, H., COSTA, E. & GUIDOTTI, A. (2003). On the putative physiological role of allopregnanolone on GABA(A) receptor function. *Neuropharmacology,* 44**,** 49-55.

PYNER, S. & COOTE, J. H. (1999). Identification of an efferent projection from the paraventricular nucleus of the hypothalamus terminating close to spinally projecting rostral ventrolateral medullary neurons. *Neuroscience,* 88**,** 949-957.

PYNER, S. & COOTE, J. H. (2000). Identification of branching paraventricular neurons of the hypothalamus that project to the rostroventrolateral medulla and spinal cord. *Neuroscience,* 100**,** 549-556.

PYNER, S., DEERING, J. & COOTE, J. H. (2002). Right atrial stretch induces renal nerve inhibition and c-fos expression in parvocellular neurones of the paraventricular nucleus in rats. *Exp Physiol,* 87**,** 25-32.

PYNER, S. (2009). Neurochemistry of the paraventricular nucleus of the hypothalamus: implications for cardiovascular regulation. *J Chem Neuroanat,* 38**,** 197-208.

QUESNELL, R. R. & BROOKS, V. L. (1997). Alterations in the baroreflex occur late in pregnancy in conscious rabbits. *Am J Obstet Gynecol,* 176**,** 692-694.

RANSON, R. N., MOTAWEI, K., PYNER, S. & COOTE, J. H. (1998). The paraventricular nucleus of the hypothalamus sends efferents to the spinal cord of the rat that closely appose sympathetic preganglionic neurones projecting to the stellate ganglion. *Exp Brain Res,* 120**,** 164-172.

ROLLS, E. T. (2000). Hippocampo-cortical and cortico-cortical backprojections. *Hippocampus,* 10**,** 380-388.

RUDOLPH, U. & MOHLER, H. (2006). GABA-based therapeutic approaches: GABAA receptor subtype functions. *Curr Opin Pharmacol,* 6**,** 18-23.

RUDOLPH, U. & KNOFLACH, F. (2011). Beyond classical benzodiazepines: novel therapeutic potential of GABAA receptor subtypes. *Nat Rev Drug Discov,* 10**,** 685-697.

SAGVOLDEN, T., PETTERSEN, M. B. & LARSEN, M. C. (1993). Spontaneously hypertensive rats (SHR) as a putative animal model of childhood hyperkinesis: SHR behavior compared to four other rat strains. *Physiol Behav,* 54**,** 1047-1055.

SALAS, S. P., ROSSO, P., ESPINOZA, R., ROBERT, J. A., VALDES, G. & DONOSO, E. (1993). Maternal plasma volume expansion and hormonal changes in women with idiopathic fetal growth retardation. *Obstet Gynecol,* 81**,** 1029-1033.

SALIBA, R. S., GU, Z., YAN, Z. & MOSS, S. J. (2009). Blocking L-type voltage-gated Ca2+ channels with dihydropyridines reduces gamma-aminobutyric acid type A receptor expression and synaptic inhibition. *J Biol Chem,* 284**,** 32544-32550.

SANNA, E., MOSTALLINO, M. C., MURRU, L., CARTA, M., TALANI, G., ZUCCA, S., MURA, M. L., MACIOCCO, E. & BIGGIO, G. (2009). Changes in expression and function of extrasynaptic GABAA receptors in the rat hippocampus during pregnancy and after delivery. *J Neurosci,* 29**,** 1755-1765.

SANZ-CLEMENTE, A., MATTA, J. A., ISAAC, J. T. & ROCHE, K. W. (2010). Casein kinase 2 regulates the NR2 subunit composition of synaptic NMDA receptors. *Neuron,* 67**,** 984-996.

SCHIMCHOWITSCH, S., MOREAU, C., LAURENT, F. & STOECKEL, M. E. (1989). Distribution and morphometric characteristics of oxytocin- and vasopressin-immunoreactive neurons in the rabbit hypothalamus. *J Comp Neurol,* 285**,** 304-324.

SCHLAICH, M. P., HERING, D., SOBOTKA, P., KRUM, H., LAMBERT, G. W., LAMBERT, E. & ESLER, M. D. (2012). Effects of renal denervation on sympathetic activation, blood pressure, and glucose metabolism in patients with resistant hypertension. *Front Physiol,* 3**,** 10.

SCHMIDT, B. & DIMICCO, J. A. (1984). Blockade of GABA receptors in periventricular forebrain of anesthetized cats: effects on heart rate, arterial pressure, and hindlimb vascular resistance. *Brain Res,* 301**,** 111-119.

SCHNEIDEREIT, M. (1985). Study of fetal organ growth in Wistar rats from day 17 to 21. *Lab Anim,* 19**,** 240-244.

SCHOUSBOE, A., SARUP, A., BAK, L. K., WAAGEPETERSEN, H. S. & LARSSON, O. M. (2004). Role of astrocytic transport processes in glutamatergic and GABAergic neurotransmission. *Neurochem Int,* 45**,** 521-527.

SCOTT-STEVENS, P., ATACK, J. R., SOHAL, B. & WORBOYS, P. (2005). Rodent pharmacokinetics and receptor occupancy of the GABAA receptor subtype selective benzodiazepine site ligand L-838417. *Biopharm Drug Dispos,* 26**,** 13-20.

SERWANSKI, D. R., MIRALLES, C. P., CHRISTIE, S. B., MEHTA, A. K., LI, X. & DE BLAS, A. L. (2006). Synaptic and nonsynaptic localization of GABAA receptors containing the alpha5 subunit in the rat brain. *J Comp Neurol,* 499**,** 458-470.

SHAFTON, A. D., RYAN, A. & BADOER, E. (1998). Neurons in the hypothalamic paraventricular nucleus send collaterals to the spinal cord and to the rostral ventrolateral medulla in the rat. *Brain Res,* 801**,** 239-243.

SHERLOCK, D. A., FIELD, P. M. & RAISMAN, G. (1975). Retrograde transport of horseradish peroxidase in the magnocellular neurosecretory system of the rat. *Brain Res,* 88**,** 403-414.

SHONIS, C. A. & WALDROP, T. G. (1993). Augmented neuronal activity in the hypothalamus of spontaneously hypertensive rats. *Brain Res Bull,* 30**,** 45-52.

SIEGHART, W., FUCHS, K., TRETTER, V., EBERT, V., JECHLINGER, M., HOGER, H. & ADAMIKER, D. (1999). Structure and subunit composition of GABA(A) receptors. *Neurochem Int,* 34**,** 379-385.

SIMMONS, D. M. & SWANSON, L. W. (2008). High-resolution paraventricular nucleus serial section model constructed within a traditional rat brain atlas. *Neurosci Lett,* 438**,** 85-89.

SOFRONIEW, M. V. (1980). Projections from vasopressin, oxytocin, and neurophysin neurons to neural targets in the rat and human. *J Histochem Cytochem,* 28**,** 475-478.

SOMOGYI, P., FRITSCHY, J. M., BENKE, D., ROBERTS, J. D. & SIEGHART, W. (1996). The gamma 2 subunit of the GABAA receptor is concentrated in synaptic junctions containing the alpha 1 and beta 2/3 subunits in hippocampus, cerebellum and globus pallidus. *Neuropharmacology,* 35**,** 1425-1444.

SPERK G., SCHWARZER, C., TSUNASHIMA, K., FUCHS, K. & SIEGHART, W. (1997). $GABA_A$ receptor subunits in the rat hippocampus I: Immunocytochemical distribution of 13 subunits. *Neuroscience*, 80(4), 987-1000

STELZER, A., SLATER, N. T. & TEN BRUGGENCATE, G. (1987). Activation of NMDA receptors blocks GABAergic inhibition in an in vitro model of epilepsy. *Nature,* 326**,** 698-701.

STELZER, A. & SHI, H. (1994). Impairment of GABAA receptor function by N-methyl-D-aspartate-mediated calcium influx in isolated CA1 pyramidal cells. *Neuroscience,* 62**,** 813-828.

STEPHENSON, F. A. (2001). Subunit characterization of NMDA receptors. *Curr Drug Targets,* 2**,** 233-239.

STERN, J. E. (2004). Nitric oxide and homeostatic control: an intercellular signalling molecule contributing to autonomic and neuroendocrine integration? *Prog Biophys Mol Biol,* 84**,** 197-215.

STOCKER, S. D., SIMMONS, J. R., STORNETTA, R. L., TONEY, G. M. & GUYENET, P. G. (2006). Water deprivation activates a glutamatergic projection from the hypothalamic paraventricular nucleus to the rostral ventrolateral medulla. *J Comp Neurol,* 494**,** 673-685.

STOREY, E. & KAUFMAN, S. (2004). Effect of pregnancy and 5alpha-pregnan-3alpha-ol-20-one on atrial receptor afferent discharge in rats. *Am J Physiol Regul Integr Comp Physiol,* 287**,** R1427-1433.

STOREY, G. P., OPITZ-ARAYA, X. & BARRIA, A. (2011). Molecular determinants controlling NMDA receptor synaptic incorpTRAoration. *J Neurosci,* 31**,** 6311-6316.

STRACK, A. M., SAWYER, W. B., PLATT, K. B. & LOEWY, A. D. (1989). CNS cell groups regulating sympathetic outflow to adrenal gland as revealed by transneuronal cell body labelling with pseudorabies virus. *Brain Res,* 491, 274-296.

STUMPF, W. E. (1990). Steroid hormones and the cardiovascular system: direct actions of estradiol, progesterone, testosterone, gluco- and mineralcorticoids, and soltriol [vitamin D] on central nervous regulatory and peripheral tissues. *Experientia,* 46**,** 13-25.

SUN, C., SIEGHART, W. & KAPUR, J. (2004). Distribution of alpha1, alpha4, gamma2, and delta subunits of GABAA receptors in hippocampal granule cells. *Brain Res,* 1029**,** 207-216.

SVED, A. F., ITO, S. & MADDEN, C. J. (2000). Baroreflex dependent and independent roles of the caudal ventrolateral medulla in cardiovascular regulation. *Brain Res Bull,* 51**,** 129-133.

SWANSON, L. W. (1977). Immunohistochemical evidence for a neurophysin-containing autonomic pathway arising in the paraventricular nucleus of the hypothalamus. *Brain Res,* 128**,** 346-353.

SWANSON, L. W., SAWCHENKO, P. E., WIEGAND, S. J. & PRICE, J. L. (1980). Separate neurons in the paraventricular nucleus project to the median eminence and to the medulla or spinal cord. *Brain Res,* 198**,** 190-195.

SWANSON, L. W. & SAWCHENKO, P. E. (1983). Hypothalamic integration: organization of the paraventricular and supraoptic nuclei. *Annu Rev Neurosci,* 6**,** 269-324.

TAKETO, M. & YOSHIOKA, T. (2000). Developmental change of GABA(A) receptor-mediated current in rat hippocampus. *Neuroscience,* 96**,** 507-514.

THOMAS, C. J. & WOODS, R. L. (2004). Do natriuretic peptides modify arterial baroreflexes in sheep? *Exp Physiol,* 89**,** 709-715.

TRICCO, A. C., VANDERVAART, S., SOOBIAH, C., LILLIE, E., PERRIER, L., CHEN, M. H., HEMMELGARN, B., MAJUMDAR, S. R. & STRAUS, S. E. (2012). Efficacy of cognitive enhancers for Alzheimer's disease: protocol for a systematic review and network meta-analysis. *Syst Rev,* 1**,** 31.

VAHID-ANSARI, F. & LEENEN, F. H. (1998). Pattern of neuronal activation in rats with CHF after myocardial infarction. *Am J Physiol,* 275**,** H2140-2146.

VAN DEN POL, A. N. (1991). Glutamate and aspartate immunoreactivity in hypothalamic presynaptic axons. *J Neurosci,* 11**,** 2087-2101.

VERKUYL, J. M., HEMBY, S. E. & JOELS, M. (2004). Chronic stress attenuates GABAergic inhibition and alters gene expression of parvocellular neurons in rat hypothalamus. *Eur J Neurosci,* 20**,** 1665-1673.

WANG, L., SPARY, E., DEUCHARS, J. & DEUCHARS, S. A. (2008). Tonic GABAergic inhibition of sympathetic preganglionic neurons: a novel substrate for sympathetic control. *J Neurosci,* 28**,** 12445-12452.

WANG, R. J., ZENG, Q. H., WANG, W. Z. & WANG, W. (2009). GABA(A) and GABA(B) receptor-mediated inhibition of sympathetic outflow in the paraventricular nucleus is blunted in chronic heart failure. *Clin Exp Pharmacol Physiol,* 36**,** 516-522.

WATKINS, N. D., CORK, S. C. & PYNER, S. (2009). An immunohistochemical investigation of the relationship between neuronal nitric oxide synthase, GABA and presympathetic paraventricular neurons in the hypothalamus. *Neuroscience,* 159**,** 1079-1088.

WOMACK, M. D., PYNER, S. & BARRETT-JOLLEY, R. (2006). Inhibition by alpha-tetrahydrodeoxycorticosterone (THDOC) of pre-sympathetic parvocellular neurones in the paraventricular nucleus of rat hypothalamus. *Br J Pharmacol,* 149**,** 600-607.

YAMADA, J., SAITOW, F., SATAKE, S., KIYOHARA, T. & KONISHI, S. (1999). GABA(B) receptor-mediated presynaptic inhibition of glutamatergic and GABAergic transmission in the basolateral amygdala. *Neuropharmacology,* 38**,** 1743-1753.

YAMORI, Y. & OKAMOTO, K. (1969). Hypothalamic tonic regulation of blood pressure in spontaneously hypertensive rats. *Jpn Circ J,* 33**,** 509-519.

YANG, Z. & COOTE, J. H. (1998). Influence of the hypothalamic paraventricular nucleus on cardiovascular neurones in the rostral ventrolateral medulla of the rat. *J Physiol,* 513 (Pt 2)**,** 521-530.

YANG, Z., BERTRAM, D. & COOTE, J. H. (2001). The role of glutamate and vasopressin in the excitation of RVL neurones by paraventricular neurones. *Brain Res,* 908**,** 99-103.

YANG, Z. & COOTE, J. H. (2003). Role of GABA and NO in the paraventricular nucleus-mediated reflex inhibition of renal sympathetic nerve activity following stimulation of right atrial receptors in the rat. *Exp Physiol,* 88**,** 335-342.

YANG, Z., HAN, D. & COOTE, J. H. (2009). Cardiac sympatho-excitatory action of PVN-spinal oxytocin neurones. *Auton Neurosci,* 147**,** 80-85.

YE, Z. Y., LI, D. P., BYUN, H. S., LI, L. & PAN, H. L. (2012a). NKCC1 Upregulation Disrupts Chloride Homeostasis in the Hypothalamus and Increases Neuronal Activity-Sympathetic Drive in Hypertension. *J Neurosci,* 32**,** 8560-8568.

YE, Z. Y., LI, L., LI, D. P. & PAN, H. L. (2012b). Casein Kinase 2-mediated Synaptic GluN2A Up-regulation Increases N-Methyl-D-aspartate Receptor Activity and Excitability of Hypothalamic Neurons in Hypertension. *J Biol Chem,* 287**,** 17438-17446.

YUAN, H., VANCE, K. M., JUNGE, C. E., GEBALLE, M. T., SYNDER, J. P., HEPLER, J. R., YEPES, M., LOW, C. M. & TRAYNELIS, S. F. (2004). The serine protease plasmin cleaves the amino terminal domain of the NR2A subunit to relieve zinc inhibition of the *N*-methyl-D-aspartate receptors. *J Biol Chem*, 284 (19), 12862-12873.

ZAHNER, M. R., LI, D. P. & PAN, H. L. (2007). Benzodiazepine inhibits hypothalamic presympathetic neurons by potentiation of GABAergic synaptic input. *Neuropharmacology,* 52**,** 467-475.

ZHANG, K. & PATEL, K. P. (1998). Effect of nitric oxide within the paraventricular nucleus on renal sympathetic nerve discharge: role of GABA. *Am J Physiol,* 275**,** R728-734.

ZHANG, K., LI, Y. F. & PATEL, K. P. (2002). Reduced endogenous GABA-mediated inhibition in the PVN on renal nerve discharge in rats with heart failure. *Am J Physiol Regul Integr Comp Physiol,* 282**,** R1006-1015.

ZHELEZNOVA, N., SEDELNIKOVA, A. & WEISS, D. S. (2008). alpha1beta2delta, a silent GABAA receptor: recruitment by tracazolate and neurosteroids. *Br J Pharmacol,* 153**,** 1062-1071.

ZHELEZNOVA, N., SEDELNIKOVA, A. & WEISS, D. S. (2009). Function and modulation of delta-containing GABA(A) receptors. *Psychoneuroendocrinology,* 34 Suppl 1**,** S67-73.

ZHENG, H., LI, Y. F., WANG, W. & PATEL, K. P. (2009). Enhanced angiotensin-mediated excitation of renal sympathetic nerve activity within the paraventricular nucleus of anesthetized rats with heart failure. *Am J Physiol Regul Integr Comp Physiol,* 297**,** R1364-1374.

ZIEGLER, D. R., CULLINAN, W. E. & HERMAN, J. P. (2005). Organization and regulation of paraventricular nucleus glutamate signaling systems: N-methyl-D-aspartate receptors. *J Comp Neurol,* 484**,** 43-56.